

**Molecular Electrostatics for Probing Hydrogen Bonds,
Halogen Bonds and Lone Pair- π Interactions and
Design of Receptors for Lone Pair Bearing Molecules**

**Thesis submitted to
Cochin University of Science and Technology
for the award of Degree of
Doctor of Philosophy
in Chemistry under the Faculty of Science**

By

**Neetha Mohan
(Reg. No. 4147)**



**Inorganic and Theoretical Chemistry Section
Chemical Sciences and Technology Division
CSIR-National Institute for Interdisciplinary Science and Technology
Thiruvananthapuram – 695 019
Kerala, India**

2014

DECLARATION

I hereby declare that the matter embodied in the Ph.D. thesis entitled “**Molecular Electrostatics for Probing Hydrogen Bonds, Halogen Bonds and Lone Pair- π Interactions and Design of Receptors for Lone Pair Bearing Molecules**” is the result of investigations carried out by me at the Inorganic and Theoretical Chemistry Section, Chemical Sciences and Technology Division, CSIR-National Institute for Interdisciplinary Science and Technology (CSIR-NIIST), Trivandrum, under the supervision of Dr. C. H. Suresh and the same has not been submitted elsewhere for a degree, diploma or title.

In keeping with the general practice of reporting scientific observations, due acknowledgement has been made wherever the work described is based on the findings of other investigators.

(Neetha Mohan)

CSIR-National Institute for Interdisciplinary Science and Technology*(Formerly Regional Research Laboratory)***Council of Scientific & Industrial Research (CSIR)**
Industrial Estate P.O., Trivandrum - 695 019
Kerala, INDIA**Dr. Cherumuttathu H. Suresh**
Principal Sct. and Head
Inorganic & Theoretical Chem. Sec., CSTD**Tel: 91-471-2535 506**
Fax: +91-471-2491 712
E-mail: sureshch@gmail.com
sureshch@niist.res.in

March 3, 2014

CERTIFICATE

This is to certify that the work embodied in the thesis entitled “**Molecular Electrostatics for Probing Hydrogen Bonds, Halogen Bonds and Lone Pair- π Interactions and Design of Receptors for Lone Pair Bearing Molecules**” has been carried out by **Ms. Neetha Mohan** under my supervision and guidance at the Inorganic and Theoretical Chemistry Section, Chemical Sciences and Technology Division, CSIR-National Institute for Interdisciplinary Science and Technology (CSIR-NIIST), Trivandrum and the same has not been submitted elsewhere for a degree. All the relevant corrections, modifications and recommendations suggested by the audience and the doctoral committee members during the pre-synopsis seminar of **Ms. Neetha Mohan** have been incorporated in the thesis.

(C. H. Suresh)
Thesis Supervisor

ACKNOWLEDGEMENT

This thesis is the result of a challenging journey, upon which many people have contributed directly or indirectly through their support and encouragement. I am truly grateful to all of them for making my journey smooth and enjoyable.

First and foremost, I would like to express my heartfelt gratitude to my research supervisor, Dr. C. H. Suresh for his timely advice, continued encouragement, thoughtful guidance and strong motivation throughout the course of my research. The experience gained while working under his mentorship and expertise will benefit me in every aspect of my career for years to come.

I am deeply indebted to Dr. Suresh Das, Director, CSIR-NIIST and former directors, Dr. B. C. Pai and Prof. T. K. Chandrasekhar for the academic support and for providing me the necessary facilities for carrying out the work in this institution.

I am thankful to Professor Shridhar R. Gadre and Anmol Kumar, IIT-Kanpur, for the insightful discussions and fruitful collaboration. I wish to thank my Doctoral Committee members Dr. Manoj Narayana Pillai and Dr. Luxmi Varma for their valuable suggestions, timely help and support.

I owe my deepest gratitude to Dr. Roschen Sasikumar, Dr. Elizabeth Jacob, Dr. S. Savithri and Dr. Mangalam Nair who have been very kind enough to extend their help at various phases of this research. I also extend my sincere thanks to Dr. K. P. Vijayalakshmi for her generous advice, encouragement and constant moral support.

I wish to thank the past and present members of Theoretical Chemistry Group; Jomon, Sajith, Bhasha, Ajitha, Sandhya, Shaija, Remya K., Rakhi, Lincy, Remya P.R., Della, Anjali, Prasanth Kumar and Dr. Prabha for their warm friendship which created a pleasant working atmosphere. I greatly appreciate the friendship and support of Ani Mathews, Panneer, Jijoy, Alex, Manju, Manoj, Sudeep, Rejitha, Fathima, Arya,

Dhaneesh, Gaurab and Shaban. Many thanks to Delishia, Geoncy, Sarath, Vidya, Ushasree, Deepthy and Arya for their invaluable friendship, support and encouragement. Thanks to my supportive home mates Surya, Dilna, Vini and Sneha.

I wholeheartedly extend my thanks to all my friends at NIIST for making my days in NIIST memorable. I would also like to thank the administrative and technical staff members of NIIST for the cooperation and help in their respective roles.

I gratefully acknowledge Council of Scientific and Industrial Research, for providing me financial support. I express my gratitude towards the NIIST-CUSAT Research Council for the timely help during the entire course of my work and thesis submission. High performance computational facilities at CSIR-NCL, Pune and CSIR-CMMACS, Bangalore is greatly acknowledged.

Mere expression of thanks does not suffice for the unconditional support, prayers and care of my family on which I have relied throughout my life. Special thanks to all my beloved teachers for enlightening me with the first glance of research.

Above all, I owe it all to the Almighty for granting me the wisdom, health and strength to undertake this research task and enabling me to its completion.

"For each new morning with its light, For rest and shelter of the night, For health and food, for love and friends, For everything Thy goodness sends."

Ralph Waldo Emerson

Neetha Mohan

Contents

	Page
Declaration	i
Certificate	ii
Acknowledgements	iii
List of Tables	ix
List of Figures	xii
List of Schemes	xix
List of Abbreviations	xx
Preface	xxii
Chapter 1: Introduction	
Part A – Noncovalent Interactions	1
1.1 An Overview of Noncovalent Interactions	1
1.1.1 Components of Noncovalent Interaction Energy	3
1.1.2 Experimental Determination of Noncovalent Interactions	6
1.1.3 Hydrogen Bonds	8
1.1.3.1 Historical Background	8
1.1.3.2 Definition of Hydrogen Bond	9
1.1.3.3 Types of Hydrogen Bonds	12
1.1.3.4 Strength and Nature of Hydrogen Bonds	14
1.1.4 Halogen Bonds	17
1.1.5 Lone Pair-π and Anion-π Interactions	23
Part B – Computational Chemistry	30
1.2 An Overview of Computational Chemistry	30
1.2.1 <i>Ab initio</i> Molecular Orbital Theory	32

1.2.2	Hartree-Fock Theory	34
1.2.3	Electron Correlation Methods	37
1.2.3.1	Configuration Interaction	38
1.2.3.2	Coupled Cluster Methods	39
1.2.3.3	Many-Body Perturbation Theory	40
1.2.4	Density Functional Theory	43
1.2.4.1	Thomas-Fermi Model	44
1.2.4.2	Hohenberg-Kohn Theorem	45
1.2.4.3	The Kohn-Sham Equations	46
1.2.4.4	Exchange-Correlation Functionals	48
1.2.4.5	Minnesota Functionals	50
1.2.5	Basis Sets	51
1.2.6	Basis Set Superposition Error	54
1.2.7	Atoms in Molecules	55
1.2.8	Molecular Electrostatic Potential	58
1.2.9	Solvation Models	61
1.3	Conclusions	63
Chapter 2: Molecular Electrostatics for Probing Lone Pairs and Lone Pair-π Interactions		
2.1	Abstract	64
2.2	Introduction	65
2.3	Computational Methods	69
2.4	Results and Discussion	70
2.4.1	MESP Topography to Quantify Lone Pairs	70
2.4.2	Lone Pair- π Complexes	77
2.4.3	Electron Density Analysis	84

2.4.4	Correlation between V_{\min} and E_{int}	87
2.4.5	Validation of V_{\min} vs E_{int} Relationship	88
2.5	Conclusions	93
Chapter 3: Hydrogen Bonds, Halogen Bonds and Dihydrogen Bonds		
3.1	Abstract	94
Part A – Accurate Binding Energies and Cation Enhanced Binding Strengths		96
3.2	Introduction	96
3.3	Computational Methods	99
3.4	Results and Discussion	101
3.4.1	Modeling Accurate Interaction Energies	101
3.4.2	Cation Enhanced Binding Strengths	107
Part B – Molecular Electrostatic Potential Analysis of Hydrogen, Halogen, and Dihydrogen Bonds		117
3.5	Introduction	117
3.6	Computational Methods	120
3.7	Results and Discussion	120
3.7.1	Electron Density Analysis	121
3.7.2	Molecular Electrostatic Potential Analysis	124
3.8	Conclusions	132
Chapter 4: Rational Design of Receptors Based on Noncovalent Interactions		
4.1	Abstract	134
Part A – Receptors for Neutral Molecules and Anions		
4.2	Introduction	136
4.3	Methods	139
4.3.1	Molecular Design Strategy	139
4.3.2	Computational Methods	140

4.4	Results and Discussion	141
Part B – Cage Receptors for Noble Gas Atoms and Molecular Hydrogen		
4.5	Introduction	152
4.6	Design Strategy and Computational Methods	154
4.7	Results and Discussion	155
4.8	Conclusions	161
	List of Publications	163
	References	164


List of Tables


			Page
1.	Table 1.1	Important classes of noncovalent interactions and their strength ranges.	3
2.	Table 2.1	MESP topography features of neutral molecules.	74
3.	Table 2.2	MESP topography features of radicals and anions.	76
4.	Table 2.3	Interaction energies (E_{int}) and distance parameters (R_{hfb} and R_{c}) for the lone pair- π complexes of HFB.	80
5.	Table 2.4	AIM topological features of HFB:lone pair complexes.	86
6.	Table 2.5	Interaction energies (E_{int}), distance parameters (R_{hfb} and R_{c}) and θ , θ' and $\Delta\theta$ values for lone pair- π complexes of 1,2,4,5-tetracyanobenzene (TCB).	90
7.	Table 2.6	Interaction energies (E_{int}), distance parameters (R_{hfb} and R_{c}) and θ , θ' and $\Delta\theta$ values for lone pair- π complexes of 2,4,6-trifluoro-1,3,5-triazine (CNF).	90
8.	Table 2.7	Interaction energies (E_{int}), distance parameters (R_{hfb} and R_{c}) and θ , θ' and $\Delta\theta$ values for lone pair- π complexes of 1,3,5-trinitrobenzene (TNB).	91
9.	Table 3.1	Interaction energies of hydrogen bond complexes calculated at M06L (E_{M06L}), MP4//M06L ($E_{\text{MP4//M06L}}$), MP2 (E_{MP2}), MP4//MP2 ($E_{\text{MP4//MP2}}$), CCSD(T)//MP2 ($E_{\text{CCSD(T)//MP2}}$), W1BD (E_{W1BD}), and reference CCSD(T) (E_{ref}) methods in kcal/mol. Reference corresponding to E_{ref} values also provided.	111
10.	Table 3.2	Interaction energies of halogen and dihydrogen bond	




- complexes calculated at M06L (E_{M06L}), MP4//M06L ($E_{MP4/M06L}$), MP2 (E_{MP2}), MP4//MP2 ($E_{MP4/MP2}$), CCSD(T)//MP2 ($E_{CCSD(T)/MP2}$), W1BD (E_{W1BD}), and reference CCSD(T) (E_{ref}) methods in kcal/mol. Reference corresponding to E_{ref} values also provided. 114
11. Table 3.3 Energetic and geometric features of $D...A...Li^+$ and $D...A...NH_4^+$ complexes. E_{int} and D are the interaction energies and intermolecular hydrogen bond distances of **D-A** complexes. E_{Li^+} , $E_{NH_4^+}$, D_{Li^+} and $D_{NH_4^+}$ are the interaction energies and interaction distances of $D...A...Li^+$ and $D...A...NH_4^+$ complexes and NSE_{Li^+} and $NSE_{NH_4^+}$ represent the corresponding stabilization energies. Energy values in kcal/mol and distances in Å units. 115
12. Table 3.4 Interaction energies (E_{nb}), AIM properties (ρ and $\nabla^2\rho$) and MESP features (ΔV_{min-A} , ΔV_{min-D} , $\Delta\Delta V_{min}$, ΔV_{n-A} , ΔV_{n-D} and $\Delta\Delta V_n$) for representative set of intermolecular complexes. 130
13. Table 4.1 Interaction energy (E_{int}) of **HFB...X**, **R_I...X**, **R_{II}...X** and **R_{III}...X** in kcal/mol. 148
14. Table 4.2 Free energy change (ΔG) of **R_I...X**, **R_{II}...X** and **R_{III}...X** complexes in kcal/mol. 149
15. Table 4.3 Binding energy values of receptor-guest complexes in aqueous phase using IPCM solvation model in kcal/mol. 149
16. Table 4.4 Interaction energy values (E_{int}) of **HFB...X**, **R_I...X**, **R_{II}...X**, **R_{III}...X** and **R_{IV}...X** in kcal/mol. 158
17. Table 4.5 Electron density ($\rho(\mathbf{r})$) and Laplacian of electron density

$(\nabla^2\rho(\mathbf{r}))$ at bcps for $\mathbf{R}_{IV...X}$ complexes. I, II, III, IV and V represent the five aromatic rings in the cage receptor. Values in au.

List of Figures


			Page
1.	Figure 1.1	Normal hydrogen bond with one acceptor, (b) bifurcated hydrogen bond and (c) trifurcated hydrogen bond.	12
2.	Figure 1.2	Schematic representation of typical hydrogen bond potential. d_0 is the equilibrium distance and d is the hydrogen bond length. Negative and positive bond energies are indicated by the terms stabilizing and destabilizing respectively. Figure adapted from [Desiraju and Steiner 1999].	15
3.	Figure 1.3	Halogen bonding between R–X and (a) lone pair of NH_3 and (b) π -electrons of benzene.	17
4.	Figure 1.4	Directional tendencies of close contacts in crystalline halides.	19
5.	Figure 1.5	Molecular electrostatic potential at 0.001 au isodensity surface of CF_4 , CF_3Cl and CF_3Br showing σ -hole. Color coding,  blue -0.009 au to red 0.054 au. Figure adapted from [Clark <i>et al.</i> , 2007].	20
6.	Figure 1.6	Lone pair- π and anion- π interactions. (a) Lone pair- π complex between hexafluorobenzene and water (b) Anion pair- π complex between hexafluorobenzene and chloride ion.	24
7.	Figure 1.7	Anion- π interaction reported by Meyer and coworkers. (a) Schematic drawing of hexakis(pyridine-2-yl)-[1,3,5]-triazine-2-4-6-triamine (L1); (b) Front view and side view of $\{[(\text{L1})_2(\text{CuCl})_3][\text{Cl}]\}^{2+}$. Atom colors: C = grey, H = white, N = dark blue, Cu = light blue and Cl = yellow. Figure adapted	

- from [Demeshko *et al.*, 2004]. **25**
8. Figure 1.8 Anion- π interaction reported by Reedijk and coworkers. (a) Schematic drawing of N,N',N'',N'''-tetrakis{2,4-bis(di-2-pyridylamino)-1,3,5-triazinyl}-1,4,8,11-tetraazacyclotetradecane (L2), (b) Crystal structure of $[\text{Cu}_4(\text{L2})\text{Cl}_4][\text{Cl}]_4(\text{H}_2\text{O})_{13}$ from two different views. Atom colors: C = grey, H = white, N = dark blue, Cu = light blue and Cl = yellow. Figure adapted from [De Hoog *et al.*, 2004]. **26**
9. Figure 1.9 Anion- π complexes of 1,3,5-triazine and trifluoro-1,3,5-triazine with multiple anion- π interactions per anion. (X= Br^- or Cl^- and Y= H or F). **27**
10. Figure 1.10 N,N-naphthalenediimide unit and its DFT computed electrostatic potential map demonstrating the electron deficient character. Color coding,  blue -0.02 au to red 0.02 au. Figure adapted from [Mohan *et al.* 2013]. **29**
11. Figure 1.11 Jacob's ladder representing the five generations of density functional from the world of Hartree to the heaven of chemical accuracy, with examples from each class. **50**
12. Figure 1.12 Molecular graph of hexafluorobenzene-nitrogen complex (M06L/6-311++G(d,p) level) showing the bond paths (lines) and different critical points (red for (3, -1) or bond CP, yellow for (3, +1) or ring CP, and green for (3, +3) or cage CP. Color-code by element: C = black, F = grey and N=blue. **56**
13. Figure 1.13 (a) MESP contour plot of hexafluorobenzene molecule

- textured on to a 0.003 au electron density surface. Color coding,  blue -0.02 au to red 0.02 au, (b) nature and location of MESP CPs of formaldehyde. **60**
14. Figure 2.1 MESP textured on the 0.003 au electron density surface for (a) HFB, (b) TCB, (c) TNB and (d) CNF demonstrating the electron deficient nature of the aromatic rings. Color coding,  blue -0.01 au to red 0.01 au. **68**
15. Figure 2.2 Representation of molecular electrostatic potential (MESP) isosurfaces for a representative set of lone pair species. The MESP minima are marked as black dots and the corresponding V_{\min} values are given in kcal/mol. **71**
16. Figure 2.3 Correlation between MESP minimum (V_{\min}) and the largest eigenvalue (LE). **73**
17. Figure 2.4 Optimized geometries of HFB-lone pair complexes at M06L/6-311++G(d,p) level along with the interaction distances in Å. **79**
18. Figure 2.5 Molecular electrostatic potential textured on the 0.003 au electron density surface for HFB-lone pair complexes. Color coding,  blue -0.02 au to red 0.02 au for neutral and free radicals and blue -0.14 au to red -0.1 au for anionic species. **84**
19. Figure 2.6 AIM molecular graphs of HFB-lone pair complexes showing the bond paths (lines) and bond critical points (red for BCPs and green for CCPs). **85**
20. Figure 2.7 Correlation between MESP V_{\min} at lone pair region and

- interaction energy of the complexes between HFB and the lone pair containing species. **88**
21. Figure 2.8 Optimized geometries of lone pair complexes of 1,2,4,5-tetracyanobenzene (TCB), 1,3,5-trinitrobenzene (TNB) and 2,4,6-trifluoro-1,3,5-triazine (CNF) with a representative set of lone pair bearing molecules. Distances in Å. **89**
22. Figure 2.9 Correlation between MESP V_{\min} at lone pair region and interaction energy of the lone pair- π complexes of (a) 2,4,6-trifluoro-1,3,5-triazine (CNF), (b) 1,2,4,5-tetracyanobenzene (TCB) and (c) 1,3,5-trinitrobenzene (TNB). **92**
23. Figure 3.1 Representative set of intermolecular D-A complexes studied. Bond distances at MP2, M06L and W1BD methods (in Å) are given in the order from top to bottom. **102**
24. Figure 3.2 Correlation between E_{W1BD} and E_{ref} values. All values in kcal/mol. **104**
25. Figure 3.3 Comparison of energy errors of MP2 and M06L methods with respect to W1BD method. **106**
26. Figure 3.4 Comparison of energy errors of MP4//MP2, MP4//M06L and CCSD(T)//MP2 methods with respect to W1BD method. **107**
27. Figure 3.5 Optimized geometries of representative $\text{D}\dots\text{A}\dots\text{Li}^+$ complexes along with the hydrogen bond distances in Å. Hydrogen bond distances of the corresponding **D-A** complexes are given in parentheses. **108**
28. Figure 3.6 Optimized geometries of representative $\text{D}\dots\text{A}\dots\text{NH}_4^+$ complexes along with the hydrogen bond distances in Å.

- Hydrogen bond distances of the corresponding **D-A** complexes are given in parentheses. **109**
29. Figure 3.7 **D-A** complexes showing bridged configurations. Bond distances in Å. **122**
30. Figure 3.8 Relationship between interaction energy (kcal/mol) and electron density (ρ) at bcp. The dotted line represents the overall correlation and the coloured lines indicate the correlation for separate classes of noncovalent complexes. **123**
31. Figure 3.9 Change in V_{\min} upon bond formation for (a) $\text{H}_2\text{O}\dots\text{H}_2\text{O}$ (b) $\text{H}_2\text{O}\dots\text{ClF}$ and (c) $\text{H}_3\text{N}\dots\text{HCCH}$. The black dots represent the location of the most negative MESP-valued point and the corresponding V_{\min} values are also depicted. **126**
32. Figure 3.10 Linear relationship between $\Delta\Delta V_{\min}$ and noncovalent interaction energy (E_{nb}). **126**
33. Figure 3.11 Linear relationship between $\Delta\Delta V_{\text{n}}$ and noncovalent interaction energy (E_{nb}). **129**
34. Figure 3.12 Change in V_{\min} upon bond formation in electron donor-acceptor-donor complexes (a) $\text{F}^-\dots\text{IF}$ and (b) $\text{F}^-\dots\text{IBr}$. The black dots represent the location of the most negative MESP-valued point and the corresponding V_{\min} values are also depicted. **129**
35. Figure 4.1 Optimized geometries of **R_I**, **R_{II}** and **R_{III}** at M06L/6-311++G(d,p) DFT method. C-C bond distances in Angstroms and C-C-C bond angles in degree are also depicted. **141**

36. Figure 4.2 MESP plots demonstrating the nature of aromatic rings in benzene, fluorobenzene, HFB, **R_I**, **R_{II}** and **R_{III}**. Color coding,  blue -0.001 a.u. to red 0.03 a.u. 142
37. Figure 4.3 MESP isosurface of value -0.01 au for HFB, **R_I**, **R_{II}** and **R_{III}** along with their V_{\min} values in kcal/mol. V_{\min} points are indicated by black dots. 143
38. Figure 4.4 Representation of MESP isosurfaces for a representative set of lone pair bearing guest molecules. The MESP minima are marked as black dots and the corresponding V_{\min} values are given in kcal/mol. 144
39. Figure 4.5 Optimized geometries of **R_I...X** complexes. Distances in Angstrom units. 145
40. Figure 4.6 Optimized geometries of **R_{II}...X** complexes. Distances in Angstrom units. 146
41. Figure 4.7 Optimized geometries of **R_{III}...X** complexes. Distances in Angstrom units. 147
42. Figure 4.8 AIM Molecular graphs of **R_I...H₂O**, **R_{II}...H₂O**, **R_{III}...H₂O** and **R_{III}...SO₄²⁻**. Small red spheres and lines represent bond critical points (BCPs) and bond paths, respectively. 150
43. Figure 4.9 (a) Optimized geometry of the cage receptor and (b) MESP textured on the 0.003 au electron density surface. 156
44. Figure 4.10 Optimized geometries of **R_{IV}...He**, **R_{IV}...Ne**, **R_{IV}...Ar** and **R_{IV}...Kr** complexes. Interaction distances in Å. 157
45. Figure 4.11 Optimized geometry of **R_{IV}...H₂** complex. Interaction distances in Å. 159

46. Figure 4.12 AIM molecular graph of the endohedral complexes of \mathbf{R}_{IV} with He, Ne, Ar and Kr. Small red spheres represent bond critical points (bcps) and red lines represent bond paths. **159**
47. Figure 4.13 AIM molecular graph of the $\mathbf{R}_{IV}\dots\mathbf{H}_2$ complex. Small red spheres represent bond critical points (bcps) and red lines represent bond paths. **160**

List of Schemes

			Page
1.	Scheme 2.1	Representation of (a) arrangement of lone pairs in a molecule and (b) orientation of the molecule in a lone pair- π complex. L denotes the atom bearing the lone pair, X and Y are the atoms bonded to L. LP is the location of the lone pair, R is the ring centre, θ is the angle which the lone pair makes with L and the nearest atom X and θ' is the angle between L, X and R.	82
2.	Scheme 3.1	Effect of cations on the strength of neighboring hydrogen bonds.	99
3.	Scheme 3.2	X-A represents the electron acceptor and D-Z represents the electron donor. D and A are the atoms participating in the interaction. MESP at the nuclei are designated with symbols V_{n-A} , $V_{n-A'}$, V_{n-D} and $V_{n-D'}$.	127
4.	Scheme 4.1	Models proposed for anion recognition. X represents the lone pair bearing molecule and the possible lone pair- π interactions are represented with dotted lines.	140
5.	Scheme 4.2	The cage receptor model, R_{IV} . X = He, Ne, Ar, Kr and H ₂ . Dotted lines represent the possible interactions of the guest molecule with the electron-deficient rings of the receptor.	154

List of Abbreviations

AIM	: Atoms in Molecules
BCP	: Bond Critical Point
BSSE	: Basis Set Superposition Error
CAHB	: Charge-Assisted Hydrogen Bonds
CC	: Coupled Cluster
CCP	: Cage Critical Point
CCSD	: Coupled Cluster Single and Double
CI	: Configuration Interaction
CSD	: Cambridge Structural Database
DFT	: Density Functional Theory
DNA	: Deoxyribonucleic Acid
DZ	: Double Zeta
ECHBM	: Electrostatic-Covalent Hydrogen Bond Model
G09	: Gaussian 09
GGA	: Generalized Gradient Approximation
GTO	: Gaussian-Type Orbitals
HF	: Hartree-Fock
HK	: Hohenberg-Kohn
IPCM	: Isodensity Polarizable Continuum Model
IUPAC	: International Union for Pure and Applied Chemistry
LCAO	: Linear Combination of Atomic Orbital
LDA	: Local-Density Approximation
LSDA	: Local Spin Density Approximation
MBPT	: Many Body Perturbation Theory

MC	: Monte Carlo
MED	: Molecular Electron Density
MIPp	: Molecular Interaction Potential with Polarization
MD	: Molecular Dynamics
MESP	: Molecular Electrostatic Potential
MM	: Molecular Mechanics
MO	: Molecular Orbital
MP	: Møller-Plesset Perturbation Theory
ONIOM	: Our N-layered Integrated Molecular Orbital + Molecular Mechanics
PCM	: Polarizable Continuum Model
PES	: Potential Energy Surface
QM	: Quantum Mechanics
QSAR	: Quantitative Structure Activity Relationship
RCP	: Ring Critical Point
RAHB	: Resonance-Assisted Hydrogen Bonds
RNA	: Ribonucleic Acid
SCF	: Self Consistent Field
SAPT	: Symmetry Adapted Perturbation Theory
STO	: Slater-Type Orbitals
UFF	: Universal Force Field
XC	: Exchange Correlation

Preface

Noncovalent interactions, such as hydrogen bonds, halogen bonds and lone pair- π interactions are central to many areas of chemistry, molecular biology and materials science. A clear understanding of the nature and relative magnitude of noncovalent interactions is indispensable for the rational design of new molecules. Despite the overwhelming importance of noncovalent interactions, their quantification has been remained as a challenging task. Molecular electrostatic potential (MESP), a property amenable to experimental observation as well as theoretical calculation, has emerged as an efficient tool to understand, interpret and quantify weak interactions. The focus of this thesis is to develop MESP based approaches to probe hydrogen bonds, halogen bonds and lone pair/anion- π interactions. Further, these insights are utilized to design molecular receptors for neutral and anionic molecules of chemical, biological and environmental relevance. The thesis is divided into four chapters.

The first part of Chapter 1 gives an overview of various noncovalent interactions and reviews the major concepts and principles that have emerged from this area. Computational chemistry is an exciting and fast-emerging field that has become crucial for most advances made in chemistry today. A brief account of various computational methods and their theoretical basis is presented in the second part of Chapter 1.

In Chapter 2, an electrostatics-based approach is proposed for probing the weak interactions between lone pair containing molecules and electron deficient π -systems. For electron-rich molecules, the negative minima in molecular electrostatic potential (MESP) topography give the location of electron localization and the MESP value at the minimum (V_{\min}) quantifies the electron rich character of that region. Interactive behavior of lone pair bearing molecules with electron deficient π -systems explored within DFT brings out good correlation of the lone pair- π interaction energy with the V_{\min} value of

the electron rich system. On the basis of the precise location of MESP minimum, a prediction on the orientation of a lone pair bearing molecule with an electron deficient π -system is possible.

The quantification and characterization of hydrogen bonds, halogen bonds and dihydrogen bonds using accurate *ab initio* and MESP approaches is presented in Chapter 3. The competence of M06L, MP2, MP4//M06L and MP4//MP2 methods for modeling accurate binding energies of noncovalent complexes featuring hydrogen bonds, halogen bonds and dihydrogen bonds is assessed. It is shown that unambiguous evidence for bond formation in hydrogen bonds, halogen bonds and dihydrogen bonds can be obtained from the MESP analysis. Compared to the electron density (ρ) at the bond critical point-based analysis, the MESP data obtained at the bonded nuclei (V_n) as well as the MESP minimum (V_{\min}) observed on the constituents of the bonded complexes are found to be effective for predicting the strength of all kinds of hydrogen bonds, halogen bonds and dihydrogen bonds. A good linear correlation obtained between a parameter based on V_n and bond strength strongly suggests that all such bonds arise from electron donor-acceptor (eDA) interactions.

Chapter 4 presents the rational design of bidentate (**R_I**), tridentate (**R_{II}**) and tetradentate (**R_{III}**) receptors capable of binding neutral molecules and anions predominantly through lone pair- π and anion- π interactions. The receptors are modeled in a stepwise manner by substituting the electron deficient core of hexafluorobenzene at 1, 3, and 5 positions with pentafluorobenzyl (C₆F₅CH₂-) groups. The tripodal platform of **R_{III}** is used for the construction of a cage receptor (**R_{IV}**) which can form stable endohedral van der Waal's complexes with noble gas atoms and molecular hydrogen.

Chapter 1

Introduction

**Part A – Noncovalent Interactions
&
Part B – Computational Chemistry**

Part A – Noncovalent Interactions

1.1 An Overview of Noncovalent Interactions

Atoms and molecules can interact together leading to the formation of either new molecules or molecular assemblies. The former which result from the partial overlap between hybrid atomic orbitals is termed covalent [Lewis 1923] while the latter which neither involves the formation or breaking of chemical bond is termed noncovalent interactions. Noncovalent interactions were first recognized in the last century by J. D. van der Waals who realized that the discrepancies between the state function of a real gas and ideal gas could be accounted for by the attractive forces existing between gas molecules [Müller-Dethlefs and Hobza 2000]. Liquefaction of helium by Kamerlingh Onnes [Onnes 1909] provided a most decisive argument about the existence of attractive intermolecular forces even between rare gas atoms such as helium which do not possess any charge or permanent electric multipole moment. Later in 1930, Fritz London made fundamental step in understanding and interpreting these interactions using the principles of quantum mechanics [London 1930a]. Noncovalent interactions exist at much greater distances compared to covalent bonds; sometimes at more than 10 Å or even 100 Å in the case of some biomacromolecules [Hobza and Müller-Dethlefs 2010].

Noncovalent interactions are the main source of stability of many molecular complexes in chemistry, nanoscience and biology. The three dimensional structure and functions of biomacromolecules like DNA, RNA and proteins result from a delicate balance between various noncovalent interactions acting between biomolecular building blocks as well as between these molecules and their surrounding environment. Although weak relative to covalent interactions, it is the large number of these interactions that occur in biomolecules and supramolecular structures that make them functionally

significant. To quote Nobel laureate Jean-Marie Lehn [Lehn 1995], “Noncovalent interactions define the inter-component bond, the action and reaction, in brief, the behavior of molecular individuals and populations”. Despite the enormous progress made in experimental and theoretical techniques, an unambiguous description of noncovalent interactions is far from reality [Müller-Dethlefs and Hobza 2000].

The term “noncovalent” encompasses an enormous range of attractive and repulsive forces which range from coordinative bonds with a strength of several hundreds of kJ/mol to weak van der Waals interactions worth only a few kJ/mol. In the very broadest sense, noncovalent interactions include electrostatic interactions occurring between permanent multipoles such as charge-charge, charge-dipole, charge-multipole, multipole-multipole interactions, induction or polarization interactions between permanent and induced multipoles and dispersion interactions between instantaneous and induced multipoles. Charge-transfer, ionic and metallic interactions, hydrogen bonds, halogen bonds, dihydrogen bonds and lithium bonds are also subsumed under noncovalent interactions. π -systems also participate in noncovalent interactions and can interact favorably with cations, anions or other π -systems leading to cation- π , anion π or π - π stacking interactions. Hydrophobic interactions represent the tendency of nonpolar groups to associate in aqueous solutions and occur in low molecular weight organic molecules and biological macromolecules. Strongest among noncovalent interactions are ion-ion interactions (bond energies ranging from 100 – 350 kJ/mol) and the strength of these interactions depend on the distance between the charges and the extent of delocalization. Interactions between ions and dipoles (ion-dipole interactions) are weaker with bond energies in the range of 20 – 200 kJ/mol. Even weaker are dipole-dipole interactions with bond energies lying between 5 – 50 kJ/mol. Hydrogen bonds are highly directional noncovalent interactions with bond strength ranging from very weak (< 12 kJ/mol) to moderate (16 – 60 kJ/mol) and strong (60 – 120 kJ/mol) [Desiraju and Steiner

2001]. The classification and strength ranges of accepted intermolecular noncovalent interactions are summarized in Table 1.1.

Table 1.1 Important classes of noncovalent interactions and their strength ranges.

Interaction	Strength Range	Example
Ion-ion	100 - 350 kJ/mol	NaCl
Ion-dipole	20 - 200 kJ/mol	Coordination Bonds
Dipole-dipole	5 - 50 kJ/mol	SO ₂ + SO ₂
Hydrogen Bonding	4 - 120 kJ/mol	Water
Halogen Bonding	10 - 200 kJ/mol	Bromine 1,4-dioxanate
Cation- π Interaction	5 - 80 kJ/mol	Na ⁺ channels
Anion- π Interaction	4 - 120 kJ/mol	Hexafluorobenzene-F ⁻ complex
π - π stacking	0 - 50 kJ/mol	Benzene crystal structure
van der Waals	< 5 kJ/mol	Crystal close packing/charge balance
Hydrophobic Effects	No measurement	Oil and water

The thesis mainly focuses on hydrogen bonds, halogen bonds and anion- π interactions which will be described in detail in the forthcoming sections.

1.1.1 Components of Noncovalent Interaction Energy

Various intermolecular noncovalent forces can be broadly classified as short-range forces that decrease exponentially with distance and long-range forces that vary as the inverse powers of distance. The total intermolecular interaction (E_{int}) energy of noncovalent complexes is partitioned into five different energy contributions on the basis of perturbation theory *viz.* electrostatic, polarization, dispersion, charge-transfer and exchange-repulsion terms.

$$E_{\text{int}} = E_{\text{ES}} + E_{\text{POL}} + E_{\text{EX}} + E_{\text{DIS}} + E_{\text{CT}} \quad (\text{Eq. 1.1})$$

where E_{ES} , E_{POL} , E_{EX} , E_{DIS} and E_{CT} represent electrostatic, polarization, exchange-repulsion, dispersion and charge-transfer energies respectively. The relative contributions of each of these components vary for specific kinds of noncovalent interactions.

Electrostatic forces arise from the classical Coulombic interactions between the static charge distributions of two molecules. These forces can be either attractive or repulsive and includes the interactions of all permanent charges and multipoles such as charge-charge, charge-dipole, dipole-dipole, dipole-quadrupole, etc. The electrostatic force of interaction, F between two point charges q_1 and q_2 separated by a distance r can be described by Coulomb's Law as,

$$F = \frac{q_1 q_2}{4\pi\epsilon r^2} \quad (\text{Eq. 1.2})$$

where ϵ is the dielectric constant of the medium. The central multipole expansion [Hirschfelder *et al.* 1964] calculates the electrostatic potential, $V(r)$ at point P at a distance r from the center of mass of any two point charges q_1 and q_2 as the sum of a finite series of charge-charge, charge-dipole, dipole-dipole, charge-quadrupole, dipole-quadrupole, quadrupole-quadrupole interactions.

$$V(r) = \frac{1}{4\pi\epsilon_0} \left(\frac{q}{r} + \frac{\mu_z \cos\theta}{r^2} + \frac{Q_{zz}(3\cos^2\theta - 1)}{2r^3} + \dots \right) \quad (\text{Eq. 1.3})$$

where μ_z is the dipole moment, Q_{zz} is the quadrupole moment and θ is the angle which the point charge makes with the center of mass and the point P. Electrostatic interaction is directional and of long range diminishing slowly as r^{-1} for charge-charge interactions, r^{-2} for charge-dipole interactions, r^{-3} for dipole-dipole and so on.

Polarization forces are highly non-additive, attractive forces arising from the deformation of the charge distribution of a nonpolar molecule by the external electric field generated by neighboring molecules possessing permanent dipole moment [Debye 1929]. The polarization component includes the interactions between all permanent

charges or multipoles and induced multipoles, such as dipole-induced dipole, quadrupole-induced dipole, etc. Polarization term is of long range and decrease faster with distance (r^{-4}). The induced dipole moment μ is given by

$$\mu = \alpha E \quad (\text{Eq. 1.4})$$

where α is the static polarizability and E is the electric field. The energy of interaction (E_{POL}) between a dipole μ and an electric field E is given by

$$E_{\text{POL}} = -\int_0^E \mu dE = -\frac{1}{2} \alpha E^2 \quad (\text{Eq. 1.5})$$

Exchange interactions are short-range repulsive interactions of quantum chemical nature which originate from charge overlap and exchange effects. This interaction can be understood in terms of the Pauli principle which prohibits any two electrons in a system from having the same set of quantum numbers. The overlap of electron density distribution of the two interacting molecules causes a fall in electron density in the intermolecular region leading to repulsion between the incompletely shielded nuclei. Unlike for the covalent bond, where the electron density between subsystems having unpaired electrons increases in the bonding region, here the electron density increases in an antibonding region, which results in mutual repulsion. Exchange potential, E_{EX} is proportional to the square of the overlap integral, S_{ij} between orbitals of two molecules.

$$E_{\text{EX}} \propto S_{ij}^2 \quad (\text{Eq. 1.6})$$

Dispersion interactions [Eisenschitz and London 1930; London 1930a; London 1930b] are less directionally specific, have a long-range character and are of vital importance in stacking interactions existing in biomacromolecules. The dispersion energy has its origin in quantum mechanics, and comes from the continuous fluctuation of charge distribution of molecules due to electron movement. The dispersion energy is proportional to the product of the polarizabilities of the subsystems and a sixth (or higher) power of reciprocal distance. Dispersion and exchange-repulsion terms are often

combined into “van der Waal’s” contribution that can be approximately described by Lennard-Jones potential ($E_{\text{vdw}} \sim Ar^{-12} - Br^{-6}$). Dispersion term has a distance dependence which decreases as r^{-6} while exchange-repulsion term increases sharply with reducing distance as r^{-12} . Charge-transfer interaction is caused by the charge transfer from the occupied molecular orbitals (MO) of monomer A to the vacant MO’s of monomer B and from the occupied MO’s of B to vacant MO’s of A and the higher order coupled interactions. Charge-transfer term decreases faster, with an approximate distance dependence of e^{-r} .

1.1.2 Experimental Determination of Noncovalent Interactions

Major efforts have been carried out to devise and employ experimental techniques to study the structure and dynamics of noncovalent clusters and to quantify noncovalent interactions. Scattering experiments, spectroscopic measurements, and X-ray diffraction are some of the experimental techniques that are widely used to gather information about noncovalent interactions. Molecular structure, though not directly observable, can be determined by measuring the rotational constants. Microwave spectroscopy, a method of very high resolution optical spectroscopy, yield the three rotational constants and consequently the moment of inertia and the most probable structure of molecular clusters [Canagaratna *et al.* 1998; Townes and Schawlow 1975]. It is extensively employed for the study of noncovalent clusters including those bound by electrostatic and dispersion interactions. However, rotational constants cannot provide an unambiguous answer regarding the structure and geometry of noncovalently bound complexes. Far-infrared vibration rotation tunneling or FIR-VRT spectroscopy [Blake *et al.* 1991] is widely used in the study of transitions between vibration-rotation-tunneling states in molecular clusters with a resolution comparable to that of microwave spectroscopy. Pugliano and Saykally carried out the first detailed experimental study of

water trimer using FIR-VRT spectroscopy and showed that water trimer exhibits a cyclic triangular structure [Pugliano and Saykally 1992]. Vibrational frequencies are directly observable characteristics of noncovalent complexes and hence vibrational spectroscopy methods based on infrared absorption or Raman effect can provide information on the structure and strength of noncovalent complexes. Zero-electron kinetic energy (ZEKE) [Müller-Dethlefs *et al.* 1984a; Müller-Dethlefs *et al.* 1984b] photoelectron spectroscopy provides high accurate information of stabilization energies of noncovalent complexes. ZEKE spectroscopy has greatly contributed to improving the knowledge on (ro)vibronic structure of cationic molecular complexes, van der Waal's complexes like Benzene...Ar complexes and hydrogen bonded complexes of the type Phenol...H₂O [Hobza and Müller-Dethlefs 2010]. Resonance-enhanced multiphoton ionization (REMPI) spectroscopy provides spectroscopic information on the excited states of neutral systems and is frequently applied to understand the structure and dynamics of molecular clusters. Zwier *et al.* [Dian *et al.* 2002a; Dian *et al.* 2002b], Mikami *et al.* [Patwari *et al.* 2001] and Kleinermanns *et al.* [Nir *et al.* 2001; Nir *et al.* 2002] have extensively employed IR-UV hole burning studies to understand the noncovalent interactions in molecules of biological interest in the gas phase. Molecular torsion balance experiments [Carroll *et al.* 2008] and chemical double mutant complex cycles [Cockroft and Hunter 2007] are of particular importance in the determination of the magnitude of π - π interactions. Atomic force microscopy (AFM) has become a method of choice for obtaining actual images of molecules and the forces that hold them together. Very recently by Zhang and coworkers [Zhang *et al.* 2013] reported a real-space visualization of the formation of hydrogen bonding in 8-hydroxyquinoline molecular assemblies on a Cu(III) substrate revealing weak O-H...O, C-H...O and C-H...N bonds using noncontact atomic force microscopy (NC-AFM). Accurate experimental determination of structure and energetics of noncovalent interactions still remains a

challenge. The progress in the understanding of noncovalent interactions can be achieved only by close cooperation between experiment and theoretical methods.

1.1.3 Hydrogen Bonds

“The discovery of the Hydrogen Bond could have won someone the Nobel Prize, but it didn't” George A. Jeffrey, Wolfram Saenger, 1991.

1.1.3.1 Historical Background

The hydrogen bond is the most important of all directional intermolecular interactions operative in determining structure, dynamics and function of a vast number of chemical and biological systems. The hydrogen bond $X-H\dots Y-Z$ is an attractive interaction in which the electropositive H atom intercedes between two electronegative species X and Y and brings them closer [Desiraju 2011]. The weak interactions between molecules containing hydroxyl groups were noted by Nernst in 1892 [Nernst 1892]. However, the first proper description of hydrogen bonding came only ten years later with the concept of “Nebenvaleanz” (minor valence) and “innerekomplexsalzbildung” developed by Werner [Werner 1902] and Hantzsch [Hantzsch 1910] to describe inter- and intra- molecular hydrogen bonding. Alfred Werner proposed that ammonium salt has a configuration where a proton lies between the ammonia molecule and the ion. Intramolecular hydrogen bonds were suggested by Oddo and Puxeddu (with the name *mesohydric form*) in 1906 to explain the properties of some *o*-hydroxyazo derivatives of eugenol [Oddo and Puxeddu 1906]. Several years later Pfeiffer made a similar proposal of an intramolecular hydrogen bond or “inner Komplexsdzbindung” between hydroxyl and carbonyl functional groups in 1-hydroxyanthraquinone [Pfeiffer *et al.* 1913]. Moore and Winmill concurred with Werner and proposed a hydrogen bonded structure of undissociated trimethyl ammonium hydroxide, thus accounting for its slight dissociation compared to tetramethyl ammonium hydroxide [Moore and Winmill 1912]. In 1920 W.

M. Latimer and W. H. Rodebush, recognized that the unusual properties of water and ice owe their existence to hydrogen bonds between water molecules [Latimer and Rodebush 1920]. They proposed that "[A] free pair of electrons on one water molecule might be able to exert sufficient force on a hydrogen held by a pair of electrons on another water molecule to bind the two molecules together.... Such an explanation amounts to saying that the hydrogen nucleus held between 2 octets constitutes a weak 'bond'." This description, based on the Lewis dot formalism, is the first to truly call this interaction a bond. Hydrogen bond was apparently quoted for the first time by Lewis in 1923 [Lewis 1923]. Pauling interpreted the structure of the $[F:H:F]^-$ ion and accounted for the residual entropy of ice using the concept of hydrogen bonding [Pauling 1931; Pauling 1935]. Since its discovery, hydrogen bonding interactions has continued to fascinate chemists and enormous theoretical and experimental efforts has been made to understand the phenomenon of hydrogen bonding. Huggins predicted the role and importance of hydrogen bond as early as in 1936: "... the most fruitful applications of hydrogen-bridge theory will be to a better understanding of the nature and behavior of complicated organic substances such as gels, proteins, starch, cellulose, sugars and other carbohydrates, chlorophyll, hemoglobin, and related substances, etc." [Huggins 1936]. The role of hydrogen bonding in the structure and function of biomolecules were brought out by the landmark papers of Pauling and Corey [Pauling and Corey 1950; Pauling *et al.* 1951] describing elements of protein structure *viz.* alpha helix and beta sheet and Watson and Crick [Watson and Crick 1953] discussing the structure of DNA double helix.

1.1.3.2 Definition of Hydrogen Bond

A number of definitions have been put forward for hydrogen bonds, the earlier one being the one proposed by Pauling in his book "The Nature of the Chemical Bond"

according to which "[U]nder certain conditions an atom of hydrogen is attracted by rather strong forces to two atoms, instead of only one, so that it may be considered to be acting as a bond between them. This is called the hydrogen bond" [Pauling 1939]. Over the years, chemists have found a large variety of hydrogen bonding interactions that do not quite fit the classical definition by Pauling. A far-sighted early definition is that of Pimental and McClellan who in 1960, defined hydrogen bond as being "said to exist when 1) there is evidence of a bond, and 2) there is evidence that this bond specifically involves a hydrogen atom already bonded to another atom" [Pimentel and McClellan 1960]. As noted by Hobza and Havlas [Hobza and Havlas 2000], "the published definitions of the H-bond are not unambiguous and many exist." A task group of International Union for Pure and Applied Chemistry (IUPAC) has reviewed this topic in depth based on theoretical and experimental knowledge acquired over the past century and proposed a short modern definition for it [Arunan *et al.* 2011a; Arunan *et al.* 2011b]. According to the definition "The hydrogen bond is an attractive interaction between a hydrogen atom from a molecule or a molecular fragment X–H in which X is more electronegative than H, and an atom or a group of atoms in the same or a different molecule, in which there is evidence of bond formation".

The IUPAC task committee recommends some criteria useful as evidence and some typical characteristics for defining a particular weak interaction as a hydrogen bond. The six criteria proposed by the committee for a hydrogen bond X–H...Y–Z are:

- a) The forces involved in the formation of a hydrogen bond are those originating from electrostatics, charge-transfer and dispersion.
- b) The X–H covalent bond is polarized and the H...Y bond strength increase with the increase in electronegativity of X.
- c) Closer the X–H...Y angle to 180°, stronger is the hydrogen bond and shorter is the H...Y distance.

- d) Hydrogen bond formation usually leads to an increase in the length of the X–H bond leading to a red shift in the infrared X–H stretching frequency and an increase in the infrared absorption cross-section for the X–H stretching vibration. The greater the lengthening of the X–H bond in X–H...Y, the stronger is the H...Y bond. Simultaneously, new vibrational modes associated with the formation of the H...Y bond are generated.
- e) Hydrogen bond formation leads to characteristic NMR signatures that typically include pronounced proton deshielding for H in X–H, through hydrogen bond spin-spin couplings between X and Y, and nuclear Overhauser enhancements.
- f) For a hydrogen bond to be detected experimentally, the Gibbs energy of formation for the hydrogen bond should be greater than the thermal energy of the system.

The typical characteristics of hydrogen bonds listed by the IUPAC committee are:

- (a) The pK_a of X–H and pK_b of Y–Z correlate strongly with the energy of the hydrogen bond formed between them.
- (b) Hydrogen bonds are considered as the partially activated precursors in proton-transfer reactions ($X-H...Y \rightarrow X...H-Y$).
- (c) Hydrogen bonding networks show cooperativity, leading to deviations from pairwise additivity in hydrogen bond properties.
- (d) Hydrogen bonds show directional preferences and influence packing modes in crystal structures.
- (e) Interaction energy of hydrogen bond correlates well with the extent of charge transfer between the donor and the acceptor.

- (f) Analysis of the electron-density topology of hydrogen bonded systems usually shows a bond path connecting H and Y and a (3, -1) bond critical point between H and Y.

1.1.3.3 Types of Hydrogen Bonds

The term hydrogen bond includes a broad spectrum of interactions and the term “hydrogen bridge” [Desiraju 2002] is meaningfully used in literature to represent the different types of hydrogen bonds. In a normal hydrogen bond, the donor atom interacts with a single acceptor. A donor can interact with two or three acceptors simultaneously resulting in bifurcated (three-center) and trifurcated hydrogen (four-center) bonds respectively, as illustrated in Figure 1.1.

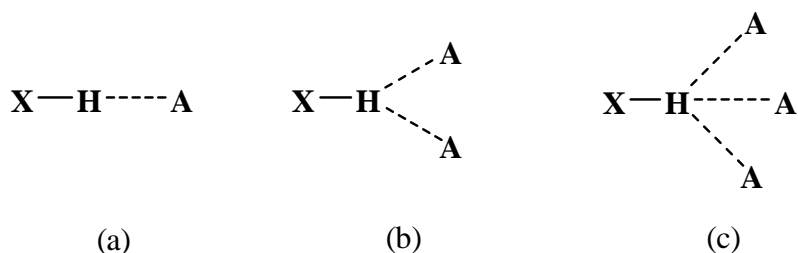


Figure 1.1 (a) Normal hydrogen bond with one acceptor, (b) bifurcated hydrogen bond and (c) trifurcated hydrogen bond.

More than one hydrogen bond can be formed at once resulting in multiple hydrogen bonding interactions. For example Adenine-Thymine base pair in DNA exhibits two intermolecular hydrogen bonds whereas Guanine-Cytosine base pair is characterized by three hydrogen bonds. The hydrogen bond donor and hydrogen bond acceptor can belong to the same molecule or different molecules; the former is termed intramolecular hydrogen bond and the latter is intermolecular hydrogen bond. Intramolecular hydrogen bonds are necessarily bent whereas intermolecular hydrogen bonds are linear or nearly linear. Hydrogen bonds can also be classified based on the nature of donor and acceptor molecules as conventional and unconventional hydrogen

bonds. Conventional hydrogen bonds have electronegative atoms O, N and Cl as proton acceptors and hence O–H...O, N–H...N, N–H...O, N–H...Cl and other similar systems are considered to be conventional hydrogen bonds. Carbon atoms or π -electrons can form hydrogen bonds and such bonds C–H...Y and X–H... π are unconventional. Hydrogen bonds can be red-shifting or blue-shifting depending on the X–H stretching frequencies of the proton donor groups. The formation of a hydrogen bond X–H...Y–Z, according to the conventional definition, is accompanied by the weakening of the covalent X–H bond with a concomitant red-shift or decrease in the X–H stretching frequency. Such hydrogen bonds are red-shifting hydrogen bonds. The red-shift of the X–H stretch vibration is regarded as the “signature of hydrogen bonding” [Allerhand and Schleyer 1963] and is the basis for several structural, spectroscopic and thermodynamic techniques for the detection of hydrogen bonding. Hobza and Špirko established the existence of a new type of hydrogen bond called improper blue-shifting hydrogen bonds in benzene dimers and other benzene complexes characterized by the strengthening of the X–H covalent bond and blue-shift in the X–H stretching frequency [Hobza *et al.* 1998]. Alabugin and coworkers showed that the structural reorganization of X–H bond in red-shift and blue-shift hydrogen bonds arise from a balance of hyperconjugative bond weakening and rehybridization bond strengthening [Alabugin *et al.* 2003]. Jemmis *et al.* suggested that the nature of the electron density distribution resulting from the electron affinity of atoms involved in the hydrogen bond donor predetermines it toward proper or improper hydrogen bonds [Joseph and Jemmis 2007]. Gilli *et al.* proposed the three types of strong hydrogen bonds where the hydrogen bond strength is enhanced by adding an electron, withdrawing an electron, or by resonance [Gilli and Gilli 2000; Gilli and Gilli 2009a; Gilli *et al.* 2009b]. These are charge-assisted hydrogen bonds, (+) CAHB and (-) CAHB and resonance-assisted hydrogen bonds (RAHB) respectively. CAHBs involve ionic

groups and are more strong compared to those found in neutral systems. In RAHBs, the enhancement of hydrogen bond strength is the result of π -electron delocalization.

Crabtree and coworkers introduced the concept of dihydrogen bonds to explain the unconventional hydrogen bonds established between metal hydrides and proton donor like O–H or N–H [Crabtree *et al.* 1996]. A dihydrogen bond is represented as M–H...H–Y where M is a metal which is less electronegative than H (usually Boron or transition metals) and Y is an electronegative element. Mikami and coworkers first reported dihydrogen bonding in the gas phase [Patwari *et al.* 2002]. The presence of one electron hydrogen bond has been revealed from both experimental [Merritt *et al.* 2006] and theoretical calculations [Alkorta *et al.* 1998] where the C atom in CH₃ radical acts as the acceptor. Very recently, Mani and Arunan [Mani and Arunan 2013] proposed ‘carbon bond’ (C...Y) analogous to hydrogen and halogen bonds wherein the tetrahedral face of CH₃ interacts with the negative centers of molecules like H₂O, H₂S and NH₃.

1.1.3.4 Strength and Nature of Hydrogen Bonds

Hydrogen bonds exhibit a continuum of strengths depending on the nature of the donor and acceptor groups; weakest hydrogen bonds are hardly distinguishable from van der Waals interaction and strongest ones are stronger than the weakest covalent bonds [Desiraju and Steiner 2001]. The energy of hydrogen bonds lies in the range of 0.5 to 40 kcal/mol. Hydrogen bonding interactions in solid, liquid and gaseous states are classified as strong, moderate and weak based on the strength of the interactions and different geometrical and spectral criteria [Jeffrey 1997]. For weak hydrogen bonds, the strength falls in the range of < 1 to 4 kcal/mol. The strength of moderate and strong hydrogen bonds ranges between 4 to 15 kcal/mol and 15 to 40 kcal/mol respectively. The schematic representation of the hydrogen bond potential for any particular donor-acceptor combination is shown in Figure 1.2 [Desiraju and Steiner 1999]. The distance

profile of the potential energy indicates that the energy is lowest at the equilibrium distance d_0 , is negative for all distances $d > d_0$ and is positive only for very short distances. The zero-energy line separates attractive (or stabilizing with energy $E < 0$) and repulsive (or destabilizing with energy $E > 0$) interactions. Every donor-acceptor combination of hydrogen bonds has its own potential energy curve with the minimum being deeper and shifted to shorter distances for stronger combinations. Figure 1.2 shows that a stabilizing interaction is associated with a repulsive force if it is shorter than the equilibrium distance.

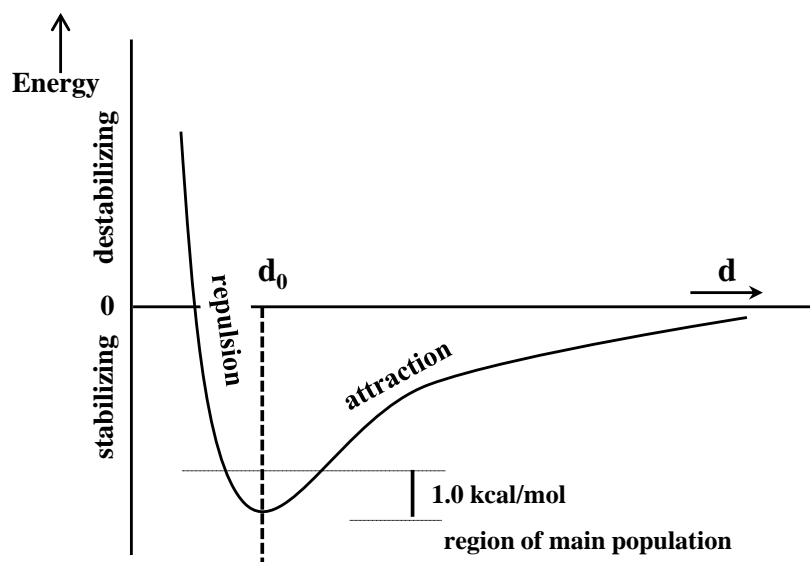


Figure 1.2 Schematic representation of typical hydrogen bond potential. d_0 is the equilibrium distance and d is the hydrogen bond length. Negative and positive bond energies are indicated by the terms stabilizing and destabilizing respectively. Figure adapted from [Desiraju and Steiner 1999].

Hydrogen bond is a complex interaction that has contributions from electrostatic (acid/base) interactions, polarization (hard/soft) effects, van der Waals (dispersion/repulsion and electron correlation) interactions and covalency (charge transfer) terms. The contributions from each term vary depending on particular donor-acceptor combination and the geometry of the hydrogen bonded complex. Different

energy decomposition schemes are employed for decomposing the hydrogen bond energy into the constituent energy terms. One of the first decomposition schemes was proposed by Kollman and Allen [Kollman and Allen 1970; Kollman and Allen 1972]. Most popular partitioning modes follow the Morokuma and Kitara decomposition scheme where the interaction energy is calculated within the Hartree-Fock one-electron approximation [Kitaura and Morokuma 1976; Morokuma 1977]. Umeyama and Morokuma analyzed different hydrogen bonded systems and proposed that the energy components of hydrogen bonds are totally distance dependent [Umeyama and Morokuma 1977]. For any hydrogen bonded complex, the long-range electrostatic term dominates over the short range charge-transfer and polarization terms at larger distances whereas the attractive electrostatic, charge-transfer and polarization terms compete with large repulsive exchange-repulsion term at relatively small distances [Desiraju 2002; Steiner 2002]. Although electrostatic contribution is the dominant factor responsible for classical hydrogen bonding, pronounced covalent character is observed in strong hydrogen bonds and the dominance of dispersive interactions is found in weak hydrogen bonds. Gilli *et al.* proposed an electrostatic-covalent hydrogen bond model (ECHBM) based on the systematic analysis of structural and spectroscopic data of a large number of O-H...O-H bonds [Gilli and Gilli 2000]. According to this model weak hydrogen bonds are electrostatic in nature. As the strength of the interaction increases, the covalent character of the bond also increases, and very strong hydrogen bonds are actually three-center four-electron covalent bonds. Desiraju claimed that the stronger hydrogen bonds are characterized by significant charge transfer from the acceptor to proton donating bond whereas weaker hydrogen bonds are mostly electrostatic in nature [Desiraju 2002]. Grabowski *et al.* characterized the covalent nature of interactions within various hydrogen bonded molecular aggregates and pointed out that the delocalization and electrostatic interaction energy are the most important attractive terms for hydrogen bond

interactions [Grabowski 2011; Grabowski *et al.* 2006]. As the interaction becomes stronger, the ratio between the delocalization and electrostatic interaction energy terms increases.

1.1.4 Halogen Bonds

A halogen bond, $R-X\dots Y-Z$ is a highly directional, electrostatically-driven noncovalent interaction between a covalently bonded halogen atom X in one molecule and a negative site Y in another molecule [Politzer *et al.* 2010]. $R-X$ is the halogen bond donor and $Y-Z$ is the halogen bond acceptor; X is a halogen atom with an electrophilic region (chlorine, bromine, iodine and astatine) and the strength of the interaction increases in the order $Cl < Br < I$. R can be another halogen atom or a large organic or inorganic residue and Y is often an atom such as oxygen, nitrogen or sulfur, that has a lone pair or π -electron of an unsaturated system (Figure 1.3).

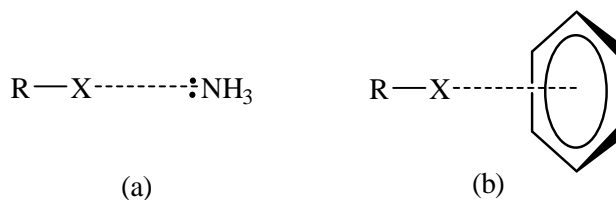


Figure 1.3 Halogen bonding between $R-X$ and (a) lone pair of NH_3 and (b) π -electrons of benzene.

The first reports of halogen acting as the Lewis acid came in the nineteenth century with the description of the complexes of Cl_2 , Br_2 and I_2 with Lewis bases such as ammonia and methylamines [Guthrie 1863; Prescott 1896; Remsen and Norris 1896]. More than 50 years later Benesi and Hildebrand reported the first cases of intermolecular donor acceptor complexes between iodine and aromatic hydrocarbons [Benesi and Hildebrand 1949]. The quantum mechanical theory of complex resonance that explained halogen bonding as a charge-transfer interaction was developed by Mulliken [Mulliken

1952] and Flurry [Flurry 1965; Flurry 1969]. Odd Hassel provided the detailed physical descriptions of the interactions in the mid-20th century from the crystal structures of molecular halogens in the complexes with organic bases and proposed that charge transfer from electron donors (Lewis bases) to electron acceptors (iodine or bromine) was responsible for these interactions [Hassel 1970; Hassel and Stromme 1958a; Hassel and Stromme 1958b]. The term “halogen bond” was first used by Dumas *et al.* in the context of experimental studies of complexes formed by CCl₄, CBr₄, SiCl₄ and SiBr₄ with tetrahydrofuran, tetrahydropyran, pyridine, anisole and di-*n*-butyl ether in organic solvents [Dumas *et al.* 1978]. The importance of halogen bonding in supramolecular self-assembly phenomena was stressed by Hassel [Hassel 1970] while the survey of Protein Data Bank (PDB) by Auffinger *et al.* in 2004 revealed the significance of such interactions in the crystal structures of biomolecular systems [Auffinger *et al.* 2004]. Extensive surveys of crystallographic data by Murray-Rust *et al.* to identify and characterize short intermolecular contact distances within the lattices of crystalline sulfides and halides revealed they show distinct patterns of attractive noncovalent interactions [Murray-Rust and Motherwell 1979; Murray-Rust *et al.* 1983]. Close contacts of halogens with electrophiles such as metal ions occur at angles 90° to 120° with the C–X bond whereas with nucleophiles such as oxygen and nitrogen, the angles were between 160° to 180° *i.e.*, along the extensions of the covalent bonds to the halogens (Figure 1.4). Such directed, near-linear interactions of halogens with nucleophiles came to be known as halogen bonds. The existence of halogen bonds initially appeared surprising and counterintuitive since both halogen atoms and halogen bond acceptors (Y) are electronegative and are typically viewed as being negatively charged.

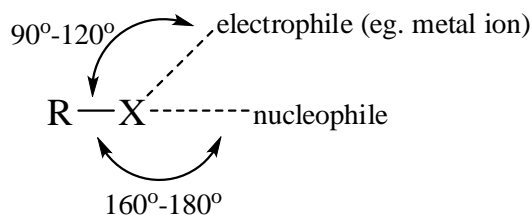


Figure 1.4 Directional tendencies of close contacts in crystalline halides.

Politzer and coworkers [Clark *et al.* 2007; Murray *et al.* 1994; Politzer *et al.* 2013] provided an advanced explanation of halogen bonding based on the concept of σ -hole. Molecular electrostatic potential studies by Brinck *et al.* showed that in $\text{H}_3\text{C}-\text{Br}$, CBr_4 and CCl_4 , the halogen atom have areas of positive electrostatic potential on the outer portion of their surfaces while the lateral sides of the halogen have negative potential [Brinck *et al.* 1992; Brinck *et al.* 1993]. This is because the half-filled p_z orbital of halogen participates in the covalent $\text{R}-\text{X}$ bond and this depletes the electron density in the outer lobe of the p_z orbital. The four p_x and p_y electrons create a belt of negative potential around the sides of the halogens thus permitting the interactions with electrophiles. Politzer *et al.* suggested the term ‘ σ -hole’ to denote this positive halogen surface region and suggested that halogen bond is an electrostatically-driven attractive interaction between a positive σ -hole on a covalently-bonded halogen atom and a negative site. The presence and magnitude of σ -hole depends on the halogen and the electron-withdrawing power of the remainder of the molecule. More electronegative halogens, F and Cl, attract enough electronic charge from the R portion of $\text{R}-\text{X}$ molecule and hence their σ -holes have a negative potential although less negative than the lateral sides of the halogen. Thus the halogen surfaces are entirely negative for H_3CF , H_3CCl and CF_4 . Molecular electrostatic potential plots of CF_4 , CF_3Cl and CF_3Br are shown in Figure 1.5 to demonstrate the concept of σ -hole. The fluorine hemispheres are negative for CF_4 . However when a chlorine or bromine is substituted, σ -hole develops on the

outermost portion of its surface, around its intersection with the C-Cl axis. The σ -hole on the bromine is progressively larger and more positive than chlorine.

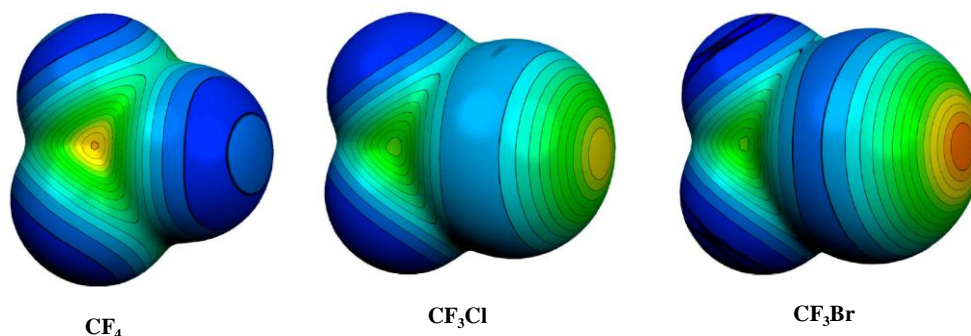



Figure 1.5 Molecular electrostatic potential at 0.001 au isodensity surface of CF_4 , CF_3Cl and CF_3Br showing σ -hole. Color coding,  blue -0.009 au to red 0.054 au. Figure adapted from [Clark *et al.* 2007].

It has been shown that covalently bonded atoms of Group IV, Group V and Group VI exhibit σ -hole interactions [Poltzer *et al.* 2013]. Frontera and coworkers [Bauzá *et al.* 2013] used tetrel bonding to refer to noncovalent interactions between electron donors and the group 14 elements, silicon, germanium and tin. Tetrel bonds have comparable strength to hydrogen bonds and other σ -hole-based interactions, are highly directional, and are expected to be valuable in crystal engineering, supramolecular chemistry, and catalysis.

Various theoretical and experimental studies have pointed out the intriguing similarities between halogen bonds and hydrogen bonds. Metrangolo and coworkers demonstrated the striking parallelism between the spectroscopic, energetic and geometric features of hydrogen bonds and halogen bonds [Metrangolo *et al.* 2005]. Quite recently it has been demonstrated that halogen bonded systems can also exhibit blue shifts as well as red shifts similar to hydrogen bonded systems [Murray *et al.* 2008; Wang *et al.* 2004]. Legon discussed the parallelism in detail and pointed out that the hydrogen bond is more likely to be nonlinear [Legon 1999; Legon 2008; Legon 2010]. Halogen bonds are found

to be more sensitive to steric hindrance due to the larger size and polarizability of halogens compared to hydrogen. Di Paolo and Sandorfy found that the infra-red bands due to solute-solvent hydrogen bonds can be significantly reduced by the introduction of a co-solute that can halogen bond with the solvent [Di Paolo and Sandorfy 1974]. Some compounds capable of co-crystalizing with both halogen bond donors and hydrogen bond donors will do so preferentially with the former [Corradi *et al.* 2000].

IUPAC recommendations 2013 [Desiraju *et al.* 2013] has proposed a definition for halogen bond which stated that “A halogen bond $R-X\dots Y-Z$ occurs when there is evidence of a net attractive interaction between an electrophilic region on a halogen atom X belonging to a molecule or a molecular fragment $R-X$ (where R can be another atom, including X, or a group of atoms) and a nucleophilic region of a molecule, or molecular fragment, $Y-Z$.” Some features useful as indications for the halogen bond, are also listed:

- a) The distance between the donor halogen atom X and the acceptor atom Y tends to be less than the sum of the van der Waals radii of X and Y.
- b) The angle $R-X\dots Y$ tends to be linear (180°) and the halogen atom X tends to align with the direction of the axis of the n -lone pair on Y or the π -bond electron pair in $Y-Z$.
- c) Halogen bond formation is usually accompanied by an increase in the length of the $R-X$ covalent bond.
- d) The strength of the halogen bond decreases with an increase in the electronegativity of X and/or decrease with the electron withdrawing ability of R.
- e) The forces involved in the formation of the halogen bond are primarily electrostatic (including polarization) and dispersion and the relative roles of the different forces may vary from one case to the other.
- f) The analysis of the electron density topology of halogen bond usually shows a bond critical point and a bond path connecting X and Y.

- g) Halogen bond formation is associated with the formation of new vibrational modes, changes in the IR, Raman absorptions and NMR signals of R-X and Y-Z and blue shifts in the UV visible spectrum of the halogen bond donor.
- h) The halogen atom X may participate in more than one halogen bond.
- i) The halogen bond may be involved in halogen transfer reactions or other reactive phenomena.

Different energy decomposition schemes have been employed to decompose the interaction energy of halogen bonds into their plausible components [Lommerse *et al.* 1996; Riley and Hobza 2008; Riley *et al.* 2009; Wang *et al.* 2007]. These studies have shown that there are five main energetic contributions to halogen bonding *viz.* electrostatic, polarization, dispersion, exchange-repulsion, and charge-transfer. The physical meaning of the contributions to the interaction energy is different for various schemes, with each scheme giving different weight for each component. Several studies have shown that electrostatic contribution is the major attractive contribution of halogen bonding interactions [Riley and Hobza 2008]. However, in a recent study Palusiak showed that the orbital interaction accounting for charge-transfer and the polarization are the most important factors responsible for the stability of halogen bonded complexes [Palusiak 2010]. Riley and Hobza pointed dispersion component has significant contribution to the total interaction energy of halogen bonds [Riley and Hobza 2008; Riley *et al.* 2013]. Politzer and coworkers provided strong evidence for the significance of electrostatic contribution from a detailed analysis of the nature of halogen bonds [Politzer *et al.* 2013]. They showed that the strength of halogen bond correlates with the positive potential of the halogen, for a given Lewis base involved in the halogen bond interaction. Using the natural energy decomposition analysis (NEDA) scheme of the interaction energy Grabowski showed that polarization is the most important

attractive term in the interaction energy with significant contributions from electrostatic and charge transfer terms [Grabowski 2013].

There is mounting evidence of the significance of halogen bonds in biological systems in ligand binding, recognition, conformational stabilization, molecular folding and drug design [Auffinger *et al.* 2004]. Auffinger *et al.* reported several interesting cases of halogen bonding in a survey of halogenated proteins and nucleic acids in the Protein Data Bank, including a strong interaction involving 5-bromouracil that stabilized a Holliday junction [Auffinger *et al.*, 2004]. Halogen bonds are found to direct ligand-protein binding, including the recognition of naturally iodinated thyroid hormones by their cognate proteins. Voth *et al.* reported that DNA junctions are stabilized more by halogen bonds than by hydrogen bonds [Carter *et al.* 2013; Voth *et al.* 2007]. Halogen bonding also finds potential applications in medicinal chemistry where halogen atoms are used as important inhibitors of proteins including those involved in carcinogenesis [Voth and Ho 2007]. The iodinated inhibitor designed to target the mitogen activated protein kinase (MEK) and a chlorinated inhibitor to the CDC2-like kinase isoform 1 (CDK1) reinforce the significance of halogen bonds in conferring specificity of inhibitors against protein kinases. Thus exploiting halogen bonding offers remarkable possibilities for the design and developments of new compounds and materials with probable applications in chemistry, biology and medicine [Politzer *et al.* 2010].

1.1.5 Lone Pair- π and Anion- π Interactions

Lone pair- π and anion- π interactions are two interaction types involving aromatic rings that have been added recently to the world of noncovalent interactions. Lone pair- π or anion- π interactions are defined as the favorable attractive interactions between the lone pairs of neutral molecules or anions and electron deficient π -electron systems of aromatic rings [Hernández-Trujillo and Vela 1996; Laidig 1991]. Schneider *et al.*

reported weak but attractive interactions between negative charges and polarizable aryl parts of host-guest systems in the early 1990s [Schnieder *et al.* 1993]. Pioneering theoretical investigations by Alkorta and coworkers in 1997 revealed the favorable nature of the interaction between π -cloud of hexafluorobenzene (C_6F_6) and several small electron-donor molecules (FH, HLi, $:CH_2^-$, HCN, and HNC) on the basis of their electron density and molecular electrostatic potential maps [Alkorta *et al.* 1997]. Gallivan and Dougherty in 1999 demonstrated the significant binding interaction between water and hexafluorobenzene in a geometry where in the oxygen lone pairs points directly into the face of the π -system and suggested that these interactions mainly arise due to attractive electrostatic forces [Gallivan and Dougherty 1999]. This was followed by numerous theoretical reports on lone pair and anion- π interactions [Alkorta *et al.* 2002; Mascali *et al.* 2002; Quiñonero *et al.* 2002a; Quiñonero *et al.* 2002b]. Figure 1.6 shows the lone pair- π and anion- π interactions in C_6F_6 -H₂O and C_6F_6 -Cl⁻ complexes.

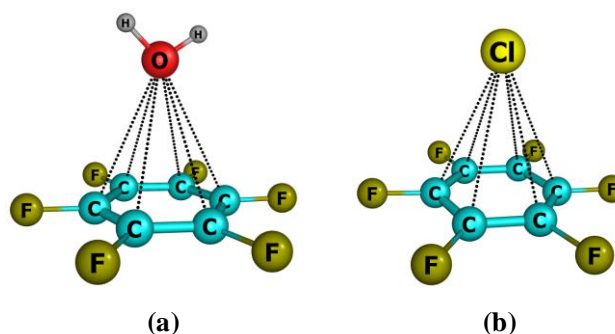


Figure 1.6 Lone pair- π and anion- π interactions. (a) Lone pair- π complex between hexafluorobenzene and water (b) Anion pair- π complex between hexafluorobenzene and chloride ion.

The first experimental proof for lone pair/anion- π interactions was provided independently in 2004 by Meyer *et al.* and Reedijk *et al.* [De Hoog *et al.* 2004; Demeshko *et al.* 2004]. Meyer *et al.* reported the attractive interaction between chloride ions and triazine in the large electron deficient ligand hexakis(pyridine-2-yl)-[1,3,5]-

triazine-2-4-6-triamine (L1), complexed with Cu(II) chloride to afford $[(L1)_2(CuCl)_3][CuCl_4][Cl]$. One of the $[Cl]^-$ counter ion establish an anion- π interaction with a triazine ring of L1 (Figure 1.7). The contact distance and angle of the anion to the ring centroid (3.11 Å and 88° respectively) are close to the theoretically predicted values by Mascal *et al.* [Mascal *et al.* 2002] and Deya *et al.* [Quiñonero *et al.* 2002b].

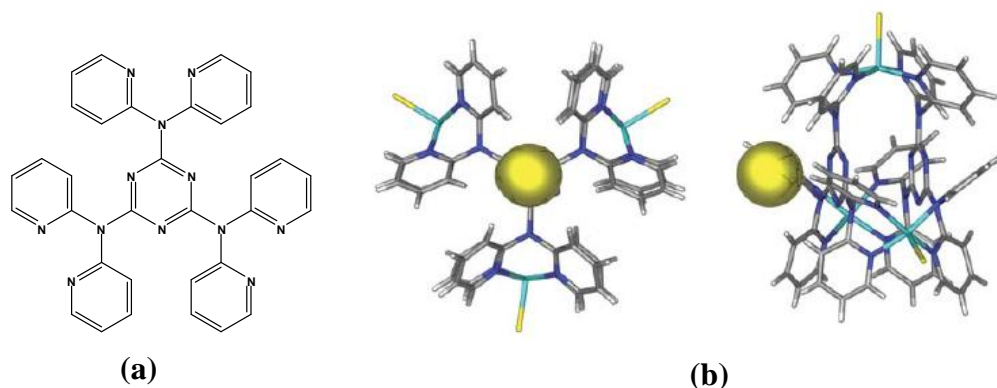


Figure 1.7 Anion- π interaction reported by Meyer and coworkers. (a) Schematic drawing of hexakis(pyridine-2-yl)-[1,3,5]-triazine-2-4-6-triamine (L1); (b) Front view and side view of $\{[(L1)_2(CuCl)_3][Cl]\}^{2+}$. Atom colors: C = grey, H = white, N = dark blue, Cu = light blue and Cl = yellow. Figure adapted from [Demeshko *et al.*, 2004].

Reedijk and coworkers demonstrated the attractive interactions between Cl^- and pyridine in a remarkable supramolecular system involving the dendritic octadentate ligand N,N',N'',N''' -tetrakis{2,4-bis(di-2-pyridylamino)-1,3,5-triazinyl}-1,4,8,11-tetraazacyclotetradecane (L2) coordinated to Cu(II) chloride to afford the ternuclear complex $[Cu_4(L2)Cl_4][Cl]_4(H_2O)_{13}$ (Figure 1.8). This complex has 16 pyridinyl rings of L2 coordinated to four different Cu(II) ions and two Cl^- ions are encapsulated in two different cavities formed by pyridinyl rings through anion- π interactions. This study prompted Reedijk *et al.* to design new triazine-based ligands and relevant systems with anion- π interactions [De Hoog *et al.* 2004].

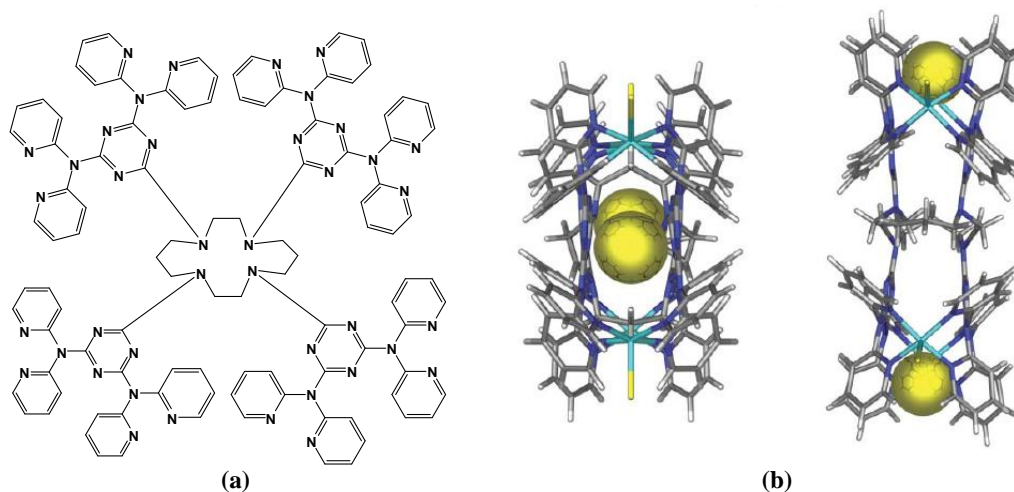


Figure 1.8 Anion- π interaction reported by Reedijk and coworkers. (a) Schematic drawing of N,N',N'',N''' -tetrakis{2,4-bis(di-2-pyridylamino)-1,3,5-triazinyl}-1,4,8,11-tetraazacyclotetradecane (L2), (b) Crystal structure of $[Cu_4(L2)Cl_4][Cl]_4(H_2O)_{13}$ from two different views. Atom colors: C = grey, H = white, N = dark blue, Cu = light blue and Cl = yellow. Figure adapted from [De Hoog *et al.*, 2004].

Reedijk and coworkers carried out a comprehensive examination of CSD and reported that anion- π contacts are quite common supramolecular bonding interactions in solid-state structures [Mooibroek *et al.* 2008]. Markedly different conclusions were drawn by Hay and Custelcean in 2009 after an exhaustive statistical analysis of anion-arene contacts in the CSD and they concluded that genuine examples of anion- π interactions with uncharged arenes are extremely rare in crystal structures [Hay and Bryantsev 2008]. CSD analyses [Hay and Custelcean 2009], spectroscopic studies [Chiavarino *et al.* 2009; Schneider *et al.* 2007] and several *ab initio* calculations [Berryman *et al.* 2007; Hay and Bryantsev 2008; Mascal *et al.* 2002] have revealed that in complexes of anions with neutral six-member aromatic rings the anion is likely to engage in aryl C-H hydrogen bonding interactions than anion- π interactions. Deyà and coworkers studied anion- π , anion- π_2 and anion- π_3 complexes of 1,3,5-triazine and trifluoro-1,3,5-triazine with Br^- and Cl^- ions using *ab initio*

calculations and demonstrated the additivity in both binding energies and geometries of anion- π interactions (Figure 1.9) [Garau *et al.* 2005]. The synergetic effect of anion- π , cation- π and π - π interactions has been demonstrated by Deyà and coworkers by means of high level *ab initio* calculations coupled with “atoms in molecules” theory and molecular interaction potential with polarization (MIPp) method [Garau *et al.* 2006].

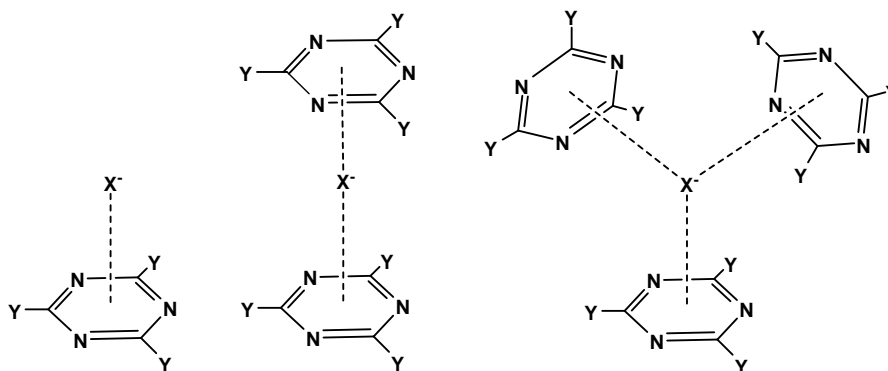


Figure 1.9 Anion- π complexes of 1,3,5-triazine and trifluoro-1,3,5-triazine with multiple anion- π interactions per anion. ($X = \text{Br}^-$ or Cl^- and $Y = \text{H}$ or F).

Elegant studies by Deyà and coworkers revealed that anion- π interactions are dominated by electrostatic and anion induced polarization contributions [Garau *et al.* 2003a; Quiñero *et al.* 2002b]. Topological analysis of electron density in anion- π interactions show that strong correlation exists between the permanent quadrupole moment, Q_{zz} of the electron deficient aromatic ring and the electrostatic component of the interaction energy [Garau *et al.* 2003a]. It has been shown that anion-induced polarization correlates with the molecular polarizability of the aromatic compound. Molecules with small magnitudes of Q_{zz} can exhibit a dual behavior by binding both cations and anions [Garau *et al.* 2004]. Garau *et al.* established that even non-electron deficient aromatic rings are capable of exhibiting anion- π interactions if the ring is interacting simultaneously with a cation on the opposite face of the ring [Garau *et al.* 2003b]. Symmetry adapted perturbation theory (SAPT) studies by Kim and coworkers on

anion- π complexes revealed that the major attractive contributions to the total interaction energy are due to electrostatic and induction energies [Garau *et al.* 2004; Kim *et al.* 2004]. They also showed that total interaction energy has significant contributions from dispersion and exchange-repulsion energies.

Egli and coworkers provided crystallographic evidence for the stabilizing influence of sugar O4' lone pair- π (nucleobase) intramolecular interactions in DNA [Berger and Egli 1997; Berger *et al.* 1996; Egli and Gessner 1995]. They also reported the role of attractive lone pair- π interactions in the conformational stability of Z-DNA at high ionic strength despite poor base pair stacking. A high-resolution X-ray structure analysis showed the existence of lone pair- π interactions between water molecules and functionally important unstacked residues in the 1.25 Å crystal structure of the ribosomal frameshifting RNA pseudoknot from beet western yellow virus [Sarkhel *et al.*, 2003]. Sankararamkrishnan and coworkers systematically analyzed 500 high-resolution protein structures and identified 286 examples which show $\pi\dots\pi$ and/or lone-pair- π interactions indicating that such interactions could stabilize secondary structures of proteins [Jain *et al.* 2007]. The presence of relevant anion- π interactions in the active site of the urate oxidase enzyme has been reported by Deyà and coworkers [Estarellas *et al.* 2011].

Anion/lone pair- π interactions holds great promise for the design of colorimetric sensors, selective anion receptors, hosts or scaffolds and catalysts of chemical and biological significance [Chifotides and Dunbar 2013]. Matile *et al.* reported synthesis and of an unprecedented synthetic ion channel based on π -acidic oligo-(para-phenylene)-N,N-naphthalenediimide (O-NDI) rods as transmembrane chloride π -slides and showed that the gradient of electron deficiency in these oligomers can be exploited to transfer anions through membranes [Matile and Mareda 2009]. The N,N-naphthalenediimide

(NDI) building unit exhibits an electron deficient character at the center of the molecule (Figure 1.10).

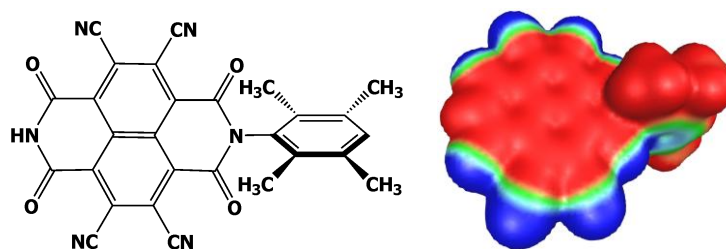



Figure 1.10 N,N-naphthalenediimide unit and its DFT computed electrostatic potential map demonstrating the electron deficient character. Color coding,  blue -0.02 au to red 0.02 au. Figure adapted from [Mohan *et al.* 2013].

Wang and coworkers demonstrated that the anion- π interaction motifs can be used in the design of receptors for ion pair recognition by synthesizing oxacalix[2]arene[2]triazine azacrown based dipotic receptor molecules that binds to ion pairs through anion- π interactions [Chen *et al.* 2011]. Experimental and theoretical calculations by Matile and coworkers showed that anion- π interactions can contribute to catalysis [Zhao *et al.* 2014]. They showed that the stabilization of anionic transition states in Kemp elimination increases with the π -acidity of the catalysts.

With the development of experimental and theoretical techniques, the realm of weak noncovalent interactions is expanding continuously with many non-conventional interactions being reported and analyzed.

Part B – Computational Chemistry

“Everything that living things do can be understood in terms of the jiggling and wiggling of atoms.” Richard Feynman, 1963

1.2 An Overview of Computational Chemistry

Computational chemistry or molecular modeling encompasses quantum mechanics, molecular mechanics, simulations, conformational analysis and other computer-based methods for understanding and predicting the behavior of molecular systems. Quantum chemistry is a branch of computational chemistry that attempts to explain the chemical phenomena through a computational solution of the basic equations of quantum mechanics. The theoretical basis for this field of chemistry embodies many of the important scientific discoveries made in the late 19th century and in the first part of the 20th century by Michael Faraday, Gustav Kirchoff, Ludwig Boltzman, Albert Einstein, Max Plank, Neils Bohr, Erwin Schrödinger and others [Cramer 2004]. Computational chemistry methods range from highly accurate ones feasible only for small systems to very approximate methods for larger systems. Depending on the formalism, these methods can be broadly classified into (a) Molecular mechanics (b) *ab initio* quantum chemical methods (c) semi-empirical quantum chemical methods (d) the density functional methods (e) molecular dynamics and Monte Carlo simulations and (f) hybrid quantum mechanics/molecular mechanics (QM/MM) methods. All these methods use different approximations to produce results of varying levels of accuracy. Except *ab initio* quantum chemical methods, all others rely on empirical information (parameters, energy levels etc.).

The molecular mechanics (MM) or force field methods [Bowen and Allinger 1991; Boyd and Lipkowitz 1982; Dinur and Hagler 1991; Weiner and Kollman 1981] use

the laws of classical physics and calculate the energy of a system as a function of the nuclear coordinates alone ignoring the electronic motions. MM calculations are based upon on a rather simple mathematical model of the system as a collection of balls (corresponding to the atoms) held together by springs (corresponding to the bonds). The energy of a molecule is expressed as a function of its resistance towards bond stretching, bond bending, and atom crowding and this energy equation is used to find the bond lengths, angles, and dihedrals corresponding to the minimum energy geometry. MM methods can invariably be used to perform calculations on systems containing significant number of atoms and, in some cases, provide answers that are as accurate as even the highest level quantum mechanical calculation in a fraction of the computer time, provided that the forcefield is carefully parameterized for the molecules studied. MM methods however, cannot throw light on electronic properties like charge distributions, nucleophilic and electrophilic behavior of molecules, electronic spectra etc.

Semi-empirical quantum mechanical methods [Pople and Beveridge 1970; Stewart 1990] are also based on Schrödinger equation and they represent a middle road between the mostly qualitative results from molecular mechanics and the highly computationally demanding quantitative results from *ab initio* methods. These methods are logically regarded as simplifications of the *ab initio* method since they use parameterizations and approximations from experimental data to provide input into mathematical models. Semi-empirical calculations are relatively inexpensive and much faster, often only with an inconsequential loss of accuracy and are generally applicable to very large molecular systems.

Computer simulations act as a bridge between microscopic length and time scales and the macroscopic world of the laboratory. Molecular dynamics (MD) and Monte Carlo (MC) methods are the two main families of simulation techniques widely employed in computational chemistry. MD methods use Newton's laws of motion to

examine the time-dependent behavior of systems, including vibrations or Brownian motion, using a classical mechanical description [Rapaport 2004; Schlick 2002]. ‘Monte Carlo’ is almost always used to refer methods that use importance sampling, a technique that generates states of low energy. MC simulation generates configurations of a system by making random changes to the positions of the species present, together with their orientations and conformations where appropriate [Doll and Freeman 1994]. MD simulations are required if one wishes to calculate time-dependent quantities while, MC methods are often appropriate to investigate systems in certain ensembles.

The hybrid QM/MM approach combines the strength of both QM (accuracy) and MM (speed) calculations, are generally applicable for the calculation of ground and excited state properties like molecular energies and structures, energies and structures of transition states, atomic charges, reaction pathways etc. [Senn and Thiel 2009]. The basic idea of QM/MM methods is to partition the system into two (or more) parts. The region of chemical interest is treated using accurate QM methods while the rest of the system is treated using MM or less accurate QM methods such as semi-empirical methods or a combination of the two. *Ab initio* quantum chemical methods and density functional methods are discussed in detail in the forthcoming section.

1.2.1 *Ab initio* Molecular Orbital Theory

The electronic structure theory aims at solving the time-independent, non-relativistic Schrödinger equation [Schrödinger 1926], which in its simplest form is

$$H\Psi = E\Psi \quad (\text{Eq. 1.7})$$

where H is the Hamiltonian operator, Ψ is the N -body wave function and E is the energy eigenvalue of the system. The Hamiltonian operator for a system of N electrons and M nuclei comprises of the nuclear and electronic kinetic energy operators and the potential energy operators corresponding to the nuclear-nuclear, nuclear-electron and electron-

electron interactions and may be written in atomic unit as:

$$H = -\sum_{i=1}^N \frac{1}{2} \nabla_i^2 - \sum_{A=1}^M \frac{1}{2M_A} \nabla_A^2 - \sum_{i=1}^N \sum_{A=1}^M \frac{Z_A}{r_{iA}} + \sum_{i=1}^N \sum_{j>i}^N \frac{1}{r_{ij}} + \sum_{A=1}^M \sum_{B>A}^M \frac{Z_A Z_B}{R_{AB}} \quad (\text{Eq. 1.8})$$

where \mathbf{R}_A and \mathbf{r}_i are the position vectors of nuclei and electrons. The distance between the i^{th} electron and A^{th} nucleus is r_{iA} ; the distance between i^{th} and j^{th} electron is r_{ij} and the distance between the A^{th} nucleus and B^{th} nucleus is R_{AB} . M_A is the ratio of the mass of the nucleus A to the mass of an electron and Z_A is the atomic number of nucleus A.

The Schrödinger equation cannot be solved exactly for any molecular systems and hence some approximations are introduced for its practical applications. A common and very reasonable approximation used is the Born Oppenheimer (BO) approximation [Born and Oppenheimer 1927] which enables the electronic and nuclear motions to be separated. BO approximation is based on the concept that the nuclear and electronic motions take place at different time scales, the latter being much smaller than the former. Thus, an electron in motion sees relatively static nuclei, while a moving nucleus feels averaged electronic motion. The electronic wave function thus depends only on the positions of the nuclei and not on their momenta. Under the BO approximation the electronic Hamiltonian (Eq. 1.8) may be written as

$$H_{\text{elec}} = -\sum_{i=1}^N \frac{1}{2} \nabla_i^2 - \sum_{i=1}^N \sum_{A=1}^M \frac{Z_A}{r_{iA}} + \sum_{i=1}^N \sum_{j>i}^N \frac{1}{r_{ij}} \quad (\text{Eq. 1.9})$$

The first term is the electronic kinetic energy operator summed over the number of electrons, N. The second term represents Coulombic attraction between N electrons and M nuclei, while Z_A are the nuclear charges. The last term attributes to the Coulombic repulsion between electrons. The eigenvalue equation involving the electronic Hamiltonian is then written as

$$H_{\text{elec}} \Phi_{\text{elec}}(\{\mathbf{r}_i\}; \{\mathbf{R}_A\}) = E_{\text{elec}} \Phi_{\text{elec}}(\{\mathbf{r}_i\}; \{\mathbf{R}_A\}) \quad (\text{Eq. 1.10})$$

where $\{\mathbf{r}_i\}$ and $\{\mathbf{R}_A\}$ are the positions of electrons and nuclei, respectively. The solution to Eq. 1.10 gives the electronic wave function (Eq. 1.11) which describes the motion of electrons and depends explicitly on the electronic coordinates and parametrically on the nuclear coordinates.

$$\Phi(\{\mathbf{r}_i\};\{\mathbf{R}_A\}) = \Phi_{\text{elec}}(\{\mathbf{r}_i\};\{\mathbf{R}_A\})\Phi_{\text{nuc}}(\{\mathbf{R}_A\}) \quad (\text{Eq. 1.11})$$

All properties can be calculated from the wave function, once the equations are solved as the expectation value of appropriate operator, $\langle \Psi | \mathcal{O} | \Psi \rangle$. An exact solution to the Schrödinger equation is not possible for any but the most trivial molecular systems and hence simplifying approximations are needed to get qualitatively correct solutions to the many body Schrödinger equation.

1.2.2 Hartree-Fock Theory

Hartree-Fock (HF) theory (also known as independent particle model or a mean field theory) [Fock 1930; Hartree 1928; Slater 1930] is an approximate method for solving the Schrödinger equation which posits that each electron's motion can be described by a single-particle function (orbital) which does not depend explicitly on the instantaneous motions of other electrons. In the HF approach, the N-electron wave function for a given state is written as a Slater determinant, an anti-symmetrized product of spin orbitals.

$$\Psi(\mathbf{x}_1, \mathbf{x}_2, \dots, \mathbf{x}_N) = \frac{1}{\sqrt{N!}} \begin{vmatrix} \chi_i(\mathbf{x}_1) & \chi_j(\mathbf{x}_1) & \dots & \chi_N(\mathbf{x}_1) \\ \chi_i(\mathbf{x}_2) & \chi_j(\mathbf{x}_2) & \dots & \chi_N(\mathbf{x}_2) \\ \cdot & \cdot & \dots & \cdot \\ \chi_i(\mathbf{x}_N) & \chi_j(\mathbf{x}_N) & \dots & \chi_N(\mathbf{x}_N) \end{vmatrix} \quad (\text{Eq. 1.12})$$

The factor $1/\sqrt{N!}$ is a normalization factor. The spin orbitals are denoted as χ 's, while \mathbf{x}_1 , \mathbf{x}_2 , etc. represent the combined spatial and spin coordinates of the respective electrons. An interesting consequence of this functional form is that the electrons are all

indistinguishable. The normalized Slater determinant can also be represented in a shorter notation as:

$$\Psi(\mathbf{x}_1, \mathbf{x}_2, \dots, \mathbf{x}_N) = |\chi_i \chi_j \dots \chi_k\rangle \quad (\text{Eq. 1.13})$$

In this notation it is presumed that electrons 1, 2, etc. sequentially occupy the spin orbitals.

In the HF method, the determinantal wave function is used to approximate the exact wave function and the energy is calculated as an expectation value of the Hamiltonian over this approximate wave function. The orbitals are found using the variational principle by minimization of the energy expectation value. Thus, the best approximate wave function can be obtained by varying all the wave function parameters, until the energy expectation value of the approximate wave function is minimized. The application of this minimizing procedure leads to the HF equations for the individual spin orbitals. HF equation is an eigenvalue equation of the form:

$$f(i)\chi(\mathbf{x}_i) = \epsilon\chi(\mathbf{x}_i) \quad (\text{Eq. 1.14})$$

where $f(i)$ is an effective one-electron operator, called the Fock operator, of the form:

$$f(i) = -\frac{1}{2}\nabla_i^2 - \sum_{A=1}^M \frac{Z_A}{r_{iA}} + V^{\text{HF}}(i) \quad (\text{Eq. 1.15})$$

where $V^{\text{HF}}(i)$ is the HF potential which is the average potential experienced by the i^{th} electron due to the presence of other electrons. Thus, the HF approximation replaces the complicated many-electron problem by a one-electron problem in which electron-electron repulsion is treated in an average way. The HF potential $V^{\text{HF}}(i)$ depends on the spin orbitals of other electrons. The solution of HF eigenvalue problem yields a set $\{\chi_k\}$ of orthonormal HF spin orbitals with orbital energies $\{\epsilon_k\}$. The N spin orbitals with the lowest energies are called the occupied orbitals and the remaining members of the set

$\{\chi_k\}$ are called virtual or unoccupied orbitals. The HF potential for the electron (1) is defined as:

$$V^{\text{HF}}(1) = \sum_j^N (J_j(1) - K_j(1)) \quad (\text{Eq. 1.16})$$

where J_j and K_j are the classical Coulomb and the exchange operators, respectively. The Coulomb operator takes into account the Coulombic repulsion between electrons, and the exchange operator represents the quantum correlation due to the Pauli exclusion principle.

$$\text{Coulomb operator, } J_j(1) = \int \chi_j(2) \frac{1}{r_{12}} \chi_j(2) d\mathbf{x}_2 \quad (\text{Eq. 1.17})$$

The exchange operator can only be written through its effect when operating on a spin orbital $\chi_i(1)$,

$$K_j(1)\chi_i(1) = \left[\int \chi_j(2) \frac{1}{r_{12}} \chi_i(2) d\mathbf{x}_2 \right] \chi_j(1) \quad (\text{Eq. 1.18})$$

Derivation of the HF equations for the closed shell systems was proposed by Roothaan and Hall [Hall 1951; Roothaan 1951]. The HF equation Eq. 1.14 may be rewritten by substituting Eq. 1.19, where the spin orbital is expressed as the linear combination of basis functions, leading to Eq. 1.20

$$\Psi_i = \sum_{\mu=1}^K C_{\mu i} \phi_{\mu} \quad i = 1, 2, \dots, K \quad (\text{Eq. 1.19})$$

where ϕ_{μ} are the basis functions corresponding to atomic orbitals, $C_{\mu i}$ are the coefficients of ϕ_{μ} and K is the total number of basis functions. Roothaan Hall equation is written as a single matrix equation,

$$\mathbf{FC} = \mathbf{SC}\epsilon \quad (\text{Eq. 1.20})$$

where ϵ are orbital energies, S is the overlap matrix and F is the Fock matrix. The Fock matrix F is the matrix representation of the Fock operator (Eq. 1.15) in the basis ϕ_μ . The Fock matrix must be diagonalized to find out the unknown molecular orbital coefficients in order to determine the eigenvalues from Roothaan Hall equation (Eq. 1.20).

The HF equation is non-linear and is solved iteratively using a procedure called self-consistent field (SCF) method in which a trial set of spin orbitals are guessed and used to construct the Fock operator. The new set of spin orbitals obtained from the solution is used to obtain a revised Fock operator, and this cycle of calculation and reformulation is repeated until the convergence criterion is satisfied. The one-electron nature of Fock operator results certain limitations to HF theory constructed using the Roothaan approach since all electron correlation is ignored other than exchange. The correlation energy is typically a small fraction of the total energy. However, it can be a very important contribution to many systems of physical and chemical interest. Further, the choice of basis set was challenging to early computational chemists. Even though the LCAO approach using hydrogenic orbitals remains attractive, this basis set requires numerical solution of the four index integrals appearing in the Fock matrix elements which is a tedious process. Since each index runs over the total number of basis functions, there are in principle N^4 total integrals to be evaluated, and this quartic scaling behavior with respect to basis set size proves to be a bottleneck in HF theory applied to essentially any molecules.

1.2.3 Electron Correlation Methods

Electron correlation methods or Post Hartree-Fock methods are a set of methods which go beyond SCF in attempting to add electron correlation in a more accurate way. Most of these methods require more flexible wave functions than that of a single determinant HF and usually it is obtained by means of excitations of electrons from

occupied to virtual orbitals. The energy contribution resulting from the correlated motion of electrons is usually denoted as the correlation energy [Boys 1950] and is defined as the difference between the exact energy and the energy obtained by the HF method *i.e.*,

$$E_{\text{corr}} = \varepsilon_0 - E_0 \quad (\text{Eq. 1.21})$$

where, ε_0 is the exact eigenvalue of H_{elec} and E_0 the “best” HF energy with the basis set extrapolated to completeness. The popular approaches that try to compute E_{corr} are the configuration interaction (CI) [Foresman *et al.* 1992; Pople *et al.* 1976], coupled cluster (CC) [Cramer 2004; Kümmel 2002], and many body perturbation theory (MBPT) [Brillouin 1934; Kelly 1969] methods.

1.2.3.1 Configuration Interaction

The most simple and easiest method to incorporate electron correlation effect into an *ab initio* molecular orbital calculation is the configuration interaction (CI). In CI, the electronic state is described with excited states which are constructed by replacing one or more occupied orbitals with a virtual orbital within the HF determinant. In general, CI wave function can be written as:

$$|\Phi\rangle = c_0|\Psi_0\rangle + \sum_{ar} c_a^r |\Psi_a^r\rangle + \sum_{\substack{a<b \\ r<s}} c_{ab}^{rs} |\Psi_{ab}^{rs}\rangle + \sum_{\substack{a<b<c \\ r<s<t}} c_{abc}^{rst} |\Psi_{abc}^{rst}\rangle + \dots \quad (\text{Eq. 1.22})$$

The first term in Eq. (1.22) represents the Slater determinant corresponding to the HF wave function and rest of the terms constitute singly, doubly, triply, ... , n-tuply excited determinants with appropriate expansion coefficients. The indices a , b , etc. signify the occupied orbitals and r , s , etc. signify the virtual orbitals involved in the electron excitations. The energy of the system is then minimized in order to determine the coefficients using linear variation approach. The number of excitations used to construct each determinant classifies the CI calculations. If only one electron has been moved from each determinant, it is called a configuration interaction single-excitation (CIS)

calculation. The CIS calculation gives an approximation to the excited states of a molecule, but do not change its ground-state energy. Single-and double excitation (CISD) calculations yield a ground-state energy that has been corrected for correlation. Triple-excitation (CISDT) and quadruple-excitation (CISDTQ) calculations are done only when very high accuracy results are desired. The configuration interaction calculation with all possible excitations is called a full CI. Full CI is important because it is the most complete possible estimation of electron correlation within the limitations imposed by the basis set. In the limit of a complete basis set full CI becomes complete CI, but is generally impractical. Truncated CI (CISD etc.) can be used as a simplification; however these methods are not size-consistent.

1.2.3.2 Coupled Cluster Methods

The coupled cluster (CC) method [Čížek 1966] introduced by Čížek and Pauldus in the 1960's is among the most robust levels of theory that can describe dynamic electron correlation. It essentially takes the basic HF molecular orbital method and constructs multi-electron wave functions using the exponential cluster operator to account for electron correlation. The CC method assumes the full CI wave function,

$$\Psi_{CC} = e^T \Psi_{HF} \quad (\text{Eq. 1.23})$$

Ψ_{HF} is a Slater determinant constructed from HF molecular orbitals and

$$e^T = 1 + T + \frac{1}{2}T^2 + \frac{1}{6}T^3 + \dots = \sum_{k=0}^{\infty} \frac{1}{k!} T^k \quad (\text{Eq. 1.24})$$

T is known as cluster operator which when acting on Ψ_{HF} produces a linear combination of excited slater determinants and can be given as

$$T = T_1 + T_2 + T_3 + \dots + T_n \quad (\text{Eq. 1.25})$$

where n is the total number of electrons and various T_i operators generate all possible determinants having i^{th} excitation from the reference.

$$T_2 = \sum_{i < j}^{\text{occ.}} \sum_{a < b}^{\text{vir.}} t_{ij}^{ab} \Psi_{ij}^{ab} \quad (\text{Eq. 1.26})$$

where the amplitudes t are determined by the constraint that (Eq. 1.23) be satisfied.

When considering the double excitation $T = T_2$ and the Taylor expansion of the exponential function in (Eq. 1.23) gives

$$\Psi_{\text{CCD}} = \left(1 + T_2 + \frac{1}{2!} T_2^2 + \frac{1}{3!} T_2^3 + \dots \right) \Psi_{\text{HF}} \quad (\text{Eq. 1.27})$$

where CCD implies coupled cluster with only the double excitation operator. The first two terms in parenthesis ($1 + T_2$) defines the configuration double excitation method and the remaining terms involve the product of excitation operators. Solving for the unknown coefficients t_{ij}^{ab} is necessary for finding the approximate solution $|\Psi_{\text{CC}}\rangle$. The coupled cluster correlation energy is determined completely by the singles and doubles coefficients and the two electron MO integrals. The cost of including single excitations (T_1) in addition to doubles defines CC singles-doubles (CCSD) model. Inclusion of connected triple excitations arising with their amplitudes from T_3 defines CCSDT and if the singles/triples coupling term is included then it is called CCSD(T). Coupled cluster calculations are size extensive but not variational. By including many excitation terms in the expansion, CC methods are computationally very expensive relative to HF calculations. Formally, CCSD scales as N^6 , CCSDT scales as N^8 and CCSD(T) scales as N^7 .

1.2.3.3 Many-Body Perturbation Theory

Møller and Plesset proposed an alternative way to tackle the problem of electron correlation based on Rayleigh-Schrödinger perturbation theory [Bartlett and Silver 1975; Krishnan and Pople 1978] in which the ‘true’ Hamiltonian operator H is expressed as the sum of a ‘zeroth order’ Hamiltonian H_0 and a perturbation U :

$$H = H_0 + \lambda U \quad (\text{Eq. 1.28})$$

The eigenfunctions of the ‘true’ Hamiltonian operator are ψ_i , with the corresponding energies E_i . The eigenfunctions of the zeroth-order Hamiltonian are written $\psi_i^{(0)}$ with energies $E_i^{(0)}$. The ground-state wave function is thus $\psi_0^{(0)}$ with energy $E_0^{(0)}$. λ is a parameter that can vary between 0 and 1; when λ is zero then H is equal to the zeroth-order Hamiltonian but when λ is one then H equals its true value. The eigenfunctions ψ_i and eigenvalues E_i of H are then expressed in powers of λ :

$$\psi_i = \psi_i^{(0)} + \lambda \psi_i^{(1)} + \lambda^2 \psi_i^{(2)} \dots = \sum_{n=0} \lambda^n \psi_i^{(n)} \quad (\text{Eq. 1.29})$$

$$E_i = E_i^{(0)} + \lambda E_i^{(1)} + \lambda^2 E_i^{(2)} + \dots = \sum_{n=0} \lambda^n E_i^{(n)} \quad (\text{Eq. 1.30})$$

$E_i^{(1)}$ is the first-order correction to the energy, $E_i^{(2)}$ is the second-order correction and so on. These energies can be calculated from the eigenfunctions as follows:

$$E_i^{(0)} = \int \psi_i^{(0)} H_0 \psi_i^{(0)} d\tau \quad (\text{Eq. 1.31})$$

$$E_i^{(1)} = \int \psi_i^{(0)} U \psi_i^{(0)} d\tau \quad (\text{Eq. 1.32})$$

$$E_i^{(2)} = \int \psi_i^{(0)} U \psi_i^{(1)} d\tau \quad (\text{Eq. 1.33})$$

$$E_i^{(3)} = \int \psi_i^{(0)} U \psi_i^{(2)} d\tau \quad (\text{Eq. 1.34})$$

To determine the corrections to the energy, it is necessary to determine the wave functions to a given order. In Møller-Plesset perturbation theory [Møller and Plesset 1934] the unperturbed Hamiltonian H_0 is the sum of the one-electron Fock operator for the N electrons.

$$H_0 = \sum_{i=1}^N f_i = \sum_{i=1}^N \left(H^{\text{core}} + \sum_{j=1}^N (J_i + K_i) \right) \quad (\text{Eq. 1.35})$$

The zeroth-order energy is the sum of orbital energies for the occupied molecular orbitals.

$$E_0^{(0)} = \sum_{i=1}^{\text{occupied}} \varepsilon_i \quad (\text{Eq. 1.36})$$

In order to calculate higher order wave functions, the form of the perturbation, U is established as the difference between the ‘real’ Hamiltonian, H and the zeroth-order Hamiltonian, H_0 . The true Hamiltonian is equal to the sum of the nuclear attraction terms and electron repulsion terms:

$$H = \sum_{i=1}^N (H^{\text{core}}) + \sum_{i=1}^N \sum_{j=i+1}^N \frac{1}{r_{ij}} \quad (\text{Eq. 1.37})$$

Hence the perturbation U is given by:

$$U = \sum_{i=1}^N \sum_{j=i+1}^N \frac{1}{r_{ij}} - \sum_{j=1}^N (J_j + K_j) \quad (\text{Eq. 1.38})$$

The first-order energy $E_0^{(1)}$ is given by:

$$E_0^{(1)} = -\frac{1}{2} \sum_{i=1}^N \sum_{j=1}^N \frac{1}{r_{ij}} [(\text{ii} | \text{jj}) - (\text{ij} | \text{ij})] \quad (\text{Eq. 1.39})$$

The sum of the zeroth-order and first-order energies corresponds to the HF energy,

$$E_0^{(0)} + E_0^{(1)} = \sum_{i=1}^N \varepsilon_i - \frac{1}{2} \sum_{i=1}^N \sum_{j=1}^N [(\text{ii} | \text{jj}) - (\text{ij} | \text{ij})] \quad (\text{Eq. 1.40})$$

To obtain an improvement on the HF energy it is necessary to use Møller-Plesset perturbation theory to at least second order. This level of theory is referred to as MP2 and

involves the integral $\int \psi_0^{(0)} U \psi_0^{(1)} dt$

The higher order wave function $\psi_0^{(1)}$ is expressed as linear combinations of solutions to the zeroth-order Hamiltonian:

$$\psi_0^{(1)} = \sum_j c_j^{(1)} \psi_j^{(0)} \quad (\text{Eq. 1.41})$$

The $\psi_j^{(0)}$ in Eq. 1.41 include single, double etc. excitations obtained by promoting electrons into virtual orbitals obtained from a HF calculation. The second order energy is given by:

$$E_0^{(2)} = \sum_i^{\text{occupied}} \sum_{j>i}^{\text{virtual}} \frac{\iint d\tau_1 d\tau_2 \chi_i(1) \chi_j(2) \left(\frac{1}{r_{12}} \right) [\chi_a(1) \chi_b(2) - \chi_b(1) \chi_a(2)]}{\epsilon_a + \epsilon_b - \epsilon_i - \epsilon_j} \quad (\text{Eq. 1.42})$$

These integrals will be non-zero only for double excitations, according to the Brillouin theorem [Brillouin 1934]. Third- and fourth-order Møller-Plesset calculations (MP3 and MP4) are also available. The advantage of many-body perturbation theory is that it is size-independent, unlike CI. However, Møller-Plesset perturbation theory is not variational and can sometimes give energies that are lower than the ‘true’ energy. Møller-Plesset calculations are computationally intensive, yet the most popular way to incorporate electron correlation in molecular quantum mechanical calculations.

1.2.4 Density Functional Theory

The foundations of density functional theory (DFT) date from the 1920s with the work of Thomas and Fermi [Fermi 1927; Fermi 1928; Thomas 1927], but it was after the work of Hohenberg, Kohn, and Sham [Hohenberg and Kohn 1964; Kohn and Sham 1965] in the 1960s that the widespread application of DFT became a reality. In contrast to Hartree-Fock theory, DFT is based on electron density, rather than on wave functions. DFT is built around the premise that the energy of an electronic system can be defined in terms of its electron probability density, $\rho(\mathbf{r})$. An important advantage of using the $\rho(\mathbf{r})$ over the wave function is the much reduced dimensionality. Regardless of how many electrons one has in the system, the density is always 3 dimensional whereas, the wave function for an N-electron system is a function of 3N spatial co-ordinates. This enables DFT to readily be applied to much larger systems with hundreds or even thousands of atoms. According to DFT formalism, the electronic energy, E is regarded as a functional

of the electron density, $E[\rho(\mathbf{r})]$, in the sense that the given function $\rho(\mathbf{r})$ corresponds a single energy, *i.e.*, a one-to-one correspondence exists between the electron density of a system and its energy.

$\rho(\mathbf{r})$ is defined as

$$\rho(\mathbf{r}) = N \int \dots \int |\Psi(x_1, x_2, \dots, x_N)|^2 d\sigma_1 d\sigma_2 \dots dx_N \quad (\text{Eq. 1.43})$$

where $\{x_i\}$ represents both spatial and spin coordinates. $\rho(\mathbf{r})$ determines the probability of finding any of the N electrons within the volume \mathbf{r} but with arbitrary spin while the other $N-1$ electrons have arbitrary positions and spin in the state represented by Ψ . This is a non-negative simple function of three variables, x , y , and z , integrating to the total number of electrons,

$$N = \int \rho(\mathbf{r}) d\mathbf{r} \quad (\text{Eq. 1.44})$$

1.2.4.1 Thomas-Fermi Model

The concept of density functional emerged for the first time in the late 1920's, in the early work of E. Fermi and L.H. Thomas, which introduced the idea of expressing the energy of a system as a function of the total electron density. In Thomas-Fermi model [Fermi 1927; Fermi 1928; Thomas 1927] the kinetic energy of the electrons is derived from the quantum statistical theory based on the uniform electron gas, but the electron-nucleus and electron-electron interactions are treated classically. Within this theory, the kinetic energy of the electron gas, $T_{\text{TF}}[\rho(\mathbf{r})]$ is defined as,

$$T_{\text{TF}}[\rho(\mathbf{r})] = \frac{3}{10} (3\pi^2)^{2/3} \int d\mathbf{r} \rho^{5/3}(\mathbf{r}) \quad (\text{Eq. 1.45})$$

From the above equation, the approximation is made that the kinetic energy of the electrons depends exclusively on the electron density. By adding the interaction between electron-nucleus and electron-electron, a total energy in terms of electron density is obtained,

$$E[\rho(\mathbf{r})] = \frac{3}{10} (3\pi^2)^{2/3} \int d\mathbf{r} \rho^{5/3}(\mathbf{r}) - Z \int \frac{\rho(\mathbf{r})}{\mathbf{r}} d\mathbf{r} + \frac{1}{2} \iint \frac{\rho(\mathbf{r}_1)\rho(\mathbf{r}_2)}{|\mathbf{r}_1 - \mathbf{r}_2|} d\mathbf{r}_1 d\mathbf{r}_2 \quad (\text{Eq. 1.46})$$

The second and third terms are the electron-nucleus and electron-electron interactions, respectively. The Thomas-Fermi kinetic energy functional is the only density functional that has an elegant mathematical derivation, but it is not accurate enough to be chemically useful. The significance of Thomas-Fermi model in the history of DFT is more as an illustration that the energy can be determined purely using the electron density. In 1951, J.C. Slater [Slater 1951], applied the same basic idea into the development of the Hartee-Fock-Slater method, nowadays considered as a predecessor of the theory of DFT. However, a formal proof of this notion came with Hohenberg-Kohn Theorem.

1.2.4.2 Hohenberg-Kohn Theorem

In 1964, Hohenberg and Kohn [Hohenberg and Kohn 1964] formulated and proved a theorem that put on solid mathematical grounds to the former ideas proposed by Thomas and Fermi. In their landmark paper Hohenberg and Kohn stated that (i) there exists a one-to-one correspondence between external potential and electron density and (ii) the ground state energy can be obtained variationally *i.e.*, the density that minimizes the total energy is the exact ground state density. A straightforward consequence of the first Hohenberg and Kohn theorem is that the ground state energy E is also uniquely determined by the ground-state charge density. The energy functional can be written as a sum of two terms:

$$E[\rho(\mathbf{r})] = \int V_{\text{ext}}(\mathbf{r})\rho(\mathbf{r})d\mathbf{r} + F[\rho(\mathbf{r})] \quad (\text{Eq. 1.47})$$

The first term arises from the interaction of the electrons with an external potential $V_{\text{ext}}(\mathbf{r})$, typically due to the Coulomb interaction with the nuclei. $F[\rho(\mathbf{r})]$ is the sum of the kinetic energy of the electrons and the contribution from the interelectronic interactions.

The minimum value in the energy corresponds to the exact ground-state electron density, enabling a variational approach to be used. The DFT equivalent of the Schrödinger equation may be written as:

$$\left(\frac{\delta E[\rho(\mathbf{r})]}{\delta \rho(\mathbf{r})} \right)_{V_{\text{ext}}} = \mu \quad (\text{Eq. 1.48})$$

where μ is a Lagrangian multiplier which can be identified with the chemical potential for the electron for its nuclei.

1.2.4.3 The Kohn-Sham Equations

Kohn and Sham [Kohn and Sham 1965] suggested a practical way to solve the Hohenberg-Kohn theorem for a set of interacting electrons. They showed that $F[\rho(\mathbf{r})]$ should be approximated as the sum of three terms:

$$F[\rho(\mathbf{r})] = E_{\text{KE}}[\rho(\mathbf{r})] + E_{\text{H}}[\rho(\mathbf{r})] + E_{\text{XC}}[\rho(\mathbf{r})] \quad (\text{Eq. 1.49})$$

where $E_{\text{KE}}[\rho(\mathbf{r})]$ is the kinetic energy, $E_{\text{H}}[\rho(\mathbf{r})]$ is the electron-electron Coulombic energy, and $E_{\text{XC}}[\rho(\mathbf{r})]$ contains contributions from exchange and correlation. The first term, $E_{\text{KE}}[\rho(\mathbf{r})]$, is defined as the kinetic energy of a system of non-interacting electrons with the same density $\rho(\mathbf{r})$ as the real system:

$$E_{\text{KE}}[\rho(\mathbf{r})] = \sum_{i=1}^N \int \psi_i(\mathbf{r}) \left(-\frac{\nabla^2}{2} \right) \psi_i(\mathbf{r}) d\mathbf{r} \quad (\text{Eq. 1.50})$$

$$\text{Hartree electrostatic energy, } E_{\text{H}}[\rho(\mathbf{r})] = \frac{1}{2} \iint \frac{\rho(\mathbf{r}_1)\rho(\mathbf{r}_2)}{|\mathbf{r}_1 - \mathbf{r}_2|} d\mathbf{r}_1 d\mathbf{r}_2 \quad (\text{Eq. 1.51})$$

The full expression for the energy of an N-electron system within the Kohn-Sham scheme now becomes:

$$E[\rho(\mathbf{r})] = \sum_{i=1}^N \int \psi_i(\mathbf{r}) \left(-\frac{\nabla^2}{2} \right) \psi_i(\mathbf{r}) d\mathbf{r} + \frac{1}{2} \iint \frac{\rho(\mathbf{r}_1)\rho(\mathbf{r}_2)}{|\mathbf{r}_1 - \mathbf{r}_2|} d\mathbf{r}_1 d\mathbf{r}_2 + E_{\text{XC}}[\rho(\mathbf{r})] - \sum_{A=1}^M \int \frac{Z_A}{|\mathbf{r} - \mathbf{R}_A|} \rho(\mathbf{r}) d\mathbf{r} \quad (\text{Eq. 1.52})$$

This equation acts to define the exchange-correlation energy functional which thus contains not only the contributions due to exchange and correlation but also a contribution due to the difference between the true kinetic energy of the system and $E_{KE}[\rho(\mathbf{r})]$. Kohn and Sham wrote the density of the system as the sum of the square moduli of a set of one-electron orbitals:

$$\rho(\mathbf{r}) = \sum_{i=1}^N |\psi_i(\mathbf{r})|^2 \quad (\text{Eq. 1.53})$$

By introducing this expression for electron density and applying the appropriate variational condition, the one-electron Kohn-Sham equation takes the form:

$$\left\{ -\frac{\nabla_1^2}{2} - \left(\sum_{A=1}^M \frac{Z_A}{r_{1A}} \right) + \int \frac{\rho(\mathbf{r}_2)}{r_{12}} d\mathbf{r}_2 + V_{XC}[\mathbf{r}_1] \right\} \psi_i(\mathbf{r}_1) = \varepsilon_i \psi_i(\mathbf{r}_1) \quad (\text{Eq. 1.54})$$

where ε_i are the orbital energies and V_{XC} is known as the exchange-correlation potential which is related to the exchange-correlation energy by:

$$V_{XC}[\mathbf{r}] = \frac{\delta E_{XC}[\rho(\mathbf{r})]}{\delta \rho(\mathbf{r})} \quad (\text{Eq. 1.55})$$

To solve the Kohn-Sham equations a self-consistent approach is followed. An initial guess of the density is fed into Eq. 1.55 from which a set of orbitals can be derived, leading to an improved value of density, which is then used in the second iteration and so on until convergence is achieved. The exchange-correlation energy, E_{XC} is generally divided into two terms, an exchange term E_X (associated with the interaction of electrons of the same spin) and a correlation term E_C (associated with the interaction of electrons of opposite spin). The corresponding functionals are exchange functional and correlation functional, respectively.

$$E_{XC}[\rho(\mathbf{r})] = E_X[\rho(\mathbf{r})] + E_C[\rho(\mathbf{r})] \quad (\text{Eq. 1.56})$$

1.2.4.4 Exchange-Correlation Functionals

Kohn-Sham DFT is formally exact, but it does not lead to the exact form of exchange-correlation functional V_{XC} . The situation is well summarized by the quotation: "DFT is the method of choice for first principles quantum chemical calculations of the electronic structure and properties of many molecular and solid systems. With the exact exchange-correlation functional, DFT would take into full account all complex many-body effects at a computation cost characteristic of mean field approximations. Unfortunately, the exact exchange-correlation functional is unknown, making it essential to pursue the quest of finding more accurate and reliable functionals" [Xu and Goddard 2004]. For practical applications of DFT, several methods have been designed by modifying the exchange-correlation potential *viz.* (i) Local density approximation (LDA) (ii) Generalized gradient approximation (GGA) (iii) meta-GGA (iv) Hybrid functionals.

The local density approximation [Dirac 1930; Fermi 1927; Thomas 1927] represents the simplest approach to represent the exchange-correlation functional. LDA implicitly assumes that the exchange-correlation energy at any point in space is a function of the electron density at that point and can be given by the electron density of a homogenous electron gas of the same density. Within the LDA approach, the exchange function is given by:

$$E_X^{\text{LDA}}[\rho(\mathbf{r})] = -\frac{3}{4} \left(\frac{3}{\pi} \right)^{1/3} \int \rho^{4/3}(\mathbf{r}) d\mathbf{r} \quad (\text{Eq. 1.57})$$

The local spin density approximation (LSDA) proposed by J.C. Slater [Slater 1951], represents a more general application of LDA, which introduces spin densities into the functionals, thereby solving several conceptual problems of LDA. The exchange functional in LSDA approach is given by:

$$E_X^{\text{LDA}}[\rho(\mathbf{r})] = -2^{1/3} \left(-\frac{3}{4} \left(\frac{3}{\pi} \right)^{1/3} \right) \int (\rho_\alpha^{4/3}(\mathbf{r}) + \rho_\beta^{4/3}(\mathbf{r})) d\mathbf{r} \quad (\text{Eq. 1.58})$$

α and β represent spin up and down, respectively.

In LDA, the correlation energy E_C per particle is difficult to obtain separately from the exchange energy. Several different formulations for this functional have been developed by Vosko, L. Wilk and M. Nusair known as Vosko-Wilk-Nusair or VWN [Vosko *et al.* 1980] by incorporating Monte Carlo results.

Generalized gradient approximation methods (GGAs) assume that the exchange-correlation energies depend not only on the density but also on the gradient of the density, $\nabla\rho(\mathbf{r})$.

$$E_{\text{XC}}[\rho_\alpha(\mathbf{r}), \rho_\beta(\mathbf{r})] \equiv \int \varepsilon_{\text{XC}}(\rho_\alpha(\mathbf{r}), \rho_\beta(\mathbf{r}), \vec{\nabla}\rho_\alpha(\mathbf{r}), \vec{\nabla}\rho_\beta(\mathbf{r})) d^3\mathbf{r} \quad (\text{Eq. 1.59})$$

The development of GGA methods, follow two main lines; one based on numerical fitting procedures proposed by Becke [Becke 1988] and a more rational-based one advocated by Perdew [Perdew 1986; Perdew *et al.* 1992]. Meta-GGA functionals represent a significant improvement over GGA methods and depend explicitly on higher order density gradients which involve derivatives of the occupied Kohn-Sham orbitals.

Hybrid density functional (H-GGA) methods combine the exchange-correlation of a conventional GGA method with a percentage of HF exchange, with a certain degree of empiricism in optimizing the weight factor for each component and the functionals that are mixed. The exact amount of HF exchange is fitted semiempirically from experimental atomization energies, ionization potentials, proton affinities, total atomic energies, and other data, for a representative set of small molecules. Hybrid-meta GGA (HM-GGA) methods represent a new class of density functionals, based on a similar concept of M-GGAs, but start from M-GGAs instead of standard GGAs. These methods

depend on HF exchange, the electron density and its gradient and the kinetic energy density.

J. Perdew presented the hierarchy of DFT approximations as Jacob’s ladder (the famous allusion from the book of Genesis), containing five different rungs, comprising the five generations of density functionals *viz.* LDA, GGA, M-GGA, H-GGA and HM-HGA, and finally the fully nonlocal description [Perdew and Schmidt 2001]. Each rung adds something more to the design elements of the lower rungs and each rung has particular strength and weaknesses (Figure 1.11). Recently, Janesko added a new rung on the Jacob’s ladder called “rung 3.5” which is an intermediate between the local and hybrid functionals [Janesko 2010; Janesko 2013].

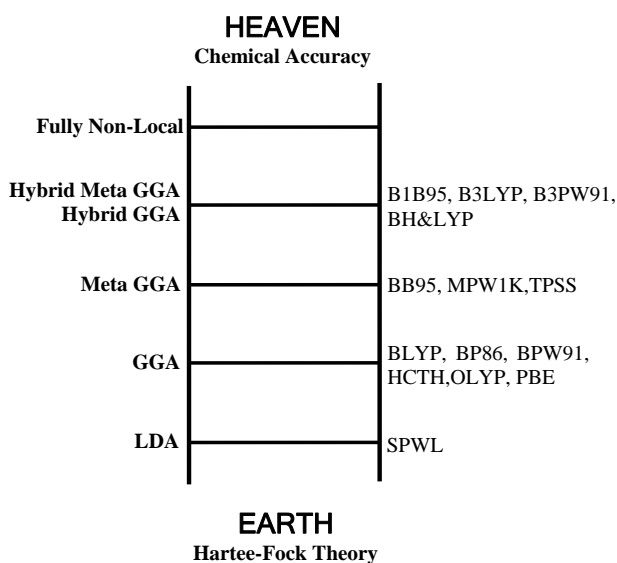


Figure 1.11 Jacob’s ladder representing the five generations of density functional from the world of Hartree to the heaven of chemical accuracy, with examples from each class.

1.2.4.5 Minnesota Functionals

Zhao and Truhlar presented and parameterized a new suite of functionals termed Minnesota functionals [Peverati and Truhlar 2011; Peverati and Truhlar 2012; Zhao *et al.* 2005a; Zhao *et al.* 2005b; Zhao and Truhlar 2006a; Zhao and Truhlar 2006b; Zhao and

Truhlar 2008a; Zhao and Truhlar 2008b]. The Minnesota functional family includes one meta-GGA (M06-L), two meta-NGAs (M11-L and MN12-L), seven global-hybrid meta-GGAs (M05, M05-2X, M06-2X, M08-HX and M08-SO), one range-separated hybrid meta-GGA (M11) and one screened exchange hybrid meta-NGA (MN12-SX). The M06 family, the most popular among these, is composed of four functionals that have similar functional forms for the DFT part, but each has parameters optimized with a different percentage of HF exchange. The four functionals are (i) M06-L, a local functional (no HF exchange) (ii) M06, a global-hybrid meta-GGA with 27% of HF exchange, leading to a well-balanced functional for overall good performance for chemistry (iii) M06-2X, a global hybrid meta-GGA with 54% HF exchange, for top-level across-the-board performances in all areas of chemistry including thermochemistry and reaction kinetics, but excluding multi-reference systems such as those containing transition metals and (iv) M06-HF, a global-hybrid meta-GGA with 100% HF exchange, suitable for calculation of spectroscopic properties of charge-transfer transitions, where elimination of self-interaction error is of prime importance. Although it was believed that one could not design a generally useful functional with 100% HF exchange, M06-HF disproved this by achieving overall performances for chemistry better than the popular B3LYP functional. The DFT calculations presented in this thesis have been carried out using M06-L functional. Being a non-hybrid meta GGA functional M06-L resides in the third rung of Jacob's ladder and can be applied for large systems with low costs.

1.2.5 Basis Sets

Basis set refers to the linear combinations of a pre-defined set of non-orthogonal one-electron wave functions used to build molecular orbitals, with the weights or coefficients to be determined. There are two main types of basis functions *viz.* Slater type orbitals (STOs) [Allen and Karo 1960] and Gaussian type orbitals (GTOs) [Boys 1950;

Feller and Davidson 1990]. The first basis sets used in molecular calculations were typically STOs, which correspond to a set of functions which decay exponentially with the distance from the nuclei. STOs have the exponential dependence: $e^{-\zeta r}$ and are given by the mathematical expression:

$$\phi_{abc}^{\text{STO}}(x, y, z) = N x^a y^b z^c e^{-\zeta r} \quad (\text{Eq. 1.60})$$

where N is the Normalization constant, a, b, c control the angular momentum ($L = a + b + c$), ζ determines the width or spread of the orbital and x, y, z represent the cartesian coordinates. STOs are not particularly amenable to implementation in molecular orbital calculations since some of the integrals in STOs are difficult to evaluate especially when the atomic orbitals are centered on different nuclei. Gaussian type orbitals have the exponential dependence $e^{-\zeta r^2}$. GTOs have the following mathematical expression:

$$\phi_{abc}^{\text{GTO}}(x, y, z) = N x^a y^b z^c e^{-\zeta r^2} \quad (\text{Eq. 1.61})$$

The computational advantage of GTOs over STOs is primarily due to the Gaussian product theorem, *viz.* the product of two GTOs is also a Gaussian function centered at the weighted midpoint of the two functions [Shavitt 1963]. In addition, the overlap and other integrals are easier to evaluate leading to huge computational savings. The Gaussian function described in Eq. 1.61 is generally known as primitive Gaussian (PGTO). It is a common practice [Stewart 1970] to bunch together a set of primitive Gaussian functions into one Gaussian function or a contracted Gaussian (CGTO),

$$\phi_{abc}^{\text{CGTO}}(x, y, z) = N \sum_{i=1}^n c_i x^a y^b z^c e^{-\zeta_i r^2} \quad (\text{Eq. 1.62})$$

where n represent the number of Gaussian's to mimic the STO and c_i represent coefficients. By contracting several primitive Gaussians into one, the computational effort can be reduced through the optimization of several coefficients in one go. The degree of complexity, and thus precision, of a basis set is defined by the number of

contracted functions employed to represent each atomic orbital, the minimum being one contracted function to describe a basis function (minimal basis set). For example the STO-3G basis set [Hehre *et al.* 1969] (where G indicates a combination of contracted Gaussian functions) is formed by a linear combination of three contracted functions for each basis function so as to resemble an STO.

For more precision and better description of the system, two or more functions can be used to describe each type of orbital, usually double-zeta (DZ) and triple-zeta (TZ) basis sets [Davidson and Feller 1986]. Pople and coworkers designed the split valence basis sets of type 'k-nlmG' where 'k' indicates how many PGTOs are used for representing the core orbitals and 'nlm' indicates both how many functions the valence orbitals are split into and how many PGTOs are used for their representation [Ditchfield *et al.* 1971]. 3-21G and 6-31G basis sets are examples of split valence basis sets [Binkley *et al.* 1980; Hehre *et al.* 1972]. Further improvements can be achieved by adding polarization or diffuse functions. Although a free isolated atom will have spherical symmetry, the atoms in a molecule or some other chemical environment will exhibit some distortions in their electron density. To take account of this effect, functions of higher angular momentum than the occupied atomic orbitals known as polarization functions are added to the basis sets. This is usually denoted as * or ** (or (d) or (d, p)) after the G in the notation of the basis sets describing the use of an extra set of d-orbitals on heavy atoms and p-orbitals on hydrogens. Similarly, diffuse functions are sometimes included in the basis set to improve the description at large distances from the nuclei and are denoted by + or ++ signs. This is especially important for anions as the additional electrons are loosely bound to nuclei.

The basis sets employed for the calculations in the thesis are (a) Pople's split valence basis set, 6-311++G(d,p) with d polarization functions for non-hydrogen atoms and p polarization function for hydrogen atom as well as diffuse functions for non-

hydrogen and hydrogen atom [Hehre *et al.* 1986], (ii) Dunning's augmented correlation consistent polarized valence triple zeta basis function, aug-cc-pvtz [Dunning 1989] and (iii) double-zeta valence plus polarization basis set (equivalent to the one used in DGauss software [Godbout *et al.* 1992]), DGDZVP.

1.2.6 Basis Set Superposition Error

Basis set superposition error (BSSE) refers to the artificial shortening of intermolecular distances and concomitant strengthening of intermolecular interactions in weakly bound clusters while using smaller basis sets. When two fragments A and B approach each other to form a new species, their basis functions overlap. Each fragment "borrows" basis functions from the nearby components, effectively increasing its basis set and improving the calculation of derived properties such as energy. The energy of the system falls not only because of the favourable intermolecular interactions but also because the basis functions on each molecule provide a better description of the electronic structure around the other molecule. One widely used method to assess the BSSE is the counterpoise correction scheme of Boys and Bernardi [Boys and Bernardi 1970] in which the entire basis set is included in all calculations. To illustrate this, consider the binding energy of the dimer (AB) *viz.* $A + B \rightarrow AB$. The binding energy (ΔE) can be expressed as,

$$\Delta E = E(AB)_{ab} - [E(A)_a + E(B)_b] \quad (\text{Eq. 1.63})$$

where $E(AB)_{ab}$, $E(A)_a$ and $E(B)_b$ represent the energy of AB, monomer A and monomer B, respectively. Subscripts indicate the corresponding basis sets for AB, A and B. In counterpoise method, the calculation of the energy of the individual species A is performed in the presence of 'ghost' orbitals of B, without the nuclei or electrons of B. A similar calculation is performed for B using the 'ghost' orbitals on A. Using counterpoise method, BSSE can be evaluated with:

$$\Delta E_{BSSE} = E(\tilde{A})_{ab} + E(\tilde{B})_{ab} - E(\tilde{A})_a - E(\tilde{B})_b \quad (\text{Eq. 1.64})$$

where $E(\tilde{A})_{ab}$ and $E(\tilde{B})_{ab}$, respectively represents the energy of monomer A and B in the structure it adopts in the dimer (AB) and with the full basis set of the dimer available. $E(\tilde{A})_a$ and $E(\tilde{B})_b$ are the energies of A and B, respectively, with only their own basis functions but again in the structure they adopt in the dimer. The correction to the binding energy can be calculated as, $\Delta E - \Delta E_{BSSE}$.

1.2.7 Atoms in Molecules

Richard Bader [Bader 1985; Bader 1991] pioneered the topographical investigation of molecular electron density (MED), one of the fundamental scalar functions that describe the probabilistic charge distribution of a molecule and developed a method called quantum theory of atoms in molecules (QTAIM). Topology of electron density $\rho(\mathbf{r})$ provides an accurate mapping of the molecule and is effectively described by a set of critical points (CPs). MED attains maximum at the nuclear positions and each atom may be described by its boundaries dependent on the balance of forces of the considered system. A critical point (CP) is a point in the electron density surface where the gradient of electron density vanishes (Eq.1.65).

$$\nabla\rho(\mathbf{r}) = i \frac{d\rho(\mathbf{r})}{dx} + j \frac{d\rho(\mathbf{r})}{dy} + k \frac{d\rho(\mathbf{r})}{dz} \longrightarrow \begin{cases} = 0 & (\text{at critical points at } \infty) \\ \neq 0 & (\text{at any other point}) \end{cases} \quad (\text{Eq.1.65})$$

The critical points may correspond to maxima, saddle points or to the local minima. The various CPs are distinguished by considering the signs of the second derivatives of electron density. The Hessian matrix is formed from the nine possible second derivatives of electron density. The Laplacian is expressed as the sum of the eigenvalues of the Hessian matrix (Eq. 1.66).

$$\nabla^2 \rho(\mathbf{r}) = \nabla \cdot \nabla \rho(\mathbf{r}) = i \frac{\partial^2 \rho(\mathbf{r})}{\partial x^2} + j \frac{\partial^2 \rho(\mathbf{r})}{\partial y^2} + \frac{\partial^2 \rho(\mathbf{r})}{\partial z^2} \quad (\text{Eq. 1.66})$$

Critical points are designated as ordered pair (r, ω) where r is the rank of the CP and ω the signature. The rank is the number of non-zero eigenvalues of the electron density at the CP and signature is the algebraic sum of the signs of eigenvalues. If one or more eigenvalue is/are zero, then the corresponding CP is termed degenerate *i.e.*, a degenerate CP has $\omega < 3$. A non-degenerate CP has all three eigenvalues non zero. There are four types of CPs of rank three: $(3, -3)$, $(3, -1)$, $(3, +1)$ and $(3, -3)$. $(3, -3)$ CP corresponds to the local maximum, the nuclear attractor; $(3, -1)$ is the bond critical point (BCP); $(3, +1)$ is the ring critical point (RCP); and $(3, -3)$ is the local maximum, called the cage critical point (CCP). Bond path (BP) is the line of maximum electron density connecting two interacting atoms or bond critical point is the minimum of electron density on the bond path. A collection of bond paths linking the nuclei of bonded atoms in equilibrium geometry with the associated critical points is known as the molecular graph. Figure 1.12 represents the molecular graph showing the bond paths and BCPs of hexafluorobenzene-nitrogen lone pair- π complex.

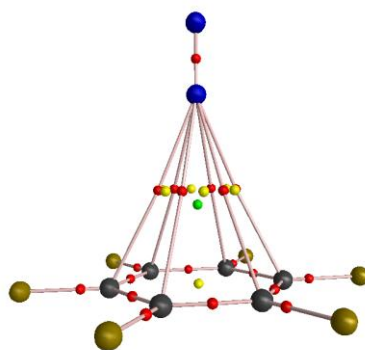


Figure 1.12 Molecular graph of hexafluorobenzene-nitrogen complex (M06L/6-311++G(d,p) level) showing the bond paths (lines) and different critical points (red for $(3, -1)$ or bond CP, yellow for $(3, +1)$ or ring CP, and green for $(3, +3)$ or cage CP). Color-code by element: C = black, F = grey and N=blue.

Analysis of BCP provides information about the nature of various interatomic interactions [Bader and Essén 1984]. The Laplacian of electron density is negative for shared interactions like covalent and polarized bonds due to the concentration of electron density in the atom-atom region. Laplacian is positive for interactions like van der Waals, ionic and hydrogen bonds where there is depletion of electron charge in the atom-atom region. Pioneering works of Boyd and Choi showed that AIM theory can be applied for the analysis of hydrogen bonds [Boyd and Choi 1985; Boyd and Choi 1986]. The values of $\rho(\mathbf{r})$ and $\nabla^2\rho(\mathbf{r})$ are important quantities to characterize hydrogen bonding in respect with strength and nature. Koch and Popelier generalized a set of eight different criteria for a hydrogen bonds based on AIM analysis [Koch and Popelier 1995; Popelier 1998; Popelier and Logothetis 1998]. The eight criteria are: (i) the presence of (3, -1) BCP and bond path linking the CP with the bonded atoms, (ii) the values of $\rho(\mathbf{r})$ at the (3, -1) BCP should lie in the range of 0.002 to 0.035 au (iii) the values of $\nabla^2(\rho(\mathbf{r}))$ should lie in the range of 0.024 to 0.139 au (iv) mutual penetration of hydrogen and acceptor atoms (v) increase in the positive charge on the hydrogen atom (vi) increase in the energy of the hydrogen atom (vii) decrease in the polarization of hydrogen atom and (viii) decrease in hydrogen atom volume. Grabowski proposed a new measure of hydrogen bond strength (Δ_{com}) using the properties of proton donating bond on the basis of detailed AIM analysis of a heterogeneous sample of hydrogen bonds, *viz.* O–H...O, O–H...N, C–H...O, C–H... π and dihydrogen bonds [Grabowski 2001]. Quantitative values of $\rho(\mathbf{r})$ and $\nabla^2(\rho(\mathbf{r}))$ are good indicators of the character and strength of halogen bonds and anion- π interactions also. Anion- π interactions are characterized by the presence of cage critical point, located along the line connecting the ion with the center of the aromatic ring and the value of electron density at the CCP is a measure of the strength of the interaction [Garau *et al.* 2003a; Garau *et al.* 2004].

1.2.8 Molecular Electrostatic Potential

Any distribution of electric charge, such as nuclei or electrons creates an electrical potential $V(\mathbf{r})$ in the surrounding space. Molecular electrostatic potential or MESP [Pullman 1990; Scrocco and Tomasi 1978] can be regarded as the potential of a molecule to interact with an electric charge located at a point \mathbf{r} . Thus a positive charge is attracted to those regions in which $V(\mathbf{r})$ is negative and is repelled from regions of positive potential. An important feature of MESP is that it is a real physical property and can be determined experimentally by X-ray diffraction techniques. MESP [Gadre and Shirsat 2000] can be rigorously and unambiguously calculated from the electron density function, $\rho(\mathbf{r})$ using the equation:

$$V(\mathbf{r}) = \sum_A^N \frac{Z_A}{|\mathbf{r} - \mathbf{R}_A|} - \int \frac{\rho(\mathbf{r}') d^3 \mathbf{r}'}{|\mathbf{r} - \mathbf{r}'|} \quad (\text{Eq. 1.67})$$

where Z_A is the charge on nucleus A located at \mathbf{R}_A and \mathbf{r}' is a dummy integration variable. The two terms refer to the bare nuclear potential and the electronic contributions, respectively. Effective localization of electron-rich regions in the molecular system thus emerges through a balance of these two terms. The above equation shows that the electrostatic potential is certainly specific to a given molecular geometry, and the value of $V(\mathbf{r})$ in any particular region depends on whether the effect of nuclei or electrons is dominant there. Thus MESP is positive in the region close to nuclei and negative in the electron-rich region. The MESP can attain positive, zero or negative values, in contrast to the behavior of electron densities in position, which can attain only non-negative values. The ESP at nuclear sites shows a discontinuity and negative value since the nuclear contribution from the corresponding atom is dropped out. The MESP at a nuclei, $V_{0,A}$ can be obtained by dropping nuclear contribution due to Z_A and can be give as:

$$V_{0,A} = \sum_{B \neq A} \frac{Z_B}{|\mathbf{R}_B - \mathbf{R}_A|} - \int \frac{\rho(\mathbf{r}') d^3 r'}{|\mathbf{r} - \mathbf{r}'|} \quad (\text{Eq. 1.68})$$

Since MESP is a one electron property, its accurate quantification is possible within a variety of theoretical methods implemented in standard *ab initio* packages. Topographical features of MESP as well as the pictorial representation of MESP in the form of contours and isosurfaces are extremely useful for exploring the structure and reactivity of molecules, intermolecular interactions, molecular recognition and a variety of chemical phenomena [Gadre *et al.* 1996; Luque *et al.* 1994; Politzer and Truhlar 1981]. Figure 1.13 (a) depicts the MESP contour plot of hexafluorobenzene molecule textured on to a 0.003 au electron density surface with the electron rich region in blue and electron deficient regions in red. In MESP topography analysis the electronic distribution of molecules is understood in terms of critical points (CPs) *i.e.*, the points at which the partial derivatives of MESP vanish. The signs of eigenvalues of the corresponding Hessian matrix indicate the nature of the CP. A CP, usually denoted as an ordered pair (R, S) of rank R and signature S, is classified according to the nature of the eigenvalues of the corresponding Hessian matrix. Rank is the number of non-zero eigenvalues of the Hessian matrix and the signature is defined as the algebraic sum of the signs of these eigenvalues. A CP possessing at least one zero eigenvalue is termed as degenerate while a non-degenerate CP has all the three eigenvalues nonzero. Four types of non-degenerate critical points for MESP exist with rank 3, *viz.* (3, -3), (3, -1), (3, +1) and (3, +3). A CP with (3, +3) character is referred to as local minimum while (3, -1) and (3,+1) are saddle points and (3, -3) is a local maximum. Figure 1.12 (b) shows the nature and location of MESP CPs of formaldehyde. MESP brings out electron rich regions like lone-pairs of electrons and π -bonds in the form of a negative valued (3, +3) minima. The most negative value of the MESP (V_{\min}) corresponds to a point at which electrostatic potential due to the electron density term dominates maximally over the bare

nuclear term, the location of it indicates the electron-dense region of a molecule [Gadre and Pathak 1990b; Gadre and Shirsat 2000; Pathak and Gadre 1990; Shirsat *et al.* 1992].

Any bonding (covalent/weak) interaction between atoms is featured by the presence of a positive valued $(3, -1)$ CP (BCP) and a positive valued $(3, +1)$ CP is the manifestation of a ring [Gadre and Shirsat 2000]. The absence of non-nuclear maxima is a main feature of MESP topography over other scalar fields in the interpretation of electronic mechanisms. Similar to the molecular electron density (MED) topography, BCPs bring out the strain in bonds by deviating from the line joining the corresponding atoms. The significance of the negative-valued MESP and their critical points in molecules and their anionic species have been widely addressed in the literature [Gadre *et al.* 1992; Gadre and Pathak 1990a; Gadre and Shrivastava 1993; Luque *et al.* 1994; Politzer and Truhlar 1981].

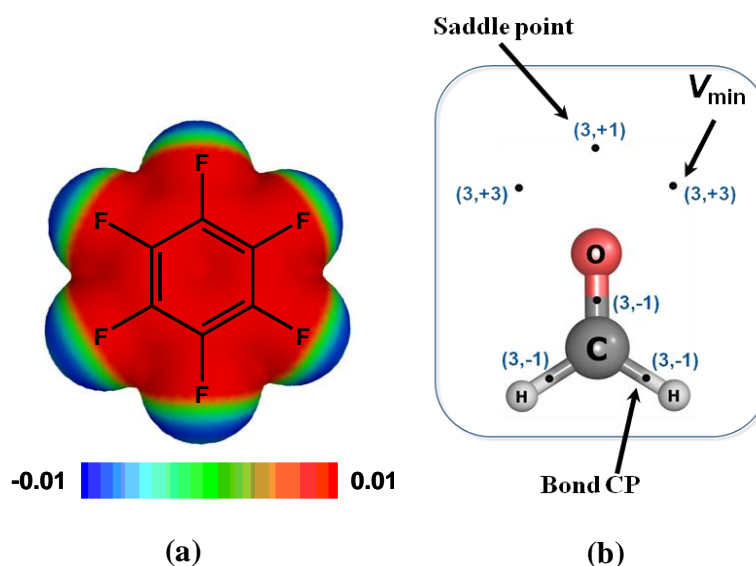


Figure 1.13 (a) MESP contour plot of hexafluorobenzene molecule textured on to a 0.003 au electron density surface, (b) nature and location of MESP CPs of formaldehyde.

In this thesis MESP is used as a predictive tool for analysing and quantifying intermolecular noncovalent interactions as well as predicting the reactive behaviour of molecules.

1.2.9 Solvation Models

Even though gas phase predictions are appropriate for many purposes, some properties such as geometry, total energy, vibrational frequency and electronic spectra are considerably affected by the surrounding environment, such as solvent. Methods for evaluating solvent effect can be broadly classified into two types; those that treat the solvent as a continuous medium (continuum solvation) and those describing the individual solvent molecules (explicit solvation) [Cramer and Truhlar 1999]. Explicit solvation models represent the most rigorously correct way of modeling chemistry in solution but are computationally expensive. Continuum models include solvent as a uniform polarizable medium with a dielectric constant ϵ and the solute \mathbf{M} is placed in a suitably shaped cavity in the medium [Foresman *et al.* 1996]. Dispersion interactions between the solvent and solute add stabilization while the creation of a hole in the medium costs energy, *i.e.* destabilization. The electric charge distribution of \mathbf{M} will polarize the medium, which in turn acts back on the molecule, thereby producing an electrostatic stabilization. Thus the free energy of solvation, ΔG_{sol} is expressed as the sum of three terms *viz.* the electrostatic (ΔG_{elec}) and dispersion-repulsion (ΔG_{disp}) contributions to free energy, and the cavitation energy (ΔG_{cav}).

$$\Delta G_{\text{sol}} = \Delta G_{\text{elec}} + \Delta G_{\text{disp}} + \Delta G_{\text{cav}} \quad (\text{Eq. 1.69})$$

SCRF (Self-Consistent Reaction Field) is a method of accounting for the effect of a polarizable solvent on the quantum system [Tomasi and Persico 1994]. The SCRF algorithm calculates the reaction field through solutions to the Poisson or Poisson--Boltzmann equation, and iteratively obtains self-consistency between the reaction field and charge distribution of the quantum system. SCRF methods vary with how they define the cavity and the reaction field. Polarizable continuum model (PCM) by Tomasi and coworkers is one of the most frequently used SCRF methods where the cavity is

defined as the union of a series of interlocking atomic spheres [Cossi *et al.* 1996]. This technique uses a numerical integration over the solute charge density and generally gives good results.

The isodensity PCM (IPCM) model defines the cavity as an isodensity surface of the molecule determined by an iterative procedure in which an SCF cycle is performed and converged using the current isodensity cavity [Foresman *et al.* 1996]. The resultant wavefunction is used to compute an updated isodensity surface, and the cycle is repeated until convergence is reached. An isodensity surface is a very natural, intuitive shape for the cavity since it corresponds to the reactive shape of the molecule possible. Self-consistent isodensity PCM (SCI-PCM) embed the cavity calculation in the SCF procedure to account for coupling between the cavity and the electron density and includes coupling terms that IPCM neglects.

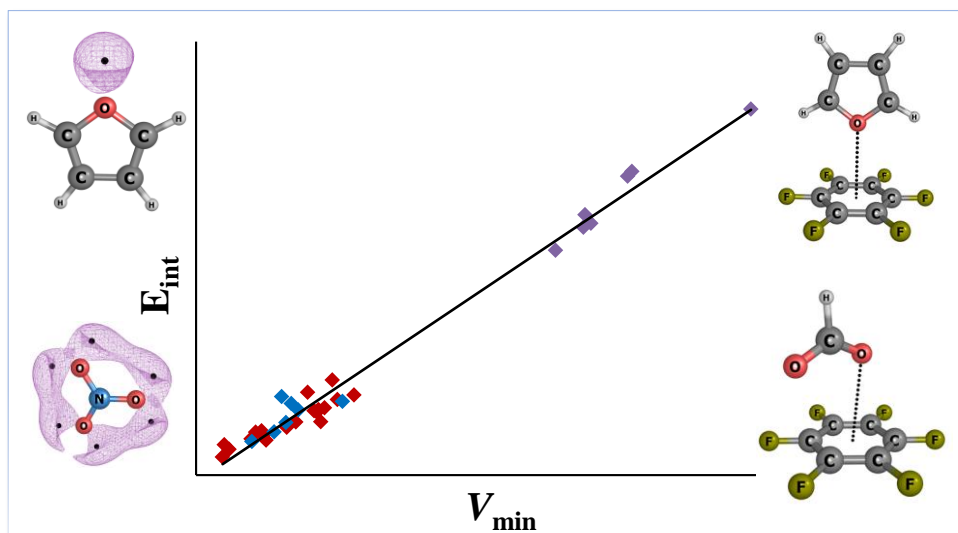
1.3 Conclusions

Noncovalent interactions are of utmost importance in various fields of chemistry and biology. The first part of Chapter 1 gives an overview of various noncovalent interactions with special emphasis to hydrogen bonds, halogen bonds and anion/lone pair- π interactions. Insights into the nature and strength of these interactions and the details of the various energetic contributions to their total interaction energy are also presented. An account of the experimental and theoretical studies that has contributed to the modern day understanding of hydrogen bonds, halogen bonds and anion/lone pair- π interactions is also discussed.

Computational chemistry methods have become crucial for many developments in chemistry today and have contributed immensely towards understanding the noncovalent interactions at the molecular level. Computational chemistry uses the laws and equations that govern the subatomic world to calculate and predict molecular structure and properties. The second part of Chapter 1 deals with the theoretical background of the methods which are commonly used in computational chemistry calculations. A detailed account of the *ab initio* and density functional theory methods used in the calculations discussed in the thesis is presented in this section. The principles and applications of atoms in molecules and molecular electrostatic potential analysis employed for the quantification and characterization of weak interactions are also outlined.

Chapter 2

Molecular Electrostatics for Probing Lone Pairs and Lone Pair- π Interactions



2.1 ABSTRACT

Lone pairs are ubiquitous in chemistry to describe molecular interactions, yet their experimental characterization has never been achieved. Using a large variety of neutral, anionic and radical systems, it is shown that molecular electrostatic potential (MESP), a property amenable to experimental observation as well as theoretical calculation can reveal lone pairs. For electron-rich molecules, the negative minima in MESP topography give the location of electron localization and the MESP value at the minimum (V_{min}) quantifies the electron-rich character of that region. Calculations at M06L/6-311++G(d,p) DFT show that among neutral molecules, N_2 exhibits the most shallow V_{min} (-11.4 kcal/mol) and imidazole possesses the deepest V_{min} (-68.4 kcal/mol). V_{min} at lone pairs of free radicals lie in the range -24.2 to -63.5 kcal/mol while anions exhibit large negative V_{min} (-155.7 to -240.3 kcal/mol). The eigenvalues of the Hessian at V_{min} and the orientation and distance of V_{min} from the lone pair bearing atom provide further characterization of a lone pair. Further, an electrostatics-based approach is proposed for probing the weak interactions between lone pair containing molecules and π -deficient molecular systems. Interactive behavior of lone pair bearing molecules with electron-deficient π -systems, viz., hexafluorobenzene, 1,3,5-trinitrobenzene, 2,4,6-trifluoro-1,3,5-triazine and 1,2,4,5-tetracyanobenzene are explored which show that good prediction on the lone pair- π interaction energy (E_{int}) can be achieved with V_{min} as it correlates linearly with E_{int} . On the basis of the precise location of MESP minimum, a prediction on the orientation of a lone pair bearing molecule with an electron-deficient π -system is possible in

majority of the cases studied. Thus, V_{min} emerges as a powerful descriptor for lone pairs and also provides good predictions on the structure of intermolecular complexes and their interaction energy.

2.2 Introduction

Lone pairs are known to play a vital role in describing the chemical and biological reactivity of molecules. Classically, a lone pair is defined as valence electron pair, bound to a nucleus, not utilized in chemical bonding. The concept of localized lone pairs originates from the classical Lewis-Langmuir theory of bonding which explain covalent bonding in molecules based on the sharing of electrons in the valence shell [Langmuir 1919a; Langmuir 1919b; Lewis 1916]. Lewis dot representation of lone pairs is well-known and widely used formalism for representing covalent bonding in molecules. The role of lone pairs in determining the shape of molecules was examined by N. V. Sidgwick and H. E. Powell [Sidgwick and Powell 1940] and later by R. J. Gillespie and R. S. Nyholm [Gillespie 1963; Gillespie and Nyholm 1957] in a popular theoretical approach known as valence shell electron pair repulsion (VSEPR) model. VSEPR model is a natural extension of the electron pair model of Lewis and delineates the importance of varying electronic repulsions among shared pair and lone pair of electrons in valence shell orbitals. The concept of hybridization was introduced by Pauling in 1931 which is an essential tool useful for suggesting the presence and probable location of lone pair orbitals [Pauling 1931]. Molecular orbital (MO) theory, a popular bonding theory, in its purest form, is based on maximum amount of delocalization of MO's. Nevertheless, localization methods need to be invoked for describing a lone pair as an electron pair localized in a non-bonded valence MO [Chesnut 2003]. However, orbitals are not observables [Humphreys 1999; Scerri 2000; Zuo *et al.* 1999]. Experiments can only

provide information about observables e.g. the electron density distribution and the entities derivable from it. Thus, characterization of lone pairs in terms of physical observables, such as the molecular electron density (MED) and molecular electrostatic potential (MESP) is more realistic and appropriate. The topological features of MED remain silent in the regime of non-bonded electrons and do not provide critical points (CPs) for lone pair regions though it yields a reliable depiction of bonding between atoms in molecules. Laplacian of the electron density, $\nabla^2\rho(\mathbf{r})$, provide the physical basis for the Lewis and VSEPR models however, locating chemically significant CPs from the Laplacian distribution [Bader 1990] is difficult. Though the scalar field of electron localization function (ELF) is suggested for the study of lone pairs, [Becke and Edgecombe 1990; Chesnut 2003] it cannot provide a quantified value for the lone pair strength. Natural bond orbital (NBO) methods [Glendening *et al.* 2002; Reed *et al.* 1988; Weinhold 1998], generally regarded as a “chemist’s basis set”, are strongly orbital based and provides localized hybrid bond and lone pair orbitals instead of delocalized description of electrons. NBO analysis makes good predictions about the number of lone pairs and the percentage participation of s and p orbitals in a particular lone pair, generally in agreement with the classical hybridization concepts, but fails to predict the geometrical location of the lone pairs. Rather, it shows the occupancy in localized and delocalized MO and cannot provide a quantitative measure of lone pair strength.

The scalar field of MESP and its topographical features [Deshmukh *et al.* 2008; Gadre and Pathak 1990; Gadre and Shirsat 2000; Mathew and Suresh 2010] are the basis of the work presented in this chapter. MESP [Murray *et al.* 1994; Politzer *et al.* 1985; Pullman 1990; Sen and Politzer 1989; Sjoberg and Politzer 1990] is a well-established analytical tool for interpreting and predicting the reactive behavior of a variety of chemical systems. Tomasi *et al.* [Tomasi *et al.* 1990; Tomasi *et al.* 1996a; Tomasi *et al.*

1996b] pioneered the applications of MESP for understanding intermolecular interactions in the early 70's. Politzer and coworkers popularized MESP as an important tool to describe various chemical properties [Politzer *et al.* 1985; Politzer and Murray 2002; Politzer *et al.* 2001] such as bonding, chemical reactivity, inductive effect and resonance. In the methods developed by Politzer and coworkers, the positive and negative regions, generated by texturing the MESP on molecular surface have been used for identifying the sites of nucleophilic and electrophilic attack respectively. In a number of studies, Gadre and coworkers [Balanarayan *et al.* 2007; Deshmukh *et al.* 2008; Sundararajan *et al.* 2002; Yeole and Gadre 2011] have shown that by studying the topographical features of MESP, quantitative information about electron-rich regions corresponding to lone pairs or π -bonds in molecules can be obtained. The most negative value of the MESP (V_{\min}) in the lone pair region or π -electron region is used as a measure of the electron-rich character of the corresponding region [Gadre *et al.* 1992; Mathew *et al.* 2007; Politzer and Murray 2002; Politzer *et al.* 2001; Suresh 2006; Suresh *et al.* 2008]. On the basis of electrostatic properties of the interacting molecules, Gadre and coworkers developed the electrostatic potential for intermolecular complexation (EPIC) model [Gadre *et al.* 1996; Gadre and Pundlik 1997; Pundlik and Gadre 1997] for predicting the orientation and interaction energies of weak molecular complexes. MESP analysis is also utilized in several other studies for identifying lone pair regions as well as to study molecular interactions [Gadre *et al.* 1992; Politzer and Murray 2002; Politzer *et al.* 2001]. MESP is calculated rigorously by using Eq. 1.67 presented in Chapter 1.

Electron-deficient aromatic rings often with halo-, nitro- and cyano- substituents have an inherent tendency to interact with lone pairs of neutral molecules and anions giving rise to lone pair- π or anion- π interactions [Hernández-Trujillo and Vela 1996; Laidig 1991]. A thorough understanding of the energetic and geometric features of lone

pair- π interactions is of prime importance in the design and development of hosts that exhibit anion and lone pair recognition property. MESP has been extensively applied for obtaining quantitative description of cation- π interactions. [Ma and Dougherty 1997; Mecozzi *et al.* 1996a; Mecozzi *et al.* 1996b; Sayyed and Suresh 2011] However, the utility of this property in the study of lone pair- π /anion- π interactions in general yet remains to be explored. The main aim of this work is to characterize and quantify lone pairs of molecules using MESP and then show that a great deal of information regarding the structure and interaction energy of lone pair bearing molecules with electron-deficient π -systems can be understood in terms of MESP topographical features. To do this study in a systematic way, the lone pair regions of a large variety of neutral, radical and anionic systems need to be investigated on the basis of V_{\min} . Further, a V_{\min} based approach is proposed for quantifying the lone pair- π /anion- π interaction energy. This approach is validated by modeling interactions of lone pair bearing molecules with electron-deficient aromatic host molecules, *viz.* hexafluorobenzene (HFB), 1,3,5-trinitrobenzene (TNB), 2,4,6-trifluoro-1,3,5-triazine or cyanuric fluoride (CNF) and 1,2,4,5-tetracyanobenzene (TCB). Figure 2.1 presents the MESP textured on the 0.003 au electron density surface of HFB, TNB, CNF and TCB demonstrating their electron-deficient nature.

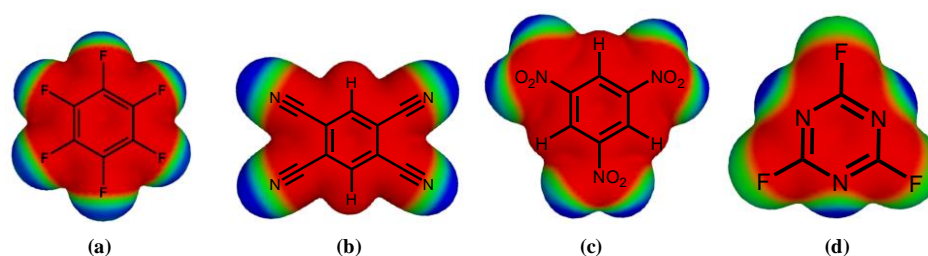



Figure 2.1 MESP textured on the 0.003 au electron density surface for (a) HFB, (b) TCB, (c) TNB and (d) CNF demonstrating the electron deficient nature of the aromatic rings. Color coding,  blue -0.01 au to red 0.01 au.

2.3 Computational Methods

Geometries of the monomers and lone pair- π complexes are fully optimized at M06-L [Zhao and Truhlar 2006] DFT functional employing 6-311++G(d,p) basis set without any symmetry constraints. Frequency calculations are performed to ensure that all the structures correspond to true energy minima containing only positive frequencies. Interaction energies of the complexes are calculated by using the supermolecule approach which gives the difference between the total energy of the complex and the sum of the isolated monomers. The computed interaction energies are corrected for basis set superposition error (BSSE) by using the counterpoise technique [Boys and Bernardi 1970]. Gaussian09 suite of programs [Frisch *et al.* 2010] is employed for all the calculations. Topological properties of molecular electron density (MED) at the bond critical points (BCP) are obtained by AIM methodology as implemented in AIM2000 program [Biegler-König and Schönbohm 2002; Biegler-König *et al.* 2001]. MESP topographical analysis of the monomers are carried out using the wave function obtained at M06L/6-311++G(d,p) level.

The location and characterization of the MESP CP is carried out using the Rapid topography mapping Fortran code developed recently by Gadre *et al.* [Yeole *et al.* 2012]. The hierarchy of their scalar field, *viz.* bare nuclear potential (BNP), molecular electron density (MED) and MESP is used for building the topography. The critical points of BNP, obtained by optimization of BNP grid points, serve as guess points for generating MED CPs. These MED CPs along with points generated inside a cube around each nuclei serve as guess points for generating MESP CPs. Guess points are optimized using L-BFGS code [Morales and Nocedal 2011]. The topography of MESP is much richer than that of BNP and MED scalar fields in terms of chemically significant CPs. The deformed atoms in molecules (DAM) procedure proposed by Rico and López *et*

al. [López *et al.* 2009; Rico *et al.* 2005; Rico *et al.* 2004] is implemented for evaluating MED and MESP and corresponding gradients at guess point during optimization. The DAM method, based on partitioning of scalar field into atomic contributions, provides a rapid and sufficiently accurate function and gradient calculation.

Topographical analysis of MESP has been carried out for locating the MESP minima for a set of 34 molecules comprising of neutral species (H_2O , N_2 , CO_2 , H_2CO , H_2S , HCN , NCCH_3 , HF , HCl , CH_3OH , PH_3 , $\text{O}(\text{CH}_3)_2$, $\text{N}(\text{CH}_3)_3$, NH_2COH , N_3H , pyrimidine, pyridine, furan, imidazole and pyrazine), anions (Cl^- , H_2PO_4^- , Br^- , NO_3^- , F^- , CH_3CO_2^- and HCO_2^-) and free radicals (OH^\bullet , $\text{CH}_3\text{O}^\bullet$, $\text{CH}_3\text{OO}^\bullet$, HCO^\bullet , $\text{CH}_3\text{CO}^\bullet$, $\text{CH}_3\text{NH}^\bullet$ and HOO^\bullet). By mapping the MESP topography, the electronic distribution of molecules is understood through the critical points (CPs), *viz.* those points in space at which all the partial derivatives of MESP vanish. There are four types of non-degenerate critical points for MESP with rank 3, *viz.* (3, -3), (3, -1), (3, +1) and (3, +3). Herein (3, +3) is referred to as local minimum (V_{\min}) while (3, -1) and (3, +1) are saddle points and (3, -3) is a local maximum. More details of MESP CP's are given in Chapter 1.

2.4 Results and Discussion

2.4.1 MESP Topography to Quantify Lone Pairs

MESP isosurfaces and minima of some representative systems are presented in Figure 2.2. The MESP topography features of neutral molecules are summarized in Table 2.1. Those of radicals and anions are reported in Table 2.2. Since the MESP minimum corresponds to a point at which electrostatic potential due to the electron density term dominates maximally over the bare nuclear term, the location of it indicates the electron-dense region of a molecule.

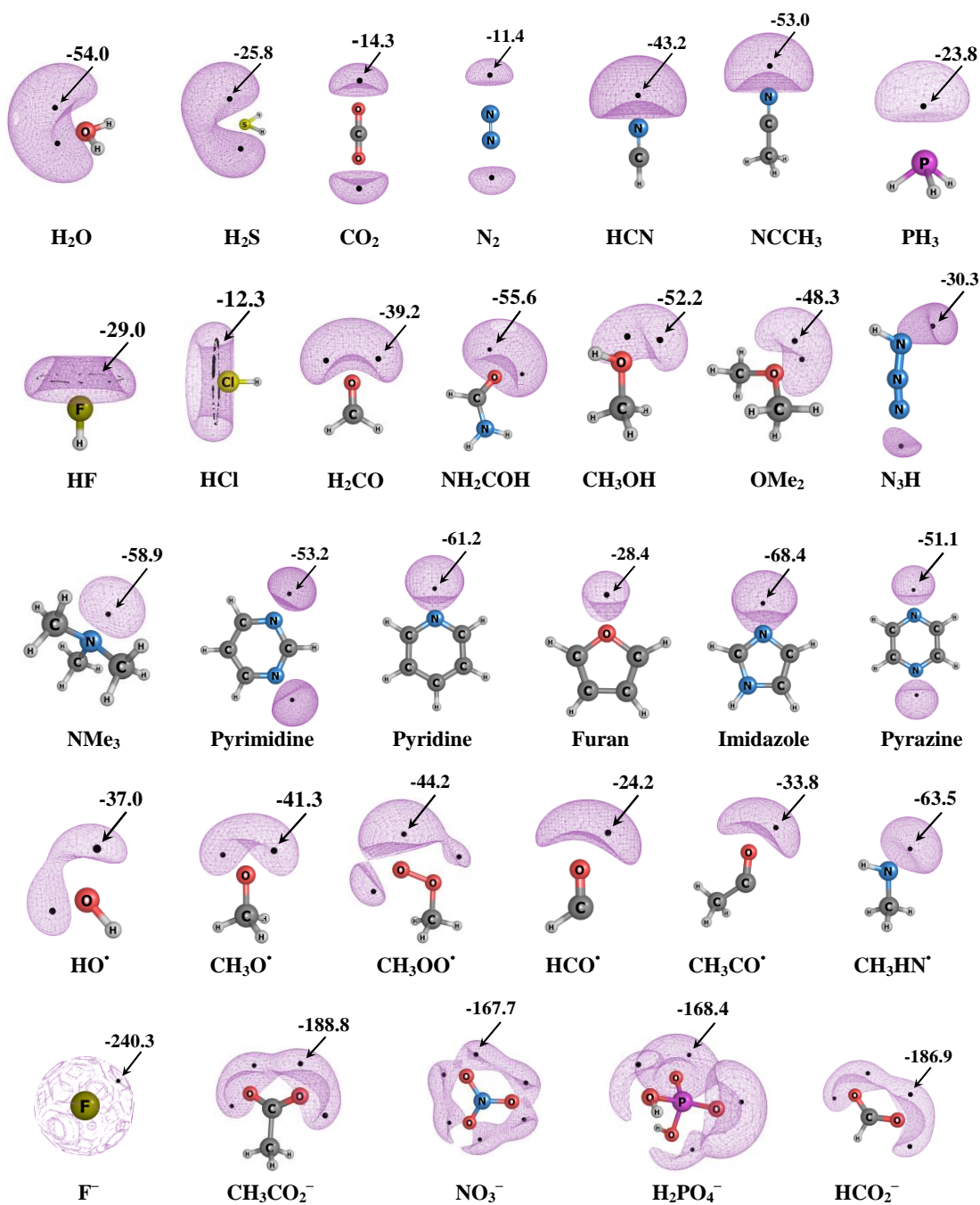


Figure 2.2 Representation of molecular electrostatic potential (MESP) isosurfaces for a representative set of lone pair species. The MESP minima are marked as black dots and the corresponding V_{\min} values are given in kcal/mol.

For the molecules given in Figure 2.2, MESP minima appear in the lone pair region. H_2O and H_2S are characterized by two such minima, one above and one below the plane of these molecules. For water, V_{\min} is -54.0 kcal/mol, which is 28.2 kcal/mol

more negative than that of H₂S. This indicates that oxygen lone pairs of water are highly electron-rich compared to those of H₂S. Although lone pair regions of HCN, pyridine, furan, imidazole, pyrazine etc. are easily recognized in the MESP topography, cases such as HCl and HF exhibit a degenerate ring of negative potential at the halogen end [Gadre *et al.* 1992; Gadre and Shirsat 2000; Murray and Sen 1996] suggesting a delocalized distribution of lone pair electrons around the halogen atom (Figure 2.2). MESP topography of F⁻, Br⁻ and Cl⁻ reveals a sphere of negative potential around the ions.

Among all the systems discussed here, fluoride anion (F⁻) exhibits the deepest V_{\min} (-240.3 kcal/mol) while the least negative V_{\min} (-11.4 kcal/mol) is observed for N₂. Imidazole has the most negative V_{\min} value (-68.4 kcal/mol) among the aromatic heterocyclic molecules while furan has the least (-28.4 kcal/mol). Similarly CH₃NH[•] and HCO[•] display the most (-63.5 kcal/mol) and the least (-24.2 kcal/mol) negative V_{\min} among free radicals, respectively. It may be noted that MESP topography reveals (3, +3) CPs in the π -electron regions of molecules as well in addition to the CPs corresponding to the lone pair regions. For instance, furan and imidazole possess one CP each above and below the C=C bond.

For all the (3, +3) CPs of MESP one of the three eigenvalues is significantly more positive compared to the other two. For instance, in the case of H₂O, among the three eigenvalues of the Hessian matrix (0.0064, 0.0327, 0.1304), the last one, *viz.* 0.1304 au is considerably more positive than the other two. The eigenvalues of NO₃⁻ (0.1769, 0.0330, 0.0148) at the deepest minimum of MESP also show a similar character with one value being considerably larger. It is noticed that for the above systems, generally one of the eigenvalues of the Hessian is at least 5 times larger than the other two. It is also seen that the eigenvalues become more positive when V_{\min} becomes more negative. Figure 2.3 depicts a linear relationship between V_{\min} and the largest eigenvalue (LE) at the

minimum. Good linear correlations for anions and neutral molecules with approximate correlation coefficient values of 0.93 and 0.94 respectively, are observed. The largest eigenvalue and corresponding eigenvector of the Hessian at the minima are shown to distinguish lone pair regions from the other types of electron localization (such as π -bonds). It has been shown that magnitude of eigenvalue at the CP that corresponds to lone pair, is numerically greater than 0.025 au and the eigenvector associated to it nearly points in the direction (angle $\leq 5^\circ$) of the atom on which it is localized [Kumar *et al.* 2014].

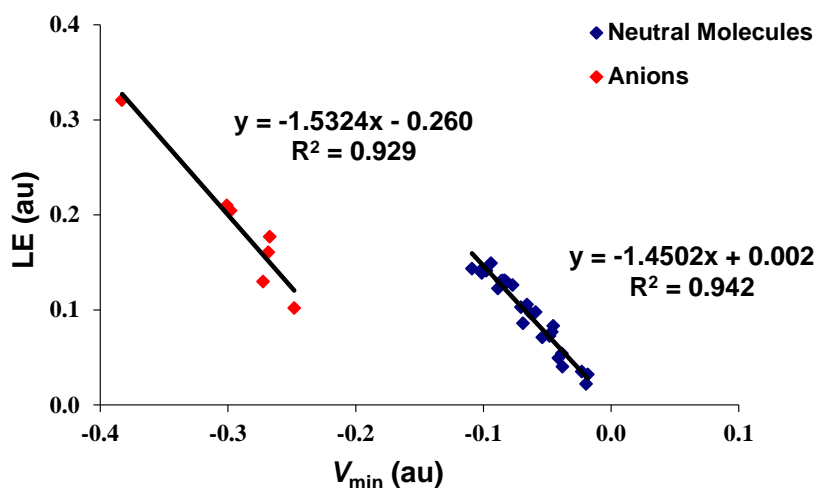


Figure 2.3 Correlation between MESP minimum (V_{\min}) and the largest eigenvalue (LE).

MESP analysis shows that the position of negative-valued minimum is useful for characterizing the region of non-bonded electrons in the molecule. Since V_{\min} value indicates the interaction energy of the molecule with a test positive charge at that location and an increase in the negative character of V_{\min} value suggests higher electron concentration at that region, V_{\min} value would qualify as a good parameter for quantifying the strength of a lone pair. This hypothesis is tested by studying the interactive behavior of all the lone pair bearing molecules with electron-deficient aromatic π -systems.

Table 2.1 MESP topography features of neutral molecules.

System	CP	No .of CPs	Distance of CP from lone pair atom (Å)	Location of CP	V_{\min} (kcal/mol)	Largest eigenvalue, LE (au)
H ₂ O	(3,+3)	2	1.24	One above and one below the plane of the molecule forming a tetrahedral structure.	-54.0	0.1304
N ₂	(3,+3)	2	1.54	Along the internuclear axis close to N atom.	-11.4	0.0320
CO ₂	(3,+3)	2	1.48	Along the internuclear axis close to O atom.	-14.3	0.0350
H ₂ CO	(3,+3)	2	1.29	Two on each side of the C2 axis close to the O atom.	-39.2	0.0960
H ₂ S	(3,+3)	2	1.78	One above and one below the plane of the molecule.	-25.8	0.0491
HCN	(3,+3)	1	1.37	Along the internuclear axis near the N atom.	-43.2	0.0858
NCCH ₃	(3,+3)	1	1.34	Along the internuclear axis near the N atom.	-53.0	0.1429
HF	Degenerate ring	-	1.30	Degenerate ring 1.30 Å away from the F end	-29.0	0.0769
HCl	Degenerate ring	-	1.90	Degenerate ring 1.90 Å away from the Cl end	-12.3	0.0219
CH ₃ OH	(3,+3)	2	1.24	Two CPs equidistant from the O atom forming 117.5° with the OH bond.	-52.2	0.1310
PH ₃	(3,+3)	1	1.88	Along the C3 axis near the P atom	-23.8	0.0403
O(CH ₃) ₂	(3,+3)	1	1.24	One above and one below the plane of the molecule near the O atom.	-48.3	0.1260

 -- Table 2.1 continued --

N(CH ₃) ₃	(3,+3)	1	1.26	Along the C3 axis close to the N atom.	-58.9	0.1491
NH ₂ COH	(3,+3)	4	1.25	Two CPs in the plane of the molecule near the O atom, two CPs above and below the plane at 1.60 Å from the N atom.	-55.6	0.1223
Pyrimidine	(3,+3)	2	1.29	One CP corresponding to each N atom lying in the plane of the molecule.	-53.2	0.1309
Pyridine	(3,+3)	1	1.28	One CP in the molecular plane at close to the N atom.	-61.2	0.1411
Furan	(3,+3)	5	1.31	One CP on the C2 axis near the O atom, one CP each above and below each C=C bond.	-28.4	0.0832
Imidazole	(3,+3)	3	1.28	One CP on the C2 near the N atom, one CP each above and below the C=C bond.	-68.4	0.1433
Pyrazine	(3,+3)	2	1.29	On the C2 axis at 1.29 Å from each N atom	-51.1	0.1291
N ₃ H	(3,+3)	2	1.41	One CP for each terminal N atom at 1.41 Å and 1.50 Å respectively.	-30.3	0.0725

Table 2.2 MESP topography features of radicals and anions.

System	CP	No .of CPs	Distance of CP from lone pair atom (Å)	Location of CP	V_{\min} (kcal/mol)	Largest eigenvalue, LE (au)
HO•	(3,+3)	2	1.29	One above and one below the plane of the molecule near the O atom.	-37.0	0.0975
CH ₃ O•	(3,+3)	2	1.28	One above and one below the C2 axis near the O atom.	-41.3	0.1056
CH ₃ OO•	(3,+3)	3	1.28	Two CPs in the molecular plane at 1.28 Å from the radical O and one CP on the adjacent O atom.	-44.2	0.1029
HCO•	(3,+3)	2	1.40	One CP in the molecular plane at 1.40 Å from the O atom and one CP on the adjacent C atom.	-24.2	0.0541
CH ₃ CO•	(3,+3)	2	1.35	One CP in the molecular plane at 1.35 Å from the O atom and one CP on the C atom.	-33.8	0.0711
CH ₃ NH•	(3,+3)	1	1.29	One CP above the C-N plane at 1.29 Å from the N atom and 123.6° with the NH bond.	-63.5	0.1387
HOO•	(3,+3)	3	1.29	Two CPs in the plane of the molecule near the radical O atom and one CP 1.40 Å from the adjacent O atom.	-38.9	0.0186
F ⁻	Degenerate surface	-	1.08	Degenerate surface at 1.08 Å from F atom.	-240.3	0.3205
CH ₃ CO ₂ ⁻	(3,+3)	4	1.15	Two CPs each on both sides of each O atom.	-188.8	0.2099

 -- Table 2.2 continued --

HCO ₂ ⁻	(3,+3)	4	1.16	Two CPs each on both sides of each O atom.	-186.9	0.2045
NO ₃ ⁻	(3,+3)	6	1.20	Two CPs each on both sides of each O atom.	-167.7	0.1769
Cl ⁻	Degenerate surface	-	1.57	Degenerate surface at 1.57 Å from Cl atom.	-171.0	0.1298
Br ⁻	Degenerate surface	-	1.74	Degenerate surface at 1.74 Å from Br atom.	-155.7	0.1019
H ₂ PO ₄ ⁻	(3,+3)	4	1.19	One CP corresponding to each O atom.	-168.4	0.1606

2.4.2 Lone Pair- π Complexes

Hexafluorobenzene (HFB) is employed as a model of an electron-deficient arene system to study lone pair- π complexes. HFB is widely utilized in the literature for the study of lone pair- π interactions and is an important binding motif used in the design of lone pair/anion sensors and receptors [Alkorta *et al.* 2002; Amicangelo *et al.* 2012; Danten 1999; Gallivan and Dougherty 1999; Kim *et al.* 2004; Quiñonero *et al.* 2002b]. The optimized geometries of a representative set of HFB-lone pair complexes are shown in Figure 2.4. Further, the interaction energy (E_{int}), equilibrium distance between the molecule and the ring centroid (R_{hfb}) and the equilibrium distance between the molecule and the nearest ring carbon atom (R_{c}) are reported in Table 2.3 for all the HFB:lone pair complexes.

In lone pair- π interactions, the lone pair should get electrostatically attracted towards the electron-deficient region of the π -system. The ring centroid of HFB is deficient of electrons due to electron withdrawing property of fluorine. Hence lone pair of guest molecules is expected to orient towards the ring centroid of HFB. However, in certain cases, slightly different orientations may be expected owing to the repulsive

interactions of the atoms of the electron-rich guest molecules with the atoms of the HFB ring. Previous studies have shown that HFB offers two binding motifs for noncovalent interaction of lone pairs; one above the centroid of the ring and the second closer to the periphery of the ring [Hay and Bryantsev 2008]. The orientation of the interacting molecules with respect to the HFB ring in the lone pair- π complexes can be explained on the basis of the topographical information of the binding molecule *i.e.*, from the location of their CPs.

Lone pair- π complexes formed by molecules with two lone pairs, *viz.* H₂S, OMe₂ and OH[•] exhibit off-center geometry with only one of the two lone pairs oriented towards the ring center. In molecules such as N₂, CO₂, HCN, N(CH₃)₃, NCCH₃, PH₃ and in all heterocyclic compounds, the lone pair is located exactly above the ring centroid. Similarly HF, HCl and the F⁻, Br⁻ and Cl⁻ anions also lie exactly above the ring centroid of HFB since their lone pairs are symmetrically distributed as degenerate rings/spheres. The remaining anions (H₂PO₄⁻, NO₃⁻, CH₃CO₂⁻ and HCO₂⁻) have more than four lone pairs and they form off-center complexes with HFB so as to generate maximum lone pair- π interaction energy. The lone pairs present on O in HCO[•] and O in CH₃CO[•] interact directly above the ring centroid of HFB. Thus the directionality of the lone pair- π interaction is determined by the strength as well as the location of the lone pairs as revealed in the MESP topography.

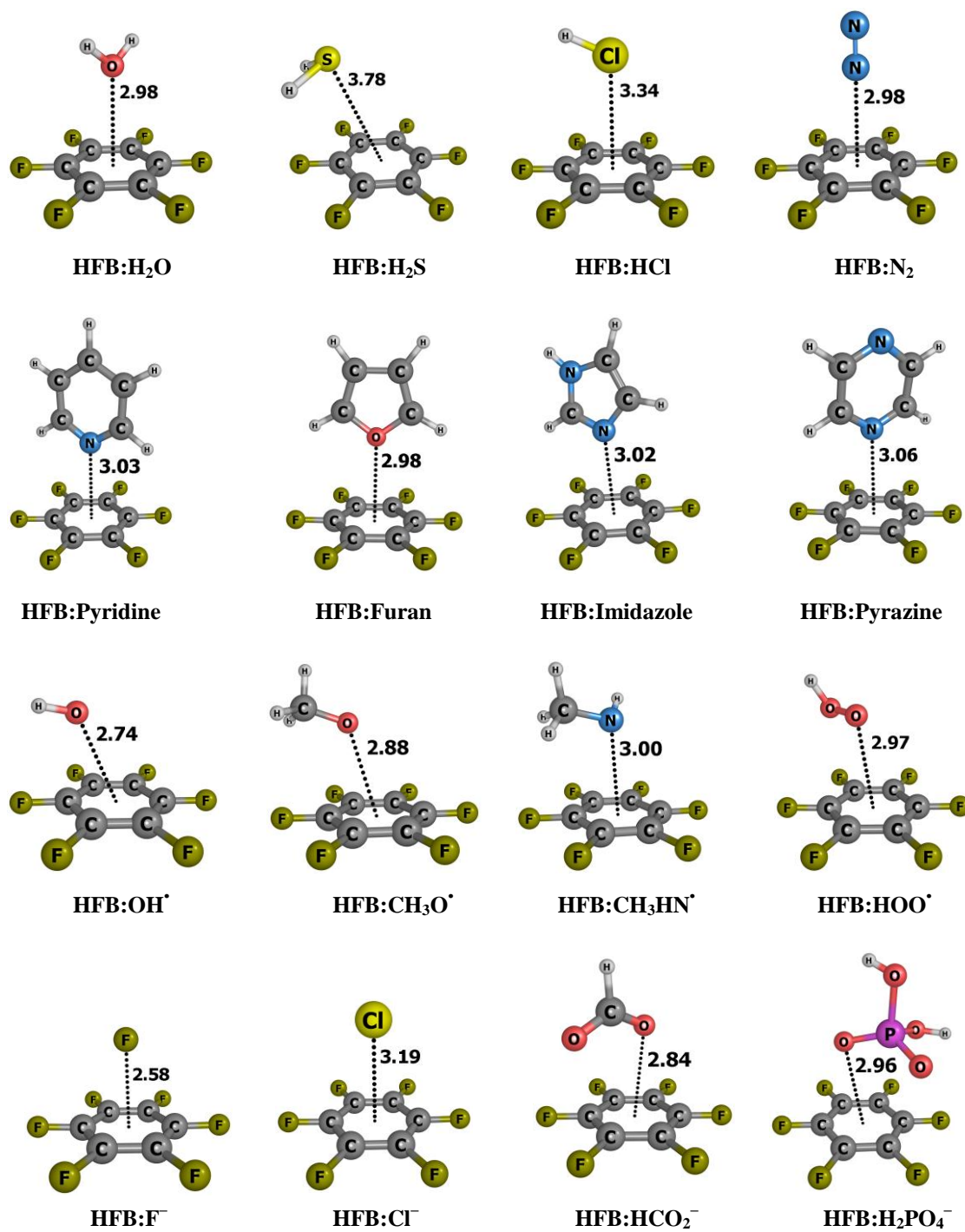


Figure 2.4 Optimized geometries of HFB-lone pair complexes at M06-L/6-311++G(d,p)

level along with the interaction distances in Å.

Table 2.3 Interaction energies (E_{int}) and distance parameters (R_{hfb} and R_{c}) for the lone pair- π complexes of HFB.

System	E_{int} (kcal/mol)	R_{hfb} (Å)	R_{c} (Å)	θ (deg)	θ' (deg)	$\Delta\theta$ (deg)
H ₂ O	-3.1	2.98	3.28	119.8	124.3	4.5
N ₂	-1.0	2.98	3.28	180.0	179.8	-0.3
CO ₂	-1.5	3.15	3.29	180.0	173.0	-7.0
H ₂ CO	-2.7	2.97	3.27	131.3	174.0	42.7
H ₂ S	-2.5	3.78	3.50	102.5	85.8	-16.7
HCN	-3.1	3.02	3.28	180.0	164.5	-15.5
NCCH ₃	-3.8	2.97	3.25	180.0	175.4	-4.6
HF	-2.3	3.08	3.37	^a	-	-
HCl	-1.7	3.34	3.61	^a	-	-
CH ₃ OH	-3.6	2.99	3.17	117.6	125.4	7.8
PH ₃	-2.1	3.47	3.73	123.3	123.9	0.6
O(CH ₃) ₂	-4.8	2.96	3.24	121.3	104.9	-16.3
N(CH ₃) ₃	-5.5	2.94	3.24	107.9	107.7	-0.2
NH ₂ COH	-3.9	2.89	3.09	138.2	169.8	31.6
Pyrimidine	-3.7	3.06	3.35	121.6	122.1	0.5
Pyridine	-4.3	3.03	3.32	121.6	121.5	-0.1
Furan	-2.5	2.98	3.28	126.6	126.5	-0.2
Imidazole	-4.6	3.02	3.23	127.8	137.6	9.8
Pyrazine	-3.7	3.06	3.35	122.2	120.8	-1.4
N ₃ H	-2.0	2.97	3.27	179.7	176.1	-3.6
HO [•]	-4.5	2.74	2.51	118.7	121.5	2.8
CH ₃ O [•]	-4.1	3.01	3.11	124.2	125.1	1.0
CH ₃ OO [•]	-5.1	3.01	3.30	107.6	96.4	-11.2
HCO [•]	-1.9	2.97	3.25	141.3	175.2	34.0

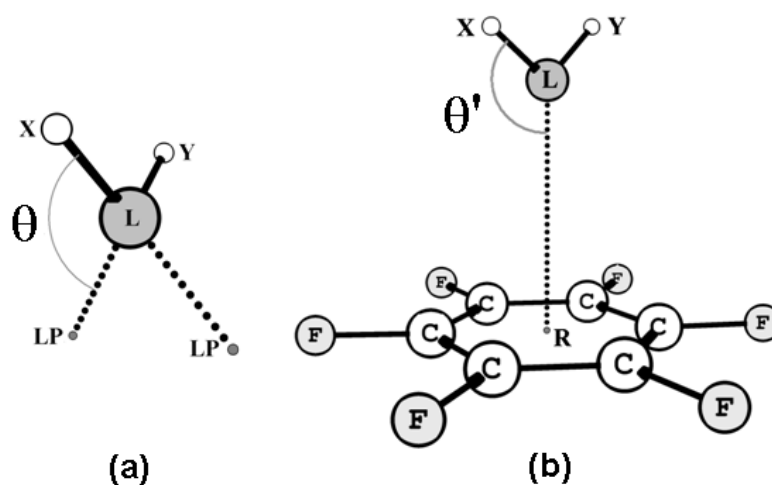
-- Table 2.3 continued --

CH ₃ CO [•]	-2.5	2.97	3.25	135.9	167.0	31.1
CH ₃ NH [•]	-4.2	3.00	3.20	123.6	126.9	3.3
HOO [•]	-3.0	2.97	3.11	120.5	96.2	-24.3
F ⁻	-21.1	2.58	2.89	- ^a	-	-
CH ₃ CO ₂ ⁻	-17.5	2.83	3.02	110.7	106.6	-4.1
HCO ₂ ⁻	-17.2	2.84	3.01	111.2	105.6	-5.6
NO ₃ ⁻	-14.3	2.80	3.04	107.1	86.4	-20.7
Cl ⁻	-14.5	3.19	3.46	- ^a	-	-
Br ⁻	-13.0	3.37	3.58	- ^a	-	-
H ₂ PO ₄ ⁻	-15.0	2.96	2.99	124.2	93.7	-30.5

^a HCl, HF, F⁻, Br⁻ and Cl⁻ exhibit degenerate CPs and hence θ , θ' and $\Delta\theta$ could not be calculated.

The extent to which a lone pair is oriented towards the ring center can be quantified if we compare the orientation of the lone pair in the free molecule with the final geometry of the lone pair- π complex. This is demonstrated in Scheme 2.1 where θ indicates the angle that the lone pair makes with the atom bearing the lone pair and a nearby atom in the monomer. Similarly, θ' indicates the angle that the centroid of the HFB makes with the lone pair bearing atom and the nearby atom. The difference between these two angles ($\theta' - \theta$) designated as $\Delta\theta$, gives a good measure of the orientation of the lone pair in the complex. From $\Delta\theta$ values, it is clear that in most of the complexes the lone pairs are oriented more or less towards the ring centroid. For instance, cases like PH₃, N(CH₃)₃, pyridine, furan, N₂, pyrimidine and CH₃O[•] have $\Delta\theta$ less than 1° indicating that the lone pair is almost perfectly aligned towards the center of the ring. Molecules such as H₂CO, CH₃CO[•], HCO[•], HOO[•], NO₃⁻ and H₂PO₄⁻ show $\Delta\theta$ values in the range 20-30°. Since these molecules contain more than two lone pairs, an optimum

configuration will maximize interactions from all the lone pairs with the HFB ring and hence the lone pairs may not necessarily point towards the centroid.



Scheme 2.1 Representation of (a) arrangement of lone pairs in a molecule and (b) orientation of the molecule in a lone pair- π complex. L denotes the atom bearing the lone pair, X and Y are the atoms bonded to L. LP is the location of the lone pair, R is the ring centre, θ is the angle which the lone pair makes with L and the nearest atom X and θ' is the angle between L, X and R.

The above discussion confirms that MESP topography analysis allows the theoretical prediction of the strength and location of lone pairs and the directionality of lone pair- π interactions. The interaction energies (E_{int}) of lone pair- π complexes range from very small in neutral molecules (N_2 and CO_2) to very large in anions (F^- and H_2PO_4^-). F^- exhibits the most stable interaction ($E_{\text{int}} = -21.1$ kcal/mol) while N_2 shows the weakest interaction ($E_{\text{int}} = -1.0$ kcal/mol). All the heteroaromatics show significant lone pair- π interaction with HFB and among them, imidazole exhibits the strongest interaction (-4.6 kcal/mol) and furan the weakest (-2.5 kcal/mol). The complex $\text{HFB}:\text{F}^-$ shows the shortest noncovalent bond distance ($R_{\text{hfb}} = 2.58$ Å) and $\text{HFB}:\text{H}_2\text{S}$ shows the longest interaction distance ($R_{\text{hfb}} = 3.78$ Å). E_{int} values suggest that HFB can be effectively used

as a lone pair sensor for a wide range of lone pair species including neutral molecules, heteroaromatics, free radicals and anions.

A quick glance at the electron density distribution of the complexes between HFB and the lone pair containing species may be obtained from Figure 2.5 which depicts MESP textured on to a 0.003 au electron density surface for some representative cases. This type of MESP plots are widely employed for identifying the electrophilic and nucleophilic regions in molecules. The MESP maps clearly indicate the interaction of the electron-deficient core of HFB (red) with the electron-rich lone pair/anion region (blue) giving rise to lone pair/anion- π interaction. Moreover, the MESP pictures provide a qualitative measure of the lone pair/anion- π interactions, analogous to the observations for cation- π interactions [Mecozzi *et al.* 1996a; Mecozzi *et al.* 1996b]. However, unlike the MESP topographical analysis, such plots cannot provide quantitative information about lone pairs or lone pair- π interactions.

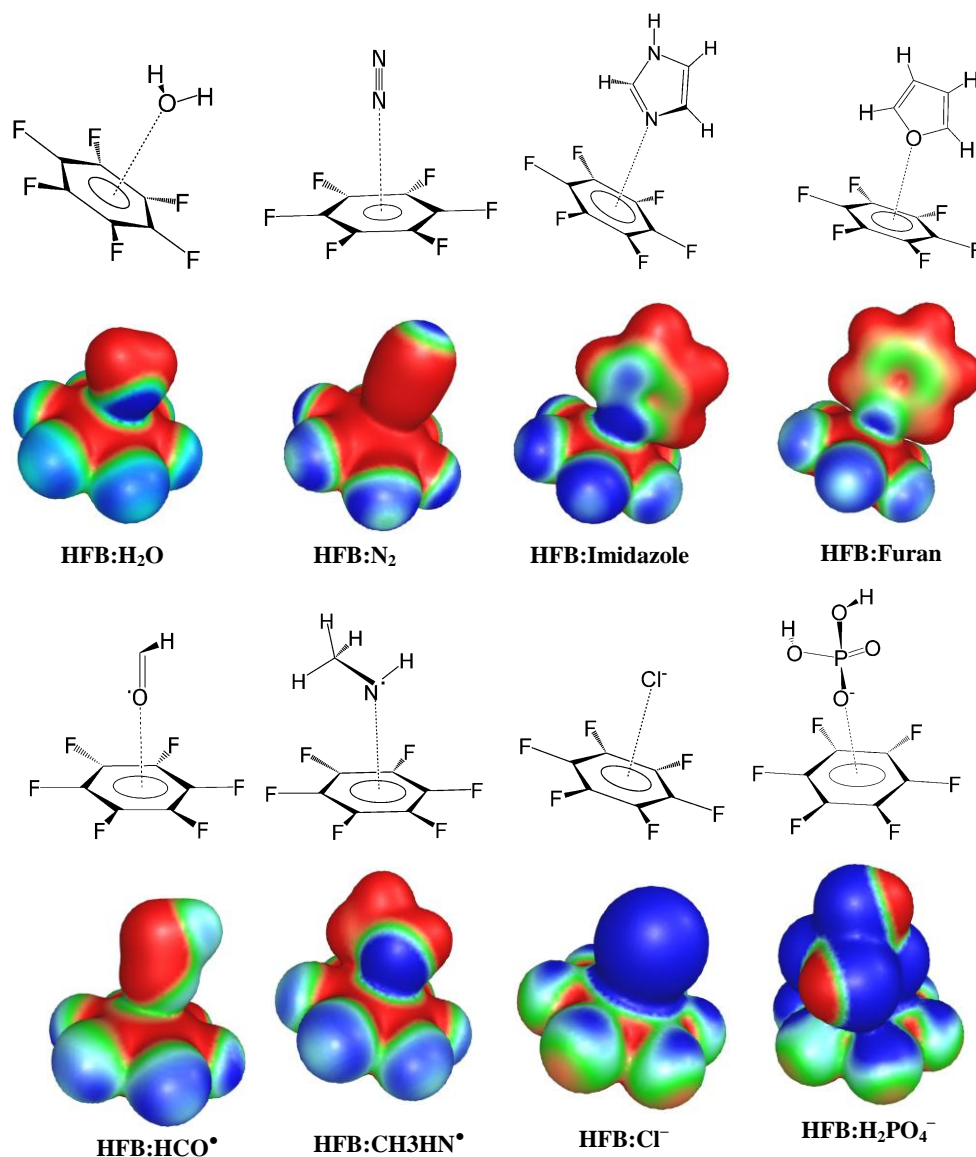


Figure 2.5 Molecular electrostatic potential textured on the 0.003 au electron density surface for HFB-lone pair complexes. Color coding blue -0.02 au to red 0.02 au for neutral and free radicals and blue -0.14 au to red -0.1 au for anionic species.

2.4.3 Electron Density Analysis

Topographical properties of molecular electron density (MED) are often employed for studying the interactive behavior, particularly the bonding features of molecules. Though a lone pair indicates an electron-rich region, MED analysis will not yield a critical feature at that site and hence it will not provide the location of a lone pair in a molecule. In this respect, MESP topography is more advantageous than MED

topography to locate non-bonded electrons in a molecule. However, MED analysis is useful for the study of bonded regions of a lone pair- π complex. It has been demonstrated [Garau *et al.* 2003] for some systems that the electron density, $\rho(\mathbf{r})$ and Laplacian of the electron density $\nabla^2\rho(\mathbf{r})$ at CPs are useful for characterizing bonding interactions. Figure 2.6 presents the AIM molecular graphs of HFB-lone pair complexes demonstrating bond paths, BCPs and CCPs.

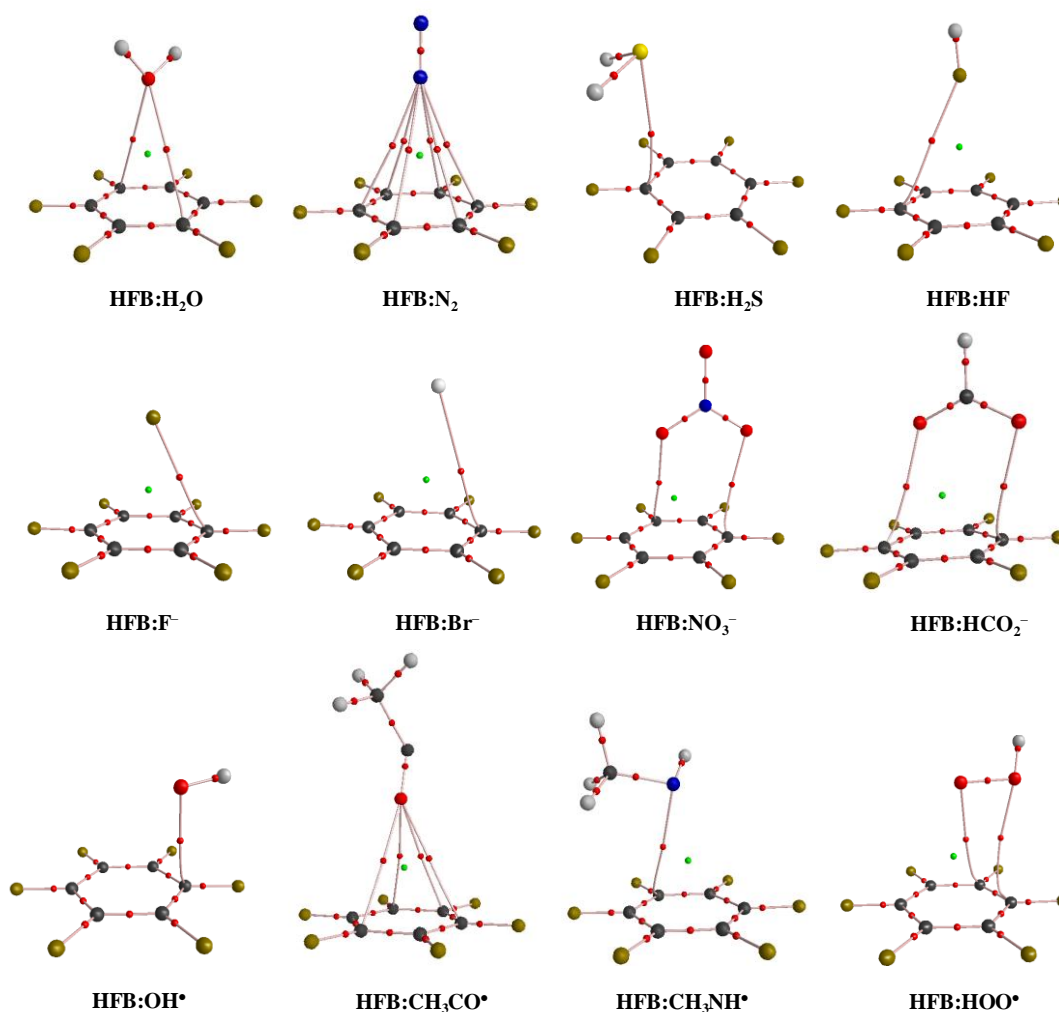


Figure 2.6 AIM molecular graphs of HFB-lone pair complexes showing the bond paths (lines) and bond critical points (red for BCPs and green for CCPs).

The presence of lone pair- π interactions in all HFB complexes is confirmed by the presence of bond critical points (BCPs) of MED which connect the atom of the lone

pair bearing molecule to at least one, several or all the ring carbon atoms of HFB. Previous studies [Bauzá *et al.* 2012; Garau *et al.* 2003] have suggested that cage critical points (CCPs) located along the line connecting the center of the aromatic ring and the electron-donor atom can be used as a unique feature for lone pair- π /anion- π interactions. In the present study, CCPs have been located for all the HFB complexes except HFB:H₂S, HFB:HO[•], HFB:CH₃O[•] and HFB:CH₃OO[•]. In these four complexes, the guest species is slightly displaced towards the periphery of the HFB ring and the deviation from normal behavior could be attributed to an additional interaction of the hydrogen atoms of H₂S, OH[•], CH₃O[•] and CH₃OO[•] with the fluorine atoms in the HFB. Table 2.4 lists the AIM topological features of HFB:lone pair complexes.

Table 2.4 AIM topological features of HFB:lone pair complexes

Lone pair species	No. of RCPs	No. of CCPs	$\rho(\mathbf{r})$ at BCP (au)	$\nabla^2\rho(\mathbf{r})$ at BCP (au)	$\rho(\mathbf{r})$ at CCP (au)	$\nabla^2\rho(\mathbf{r})$ at CCP (au)
H ₂ O	3	1	0.006	0.022	0.005	-0.006
N ₂	7	1	0.006	0.023	0.005	-0.006
CO ₂	2	1	0.005	0.019	0.003	-0.003
H ₂ CO	3	1	0.005	0.021	0.004	-0.005
H ₂ S	1	0	0.007	0.019	- ^a	-
HCN	2	1	0.007	0.022	0.005	-0.006
NCCH ₃	2	1	0.007	0.024	0.005	-0.006
HF	2	1	0.004	0.016	0.003	-0.004
PH ₃	7	1	0.006	0.017	0.005	-0.005
OMe ₂	2	1	0.007	0.025	0.005	-0.006
NMe ₃	5	1	0.009	0.028	0.007	-0.008
NH ₂ COH	2	1	0.008	0.030	0.005	-0.006
Pyrimidine	4	1	0.007	0.021	0.005	-0.006

-- Table 2.4 continued --

Pyridine	4	1	0.007	0.022	0.005	-0.006
Furan	4	1	0.006	0.022	0.005	-0.006
N ₃ H	3	1	0.006	0.023	0.005	-0.006
OH [•]	1	0	0.023	0.083	- ^a	-
CH ₃ O [•]	1	0	0.014	0.053	- ^a	-
CH ₃ OO [•]	3	0	0.008	0.030	- ^a	-
HCO [•]	2	1	0.005	0.020	0.004	-0.005
CH ₃ CO [•]	5	1	0.006	0.022	0.004	-0.005
CH ₃ NH [•]	2	1	0.008	0.025	0.005	-0.006
HOO [•]	3	1	0.008	0.029	0.005	-0.006
F ⁻	2	1	0.012	0.047	0.008	-0.011
CH ₃ CO ₂ ⁻	3	1	0.014	0.047	0.006	-0.008
HCO ₂ ⁻	3	1	0.013	0.044	0.006	-0.007
NO ₃ ⁻	3	1	0.013	0.045	0.006	-0.008
Br ⁻	2	1	0.007	0.022	0.005	-0.005
H ₂ PO ₄ ⁻	4	1	0.011	0.040	0.005	-0.006

^a CCPs not located

2.4.4 Correlation between V_{\min} and E_{int}

Since the strength of lone pair- π interaction depends on the electron-rich nature of the interacting lone pair which is directly reflected in the MESP value at the minimum, it should be possible that the characterization of lone pair strength using MESP may provide a simple approach to quantify lone pair- π interactions. Figure 2.7 depicts the relationship between E_{int} and V_{\min} value for complexes between HFB and the lone pair bearing molecules. An excellent linear correlation is observed between the two quantities. Small deviation shown by the systems HFB:O(CH₃)₂, HFB:HO[•] and HFB:CH₃O[•] could be due to the additional stabilization provided by the interaction of

side-chain hydrogen atoms with the fluorine atoms of HFB ring. A more negative V_{\min} corresponds to higher E_{int} . This suggests that the ability of a molecule to form a lone pair- π interaction with HFB can be assessed in terms of the V_{\min} value corresponding to the lone pair in the molecule.

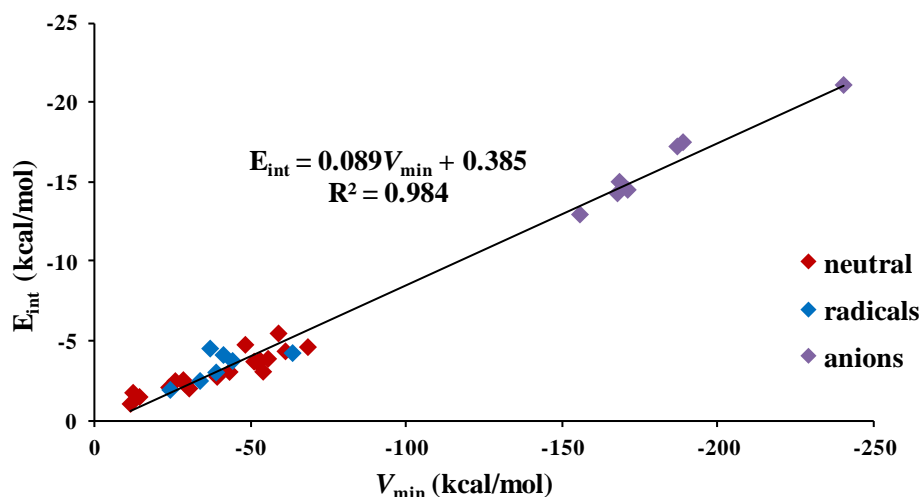


Figure 2.7 Correlation between MESP V_{\min} at lone pair region and interaction energy of the complexes between HFB and the lone pair containing species.

2.4.5 Validation of V_{\min} vs E_{int} Relationship

The relationship between V_{\min} and E_{int} is further validated by modeling lone pair- π complexes of 1,3,5-trinitrobenzene (TNB), 2,4,6-trifluoro-1,3,5-triazine or cyanuric fluoride (CNF) and 1,2,4,5-tetracyanobenzene (TCB) with a representative set of lone pair bearing molecules (H_2O , N_2 , CO_2 , H_2S , HCN , $\text{O}(\text{CH}_3)_2$, $\text{N}(\text{CH}_3)_3$, pyridine, furan, imidazole, HCO^\bullet , $\text{CH}_3\text{O}^\bullet$, Cl^- , H_2PO_4^- , Br^- , NO_3^- and HCO_2^-). Representative set of lone pair- π complexes of TNB, TCB and CNF are shown in Figure 2.8.

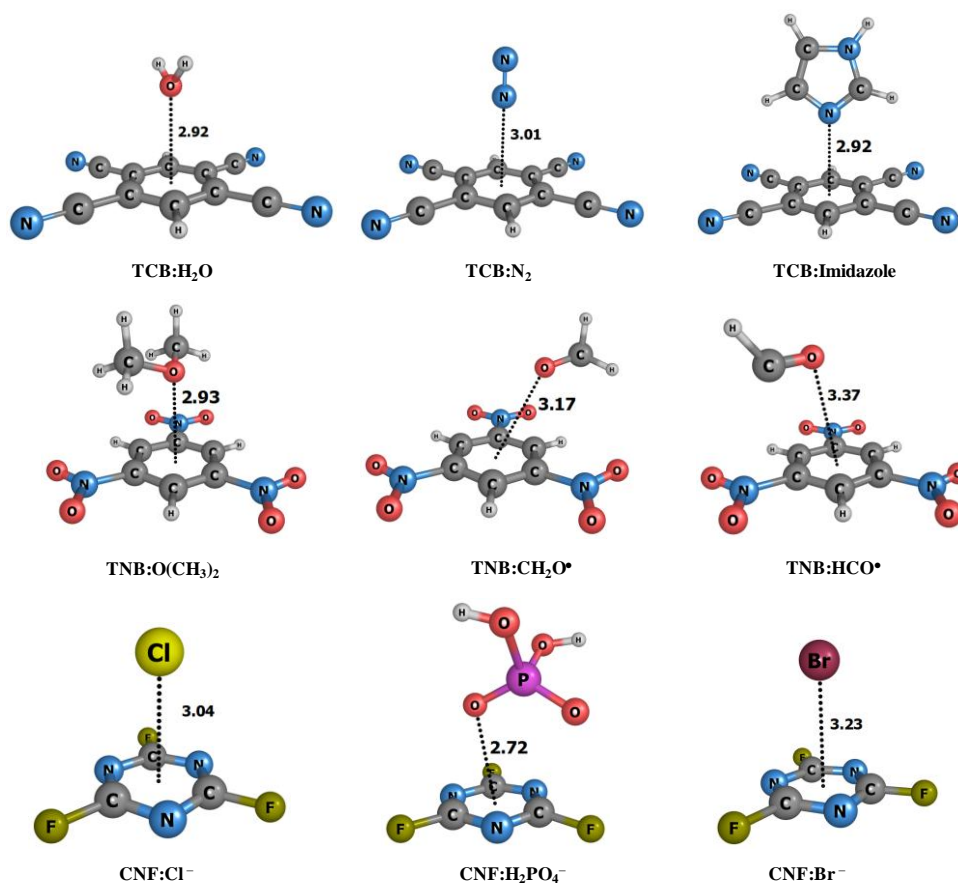


Figure 2.8 Optimized geometries of lone pair- π complexes of 1,2,4,5-tetracyanobenzene (TCB), 1,3,5-trinitrobenzene (TNB) and 2,4,6-trifluoro-1,3,5-triazine (CNF) with a representative set of lone pair bearing molecules. Distances in Å.

The correlation diagrams between E_{int} and V_{min} for TNB, CNF and TCB are depicted in Figure 2.9. The excellent linear correlation between the two quantities for all the three molecules confirms the ability of V_{min} to predict lone pair- π interaction energy. Hence, the value of MESP at the minimum, V_{min} is proposed as a useful descriptor for studying the interactive behavior of a lone pair bearing molecule with electron-deficient π -systems. The values of E_{int} , R_{hfb} , R_{c} , θ , θ' and $\Delta\theta$ for lone pair- π complexes of TCB, CNF and TNB, are given in Table 2.5, Table 2.6 and Table 2.7, respectively.

Table 2.5 Interaction energies (E_{int}), distance parameters (R_{hfb} and R_{c}) and θ , θ' and $\Delta\theta$ values for lone pair- π complexes of 1,2,4,5-tetracyanobenzene (TCB).

System	E_{int} (kcal/mol)	R_{hfb} (Å)	R_{c} (Å)	θ (deg)	θ' (deg)	$\Delta\theta$ (deg)
H ₂ O	-5.0	2.92	3.24	119.8	128.1	8.3
N ₂	-1.5	3.01	3.32	180	179.5	-0.5
CO ₂	-2.2	3.12	3.42	180	178.9	-1.1
H ₂ S	-3.1	4.32	3.68	102.5	98.1	-4.4
N(CH ₃) ₃	-7.6	3.00	3.28	107.9	133.5	25.6
O(CH ₃) ₂	-6.3	2.92	3.19	121.3	110.5	-10.8
Imidazole	-7.1	2.92	3.21	127.8	128.3	0.5
Pyridine	-6.6	2.97	3.28	121.6	121.2	-0.4
Furan	-4.6	3.17	3.29	126.6	94.6	-32.0
HCO [•]	-2.8	3.83	3.11	141.3	141.5	0.2
CH ₃ O [•]	-3.7	3.75	3.04	124.2	109.5	-14.7
H ₂ PO ₄ ⁻	-16.7	2.84	3.00	124.2	96.4	-27.8
NO ₃ ⁻	-18.6	2.77	3.06	107.1	87.6	-19.5
Cl ⁻	-16.8	3.36	2.88	^a	-	-
Br ⁻	-14.5	3.54	3.07	^a	-	-
HCO ₂ ⁻	-22.3	2.73	3.00	111.2	106.0	-5.2

^a Br⁻ and Cl⁻ exhibit degenerate CPs and hence θ , θ' and $\Delta\theta$ could not be calculated.

Table 2.6 Interaction energies (E_{int}), distance parameters (R_{hfb} and R_{c}) and θ , θ' and $\Delta\theta$ values for lone pair- π complexes of 2,4,6-trifluoro-1,3,5-triazine (CNF).

System	E_{int} (kcal/mol)	R_{hfb} (Å)	R_{c} (Å)	θ (deg)	θ' (deg)	$\Delta\theta^{\text{a}}$ (deg)
H ₂ O	-4.2	2.98	3.21	119.8	137.3	17.5
N ₂	-1.2	3.12	3.41	180	178.5	-1.5
CO ₂	-1.9	3.08	3.37	180	179.8	-0.2

-- Table 2.6 continued --

H ₂ S	-3.4	4.20	3.59	102.5	97.1	-5.4
N(CH ₃) ₃	-8.1	2.98	3.28	107.9	107.6	-0.3
O(CH ₃) ₂	-6.1	2.93	3.22	121.3	108.9	-12.4
Imidazole	-8.7	3.21	3.48	127.8	91.5	-36.3
Pyridine	-7.3	3.18	3.43	121.6	92.2	-29.4
Furan	-6.9	3.25	3.26	126.6	94.6	-32.0
HCO [•]	-3.6	3.37	3.34	141.3	96.7	-44.6
CH ₃ O [•]	-5.0	3.17	2.67	124.2	135.9	11.7
H ₂ PO ₄ ⁻	-27.9	2.81	2.93	124.2	95.5	-28.7
NO ₃ ⁻	-27.9	3.14	2.50	107.1	103.4	-3.7
Cl ⁻	-31.5	3.21	2.51	- ^a	-	-
Br ⁻	-29.4	3.41	2.72	- ^a	-	-
HCO ₂ ⁻	-34.7	2.75	3.04	111.2	98.7	-12.5

^a Br⁻ and Cl⁻ exhibit degenerate CPs and hence θ , θ' and $\Delta\theta$ could not be calculated.

Table 2.7 Interaction energies (E_{int}), distance parameters (R_{hfb} and R_{c}) and θ , θ' and $\Delta\theta$ values for lone pair- π complexes of 1,3,5-trinitrobenzene (TNB).

System	E_{int} (kcal/mol)	R_{hfb} (Å)	R_{c} (Å)	θ (deg)	θ' (deg)	$\Delta\theta^{\text{a}}$ (deg)
H ₂ O	-4.7	2.92	3.24	119.8	128.1	8.3
N ₂	-1.4	3.01	3.32	180	179.5	-0.5
CO ₂	-2.2	3.12	3.42	180	178.9	-1.1
H ₂ S	-4.2	4.32	3.68	102.5	98.1	-4.4
N(CH ₃) ₃	-8.1	3.00	3.28	107.9	133.5	25.6
O(CH ₃) ₂	-6.1	2.92	3.19	121.3	110.5	-10.8
Imidazole	-7.9	2.92	3.21	127.8	128.3	0.5
Pyridine	-6.9	2.97	3.28	121.6	121.2	-0.4
Furan	-1.1	3.17	3.29	126.6	94.6	-32.0

-- Table 2.7 continued --

HCO [•]	-5.1	3.83	3.11	141.3	141.5	0.2
CH ₃ O [•]	-6.9	3.75	3.04	124.2	109.5	-14.7
H ₂ PO ₄ ⁻	-29.5	2.84	3.00	124.2	96.4	-27.8
NO ₃ ⁻	-28.2	2.77	3.06	107.1	87.6	-19.5
Cl ⁻	-30.7	3.36	2.88	- ^a	-	--
Br ⁻	-28.6	3.54	3.07	- ^a	-	-
HCO ₂ ⁻	-34.7	2.73	3.00	111.2	106.0	-5.2

^a Br⁻ and Cl⁻ exhibit degenerate CPs and hence θ , θ' and $\Delta\theta$ could not be calculated.

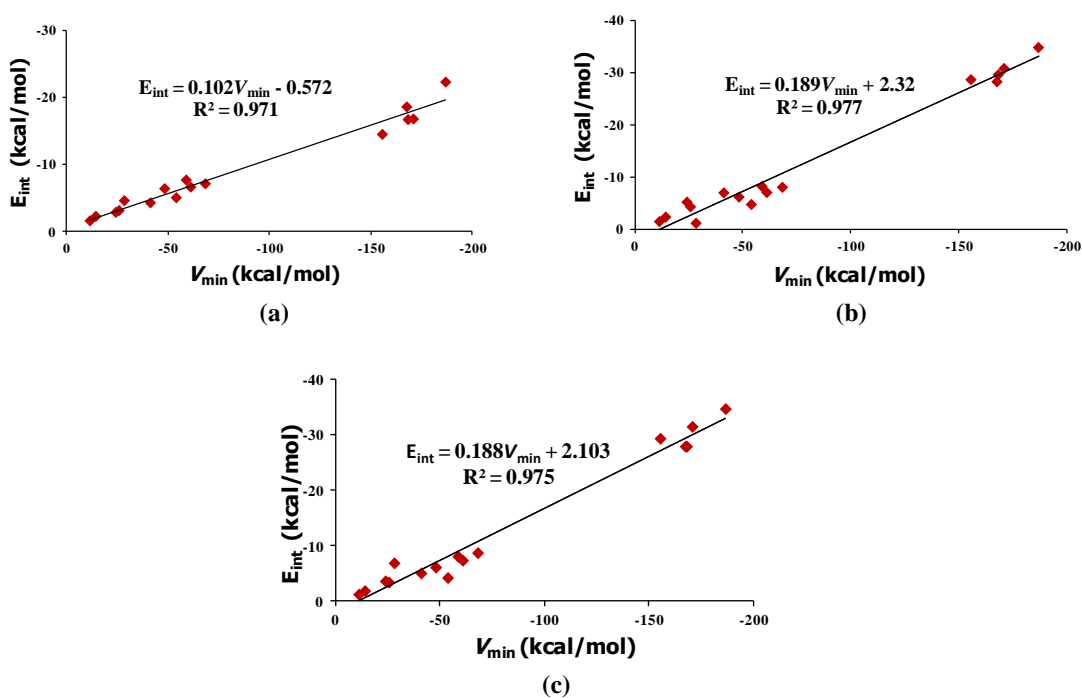


Figure 2.9 Correlation between MESP V_{\min} at lone pair region and interaction energy of the lone pair- π complexes of (a) 2,4,6-trifluoro-1,3,5-triazine (CNF), (b) 1,2,4,5-tetracyanobenzene (TCB) and (c) 1,3,5-trinitrobenzene (TNB).

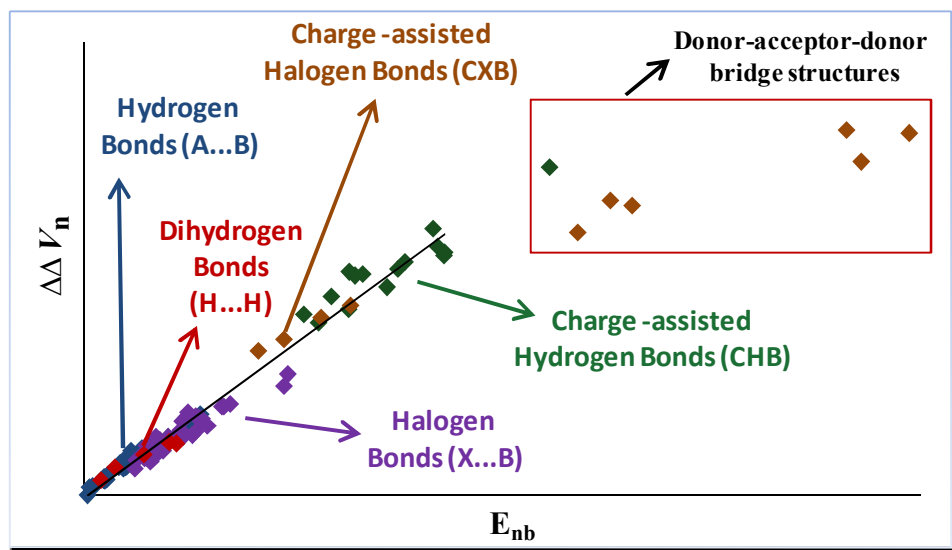
2.5 Conclusions

Lone pairs play an important role in determining the reactivity, particularly the interactive behavior of molecules with electron-deficient systems. The present study has brought out that MESP topographical analysis provides a simple and effective way to characterize the electron-rich lone pair region of a molecule. The precise location of the MESP minimum can suggest the possible location of the lone pair region and enables a prediction on the orientation of the lone pair bearing molecule when it complexes with an electron-deficient π -system. MESP value of the minimum can be used as a good descriptor to measure the strength of the interaction between the lone pair bearing molecule and an electron-deficient π -system. V_{\min} provides an *a priori* prediction on the lone pair- π interaction energy. The ability of electron-deficient aromatic rings to effectively sense a variety of lone pair bearing species is remarkable and hence highly fluorinated aromatic hydrocarbon moieties could be utilized as synthons in the design of sensors for lone pairs as well as volatile organic compounds in the atmosphere.

Chapter 3

Hydrogen Bonds, Halogen Bonds and Dihydrogen Bonds

Part A – Accurate Binding Energies and Cation Enhanced Binding Strengths
&
Part B – Molecular Electrostatic Potential Analysis of Hydrogen, Halogen, and Dihydrogen Bonds



3.1 ABSTRACT

In part A of this chapter, the interaction energies of 52 noncovalent complexes displaying hydrogen, halogen and dihydrogen bonds in the weak, medium and strong regimes have been computed at MP2, M06L and WIBD methods. Among these methods, the most accurate estimation of the noncovalent bond strength is obtained with WIBD method which shows the lowest mean absolute deviation (MAD) of the bond strength (0.19 kcal/mol) in comparison with the accurate CCSD(T) energy data reported in the literature. Compared to WIBD, MP2 underestimates interaction energies while M06L shows more accurate behavior than MP2 except for halogen and charge-assisted hydrogen bonds. Hybrid methods viz. MP4//MP2, MP4//M06L and CCSD(T)//MP2 yield interaction energies very close to those obtained from WIBD with MAD 0.14 kcal/mol, 0.16 kcal/mol and 0.27 kcal/mol, respectively. Cation complexation (Li^+ , NH_4^+) on the electron acceptor site of noncovalent complexes studied using the MP4//MP2 method shows that the polarization effect of the cation enhances more electron donation from the donor to the noncovalent bonding regions leading to substantial enhancement in the binding energy (~ 141 to 566 % for Li^+ and ~ 105 to 539 % for NH_4^+). Thus, in the presence of a cation, a noncovalent bond in the weak regime is promoted to the medium regime and that in the medium regime is promoted the strong regime.

In part B of this chapter, the nature of hydrogen bonds, halogen bonds and dihydrogen bonds in a variety of intermolecular donor-acceptor (D-A) complexes has been investigated at high level ab initio MP4//MP2 method coupled with

*Atoms in Molecules (AIM) and Molecular Electrostatic Potential (MESP) approaches. Electron density ρ at bond critical point correlates well with interaction energy (E_{nb}) for each homogeneous sample of complexes, but its applicability to the entire set of complexes is not satisfactory. Analysis of MESP minimum (V_{min}) and MESP at the nuclei (V_n) shows that in all **D-A** complexes, MESP of **A** becomes more negative and that of **D** becomes less negative suggesting donation of electrons from **D** to **A** leading to electron donor-acceptor (eDA) interaction between **A** and **D**. MESP based parameter $\Delta\Delta V_n$ measures donor-acceptor strength of the eDA interactions as it shows a good linear correlation with E_{nb} for all **D-A** complexes ($R^2 = 0.976$) except the strongly-bound bridged structures. The bridged structures are classified as donor-acceptor-donor complexes. MESP provides a clear evidence for hydrogen-, halogen- and dihydrogen bond formation and defines them as eDA interactions in which hydrogen acts as electron acceptor in hydrogen- and dihydrogen bonds while halogen acts as electron acceptor in halogen bonds.*

Part A – Accurate Binding Energies and Cation Enhanced Binding Strengths

3.2 Introduction

Hydrogen bonds, halogen bonds and dihydrogen bonds play critical roles in chemical reactivity, molecular recognition, drug-receptor binding, crystal design, self-assembly and in determining biomolecular structure [Fersht 1987; Garrett and Grisham 1995; Jeffrey and Saenger 1994; Mingos and Braga 2004; Rebek *et al.* 1987; Yap *et al.* 1995]. These noncovalent interactions have numerous properties running in parallel in terms of strength and directionality [Bent 1968; Desiraju and Parthasarathy 1989; Grabowski 2013; Kovács and Varga 2006; Legon 1998; Legon 1999]. Since these interactions exhibit a continuum of strengths [Desiraju 2002; Parthasarathi *et al.* 2006], an accurate and quantitative account of the geometries and interaction energies is required for a thorough understanding of bonding. The strength of hydrogen bonds, halogen bonds and dihydrogen bonds arise from electrostatics, polarization, charge transfer, exchange-repulsion and dispersion effects and the relative contribution from each term vary depending on the nature of the donor and acceptor molecules involved [Morokuma 1977]. Electrostatic contribution dominates the classical type of hydrogen bonding interaction, while pronounced covalent character is found in strong hydrogen bonding and a dominance of dispersive interaction is observed in weak hydrogen bonds [Gilli and Gilli 2009; Gilli *et al.* 1994; Grabowski 2011; Grabowski and Sokalski 2005]. Hence, a balanced description of all the bonding components are required for obtaining accurate interaction energies of noncovalent complexes. Advanced quantum mechanical (QM) methods, teamed up with the developments in computer hardware have made it possible to determine noncovalent interaction energies with

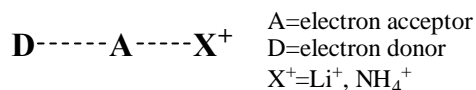
accuracy close to experimental results [Müller-Dethlefs and Hobza 2000]. Among the QM methods, density functional theory (DFT) [Hohenberg and Kohn 1964; Kohn and Sham 1965; Parr and Yang 1989] methods provide a good balance between computational cost and accuracy. Performance of DFT methods for the study of noncovalent interactions has been widely discussed and benchmarked [Hobza 2004; Thanthiriwatte *et al.* ; Zhao *et al.* 2005; Zhao and Truhlar 2005a]. Some improved DFT functionals have been recently developed [Zhao and Truhlar 2004; Zhao and Truhlar 2005b; Zhao and Truhlar 2006; Zhao and Truhlar 2008] to describe noncovalent complexes dominated by the dispersion interactions. In general, almost all the traditional local, non-local and even the highly parameterized exchange-correlation density functionals are unable to give accurate estimation of the energies of dispersion dominated complexes [Janowski and Pulay 2007; Kristyán and Pulay 1994; Perez-Jorda and Becke 1995]. Very recently, Remya and Suresh [Remya and Suresh 2013] have shown that the performance of the Minnesota functional M06L is superior to several other DFT methods implemented in Gaussian09 to obtain accurate geometry and interaction energies of noncovalent intermolecular complexes. High level *ab initio* methods accounting for electron correlation with large basis sets are recommended [Tsuzuki *et al.* 2000] for noncovalent complexes. Coupled cluster with singles and doubles including perturbative triples or CCSD(T) [Paldus *et al.* 1972; Pople *et al.* 1987] method is considered as one of the best methods to achieve chemical accuracy. However, applicability of this method is limited to the study of very small complexes owing to very high computational cost which scales to N^7 where N is the number of basis functions used. Møller-Plesset perturbation theory [Moller and Plesset 1934] to the second order (MP2) is one of the least expensive *ab initio* methods which capture a large portion of the electron correlation energy and scales to the N^5 scale on computational complexity [Raghavachari

and Anderson 1996]. If N^7 complexity is affordable, the method of choice would be the MP4 method [Raghavachari and Pople 1978] which gives accuracy close to CISD.

The main aim of this work is to obtain accurate quantitative data on interaction energies of hydrogen bonds, halogen bonds and dihydrogen bonds in a large variety of intermolecular complexes. The accurate energy data would be useful for future benchmarking of computational methods and also aid in parameterizing molecular mechanics force fields for modeling and simulation studies. Further, the effect of cations on modulating the strength of noncovalent interaction will be assessed. Cations are omnipresent in the environment as well as in the human body and they play vital roles in the structure and function of proteins and nucleic acids as well as in the catalytic processes of enzymes. Rode and coworkers investigated the influence of metal ions on neighboring hydrogen bonds and showed that polarization effects of cations can alter the donor-acceptor interactions in hydrogen bonded systems, influence the binding energies and significantly alter the equilibrium geometry of hydrogen bonds [Limtrakul *et al.* 1987; Rode 1980; Rode and Sagarik 1982; Sagarik and Rode 1981]. Rode and Sagarik showed that binding of Mg^{2+} to the O(2) atom of thymine can cause considerable hydrogen bond stabilization of the A6T pair [Sagarik and Rode 1983a; Sagarik and Rode 1983b]. Cations also exhibit crucial influence on the dynamics of proton transfer processes and it has been demonstrated that electrically charged groups in the vicinity of a hydrogen bond can have profound effects on the energetics of proton transfer within that bond, even when the ion is fairly distant from the bond [Szczesniak and Scheiner 1985]. It is well known that coexistence of two interactions can either cause the strengthening of one interaction at the expense of the other or can cause either the strengthening or weakening of both interactions [Alkorta *et al.* 2010]. In other words, cooperativity effects are present in systems where two or more noncovalent interactions

coexist [Alkorta *et al.* 2010; Frontera *et al.* 2006; Garau *et al.* 2005; Liu and Xu 2011; Mahadevi and Sastry 2014; Vijay *et al.* 2008].

This chapter presents an investigation of the interaction energies of intermolecular complexes of the type **D-A** where the bond formation leads to some amount of electron donation from **D** to **A**. The methods selected for the study are W1BD, MP2, M06L and hybrid combinations MP4//MP2, MP4//M06L and CCSD(T)//MP2. The situation where **D-A** interaction is perturbed by second noncovalent interaction provided by a cation in the vicinity of **A** (Scheme 3.1) is also probed. A comprehensive investigation of the stabilization effect of monovalent cations *viz.* Li^+ and NH_4^+ in the vicinity of the electron acceptor molecule on the **D-A** type noncovalent complexes shows that the interaction of the cation with **A** will have a profound influence on **D** to donate more electrons for the **D-A** noncovalent bond formation.



Scheme 3.1 Effect of cations on the strength of neighboring hydrogen bonds.

3.3 Computational Methods

All noncovalent **D-A** complexes are optimized at W1BD [Barnes *et al.* 2009; Martin and De Oliveira 1999; Parthiban and Martin 2001], MP2 [Moller and Plesset 1934] and M06L [Zhao and Truhlar 2006] methods. W1BD method is a variation of Weizmann-1 theory, where coupled cluster is replaced with Brueckner doubles (BD) method. The algorithm for the calculation of energy in W1BD method includes several computational steps including geometry optimization and frequency calculation at B3LYP/cc-pVTZ+d method followed by an extrapolation scheme comprising of single point calculations at BD(T)/augh-cc-pVDZ+2df, BD(T)/augh-cc-pVTZ+2df, BD/augh-cc-pVQZ+2df, BD(T)/MTSmall, BD(T,Full)/MTSmall for getting accurate energies.

Strictly speaking W1BD is not an *ab initio* method since its empirical parameter is derived from W2 calculations and not from experiments. It is more expensive, accurate and a recommended method for obtaining very accurate energies [Barnes *et al.* 2009; Martin and De Oliveira 1999; Parthiban and Martin 2001]. The MP2 is a widely used *ab initio* choice for estimating the interaction energies of hydrogen bonded complexes which is size extensive and gives a good fraction of the correlation energy (80-90%) [Jensen 1999]. M06L is local meta-GGA exchange-correlation functional recommended for thermochemistry, thermochemical kinetics, and noncovalent interactions. Pople's split-valence triple-zeta basis set, 6-311++G(d,p) [Hehre *et al.* 1986] with polarization and diffuse functions is used on all atoms for MP2 and M06L optimizations. The 6-311++G(d,p) basis set is chosen since it is recommended for obtaining satisfactory geometries at affordable computational cost over the large basis sets with more basis functions [Wiberg 2004]. The BSSE corrected interaction energies are calculated using supermolecule approach. The accuracy of the interaction energies calculated from WIBD, MP2 and M06L methods are assessed by comparing against the CCSD(T) energies available in the literature. Further, MP4 [Raghavachari and Pople 1978] single point energy calculations are performed on the MP2 and M06L optimized geometries. Since MP4 scales the same as CCSD(T) *viz.* N^7 , CCSD(T) single point energy evaluations on MP2 optimized geometries is also performed. The basis set used for single point calculations is Dunning's augmented correlation-consistent polarized valence triple zeta basis set, aug-cc-pVTZ [Dunning 1989]. The Gaussian09 suite of programs [Frisch *et al.* 2010] is employed for all the computations. The effect of cations on the strength and nature of all the intermolecular complexes are evaluated by placing monovalent cations NH_4^+ and Li^+ in the vicinity of the electron acceptor molecule without imposing any symmetry constraints. The BSSE corrected interaction energies are calculated using supermolecular approach using the hybrid MP4//MP2 method.

Vibrational frequency analysis is performed on all optimized structures to ensure that each minimum is true containing only positive frequencies.

3.4 Results and Discussion

3.4.1 Modeling Accurate Interaction Energies

The selected set of 52 intermolecular complexes includes conventional (possessing N, O, S, P or halogens as electron donors) and nonconventional hydrogen bonds (with C-H groups as electron acceptors and π -electrons or carbon as electron donors), charge-assisted hydrogen bonds (CAHB), halogen bonds (XB) and dihydrogen bonds (HH). Charge-assisted hydrogen bonds, characterized by their partial covalent character [Desiraju 2002; Gilli *et al.* 1994; Madsen *et al.* 1998; Schiøtt *et al.* 1998] and very high stabilization energy, have either the donor or acceptor species charged. Dihydrogen bonds can also be considered as unconventional hydrogen bonds established between metal hydrides and proton donors where the metal-hydrogen σ -bond acts as an efficient electron donor. Figure 3.1 shows a representative set of intermolecular complexes selected for this work. The selected data set covers complexes featuring very weak, medium and strong interactions with energies ranging from less than 1 kcal/mol to over 25 kcal/mol. The notations E_{MP2} , E_{M06L} and E_{W1BD} indicate the interaction energies at MP2, M06L and W1BD methods, respectively. The notation $E_{MP4/MP2}$ represents the interaction energy calculated from MP4 single point calculation on the MP2 geometries, $E_{MP4/M06L}$ represents the interaction energy calculated from MP4 single point calculation on the M06L geometries and $E_{CCSD(T)/MP2}$ represents the interaction energy calculated from CCSD(T) single point calculation on the MP2 geometries. The interactions energies are assessed based on the mean absolute deviation (MAD) of the W1BD energy values from the energies calculated using the tested methods.

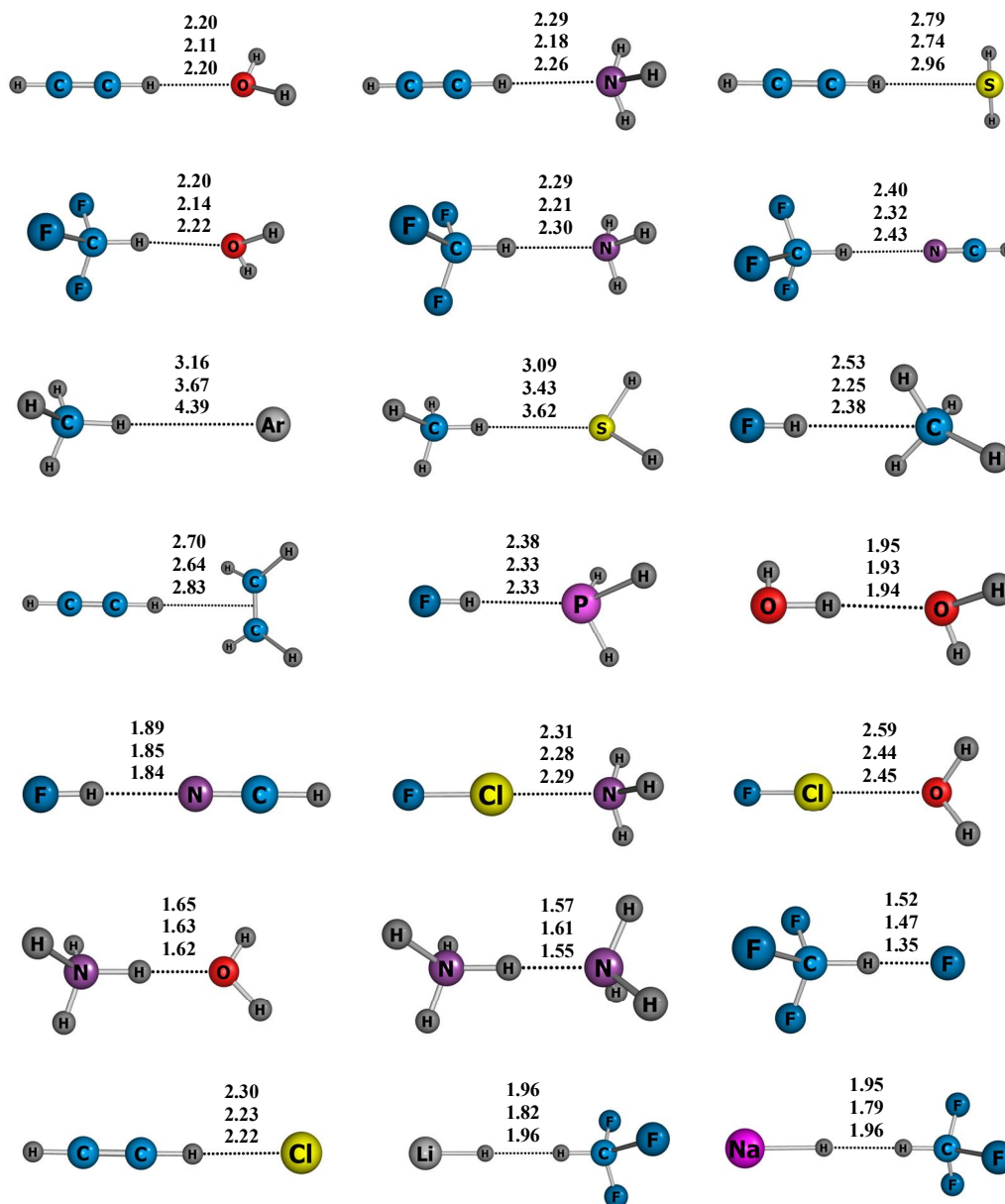


Figure 3.1 Representative set of intermolecular D-A complexes studied. Bond distances at MP2, M06L and W1BD methods (in Å) are given in the order from top to bottom.

The reference CCSD(T) interaction energies collected from literature are represented as E_{ref} . The E_{ref} , E_{MP2} , $E_{\text{MP4}/\text{MP2}}$, E_{M06L} , $E_{\text{MP4}/\text{M06L}}$, $E_{\text{CCSD(T)}/\text{MP2}}$ and E_{W1BD} for hydrogen bond complexes are presented in Table 3.1 and those for halogen and dihydrogen bond complexes are given in Table 3.2. The E_{ref} values represent an assortment of interaction energies calculated at different optimization levels and different

extrapolation schemes. However, E_{ref} represent high quality energy data and hence E_{ref} values are used as reference to assess the accuracy of other methods.

A close analysis of interaction energies indicate that W1BD method performs extremely well for hydrogen, halogen and dihydrogen bonds which are evident from the very close agreement between E_{W1BD} and E_{ref} values. Exceptionally good performance is found for hydrogen bonds where E_{W1BD} vary only ~ 0.1 kcal/mol from the E_{ref} for all complexes except Ar...HCH₃ and HF...HCH₃. In the case of Ar...HCH₃, E_{W1BD} is -0.07 kcal/mol which is significantly smaller than the reported CCSD(T)/CBS interaction energy of -0.40 kcal/mol [Patkowski 2013]. Since these complexes are dispersion dominated, the deviations in E_{W1BD} from E_{ref} could possibly indicate a weaker performance of W1BD to model dispersion energies. Deviation in the energy values may also be observed for halogen bonded complexes. However, in the whole data set, E_{W1BD} only vary < 0.5 kcal/mol from E_{ref} with two exceptions H₃N...ClF and H₂S...ClF where the interaction energy is slightly over estimated compared to the reported CCSD(T)/aug-cc-pVTZ energy values [Li *et al.* 2010]. MAD of E_{W1BD} from E_{ref} is only 0.19 kcal/mol and Figure 3.2 depicts a near perfect linear correlation between them which show that W1BD method is indeed a very good choice for studying the energetics of hydrogen, halogen and dihydrogen bond complexes. Nevertheless, the method becomes prohibitively expensive when the system contains more than 50 electrons. It may be noted that the MAD of E_{MP2} from E_{ref} is 0.41 kcal/mol whereas MAD of E_{M06L} from E_{ref} is 1.05 kcal/mol. This shows that the performance of MP2 method for modeling the strength of intermolecular noncovalent interactions is fairly good whereas M06L shows larger deviation with respect to the E_{ref} values. Since E_{W1BD} agrees very well with E_{ref} and E_{ref} values are available only for a limited number of systems, the former is used as a benchmark to compare the performance of MP2 and M06L, MP4//MP2 and MP4//M06L methods.

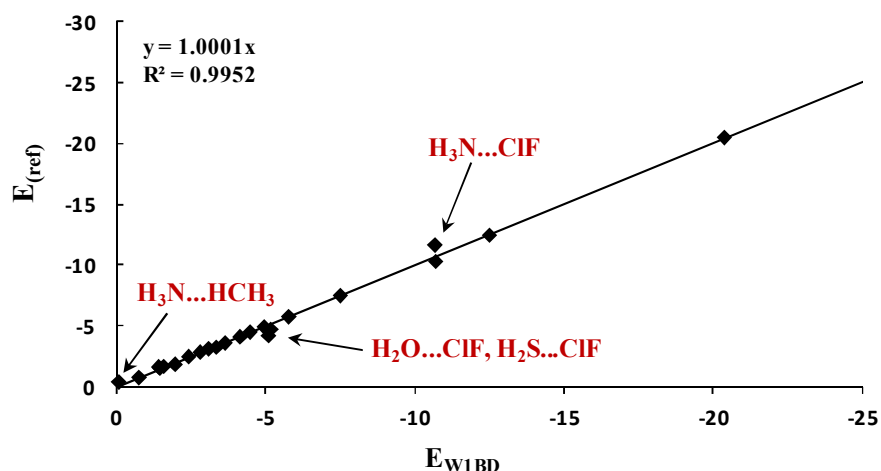


Figure 3.2 Correlation between E_{W1BD} and E_{ref} values. All values in kcal/mol.

The accuracy of MP2 energies greatly depend on the choice of basis set used in the calculation. For example, MP2 predicts repulsive interaction for $H_2S...HCH_3$ and $Ar...HCH_3$ complexes with E_{MP2} 0.04 and 0.05 kcal/mol, respectively using 6-311++G(d,p) basis set whereas it predicts attractive interaction for $Ar...HCH_3$ with higher basis sets [Parthasarathi *et al.* 2006]. This also suggest that 6-311++G(d,p) basis set is not quite adequate for studying these type of complexes dominated by dispersion. MAD of E_{MP2} from E_{W1BD} is 0.41 kcal/mol whereas MAD of E_{M06L} from E_{W1BD} is 0.81, almost twice that of MP2. The deviation of MP2 and M06L energies with respect to standard W1BD energies for all complexes can be understood from Figure 3.3. It is clear that MP2 underestimates the interaction energies for most of the complexes. The errors of MP2 energies with respect to W1BD energies *i.e.*, $E_{W1BD}-E_{MP2}$ values are < 1.5 kcal/mol for all neutral hydrogen bonds and dihydrogen bonds except $H_2CO...HF$. Larger deviations from W1BD energies are observed for halogen bonds with highest error of -2.5 kcal/mol for $H_2S...CIF$. M06L method underestimates the interaction energies for most of the neutral hydrogen bonds with errors < 1 kcal/mol, while the energies are overestimated for all charge-assisted hydrogen bonds, halogen bonds and dihydrogen bonds. Maximum

deviation is observed for $\text{H}_3\text{N}\dots\text{ClF}$, $\text{H}_2\text{S}\dots\text{ClF}$ and $\text{F}^-\dots\text{HCF}_3$. For instance, E_{W1BD} and E_{M06L} for $\text{H}_2\text{S}\dots\text{ClF}$ is -5.09 and -9.85 kcal/mol, respectively suggesting that the interaction energy is over estimated by 4.76 kcal/mol at M06L level. In general, MP2 underestimates interaction energies while M06L shows more accurate behavior than MP2 except for halogen and charge-assisted hydrogen bonds compared to W1BD.

The MP4 single point calculation on MP2 optimized geometry greatly improves the interaction energy values. For instance, the interaction is attractive in $\text{H}_2\text{S}\dots\text{HCH}_3$ and $\text{Ar}\dots\text{HCH}_3$ with $E_{\text{MP4//MP2}}$ values -0.37 and -0.23 kcal/mol, respectively. MP4 single point calculation on M06L geometries also show remarkable improvement in the interaction energy values. MAD of $E_{\text{MP4//MP2}}$ from E_{W1BD} is 0.14 kcal/mol and MAD of $E_{\text{MP4//M06L}}$ from E_{W1BD} is 0.16, respectively. MP4//M06L calculation yields more accurate energies for halogen and charge-assisted hydrogen bonds than M06L. E_{M06L} value -9.85 kcal/mol observed for $\text{H}_2\text{S}\dots\text{ClF}$ has become -4.23 kcal/mol at MP4//M06L level which is close to E_{W1BD} value -5.09 kcal/mol. Similarly in the case of $\text{H}_3\text{N}\dots\text{ClF}$, $E_{\text{MP4//M06L}}$ (-10.20 kcal/mol) and E_{W1BD} (-10.67 kcal/mol) are in very good agreement compared to E_{M06L} (-15.7 kcal/mol). Figure 3.4 presents the errors of $E_{\text{MP4//MP2}}$, $E_{\text{MP4//M06L}}$ and $E_{\text{CCSD(T)//MP4}}$ with respect to E_{W1BD} . This figure clearly indicates that upon MP4 single point calculation the errors are scaled down significantly for both MP2 and M06L methods. The largest deviation is shown by $\text{FCl}\dots\text{SH}_2$ complex in both MP4//MP2 and MP4//M06L methods with error values -0.65 and -0.86 kcal/mol respectively. Thus MP4/aug-cc-pvtz single point calculations on MP2/6-311++G(d,p) and M06L/6-311++G(d,p) geometries significantly improve the description of the energetics of the hydrogen, halogen and dihydrogen bonds. CCSD(T) single point energy calculations on MP2 optimized geometries also yields more accurate interaction energy values for hydrogen bonds, halogen bonds and dihydrogen bonds with a MAD of 0.27 from E_{W1BD} values. Among the three hybrid methods $E_{\text{MP4//MP2}}$ method emerges the best for the

estimation of interaction energies of intermolecular **D-A** complexes with the lowest MAD with respect to the benchmark W1BD energies. Hence geometry optimization at MP2/6-311++G(d,p) level followed by single point MP4 calculation using a higher basis set (aug-cc-pvtz) is suggested as good hybrid method for modeling accurate interaction energies of noncovalent complexes. It is also evident that with a judicious choice of basis set, MP2 is a good choice for the study of **D-A** complexes. BSSE correction must be incorporated in MP2 and MP4 calculations since the calculated BSSE values are substantially large for these methods which agree with the fact that failure in BSSE correction would lead to erroneous conclusions in the study of weak interactions [Zhu *et al.* 2000]. M06L optimizations though insufficient for halogen and charge-assisted hydrogen bonds can yield good interaction energies for noncovalent complexes when coupled with MP4 single point calculation. MP4//M06L method can be thus considered as a good *ab initio*-DFT hybrid method for studying the energetics of hydrogen bonds, halogen bonds and dihydrogen bonds.

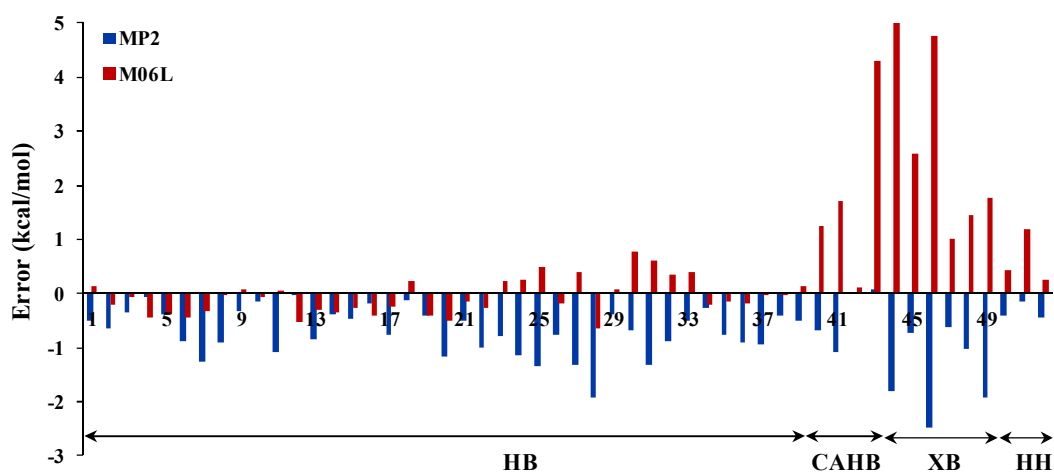


Figure 3.3 Comparison of energy errors of MP2 and M06L methods with respect to W1BD method.

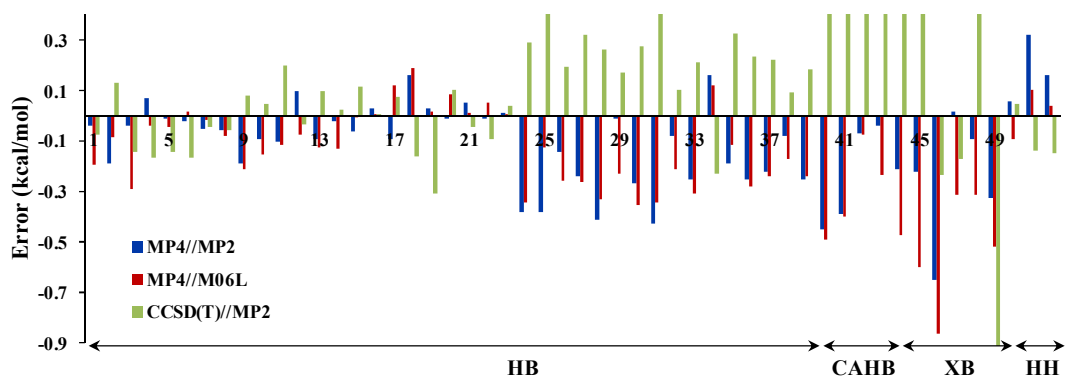


Figure 3.4 Comparison of energy errors of MP4//MP2, MP4//M06L and CCSD(T)//MP2 methods with respect to W1BD method.

3.4.2 Cation Enhanced Binding Strengths

The presence of cations *viz.* Li^+ and NH_4^+ in the vicinity of the electron acceptor molecule of hydrogen bonds, halogen bonds and dihydrogen can have two possible effects on the interaction between the electron donor and the acceptor; one in which interaction is strengthened and the other in which the cation disrupts the interaction either by interfering in the intermolecular interaction or by nucleophilic attack. In many hydrogen bonded complexes, the cation directly interacts with the electron acceptor leading to significant stabilization of the interactions. These complexes are characterized by higher interaction energies and shorter interaction distances. In certain cases, the minimal energy structures correspond to sandwich complexes of the type $\text{D}\dots\text{X}\dots\text{A}$, where the cation interacts with both the donor and acceptor. For instance the proximity of Li^+ and NH_4^+ with $\text{H}_2\text{O}\dots\text{HCCH}$ lead to $\text{H}_2\text{O}\dots\text{Li}^+\dots\text{HCCH}$ and $\text{H}_2\text{O}\dots\text{NH}_4^+\dots\text{HCCH}$ complexes, respectively. In a relatively fewer number of complexes particularly in halogen bonded complexes, the minimum energy structure correspond to the nucleophilic attack of the cation with one of the atoms of the electron acceptor. However, because the ultimate aim is to study cation enhanced bond strengths, the focus is on those geometries where the intermolecular interactions are not disturbed but strengthened by the presence

of the cation. The Li^+ and NH_4^+ adducts are designated as $\text{D}\dots\text{A}\dots\text{Li}^+$ and $\text{D}\dots\text{A}\dots\text{NH}_4^+$ respectively. The notations E_{Li^+} and $E_{\text{NH}_4^+}$ represent the Li^+ and NH_4^+ enhanced interaction energies and D_{Li^+} and $D_{\text{NH}_4^+}$ represent the corresponding intermolecular hydrogen bond distances. Figure 3.5 and Figure 3.6 presents the geometries of a representative set of $\text{D}\dots\text{A}\dots\text{Li}^+$ and $\text{D}\dots\text{A}\dots\text{NH}_4^+$ complexes. The E_{Li^+} , $E_{\text{NH}_4^+}$, D_{Li^+} and $D_{\text{NH}_4^+}$ along with the percentage increase in interaction energies are listed in Table 3.3.

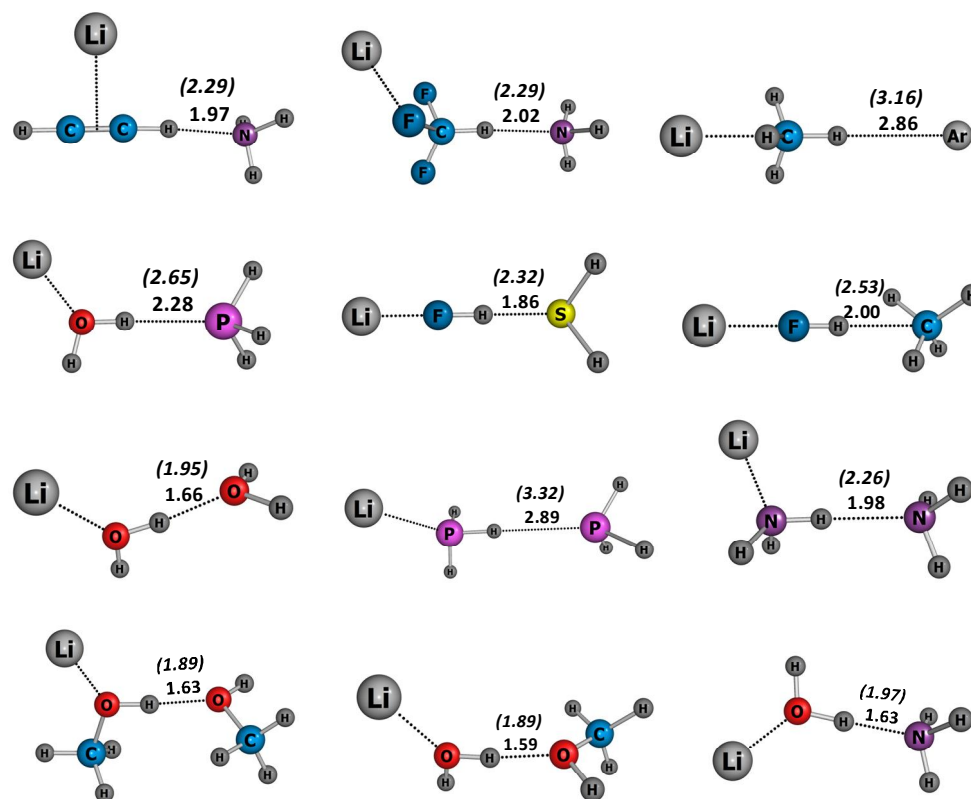


Figure 3.5 Optimized geometries of representative $\text{D}\dots\text{A}\dots\text{Li}^+$ complexes along with the hydrogen bond distances in \AA . Hydrogen bond distances of the corresponding **D-A** complexes are given in parentheses.

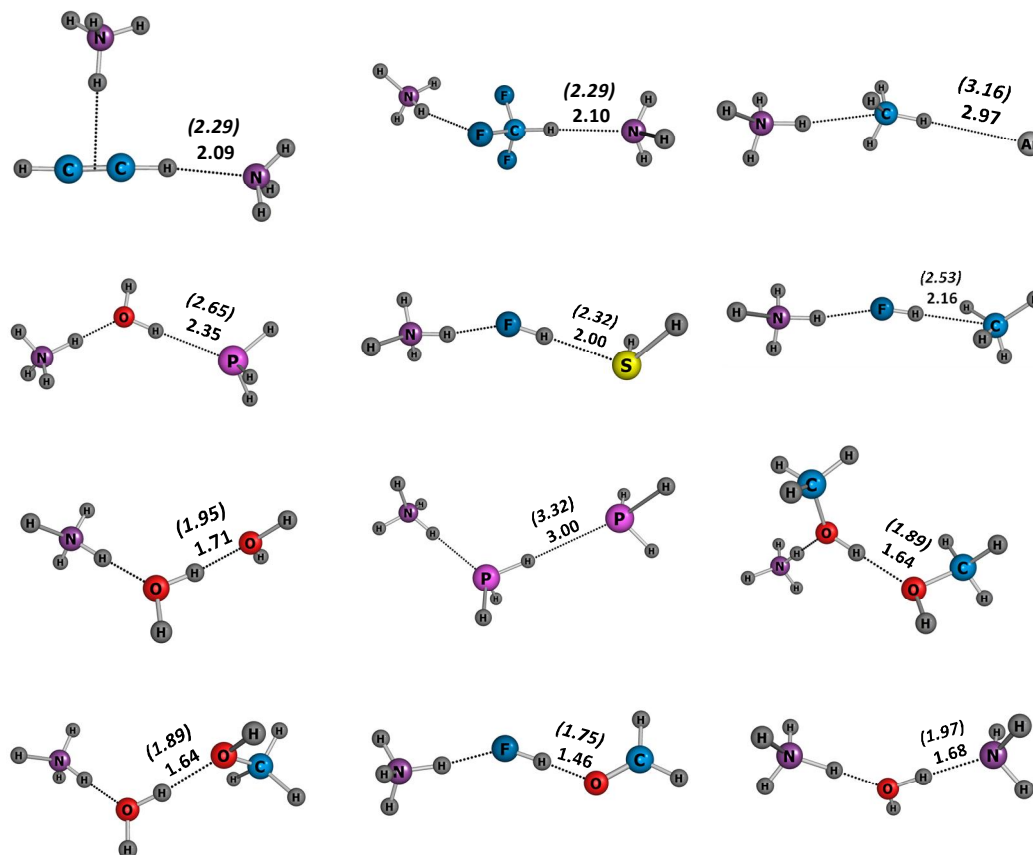


Figure 3.6 Optimized geometries of representative $D...A...NH_4^+$ complexes along with the hydrogen bond distances in Å. Hydrogen bond distances of the corresponding **D-A** complexes are given in parentheses.

The cation enhanced interaction energies are measured in terms of net stabilization energy (NSE) which is the difference between interaction energies before and after complexing the cation; NSE_{Li^+} and $NSE_{NH_4^+}$ represent the net stabilization energies on complexation with Li^+ and NH_4^+ respectively (Table 3.3).

E_{Li^+} , and $E_{NH_4^+}$ values are significantly higher than the corresponding energy values in all **D-A** complexes which indicate the stabilization effect of metal ions in their neighborhood. The stabilization effect of cations is also evident from the shortening of the intermolecular hydrogen bond distances observed in all the cases. The NSE values ranges from 0.32 to 19.44 kcal/mol in $D \cdots A \cdots Li^+$ complexes with an average shortening

of ~ 0.38 in the intermolecular hydrogen bond distances. The ternary complex, $\text{Ar}\dots\text{HCH}_3\dots\text{Li}^+$ ($E_{\text{Li}^+} = -0.55$ kcal/mol) is about 2.4 times more stable than $\text{Ar}\dots\text{HCH}_3$ complex ($E_{\text{int}} = -0.23$ kcal/mol). Here, the $\text{C-H}\dots\text{Ar}$ distance is shortened by 0.31 . The cation induced enhancement in interaction energy is more pronounced in the weak homodimer $\text{H}_3\text{P}\dots\text{H}_3\text{P}$ which show a 6.7 fold increase in interaction energy and a shortening in hydrogen bond distance by 0.31 on the proximity of Li^+ . The NSE is the highest for $\text{HCN}\dots\text{HF}\dots\text{Li}^+$ ($\text{NSE}_{\text{Li}^+} = 19.77$ kcal/mol) and lowest for, $\text{Ar}\dots\text{HCH}_3\dots\text{Li}^+$ ($\text{NSE}_{\text{Li}^+} = 0.32$ kcal/mol).

The stabilization effect of NH_4^+ on hydrogen bond strength is relatively less compared to Li^+ . The NSE of $\text{D}\dots\text{A}\dots\text{NH}_4^+$ complexes ranges from 0.24 kcal/mol to 12.26 kcal/mol and the average shortening of the hydrogen bonds distances is 0.28 . While the interaction of Li^+ with $\text{H}_3\text{N}\dots\text{H}_3\text{N}$ has considerable stabilization effect on the strength of the hydrogen bond with a NSE of 10.24 kcal/mol, the interaction of NH_4^+ with $\text{H}_3\text{N}\dots\text{H}_3\text{N}$ disrupts the hydrogen bonded NH_3 dimer and forms a much stronger $\text{H}_3\text{N}\text{H}\text{NH}_3^+\dots\text{NH}_3$ complex. The NSE values of ternary $\text{D}\dots\text{A}\dots\text{NH}_4^+$ complexes follow the same trend as in the $\text{D}\dots\text{A}\dots\text{Li}^+$ complexes with the highest NSE for $\text{HCN}\dots\text{HF}\dots\text{NH}_4^+$ ($\text{NSE}_{\text{Li}^+} = 13.05$ kcal/mol) and lowest for $\text{Ar}\dots\text{HCH}_3\dots\text{NH}_4^+$ ($\text{NSE}_{\text{Li}^+} = 0.24$ kcal/mol). The stabilization effect of Li^+ and NH_4^+ on $\text{CH}\dots$ interaction is also investigated by using the prototype $\text{C}_6\text{H}_6\dots\text{CH}_4$ dimer. The NSE for $\text{C}_6\text{H}_6\dots\text{CH}_4\dots\text{Li}^+$ and $\text{C}_6\text{H}_6\dots\text{CH}_4\dots\text{NH}_4^+$ are 5.72 and 3.61 kcal/mol, respectively which signify substantial strengthening of the interaction. Thus, the interaction energies, NSE values and the interaction distances indicate that polarization effects of the cations can lead to substantial increase in the strength of hydrogen bonds.

Table 3.1 Interaction energies of hydrogen bond complexes calculated at M06L (E_{M06L}), MP4/M06L ($E_{MP4/M06L}$), MP2 (E_{MP2}), MP4//MP2 ($E_{MP4//MP2}$), CCSD(T)//MP2 ($E_{CCSD(T)//MP2}$), W1BD (E_{W1BD}), and reference CCSD(T) (E_{ref}) methods in kcal/mol. Reference corresponding to E_{ref} values also provided.

Sl.No.	Complex	E_{M06L}	$E_{MP4/M06L}$	E_{MP2}	$E_{MP4//MP2}$	$E_{CCSD(T)//MP2}$	E_{W1BD}	E_{ref}
1	H ₃ N...HCCH	-3.77	-3.45	-3.15	-3.60	-3.71	-3.64	-3.60 [Liu and Xu 2011]
2	H ₂ S...HCCH	-1.37	-1.50	-0.95	-1.40	-1.46	-1.59	
3	H ₂ O...HCCH	-2.73	-2.51	-2.46	-2.76	-2.94	-2.80	-2.85 [ezá <i>et al.</i> 2011]
4	HCN...HCCH	-2.06	-2.46	-2.43	-2.57	-2.67	-2.50	
5	H ₃ CCN...HCCH	-2.71	-3.04	-2.71	-3.08	-3.23	-3.09	
6	H ₂ CO...HCCH	-2.59	-3.06	-2.17	-3.02	-3.21	-3.04	
7	HF...HCCH	-4.05	-4.37	-3.14	-4.34	-4.43	-4.39	
8	HCl...HCCH	-2.81	-2.75	-1.91	-2.78	-2.88	-2.83	
9	H ₃ N...HCF ₃	-4.38	-4.10	-3.99	-4.12	-4.23	-4.31	
10	H ₂ O...HCF ₃	-3.38	-3.29	-3.30	-3.35	-3.39	-3.44	
11	H ₂ S...HCF ₃	-2.22	-2.06	-1.09	-2.07	-1.97	-2.17	
12	HCN...HCF ₃	-2.68	-3.12	-3.18	-3.30	-3.23	-3.20	
13	HCl...HCF ₃	-1.68	-1.83	-1.12	-1.87	-1.86	-1.96	

-- Table 3.1 continued --

14	H ₃ N...HCH ₃	-0.40	-0.62	-0.36	-0.73	-0.73	-0.75	-0.77 [MacKie and DiLabio 2011]
15	H ₂ S...HCH ₃	-0.17	-0.42	0.04	-0.37	-0.31	-0.43	
16	H ₃ CCN...HCH ₃	-0.27	-0.67	-0.48	-0.70	-0.67	-0.67	
17	HF...HCH ₃	-1.18	-1.53	-0.65	-1.32	-1.34	-1.41	-1.64 [MacKie and DiLabio 2011]
18	Ar...HCH ₃	-0.30	-0.26	0.05	-0.23	-0.23	-0.07	-0.40 [Patkowski 2013]
19	C ₂ H ₂ ...C ₂ H ₂	-1.03	-1.47	-1.05	-1.48	-1.76	-1.45	-1.52 [ezá <i>et al.</i> 2011]
20	HF...C ₂ H ₄	-3.98	-4.56	-3.30	-4.47	-4.38	-4.48	-4.50 [MacKie and DiLabio 2011]
21	H ₃ P...H ₂ O	-2.26	-2.43	-1.93	-2.47	-2.47	-2.42	-2.49 [Lane and Kjaergaard 2009]
22	H ₂ CO...H ₂ O	-4.85	-5.16	-4.13	-5.10	-5.20	-5.11	
23	H ₃ P...HF	-4.99	-4.76	-3.95	-4.76	-4.71	-4.75	
24	H ₂ O...HF	-8.94	-8.35	-7.55	-8.31	-8.40	-8.69	
25	H ₂ S...HF	-5.53	-4.91	-3.71	-4.66	-4.56	-5.04	
26	HCN...HF	-7.32	-7.24	-6.73	-7.36	-7.30	-7.50	-7.49 [MacKie and DiLabio 2011]
27	H ₃ N...HF	-12.90	-12.24	-11.18	-12.26	-12.18	-12.50	-12.45 [Botschwina and Oswald 2005]
28	H ₂ CO...HF	-7.66	-7.99	-6.40	-7.91	-8.05	-8.32	
29	NCH...HCl	-4.74	-4.42	-4.26	-4.64	-4.48	-4.65	
30	H ₂ O...HCl	-6.14	-5.00	-4.68	-5.08	-5.07	-5.35	

-- Table 3.1 continued --

31	H ₂ S...HCl	-3.94	-3.01	-2.04	-2.92	-2.82	-3.35	-3.26 [Pernal <i>et al.</i>]
32	PH ₃ ...HCl	-3.43	-2.87	-2.20	-3.00	-2.98	-3.08	
33	OH ₂ ...OH ^F	-6.04	-5.33	-5.13	-5.39	-5.43	-5.64	
34	PH ₃ ...PH ₃	-0.25	-0.58	-0.18	-0.62	-0.69	-0.46	
35	H ₂ S...H ₂ S	-1.43	-1.46	-0.80	-1.38	-1.24	-1.57	-1.68 [Mintz and Parks 2012]
36	CH ₃ HO...HOCH ₃	-5.59	-5.49	-4.85	-5.52	-5.54	-5.77	-5.76 [ezá <i>et al.</i> 2011]
37	HCl...HCl	-1.94	-1.72	-1.03	-1.74	-1.74	-1.96	-1.85 [Tuma <i>et al.</i> 1999]
38	H ₃ N...H ₃ N	-3.06	-2.92	-2.69	-3.01	-3.00	-3.09	-3.13 [ezá and Hobza 2013]
39	H ₂ O...H ₂ O	-5.08	-4.71	-4.45	-4.70	-4.77	-4.95	-4.92 [ezá <i>et al.</i> 2011]
40	H ₂ O...NH ₄ ⁺	-21.62	-19.89	-19.72	-19.93	-20.61	-20.38	-20.45 [Boese <i>et al.</i> 2007]
41	H ₃ N...NH ₄ ⁺	-27.87	-25.75	-25.07	-25.76	-26.32	-26.15	
42	Cl ⁻ ...HCCH	-10.81	-10.63	-10.70	-10.63	-10.26	-10.70	-10.29 [Botschwinaa and Oswald 2002]
43	F ⁻ ...HCF ₃	-30.13	-25.61	-25.93	-25.80	-26.84	-25.84	

Table 3.2 Interaction energies of halogen and dihydrogen bond complexes calculated at M06L (E_{M06L}), MP4//M06L ($E_{MP4/M06L}$), MP2 (E_{MP2}), MP4//MP2 ($E_{MP4/MP2}$), CCSD(T)//MP2 ($E_{CCSD(T)/MP2}$), W1BD (E_{W1BD}), and reference CCSD(T) (E_{ref}) methods in kcal/mol. Reference corresponding to E_{ref} values also provided.

SI.No.	Complex	E_{M06L}	$E_{MP4/M06L}$	E_{MP2}	$E_{MP4/MP2}$	$E_{CCSD(T)/MP2}$	E_{W1BD}	E_{ref}
44	H ₃ N...ClF	-15.71	-10.20	-8.86	-10.46	-9.09	-10.67	-11.64 [Hill and Hu 2013]
45	H ₂ O...ClF	-7.76	-4.57	-4.43	-4.95	-4.53	-5.17	- 4.73 [Li <i>et al.</i> 2010]
46	H ₂ S...ClF	-9.85	-4.23	-2.61	-4.44	-3.75	-5.09	- 4.20 [Li <i>et al.</i> 2010]
47	HCN...ClF	-5.96	-4.64	-4.33	-4.97	-4.32	-4.95	
48	H ₃ CCN...ClF	-7.57	-5.80	-5.09	-6.02	-5.30	-6.11	
49	H ₂ CO...ClF	-7.70	-5.43	-4.02	-5.62	-5.06	-5.94	
50	LiH...HCF ₃	-6.45	-5.92	-5.59	-6.06	-5.96	-6.01	
51	NaH...HCF ₃	-7.45	-6.36	-6.11	-6.57	-6.39	-6.26	
52	LiH...HCCH	-4.38	-4.18	-3.7	-4.30	-4.29	-4.14	-4.12 [Cybulski <i>et al.</i> 2003]

Table 3.3 Energetic and geometric features of $D...A...Li^+$ and $D...A...NH_4^+$ complexes. E_{int} and D are the interaction energies and intermolecular hydrogen bond distances of **D-A** complexes. E_{Li^+} , $E_{NH_4^+}$, D_{Li^+} and $D_{NH_4^+}$ are the interaction energies and interaction distances of $D...A...Li^+$ and $D...A...NH_4^+$ complexes and NSE_{Li^+} and $NSE_{NH_4^+}$ represent the corresponding stabilization energies. Energy values in kcal/mol and distances in Å units.

Complex	E_{int} (kcal/mol)	D (Å)	E_{Li^+} (kcal/mol)	NSE_{Li^+} (kcal/mol)	D_{Li^+} (Å)	$E_{NH_4^+}$ (kcal/mol)	$NSE_{NH_4^+}$ (kcal/mol)	$D_{NH_4^+}$ (Å)
Ar...HCH ₃	-0.23	3.164	-0.55	0.32	2.858	-0.47	0.24	2.971
H ₃ N...HCCH	-3.60	2.291	-12.81	9.21	1.974	-10.37	6.77	2.091
H ₃ N...HCF ₃	-4.12	2.291	-13.02	8.90	2.021	-10.29	6.17	2.097
C ₆ H ₆ ...CH ₄	-1.58	2.575	-7.30	5.72	2.276	-5.20	3.61	2.378
H ₃ P...H ₂ O	-2.47	2.649	-10.94	8.47	2.276	-8.62	6.15	2.345
H ₂ S...HF	-4.66	2.321	-17.66	12.99	1.858	-12.91	8.25	2.003
H ₂ CO...HF	-7.91	1.759	-26.26	18.36	1.327	-20.17	12.26	1.462
HCl...HCl	-1.74	2.666	-6.84	5.10	2.218	-5.16	3.42	2.380
H ₂ S...H ₂ S	-1.38	2.837	-6.19	4.81	2.489	-5.19	3.81	2.592
H ₂ O...H ₂ O	-4.70	1.950	-16.52	11.82	1.660	-13.88	9.18	1.710
H ₃ P...H ₃ P	-0.62	3.321	-4.13	3.51	2.890	-3.22	2.60	2.996

-- Table 3.3 continued --

H ₃ N...H ₃ N	-3.01	2.263	-13.25	10.24	1.976	-19.25	16.24	1.750
NCH...HCl	-4.64	2.106	-18.12	13.48	1.630	-14.12	9.48	1.793
H ₂ O...HF	-8.31	1.732	-26.29	17.98	1.349	-20.23	11.93	1.468
H ₂ O...HCl	-5.08	1.902	-17.95	12.87	1.450	-13.95	8.87	1.638
CH ₃ HO...HOCH ₃	-5.52	1.886	-17.54	12.02	1.628	-15.22	9.70	1.644
HF...HCF ₃	-1.32	2.531	-6.40	5.08	2.000	-4.24	2.92	2.157
H ₂ O...HOCH ₃	-5.40	1.894	-18.83	13.43	1.593	-15.62	10.22	1.641
H ₃ P...H ₂ S	-1.47	2.949	-6.89	5.43	2.534	-5.33	3.87	2.648
HCN...HF	-7.36	1.889	-26.80	19.44	1.445	-20.40	13.05	1.572
H ₃ N...H ₂ O	-5.77	1.974	-21.37	15.60	1.627	-17.73	11.96	1.680
LiH...HCF ₃	-6.06	1.956	-20.26	14.20	1.563	-18.88	12.82	1.682

Part B

Molecular Electrostatic Potential Analysis of Hydrogen, Halogen, and Dihydrogen Bonds

3.5 Introduction

Hydrogen bonding is one of the most important, widely discussed and highly debated interactions in chemistry [Buckingham *et al.* 1988; Desiraju 2002; Gilli and Gilli 2000; Gilli and Gilli 2009; Gilli *et al.* 1994; Gotch and Zwier 1990; Grabowski 2001; Grabowski 2004; Grabowski 2011; Kollman *et al.* 1975; Morokuma 1977; Müller-Dethlefs and Hobza 2000]. Desiraju [Desiraju 2002] described it as an 'interaction without borders' to express the large variations in covalent, electrostatic, and van der Waals energy components of a hydrogen bond. Despite the extensive research over years, the perception of hydrogen bonds continues to evolve and a universally accepted definition of hydrogen bond remains elusive in the literature. A task group of IUPAC has reviewed this topic in depth based on theoretical and experimental knowledge acquired over the past century and proposed a short modern definition for it [Arunan *et al.* 2011; Desiraju *et al.* 2013]. Halogen bonds are highly directional noncovalent interactions that occur between an electron donor and a halogen atom in another molecule. Detailed report of IUPAC recommendations for defining hydrogen bonds and halogen bonds is provided in Chapter 1. Politzer *et al.* [Brinck *et al.* 1992; Brinck *et al.* 1993; Clark *et al.* 2007; Murray *et al.* 1994; Politzer *et al.* 2013] demonstrated that halogen bond is an electrostatically-driven interaction between positive σ -hole (a region of positive electrostatic potential on the outer side of the halogen) of the halogen and the negative potential of the base. Crabtree and coworkers [Crabtree *et al.* 1996] showed that

hydrogen atom in metal hydrides and H_3NBH_3 can form unusual hydrogen bonding interaction with a hydrogen atom in another molecule. The resulting H...H interactions are called dihydrogen bonds. In systems showing hydrogen bonds, halogen bonds and dihydrogen bonds, one atom in the bonded region accepts electron density from the other [Jonas *et al.* 1994; Mulliken and Person 1969; Ratajczak and Orville-Thomas 1980] and hence these interactions can be viewed as interaction between a Lewis base acting as electron donor (**D**) and a Lewis acid acting as electron acceptor (**A**).

Bader's 'Atoms in Molecules' (AIM) [Bader 1985; Bader 1990; Bader 1991] and molecular electrostatic potential (MESP) [Murray *et al.* 1994; Politzer *et al.* 1985; Pullman 1990; Sen and Politzer 1989; Sjoberg and Politzer 1990] analyses are important theoretical tools for eliciting noncovalent interactions. Numerous studies [Knop *et al.* 2003; Koch and Popelier 1995; Parthasarathi *et al.* 2006; Popelier 1998; Popelier and Logothetis 1998; Suresh *et al.* 2009] have shown that AIM topological parameters *viz.* electron density (ρ) at the bond critical point (bcp) and its Laplacian ($\nabla^2\rho$) are important quantities to characterize the strength and nature of hydrogen bonds, halogen bonds and dihydrogen bonds. There have been various reports [Grabowski 2001; Knop *et al.* 2003; Parthasarathi *et al.* 2006; Popelier 1998; Popelier and Logothetis 1998; Suresh *et al.* 2009] where ρ correlates with the interaction energy and length of the hydrogen bond. Sathyamurthy [Parthasarathi *et al.* 2006] *et al.* attempted to understand the concept of hydrogen bonding without borders using the topological properties of electron density and showed that the electron density at the hydrogen bond critical point increases approximately linearly with increasing stabilization energy in going from weak to moderate and strong hydrogen bonds. The most negative valued MESP point of a molecule, designated as V_{\min} symbolizes the sites of electron localization in a molecule [Mathew and Suresh 2010; Suresh and Gadre 2007] and has been used successfully in predicting the sites and directionality of hydrogen bonds in a variety of

systems [Bobadova-Parvanova and Galabov 1998; Gadre and Bhadane 1997; Gadre and Pundlik 1997; Galabov and Bobadova-Parvanova 1999; Kollman *et al.* 1975; Leroy *et al.* 1976 ; Politzer and Murray 1991]. Kollman *et al.* [Kollman *et al.* 1975] showed the existence of good correlation between hydrogen bond energies and the magnitude of MESP at fixed distance from the proton acceptors in a series of complexes between HF and various acceptors. Recently, in a series of works [Bobadova-Parvanova and Galabov 1998; Dimitrova *et al.* 2002; Dimitrova *et al.* 2003; Galabov and Bobadova-Parvanova 1999; Galabov *et al.* 2003] Galabov *et al.* showed that MESP at the site of electron donor atom could be successfully used as reactivity descriptor for the study of hydrogen bonding. However, most of these works consider hydrogen bond complexes with either donor or acceptor molecules fixed and hence the applicability of these parameters for a heterogeneous sample of complexes with different proton donors and/or acceptors is limited.

In this chapter it is shown that for a large variety of intermolecular hydrogen bonds, halogen bonds and dihydrogen bonds, a simple definition suggesting them as electron donor-acceptor (eDA) interaction holds good. The results are based on high level *ab initio* interaction energy data and topographical features of ρ distribution and MESP. The value of ρ at bcp, V_{\min} and V_n are used as electronic descriptors to quantify the strength and characteristics of eDA interactions of a large variety of complexes. Among ρ , V_{\min} and V_n , the last quantity is highly suited to measure the electron donating power of donor as well as electron accepting power of acceptor. A strong correlation between interaction energy and donor-acceptor strength is obtained for all the complexes which prove that they all belong to the same class, eDA complex.

3.6 Computational Methods

The interaction energies of all D-A complexes are calculated using the hybrid MP4//MP2 method recommended in Part A of this chapter. Gaussian 09 suite of programs [Frisch *et al.* 2010] is employed for all the computations. The topological properties of electron density at bond critical points (bcp) have been studied using AIM methodology with AIM2000 program [Biegler-König and Schönbohm 2002; Biegler-König *et al.* 2001]. MESP topographical analysis of the monomers and the intermolecular complexes are carried out at MP4/aug-cc-pvtz level. MESP, $V(\mathbf{r})$ at any point with the position vector \mathbf{r} can be calculated using the equation 1.67 given in Chapter 1. $V(\mathbf{r})$ is strongly dependent on the local charges around point \mathbf{r} , the positive charges on the neighboring nuclei, and the electron density in closer vicinity of point \mathbf{r} . V_{\min} have been located for the donor and acceptor molecules in their isolated and bound state in the noncovalent complex. MESP at the nuclei (V_n) of the atoms participating in the nonbonded interactions is also evaluated using equation 1.68 (Chapter 1). The nuclei centered quantity, V_n measures the electrostatic potential at the position of the atom 'n' due to all the electrons and rest of the nuclei. It is a local molecular property associated with the particular atom center. MESP at each atom of the donor and acceptor molecules is obtained from the standard output of the Gaussian09 program.

3.7 Results and Discussion

The set of intermolecular noncovalent complexes studied in Part A is of this chapter expanded to a total of 104 complexes that are classified into four categories, *viz.* (i) hydrogen bonds in neutral complexes (A...B), (ii) charge-assisted hydrogen bonds (CHB), (iii) halogen bonds (X...B), (iv) charge-assisted halogen bonds (CXB) and (v) dihydrogen bonds (H...H). The category A...B includes complexes where both donor and acceptor molecules are neutral; it has three subclasses: C-H...Y (hydrogen bonds

formed between C-H of C₂H₂, CF₃H and CH₄ and conventional electron donor molecules), X-H... (hydrogen bonds where the electron donor is a π -system) and X-H...Y (hydrogen bonds with HCl, HF, H₂O, PH₃, H₂S, CH₃OH and HBr as electron donors/acceptors) complexes. The halogen bonded complexes of diatomic interhalogen compounds IF, ICl, IBr, ClF, BrF and BrCl with Lewis bases H₂S, NH₃, H₂O, HCN, NCCH₃ and OCH₂ are studied. CHB and CXB includes noncovalent complexes connected through relatively strong hydrogen bonds and halogen bonds, respectively where either the donor or acceptor species is charged *i.e.*, hydrogen/halogen bonds in anionic systems and cationic systems. These bonds are characterized by their partial covalent character [Desiraju 2002; Gilli *et al.* 1994; Madsen *et al.* 1998; Schiøtt *et al.* 1998]. Dihydrogen bond complexes of BeH₂, LiH, NaH and BH₄ as electron donors with different electron acceptors are also included. E_{nb} represents the interaction energy calculated at MP4//MP2 method and the standard notations ρ and $\nabla^2\rho$ are used to indicate the electron density at the bond critical point (bcp) of the electron donor-acceptor bond and the Laplacian of the electron density at the bcp. The accuracy of E_{nb} calculated with MP4//MP2 method is very close to the 'gold standard' CCSD(T) benchmark values available in the literature with mean absolute deviation 0.25 kcal/mol. The E_{nb} values range from < 1 kcal/mol to 59 kcal/mol and covers very weak, medium and strong interactions. Table 3.4 presents the E_{nb} values of a representative set of complexes along with ρ and $\nabla^2\rho$ at bcp.

3.7.1 Electron Density Analysis

The values of ρ and $\nabla^2\rho$ at bcp for H...H and most of the A...B complexes fall in the typical range [Koch and Popelier 1995] proposed for ρ (0.002 ó 0.035 au) and $\nabla^2\rho$ (0.024 ó 0.139 au). However, for most of XB, CHB and CXB complexes, higher values of ρ and $\nabla^2\rho$ are observed indicating the presence of remarkably stronger interactions.

Nonetheless, except $\text{H}_3\text{O}^+\dots\text{H}_2\text{O}$, all other **D-A** systems exhibit typical closed-shell interactions by virtue of their positive $\nabla^2\rho$ values. $\text{H}_3\text{O}^+\dots\text{H}_2\text{O}$ represent a Zundel ion [Schuster *et al.* 1976] and have $\nabla^2\rho$ value of -0.564 au which is characteristic of a bond with covalent nature. Anionic CXB complexes *viz.* $\text{F} \dots\text{IF}$, $\text{F} \dots\text{BrF}$, $\text{Cl} \dots\text{IF}$, $\text{Cl} \dots\text{BrF}$, $\text{F} \dots\text{IBr}$ and $\text{Cl} \dots\text{IBr}$ are characterized by bridged structures and exceptionally high interaction energy values which fall in the range of 35 to 59 kcal/mol (Figure 3.7). For instance, in the case of $\text{F} \dots\text{IF}$, the position of I is symmetric with respect to both the F atoms meaning that the complex is a resonance combination of $\text{F} \dots\text{IF}$ and $\text{F}\dots\text{IF}$. Similar bonding scenario is seen in $\text{F} \dots\text{BrF}$, $\text{Cl} \dots\text{IF}$, $\text{Cl} \dots\text{BrF}$, $\text{F} \dots\text{IBr}$ and $\text{Cl} \dots\text{IBr}$. The cationic complex $\text{H}_3\text{O}^+\dots\text{H}_2\text{O}$ also exhibits a bridged configuration ($\text{H}_2\text{O}\dots\text{H}^+\dots\text{OH}_2$) with the H^+ placed at 1.19 and 1.20 from each of the two H_2O molecules (Figure 3.7).

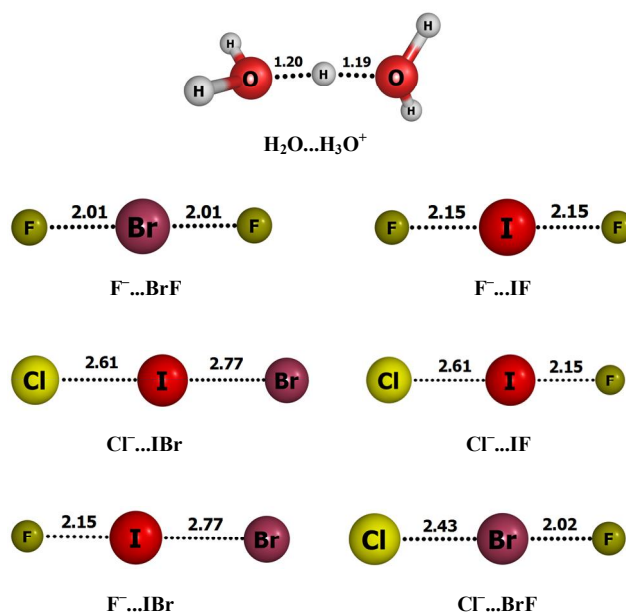


Figure 3.7 **D-A** complexes showing bridged configurations. Bond distances in Å.

It is well established that the topological parameters at bcp correlate with E_{nb} for a variety of noncovalent complexes. Sathyamurthi *et al.* [Parthasarathi *et al.* 2006] used a set of intermolecular complexes of varying strengths from van der Waals to covalent

limit and showed a linear relationship between ρ and E_{nb} as well as $\nabla^2\rho$ and E_{nb} . They also demonstrated a smooth change in the nature of the noncovalent interaction from van der Waals to classical hydrogen bonding and strong hydrogen bonding. Figure 3.8 depicts the relationship between interaction energy and electron density at bcp for all D-A complexes.

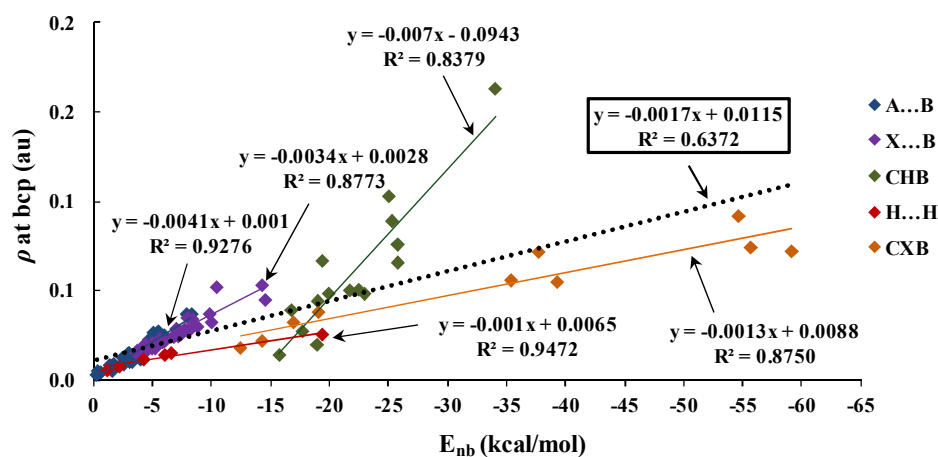


Figure 3.8 Relationship between interaction energy (kcal/mol) and electron density (ρ) at bcp. The dotted line represents the overall correlation and the coloured lines indicate the correlation for separate classes of noncovalent complexes.

The correlation between ρ and E_{nb} is very good for each homogenous sample of complexes. However, for the heterogeneous sample of complexes comprising of neutral (A...B), halogen bonded (X...B), dihydrogen bonded (H...H) and charge-assisted hydrogen bonded (CHB) and charge-assisted halogen bonded (CXB) systems (Figure 3.7), the correlation is found to be poor ($R^2 = 0.64$). For instance, in A...B complexes E_{nb} vs ρ correlation holds good with R^2 value of 0.927. Likewise, satisfactory correlations exist for X...B, CHB, CXB and H...H bonds too with the R^2 values 0.877, 0.837, 0.875 and 0.947, respectively. Thus, although ρ at bcp correlates reasonably well with E_{nb} for each homogenous sample of intermolecular complexes, its applicability for the whole set

is not satisfactory. These results clearly suggest that the applicability of AIM parameters is not quite adequate to describe a large variety of complexes on a uniform scale [Grabowski 2001].

3.7.2 Molecular Electrostatic Potential Analysis

The recent IUPAC recommendations gives emphasis on the key words 'attractive interaction' and 'evidence of bond formation' to define a hydrogen bonds or a halogen bond. Since bonding unequivocally means an attractive interaction, proving the bond formation with proper 'evidence' attains paramount importance. An attractive or repulsive interaction is bound to change the ρ distribution and hence a quantity directly related and very sensitive to ρ and amenable to experimental determination is highly useful to discover the bond formation. MESP is such a quantity and it connects ρ via eq. 1.67. Any change in ρ distribution due to bond formation between **D** and **A** molecules will be well reflected in their MESP features. The electronic changes that accompany the bond formation can be clearly understood by comparing V_{\min} values of isolated **D** and **A** molecules (designated as $V_{\min-A}$ and $V_{\min-D}$, respectively) with V_{\min} values of **D** and **A** molecules in the complex (designated as $V_{\min-A'}$ and $V_{\min-D'}$, respectively). Hence, the electronic reorganization during the bond formation can be quantified as $\hat{\epsilon} V_{\min-D} = V_{\min-D'} - V_{\min-D}$ for donor and $\hat{\epsilon} V_{\min-A} = V_{\min-A'} - V_{\min-A}$ for acceptor (Table 3.4). For all the complexes, $\hat{\epsilon} V_{\min-D}$ is positive indicating the loss in electron density from **D** and $\hat{\epsilon} V_{\min-A}$ is negative indicating gain in electron density by **A**. Thus, **A** becomes more electron rich at the expense of **D** meaning that the interaction between **D** and **A** can be best described as electron donor-acceptor (eDA) interaction. To illustrate this point, MESP plots of a representative set of complexes are given in Figure 3.9 along with their V_{\min} values. In the formation of H₂O dimer (H₂O...H₂O), one of the H₂O molecules (**A**) gains electron density at the expense of the other (**D**) (Figure 3.9 a). In this case, $V_{\min-D}$ and $V_{\min-D'}$ are -

50.45 and -34.51 kcal/mol, respectively and $V_{\text{min-A}}$ and $V_{\text{min-A}'}$ are -50.45 and -63.82 kcal/mol, respectively. $\hat{e}V_{\text{min-A}}$ and $\hat{e}V_{\text{min-D}}$ are 15.95 and -13.37 kcal/mol, respectively which indicates that a significant amount of electron density of **D** has been transferred to **A** during the formation of the noncovalent complex. Another interesting observation is that the magnitude of $\hat{e}V_{\text{min-A}}$ depends on the electron donating ability of the **D** in **D-A**. For instance, in the case of C-H...Y systems H₃N...HCCH and H₂S...HCCH, V_{min} value -22.29 kcal/mol of the isolated HCCH is changed to -32.38 kcal/mol for the former and -26.73 kcal/mol for the latter which accounts for the stronger electron donating power NH₃ ($\hat{e}V_{\text{min-A}}$ -10.09 kcal/mol) than H₂S ($\hat{e}V_{\text{min-A}}$ -4.44 kcal/mol). The $\hat{e}V_{\text{min-A}}$ of negatively charged systems are more negative than neutral ones which indicate a greater shift of electron density towards the acceptor side. This interpretation of $\hat{e}V_{\text{min-D}}$ and $\hat{e}V_{\text{min-A}}$ suggests that the quantity $\hat{e}\hat{e}V_{\text{min}} = \hat{e}V_{\text{min-D}} \hat{o} \hat{e}V_{\text{min-A}}$ could be used as a measure of the donor-acceptor strength of the noncovalent interaction. A reasonably good linear correlation between $\hat{e}\hat{e}V_{\text{min}}$ and E_{nb} is obtained (Figure 3.10) which suggests that the strength of the noncovalent bond is directly related with the donor-acceptor strength. Since V_{min} measures the work done in bringing a unit test positive charge from infinity to the location of the V_{min} , it is an energetic measure on the electrostatic influence. V_{min} is also related with the charge transfer by virtue of its relation to the continuous electron distribution and hence reflects the charge transfer taking place in the system due to non-covalent binding.

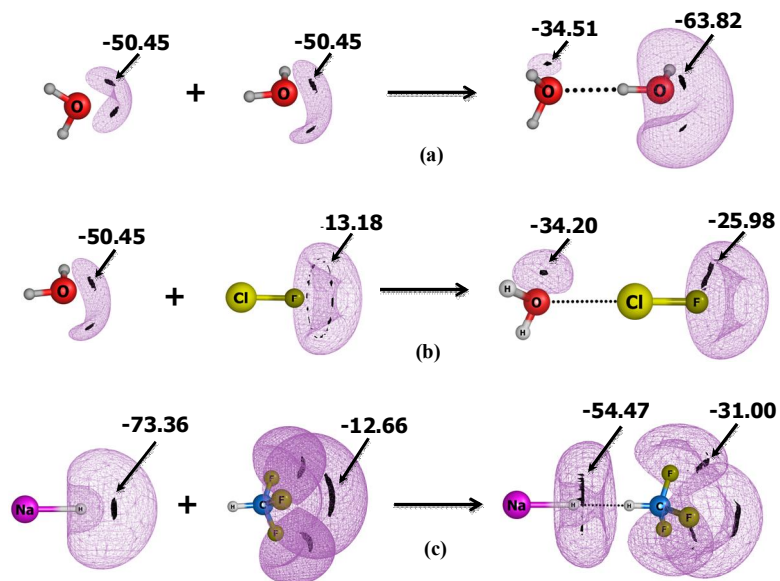


Figure 3.9 Change in V_{\min} upon bond formation for (a) $\text{H}_2\text{O} \dots \text{H}_2\text{O}$ (b) $\text{H}_2\text{O} \dots \text{ClF}$ and (c) $\text{H}_3\text{N} \dots \text{HCCH}$. The black dots represent the location of the most negative MESP-valued point and the corresponding V_{\min} values are also depicted.

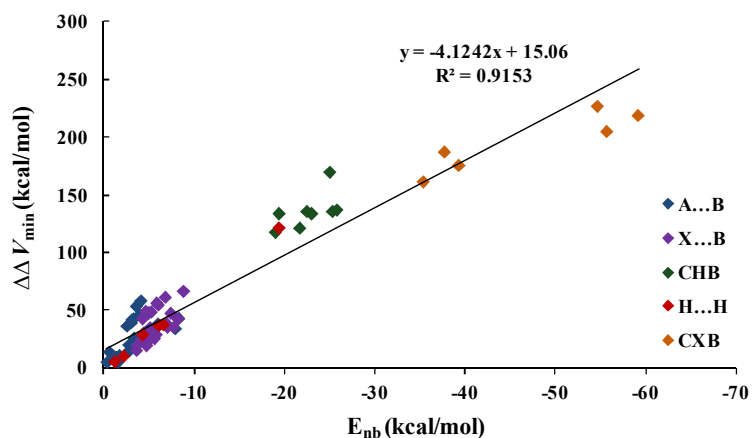
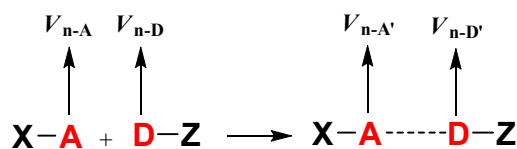


Figure 3.10 Linear relationship between $\Delta\Delta V_{\min}$ and noncovalent interaction energy (E_{nb}).

The V_{\min} approach to measure the donor-acceptor strength is not possible in some cases because of the absence of a local V_{\min} in **D** or **A** of the **D-A** complex and such systems include $\text{Ar} \dots \text{HCH}_3$, $\text{H}_3\text{P} \dots \text{H}_2\text{O}$, $\text{H}_3\text{P} \dots \text{H}_2\text{S}$, $\text{H}_3 \dots \text{HF}$, $\text{H}_3\text{P} \dots \text{HCl}$, $\text{H}_3\text{N} \dots \text{ClF}$ and

all cationic systems. Further, being a sensitive spatial property, V_{\min} can be affected by secondary interactions from other parts of the molecule and this may be the reason for not finding a strong linear correlation between $\Delta\Delta V_{\min}$ and E_{nb} ($R = 0.910$). On the other hand, the nucleus-centered quantity V_n is less sensitive to secondary interactions and all systems including cations show V_n . V_n at the donor (V_{n-D}) and acceptor (V_{n-A}) atoms in free molecules as well as V_n at the donor ($V_{n-D'}$) and acceptor atoms ($V_{n-A'}$) in complexes are computed and the quantities $\Delta V_{n-A} = V_{n-A'} - V_{n-A}$ and $\Delta V_{n-D} = V_{n-D'} - V_{n-D}$ are calculated (Scheme 3.2 and Table 3.4). The quantities ΔV_{n-D} and ΔV_{n-A} can be considered as electron donating ability and electron accepting ability of the acceptor and donor atoms, respectively. In all the A...B, X...B, CA and H...H type complexes, ΔV_{n-D} is positive and ΔV_{n-A} is negative indicating that **D** donates electron density to **A** during bond formation. This result is very similar to that obtained from V_{\min} analysis and also means that $\Delta\Delta V_n = \Delta V_{n-D} - \Delta V_{n-A}$ could be used as a good descriptor to measure the donor-acceptor power of the **D-A** complex.



Scheme 3.2 X-A represents the electron acceptor and D-Z represents the electron donor. **D** and **A** are the atoms participating in the interaction. MESP at the nuclei are designated with symbols V_{n-A} , $V_{n-A'}$, V_{n-D} and $V_{n-D'}$.

A single linear correlation exists between $\hat{\hat{V}}_n$ and E_{nb} for all the **D-A** complexes except the bridged ones as shown in Figure 3.11. This correlation has R^2 value 0.976 suggesting that V_n can be effectively used for describing the bonding strength of all the **D-A** complexes irrespective of which category they belong to, *viz.* hydrogen bonds, halogen bonds, charge-assisted hydrogen bonds, charge-assisted

halogen bonds and dihydrogen bonds. The correlations of \hat{V}_{\min} and \hat{V}_n with E_{nb} also suggest the dominance of electrostatic contribution to the total interaction energy of noncovalent complexes. The exclusion of the bridged systems ($\text{H}_3\text{O}^+ \dots \text{H}_2\text{O}$, $\text{F} \dots \text{I} \dots \text{F}$, $\text{F} \dots \text{Br} \dots \text{F}$, $\text{Cl} \dots \text{I} \dots \text{F}$, $\text{Cl} \dots \text{Br} \dots \text{F}$, $\text{F} \dots \text{I} \dots \text{Br}$ and $\text{Cl} \dots \text{I} \dots \text{Br}$) from the linear correlation is justified because in such systems, the central atom show strong electron accepting interactions from two other atoms compared to only such interaction in non-bridged structures. The electronic reorganization during the bond formation in bridged anionic CXB complexes is demonstrated by means of MESP plots in Figure 3.12. In $\text{F} \dots \text{IF}$ complex, I is placed symmetrically with respect to both the F atoms making it difficult to distinguish which F atom is the electron donor. This suggests the possibility of a resonance combination of $\text{F} \dots \text{IF}$ and $\text{F} \dots \text{IF}$ and equal sharing of negative charge on both F atoms. Hence we may assume that central iodine accepts charge density from both the F atoms leading to a donor-acceptor-donor interaction in the bridged complex. This argument is further supported by the fact the both F atoms show the same V_{\min} value in the complex (-158.20 kcal/mol) and a large enhancement in the negative MESP on the iodine atom (-110.63 kcal/mol). The MESP plot of $\text{F} \dots \text{IBr}$ too suggests the electron accepting interaction of iodine with partially negatively charged F and Br atoms. Energy decomposition analysis (EDA) by Wolters and Bickelhaupt [Wolters and Bickelhaupt 2012] has shown that halogen bonded trihalides of the type $\text{DX} \dots \text{A}$ (D, X, A = F, Cl, Br, I) are generally associated with a weaker electrostatic attraction and a significantly strong covalent component arising from the stabilizing HOMO δ LUMO interaction between the np-type lone pair on the halogen accepting fragment, A and the D-X antibonding * LUMO on the halogen bond donating fragment DX.

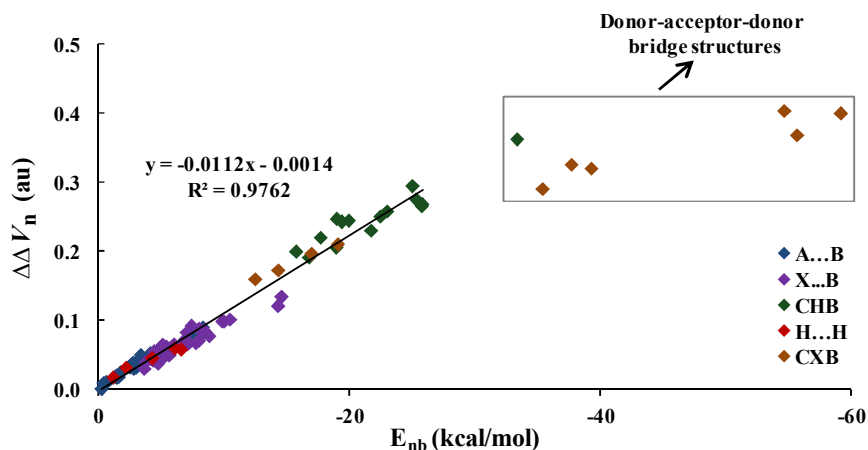


Figure 3.11 Linear relationship between $\Delta\Delta V_n$ and noncovalent interaction energy (E_{nb}).

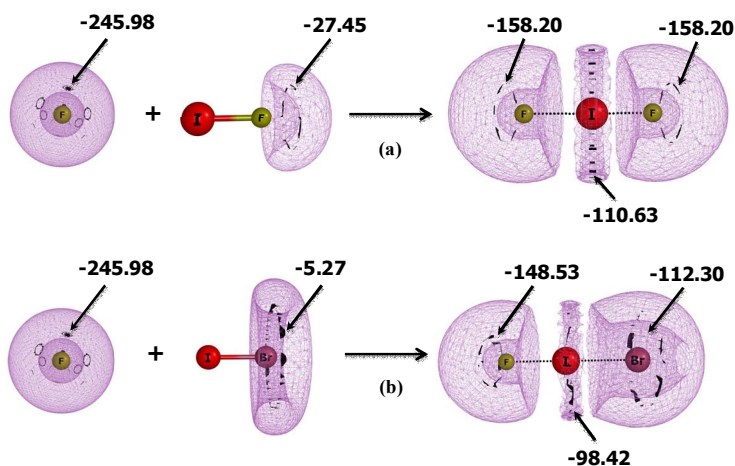


Figure 3.12 Change in V_{min} upon bond formation in electron donor-acceptor-donor complexes (a) F ...IF and (b) F ...IBr. The black dots represent the location of the most negative MESP-valued point and the corresponding V_{min} values are also depicted.

The significance of the correlation between $\Delta\Delta V_n$ and E_{nb} is that MESP approach unifies all kinds of hydrogen bonds, halogen bonds and dihydrogen bonds as electron donor-acceptor (eDA) interactions. Hence a hydrogen bond could be considered as an eDA interaction in which a hydrogen atom acts as an electron acceptor. This interpretation is also applicable for dihydrogen bonds. Similarly a halogen bond may be defined as an eDA interaction in which a halogen atom acts as the electron acceptor.

Table 3.4 Interaction energies (E_{nb}), AIM properties (ρ and $\nabla^2\rho$) and MESP features ($\hat{e} V_{\min-A}$, $\hat{e} V_{\min-D}$, $\hat{e} \hat{e} V_{\min}$, $\hat{e} V_{n-A}$, $\hat{e} V_{n-D}$ and $\hat{e} \hat{e} V_n$) for representative set of intermolecular complexes.

Complex	E_{nb} (kcal/mol)	ρ (au)	$\nabla^2\rho$ (au)	$\hat{e} V_{\min-A}$ (kcal/mol)	$\hat{e} V_{\min-D}$ (kcal/mol)	$\hat{e} \hat{e} V_{\min}$ (kcal/mol)	$\hat{e} V_{n-A}$ (au)	$\hat{e} V_{n-D}$ (au)	$\hat{e} \hat{e} V_n$ (au)
Ar...HCH ₃	-0.23	0.003	0.011				-0.0005	0.0005	0.0009
H ₂ S...HCH ₃	-0.37	0.005	0.016	-4.15	0.56	4.72	-0.0088	0.0007	0.0096
H ₃ P...H ₂ S	-1.47	0.008	0.020				-0.0097	0.0080	0.0177
H ₂ S...H ₂ S	-1.38	0.008	0.024	-4.14	4.39	8.53	-0.0087	0.0091	0.0178
H ₃ P...H ₂ O	-2.47	0.013	0.031				-0.0185	0.0134	0.0319
H ₄ C ₂ ...HF	-4.47	0.018	0.040	-10.10	14.33	24.43	-0.0253	0.0257	0.0510
H ₃ P...H ₃ P	-0.62	0.004	0.011	-3.66	9.89	13.55	-0.0075	0.0023	0.0098
H ₂ O...H ₂ O	-4.70	0.023	0.085	-13.37	15.94	29.30	-0.0303	0.0260	0.0563
H ₃ BH...HF	-19.38	0.025	0.057	-105.30	15.88	121.17	-0.2005	0.0423	0.2428
HBeH...HCCH	-1.17	0.006	0.018	-2.81	2.49	5.30	-0.0079	0.0098	0.0176
LiH...HCCH	-4.26	0.011	0.027	-18.37	10.29	28.66	-0.0413	0.0041	0.0454

-- Table 3.4 continued --

LiHf HCF ₃	-6.06	0.014	0.033	-15.89	20.71	36.60	-0.0473	0.0121	0.0594
CF ₃ H...HNa	-6.57	0.015	0.033	-18.34	18.89	37.22	-0.0537	0.0195	0.0732
H ₂ O...H ₄ N ⁺	-19.93	0.048	0.127				-0.0434	0.2011	0.2445
C ₆ H ₆ ...H ₄ N ⁺	-18.93	0.020	0.054				-0.0519	0.1537	0.2055
ClO ⁻ ...H ₂ O	-19.38	0.067	0.125	-113.14	20.33	133.47	-0.2028	0.0405	0.2433
ClO ⁻ ...HF	-22.46	0.051	0.155	-110.27	24.91	135.18	-0.2148	0.0355	0.2504
ClO ₂ ⁻ ...HF	-25.32	0.089	0.092	-117.53	-17.70	135.22	-0.2190	0.0559	0.2750
H ₃ N...ClF	-10.46	0.052	0.139				-0.0398	0.0615	0.1013
H ₂ O...ClF	-4.95	0.021	0.101	-12.80	16.25	29.05	-0.0242	0.0315	0.0557
H ₂ S...ClF	-4.44	0.020	0.062	-10.92	10.98	21.90	-0.0172	0.0249	0.0420
HCN...BrCl	-4.30	0.015	0.065	-10.08	32.47	42.55	-0.0210	0.0208	0.0418
H ₃ CCN...BrCl	-5.24	0.018	0.075	-13.23	35.02	48.25	-0.0273	0.0202	0.0474
H ₂ CO...BrCl	-4.73	0.018	0.078	-8.73	10.48	19.21	-0.0159	0.0218	0.0377
F...FI	-59.15	0.072	0.283	-130.75	87.79	218.54	-0.2183	0.1817	0.4000
CH ₂ Cl...NH ₃	-16.96	0.032	0.104				-0.0319	0.1645	0.1964

3.8 Conclusions

In Part A of this chapter, the competence of M06L, MP2, MP4//M06L, MP4//MP2 and CCSD(T)//MP2 methods for modeling accurate binding energies of noncovalent complexes featuring hydrogen bonds, halogen bonds and dihydrogen bonds is assessed by comparing the energies calculated using these methods against highly accurate W1BD benchmark energies. Though M06L method is reliable for calculating the binding energies of neutral hydrogen bond complexes, it overestimates the energies of charge-assisted hydrogen bonds, halogen bonds and dihydrogen bonds. However, the MP4//M06L method yields noteworthy improvement on the energy data, making this hybrid method a good *ab initio*-DFT choice for estimating noncovalent interaction energies. The energy values of hydrogen bonds, halogen bonds and dihydrogen bonds are underestimated at MP2 level while MP4//MP2 and CCSD(T)//MP2 methods reproduces energies very close to W1BD accuracy. Hence MP4//MP2 and CCSD(T)//MP2 methods as are good hybrid *ab initio* choices for modeling the interaction energies of noncovalent complexes. The interaction energy data shows that geometry optimization at an *ab initio* or DFT method followed by single point energy calculation using MP4 or CCSD(T) level (viz. MP4//MP2, MP4//M06L and CCSD(T)//MP2) at a higher basis set can yield interaction energy values with accuracy close to computationally expensive CCSD(T) and W1BD methods. The enhancing effect of monovalent cations on the strength of hydrogen bonds is very high which promotes a noncovalent bond in the weak regime to the medium regime and that in the medium regime to the strong regime.

In Part B of this chapter, high level *ab initio* calculations coupled with atoms-in-molecules (AIM) and molecular electrostatic potential (MESP) approaches have been used for the study of a variety of intermolecular hydrogen bonds, halogen bonds and dihydrogen bonds to devise descriptor to quantify these noncovalent interactions.

Although ρ values prove to be effective within a homogenous sample of **D-A** complexes where either the electron donor or acceptor is fixed, the applicability of these parameters for a heterogeneous sample of **D-A** complexes with different electron donors and/or acceptors is limited. An analysis of the V_{\min} values of donor and acceptor molecules before and after complex formation shows that there is a considerable rearrangement of electron density within each monomer during the bond formation. A strong linear correlation is established between a parameter based on V_n viz. $\Delta\Delta V_n$ and E_{nb} of all the complexes. The MESP at the nucleus emerges as an effective parameter to describe electron donor-acceptor interactions irrespective of the nature and strength of the interactions. To conclude, hydrogen bond can be considered as an eDA interaction in which a hydrogen atom acts as an electron acceptor whereas a halogen bond is as an eDA interaction in which a halogen atom acts as the electron acceptor. It is also shown that charge-assisted bridged complexes belong to a new category of donor-acceptor-donor complexes.

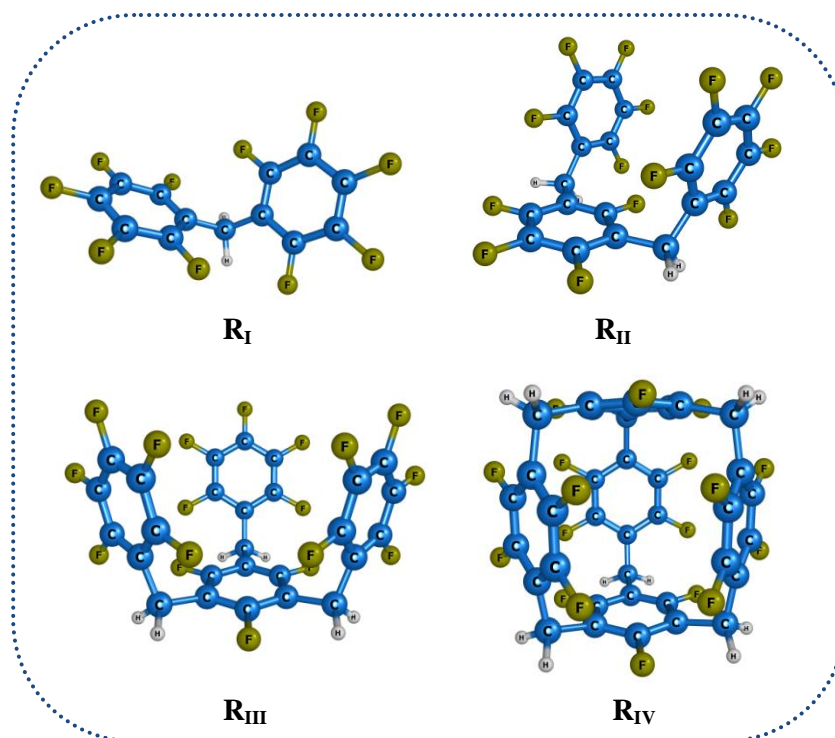
Chapter 4

Rational Design of Receptors Based on Noncovalent Interactions

Part A – Receptors for Neutral Molecules and
Anions

&

Part B – Cage Receptors for Noble Gas Atoms
and Molecular Hydrogen



4.1 ABSTRACT

In Part A of this chapter, mono, di, and tri pentafluorobenzyl substituted hexafluorobenzene (HFB) scaffolds \mathbf{R}_I , \mathbf{R}_{II} and \mathbf{R}_{III} are proposed as promising receptors for molecules of chemical, biological and environmental relevance, viz. N_2 , O_3 , H_2O , H_2O_2 , F^- , Cl^- , BF_4^- , NO_3^- , ClO^- , ClO_2^- , ClO_3^- , ClO_4^- and SO_4^{2-} . The receptor-guest complexes modelled using M06L/6-311++G(d,p) DFT show remarkable increase in the complexation energy (E_{int}) with increase in the number of fluorinated aromatic moieties in the receptor. Electron density analysis shows that fluorinated aromatic moieties facilitate the formation of large number of lone pair- π interactions around the guest molecule. Lone pair strength of guest molecules quantified in terms of the absolute minimum (V_{min}) of molecular electrostatic potential show that E_{int} strongly depends on the electron-deficient nature of the receptor as well as strength of lone pairs in the guest molecule. Compared to HFB, \mathbf{R}_I exhibits 1.1 to 2.5-fold, \mathbf{R}_{II} shows 1.6 to 3.6-fold and the bowl-shaped \mathbf{R}_{III} gives 1.8 to 4.7-fold increase in the magnitude of E_{int} . For instance, in the cases of $HFB...F^-$, $\mathbf{R}_I...F^-$, $\mathbf{R}_{II}...F^-$ and $\mathbf{R}_{III}...F^-$ the E_{int} values are -21.1, -33.7, -38.1 and -50.5 kcal/mol, respectively. The results strongly suggest that tuning lone pair- π interaction provides a powerful strategy to design receptors for small molecules and anions.

Highly fluorinated aromatic cores are electron-deficient and provide stabilizing interactions with inert gases. In Part B of this chapter, a fluorinated cage receptor molecule (\mathbf{R}_{IV}) capable of forming stable endohedral complexes with noble gas atoms and molecular hydrogen designed by pentafluorobenzyl

*(C₆F₅CH₂-) substitution of hexafluorobenzene core is reported. The van der Waals complexes of rare gas atoms (He, Ne, Ar and Kr) with **R_{IV}** studied at M06L/6-311++G(d,p) density functional theory show that ~5 to 8-fold increase in interaction energy can be achieved using **R_{IV}** compared to the unsubstituted hexafluorobenzene. Hexafluorobenzene (HFB) stabilizes He, Ne, Ar, and Kr by -0.69, -0.93, -0.76, and -1.00 kcal/mol. The inert gas stabilization increases steadily with the cage receptor molecule with E_{int} values -4.07, -5.97, -6.00, and -6.11 kcal/mol for He, Ne, Ar and Kr respectively. The efficiency of **R_{IV}** to trap and store molecular hydrogen is evident from the highly stable **R_{IV}...H₂** complex with an E_{int} value of -7.08 kcal/mol.*

Part A – Receptors for Neutral Molecules and Anions

4.2 Introduction

The design and synthesis of novel receptor systems for charged and neutral small molecules is a particularly relevant and challenging field that has spurred the interest of synthetic and theoretical chemists [Beer and Gale 2001; Dietrich 1993; Joyce *et al.* 2010; McKee *et al.* 2003]. Receptors capable of selective binding to small molecules find potential applications in varying fields including chemical and biological recognition, drug delivery, environmental chemistry, bio-sensing, catalysis, chemical separation and storage. Molecular recognition processes are mainly based on the combination of various attractive noncovalent interactions between receptor and substrate like electrostatic, dipole, dispersion, π -stacking, hydrogen bonding interactions and coordination to Lewis acids [Schmidtchen and Berger 1997]. Relatively few systems capable of molecular recognition of small gaseous substrates have been reported which include cyclodextrins, hemicarcerands, cryptophanes and porphyrins [Dietrich 1993; Graf and Lehn 1976]. Higher degree of design is required to make complementary receptors to anionic guests since they exhibit a multitude of geometries ranging from linear to spherical and even more complex structures as in the case of poly anions like DNA [Bianchi *et al.* 1997]. Larger size of anions leading to lower charge to mass ratio, sensitivity of anions to pH and protonation under acidic conditions also adds to the complexity involved in the design of anion hosts. The field of anion receptor chemistry emerged with a seminal communication by Simmons and Park [Park and Simmons 1968a; Park and Simmons 1968b] reporting the synthesis of a macrobicyclic ammonium based receptor for the

binding of chloride ions. The highly specific transport of sulphate and phosphate across biological membranes regulated by neutral anion binding proteins motivated research efforts for the synthesis of neutral receptors. Crystal structures [Pflugrath and Quioco 1988] have revealed that the sulfate binding protein binds the anion through precisely positioned hydrogen bonding interactions between the sulfate anion and the NH groups of the protein backbone, serine OH, or tryptophan NH groups [He and Quioco 1991; Luecke and Quioco 1990; Pflugrath and Quioco 1985]. On the basis of these initial findings, a myriad of synthetic anion receptors have been designed utilizing hydrogen bonding [Amendola *et al.* 2010a; Amendola *et al.* 2010b; Begum *et al.* 2006; Bondy and Loeb 2003; Choi and Hamilton 2003; Lhoták 2005; Li *et al.* 2010; Llinares *et al.* 2003; Yoon *et al.* 2006] for anion recognition which include macrocyclic polyammonium/guanidinium, amides, urea, thiourea and functionalized calixarenes based receptors.

Compelling evidence for lone pair- π and anion- π interactions from theoretical [Alkorta *et al.* 1997; Alkorta *et al.* 2002; Mascali *et al.* 2002; Quiñero *et al.* 2002b], experimental [De Hoog *et al.* 2004; Estarellas *et al.* 2011; Estarellas *et al.* 2009; Garcia-Raso *et al.* 2007; Kim *et al.* 2004; Schottel *et al.* 2008] and data base studies [Ahuja and Samuelson 2003; Casellas *et al.* 2006; Mooibroek *et al.* 2008; Quiñero *et al.* 2002a; Quiñero *et al.* 2002b] have opened an alternative route for the recognition of charged and neutral molecules bearing lone pairs by neutral hosts. Haloaromatics and electron-deficient aromatic rings like hexafluorobenzene, s-triazine, tetracyanobenzene, hexaazatriphenylene and tricyanobenzenes characterized by large negative quadrupole moments are widely employed as anion binding units for the recognition of anions [Alkorta *et al.* 2002; Mascali *et al.* 2002; Mooibroek *et al.* 2008]. Receptors capable of multiple lone pair- π interactions with the guest molecules in a cooperative fashion are required for efficient and selective recognition of lone

pairs [Mascal *et al.* 2002]. Recently, Deya *et al.* demonstrated the additivity of anion- π interactions using *ab initio* calculations with the goal of designing neutral anion receptors [Garau *et al.* 2005]. Literature reports on highly selective anion receptors and channels [Dawson *et al.* 2010; Gorteau *et al.* 2006; Hay and Bryantsev 2008; Matile and Mareda 2009; Sakai *et al.* 2010] based on anion- π interactions marks the rapid progress in the field. Mascal [Mascal 2006] theoretically predicted and experimentally synthesized several 1,3,5-cyclophane-based receptors incorporating triazine, cyanuric acid, or boroxine rings which show selective recognition towards fluoride ions by a combination of anion- π interactions and ion-pair reinforced hydrogen bonding. Matile *et al.* [Matile and Mareda 2009] recently reported the synthesis and use of oligomer of NDIs for making anion- π slides that can be exploited to transfer anions through membranes. The interaction of hexafluorobenzene (HFB) with electron-rich systems are well documented and is beneficially exploited as a key binding motif for the design of lone pair and anion sensors and receptors [Alkorta *et al.* 2002; Amicangelo *et al.* 2012; Danten 1999; Gallivan and Dougherty 1999; Kim *et al.* 2004; Mohan *et al.* 2013; Quiñonero *et al.* 2002b]. Very recently, Meyer *et al.* [Bretschneider *et al.* 2013] reported the synthesis of two neutral anion receptors *viz.* 1,3-bis(pentafluorophenyl-imino)isoindoline and 3,6-di-tert-butyl-1,8-bis(pentafluorophenyl)-9H-carbazole that exploit anion- π interactions to bind chloride and bromide ions.

Herein, neutral molecular receptors capable of binding lone pairs in molecules including anions through multiple lone pair- π interactions are proposed using density functional theory (DFT) calculations. HFB is used as a scaffold and is substituted with pentafluorobenzyl groups ($C_6F_5CH_2-$) to model bidentate receptor (**R_I**), tridentate receptor (**R_{II}**) and a tetridentate receptor (**R_{III}**) (Scheme 4.1). The $C_6F_5CH_2-$ arms of the receptor molecules are expected to show orientation toward the electron-rich lone pair regions of the incoming molecule. Since the selective recognition of anions have

biological, chemical and environmental implications, the proposed receptor models could serve as excellent lead molecules towards the synthesis of anion receptors with potential medicinal and biological applications.

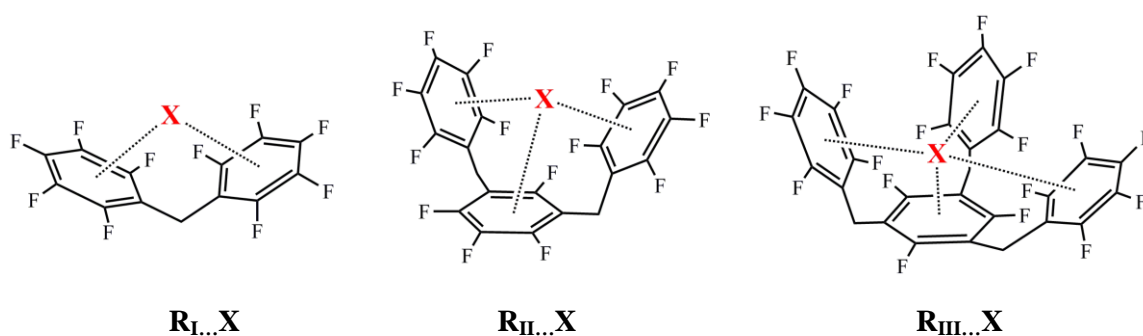
4.3 Methods

4.3.1 Molecular Design Strategy

Hexafluorobenzene (HFB), due to its electron-deficient nature, can bind effectively to lone pairs in neutral molecules, anions and free radicals [Alkorta *et al.* 1997; Alkorta *et al.* 2002; Mohan *et al.* 2013]. In order to improve the selectivity and binding affinity of HFB, pentafluorobenzyl ($C_6F_5CH_2-$) substitution on HFB core is done. Substituting one F- with $C_6F_5CH_2-$ leads to the receptor **R_I**, a bis(perfluoroaryl)methane molecule with bidentate functionality. The synthetic approach of **R_I** by the desulfurization of sulfone-stabilized carbanions is reported in literature [Chambers and Todd 1985], however the utility of this molecule as a receptor for lone pair bearing molecules has not been investigated. **R_{II}** is a fluorinated 1, 3-dibenzylbenzene molecule designed by substituting the HFB core with two $C_6F_5CH_2-$ groups at 1 and 3 positions. The three electron-deficient rings in **R_{II}** make it a suitable receptor for the recognition of molecules with three lone pair bearing atoms like O_3 and NO_3^- . The tetradentate receptor (**R_{III}**) is a fluorinated 1, 3, 5-tribenzylbenzene molecule designed by substituting HFB core with $C_6F_5CH_2-$ groups at 1, 3 and 5 positions. **R_{III}** is bowl-shaped and has four electron-deficient rings which can bind to anions with tetrahedral geometry like SO_4^{2-} and ClO_4^- . The three receptor models **R_I**, **R_{II}** and **R_{III}** and their possible lone pair- π interactions with any lone pair bearing molecule is presented in Scheme 4.1.

The interactions of **R_I**, **R_{II}** and **R_{III}** with different lone pair bearing neutral and anionic molecular systems of chemical, biological and environmental significance *viz.* N_2 , O_3 , H_2O , H_2O_2 , F^- , Cl^- , BF_4^- , NO_3^- , ClO^- , ClO_2^- , ClO_3^- , ClO_4^- and SO_4^{2-} have been

analyzed for their ability to form lone pair- π /anion- π interactions. The chlorine oxyanion family *viz.* Cl^- , ClO^- , ClO_2^- , ClO_3^- and ClO_4^- is chosen due to their environmental significance and also to understand the effect of sequential increase in the number of lone pair bearing atoms on the binding energy.



Scheme 4.1 Models proposed for anion recognition. X represents the lone pair bearing molecule and the possible lone pair- π interactions are represented with dotted lines.

4.3.2 Computational Methods

The geometries of all the receptor models and the complexes of the receptors with various lone pair bearing molecules are optimized at M06L level [Zhao and Truhlar 2006] using 6-311++G(d,p) basis set by means of Gaussian09 [Frisch *et al.* 2010] suite of programs. The binding energies are calculated using supermolecule approach with correction for basis set superposition error (BSSE) using counterpoise technique [Boys and Bernardi 1970a]. Solvation energies of a representative set of host-guest complexes are calculated using single point energy calculations at isodensity polarized continuum model (IPCM) [Foresman *et al.* 1996] at the same level of theory. IPCM model is more realistic and accurate since the solvation cavity is defined based on the isosurface of electron density. The topological properties of electron density at bond critical points (bcps) have been studied using ‘atoms-in-molecules’ (AIM) methodology with AIM2000 program [Biegler-König and Schönbohm 2002; Biegler-König *et al.* 2001]. Molecular

electrostatic potential analysis (MESP) is used to quantify the electron-rich character of the guest molecules. MESP topography of the receptor molecules are also analyzed at same level of theory.

4.4 Results and Discussion

The optimized geometries of **R_I**, **R_{II}** and **R_{III}** are presented in Figure 4.1. While HFB has all the ring C-C-C bond angles and C-C bond lengths equal *i.e.*, 120° and 1.39 Å respectively, substitution with C₆F₅CH₂- groups causes slight distortion of the C-C-C bond angles in **R_I**, **R_{II}** and **R_{III}**. In all the cases, C-C-C bond angle at the ipso carbon for the ring is decreased (by approximately 3 - 5°) while other C-C-C bond angles of the rings are increased (by approximately 2 - 5°). However, the C-C bond lengths remain more or less the same in all the receptors.

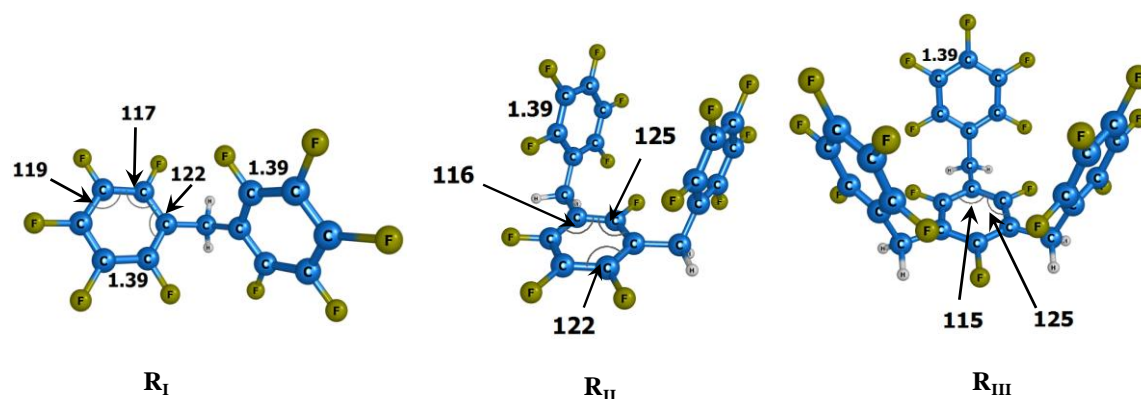


Figure 4.1 Optimized geometries of **R_I**, **R_{II}** and **R_{III}** at M06L/6-311++G(d,p) DFT method. C-C bond distances in Angstroms and C-C-C bond angles in degree are also depicted.

A qualitative picture of the electron-deficient nature of the fluorinated receptors can be understood from the MESP plots presented in Figure 4.2 where the regions of most negative potential appear blue and regions of most positive potential appear red. The π -region of benzene is evident from the large negative MESP on the ring.

Monofluorobenzene also shows negative MESP over the aromatic ring. With hexafluoro substitution, MESP over the ring becomes positive indicating highly electron-deficient HFB. The reversal of electrostatics in HFB can be attributed to the combined electron withdrawing power of six fluorine atoms. The receptors **R_I**, **R_{II}** and **R_{III}** also show highly electron-deficient nature of aromatic rings. In the fluorinated aromatics, F atoms show blue-colored MESP which correspond to their lone pair regions. Since F atoms withdraw π -electron density from the aromatic rings, an increase in the negative character of V_{\min} on F can indicate increased electron deficiency on the aromatic rings. The MESP isosurface of HFB and the three receptor molecules are shown in Figure 4.3 along with their V_{\min} values. It shows that compared to HFB having V_{\min} -6.6 kcal/mol on F atoms, the F atoms of **R_I**, **R_{II}** and **R_{III}** show progressively more negative V_{\min} , viz. -9.2, -11.0 and -14.1 kcal/mol respectively, suggesting that more fluorine substitution increases the electron deficiency on the aromatic rings. The larger electron-deficient nature of the aromatic rings will enable the receptor molecules to establish stronger electrostatic influence on lone pair- π interactions.

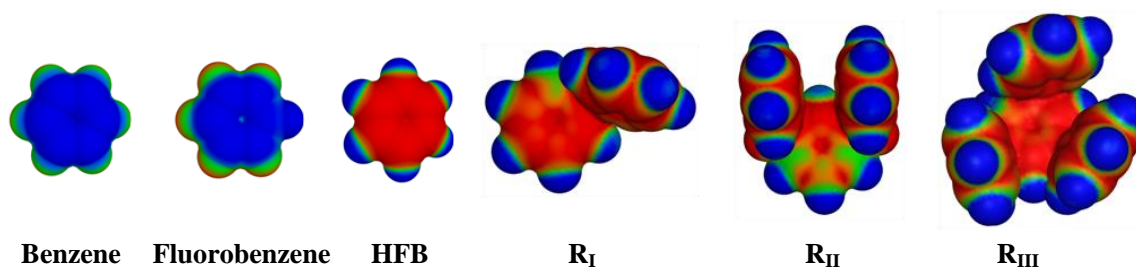



Figure 4.2 MESP plots demonstrating the nature of aromatic rings in benzene, fluorobenzene, HFB, **R_I**, **R_{II}** and **R_{III}**. Color coding,  blue -0.001 a.u. to red 0.03 a.u.

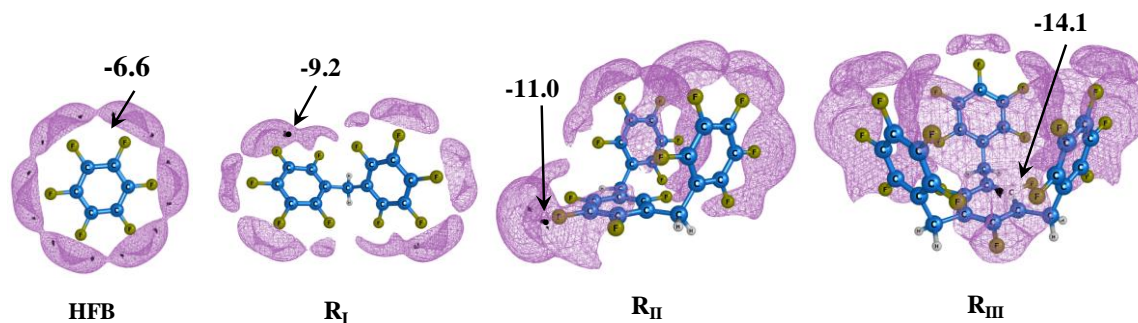


Figure 4.3 MESP isosurface of value -0.01 au for HFB, \mathbf{R}_I , \mathbf{R}_{II} and \mathbf{R}_{III} along with their V_{\min} values in kcal/mol. V_{\min} points are indicated by black dots.

MESP isosurfaces and MESP minima of some representative lone pair bearing molecules are presented in Figure 4.4. Table 4.1 reports the V_{\min} values of all guest molecules. In Chapter 2 it has been shown that V_{\min} quantifies the electron-rich character of a lone pair and provides good prediction on the lone pair- π interaction energy (E_{int}) with any electron-deficient π -system as V_{\min} correlates linearly with E_{int} . [Kumar *et al.* 2014; Mohan *et al.* 2013] The location of the lone pair region also enables a prediction on the orientation of the lone pair bearing molecule in the lone pair- π complex [Mohan *et al.* 2013]. Among all the systems discussed here, sulfate anion (SO_4^{2-}) exhibits the deepest V_{\min} (-279.6 kcal/mol) while the least negative V_{\min} (-3.6 kcal/mol) is observed for Cl_2 . The negative character of V_{\min} follows the order, $\text{Cl}_2 < \text{N}_2 < \text{O}_3 < \text{H}_2\text{O}_2 < \text{H}_2\text{O} < \text{ClO}_4^- < \text{BF}_4^- < \text{ClO}_3^- < \text{NO}_3^- < \text{Cl}^- < \text{ClO}_2^- < \text{ClO}^- < \text{F}^- < \text{SO}_4^{2-}$. In the chlorine oxyanion family, hypochlorite anion (ClO^-) possesses the most negative V_{\min} (-205.9 kcal/mol) while ClO_4^- has the least electron-rich character with a V_{\min} of -139.9 kcal/mol. The interaction energies of the receptor guest complexes are also expected to follow the same trend.

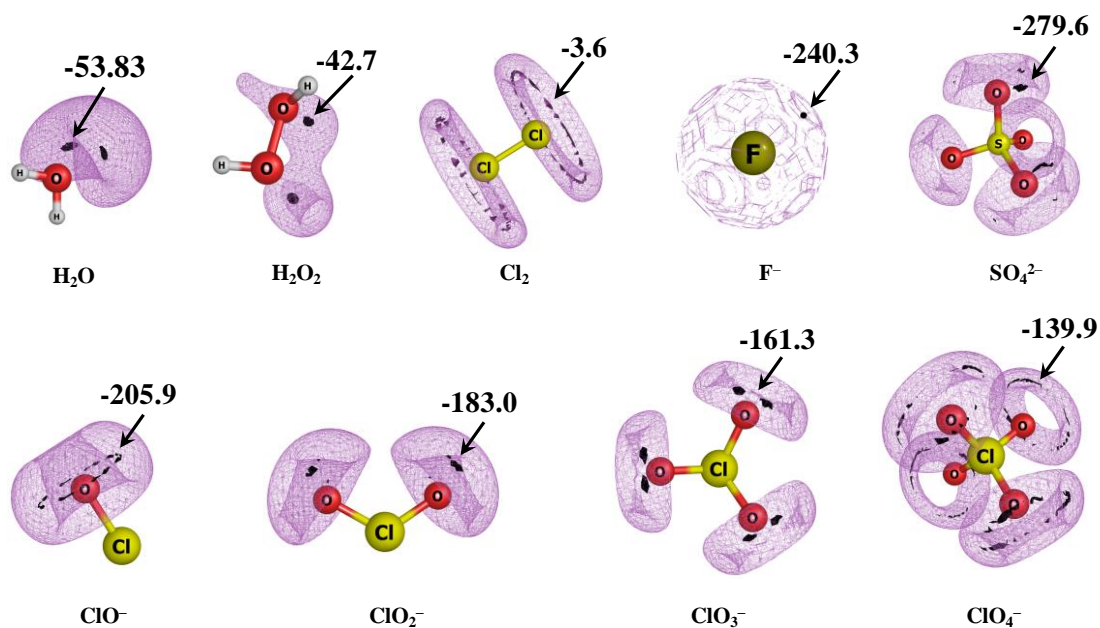


Figure 4.4 Representation of MESP isosurfaces for a representative set of lone pair bearing guest molecules. The MESP minima are marked as black dots and the corresponding V_{\min} values are given in kcal/mol.

The optimized geometries of $\mathbf{R}_I \dots \mathbf{X}$, $\mathbf{R}_{II} \dots \mathbf{X}$ and $\mathbf{R}_{III} \dots \mathbf{X}$ complexes are given in Figure 4.5, 4.6 and 4.7 respectively. Table 4.1 reports the BSSE-corrected interaction energies (E_{int}) of $\mathbf{HFB} \dots \mathbf{X}$, $\mathbf{R}_I \dots \mathbf{X}$, $\mathbf{R}_{II} \dots \mathbf{X}$ and $\mathbf{R}_{III} \dots \mathbf{X}$ complexes in kcal/mol. E_{int} values of $\mathbf{HFB} \dots \mathbf{X}$ allows a comparison of the enhancement in binding energies in \mathbf{R}_I , \mathbf{R}_{II} and \mathbf{R}_{III} achieved by $\text{C}_6\text{F}_5\text{CH}_2^-$ substitution on the HFB core. The optimum configuration of the guest molecules in all $\mathbf{R}_I \dots \mathbf{X}$ complexes is such as to maximize the interactions from all the lone pairs with the electron-deficient arms of the receptor. For instance in $\mathbf{R}_I \dots \text{H}_2\text{O}$, the lone pairs of the O atom are oriented to each of the C_6F_5^- arm of the receptor forming two lone pair- π interactions with interaction distances of 3.38 and 3.34 Å respectively. In molecules like H_2O_2 , H_2O , F^- , Cl^- , O_3 , ClO_4^- , BF_4^- and SO_4^{2-} the interacting atoms are located almost equidistant from the two electron-deficient rings of the receptor molecule. F^- forms two anion- π interactions with \mathbf{R}_I at an interaction distance of 2.90 Å from both the perfluoroaryl rings in $\mathbf{R}_I \dots \text{F}^-$ complex.

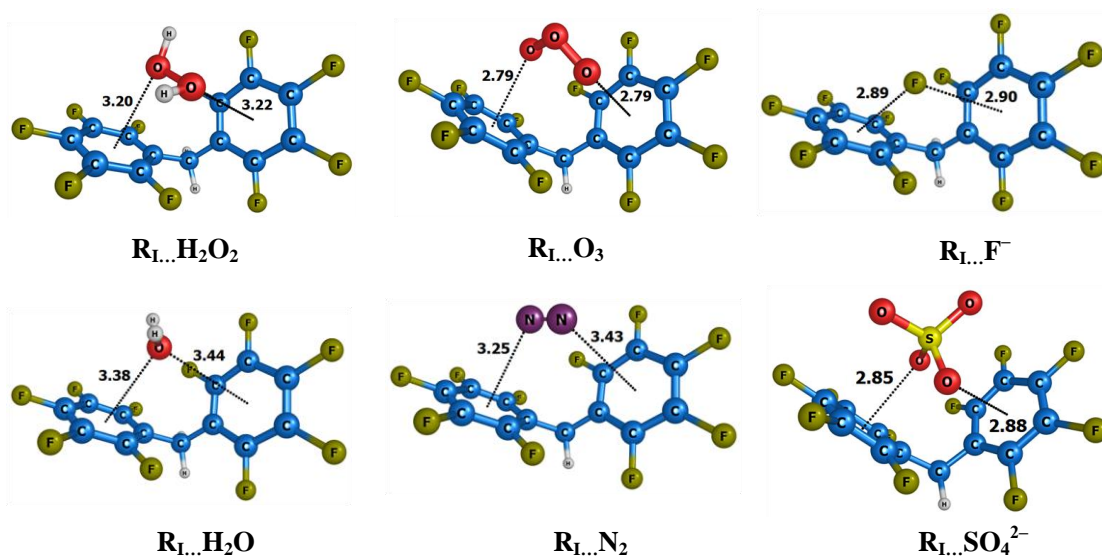


Figure 4.5 Optimized geometries of $\mathbf{R_I...X}$ complexes. Distances in Angstrom units.

The presence of multiple lone pair- π interactions is amply justified by a drastic increase in the magnitude of E_{int} . The percentage increase in the magnitude of E_{int} values in $\mathbf{R_I...X}$ compared to $\mathbf{HFB...X}$ is 11.2 - 174.8% which imply that molecules which can provide multiple interaction sites can indeed be used as effective recognition motifs for anions and lone pair bearing molecules. SO_4^{2-} exhibits the most stable interaction with $\mathbf{R_I}$ giving an E_{int} of -48.6 kcal/mol while the least stable interaction with $\mathbf{R_I}$ is shown by N_2 molecule ($E_{\text{int}} = -2.6$ kcal/mol). The binding affinity of the guest molecules towards $\mathbf{R_I}$ follows the order, $\text{N}_2 < \text{H}_2\text{O} < \text{Cl}_2 < \text{H}_2\text{O}_2 < \text{O}_3 < \text{ClO}_3^- < \text{ClO}_4^- < \text{BF}_4^- < \text{NO}_3^- < \text{Cl}^- < \text{ClO}_2^- < \text{ClO}^- < \text{F}^- < \text{SO}_4^{2-}$. Among the chlorine oxyanion family, ClO^- binds more strongly with $\mathbf{R_I}$ ($E_{\text{int}} = -18.6$ kcal/mol) while ClO_2^- exhibits the weakest binding ($E_{\text{int}} = -13.8$ kcal/mol).

Optimized geometries of $\mathbf{R_{II}...X}$ complexes presented in Figure 4.6 clearly show the presence of at least three lone pair- π interactions in all the complexes. A significant increase in the magnitude of E_{int} (13.5 - 45.2%) is observed for $\mathbf{R_{II}...X}$ compared to $\mathbf{R_I...X}$ (for $X = \text{O}_3$, E_{int} is nearly unchanged) which presumably is the result of multiple interactions between the host and guest. The most significant enhancement in the

magnitude of E_{int} is observed for $\mathbf{R}_{\text{II}}\dots\text{N}_2$ which is ~ 1.5 times higher than that of $\mathbf{R}_{\text{I}}\dots\text{N}_2$. The E_{int} values of various molecules with \mathbf{R}_{II} suggest the following trend in binding affinity: $\text{N}_2 < \text{O}_3 < \text{H}_2\text{O} < \text{Cl}_2 < \text{H}_2\text{O}_2 < \text{BF}_4^- < \text{ClO}_4^- < \text{ClO}_3^- < \text{NO}_3^- < \text{Cl}^- < \text{ClO}_2^- < \text{ClO}^- < \text{F}^- < \text{SO}_4^{2-}$. In the case of chlorine oxyanion family, E_{int} and V_{min} follow the same trend where ClO_4^- with the least negative V_{min} forms the least stable complex ($E_{\text{int}} = -22.1$ kcal/mol) while ClO^- with the most negative V_{min} forms the most stable complex ($E_{\text{int}} = -30.7$ kcal/mol).

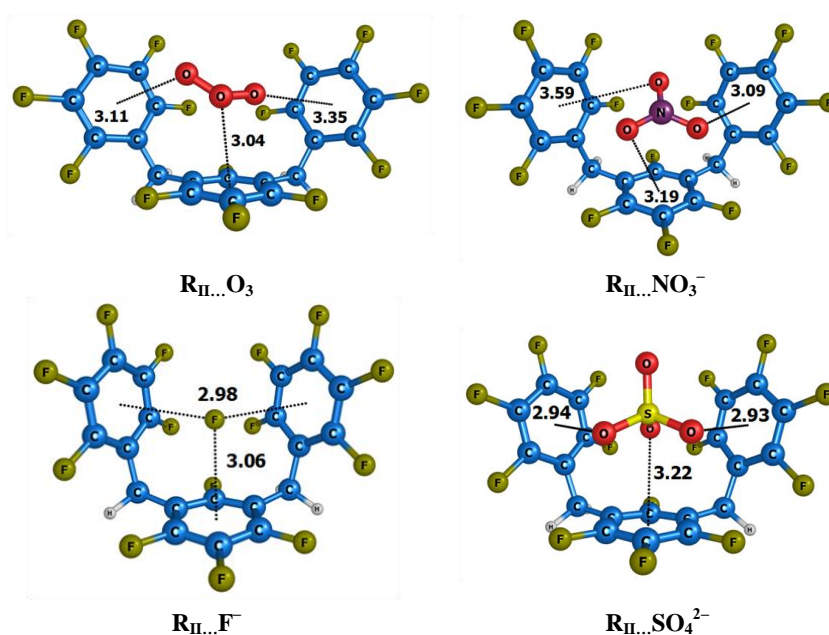


Figure 4.6 Optimized geometries of $\mathbf{R}_{\text{II}}\dots\mathbf{X}$ complexes. Distances in Angstrom units.

Tripodal receptors, hypothesized to be between cyclic and acyclic receptors are considered to bind more effectively to anionic ligands than the acyclic ones and are widely used as recognition components in various optical sensors and ion-selective membranes [Kuswandi *et al.* 2006]. In the tetradentate tripodal receptor \mathbf{R}_{III} , the guest molecules are locked into the cavity of the receptor by four or more lone pair/anion- π interactions between the arms of \mathbf{R}_{III} and \mathbf{X} (Figure 4.7).

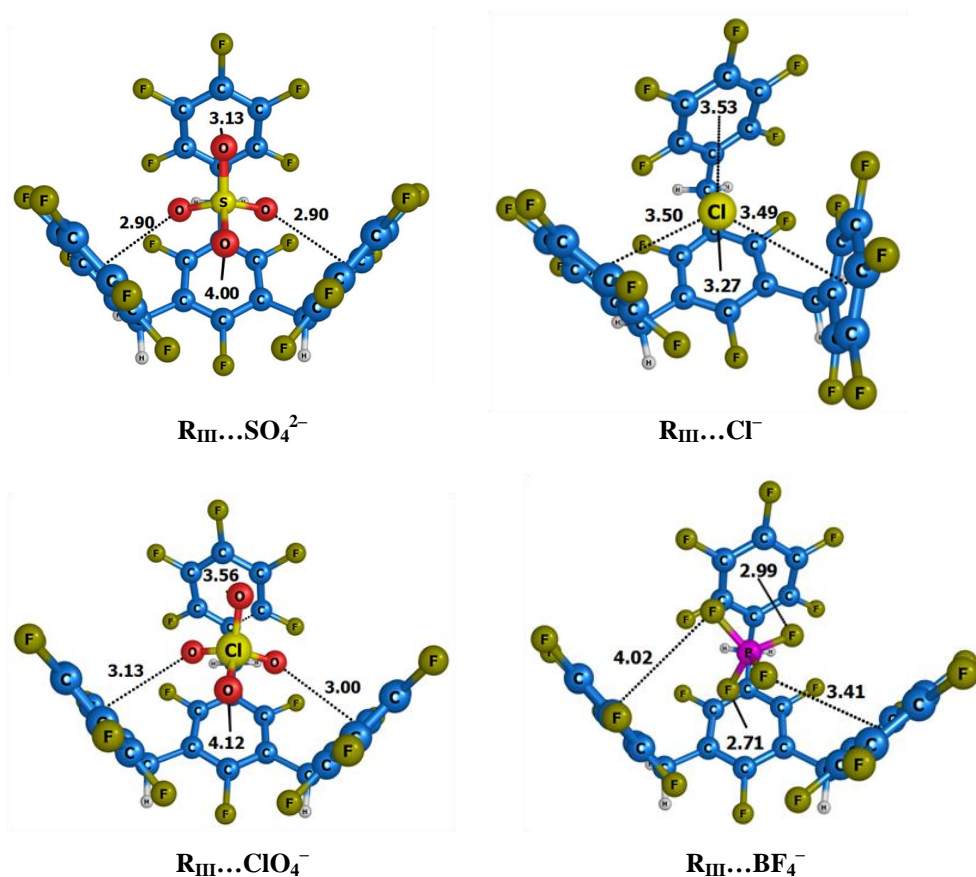


Figure 4.7 Optimized geometries of $\mathbf{R_{III}} \dots \mathbf{X}$ complexes. Distances in Angstrom units.

A significant enhancement ~ 9.4 to 37.8 % in E_{int} is observed for $\mathbf{R_{III}} \dots \mathbf{X}$ complexes compared to $\mathbf{R_{II}} \dots \mathbf{X}$ complexes. The trend for the interaction remains more or less the same with N_2 and SO_4^{2-} being the least and most interacting species, respectively. The geometrical parameters as well as the interaction energy data suggests that $\mathbf{R_{III}}$ can be effectively used for binding tetrahedral anions with four electron-rich centers like SO_4^{2-} , BF_4^- and ClO_4^- . The boost in E_{int} for $\mathbf{R_{III}}$ is more pronounced in less electron-rich neutral systems like Cl_2 and N_2 . $\mathbf{R_{III}} \dots \mathbf{X}$ complexes of Cl_2 and N_2 show 293% and 371 % enhancement in E_{int} compared to the corresponding $\mathbf{HFB} \dots \mathbf{X}$ complexes. In the chloride oxyanion family, the trend in V_{min} is reproduced in the interaction energy data of all the receptors with ClO^- exhibiting the most and ClO_4^- the least binding. This suggests that the interaction energy data has close association with the electron-rich nature of the guest molecules.

Table 4.1 Interaction energy (E_{int}) of **HFB...X**, **R_I...X**, **R_{II}...X** and **R_{III}...X** in kcal/mol.

X	$V_{\text{min-X}}$	E_{int}			
		HFB...X	R_I...X	R_{II}...X	R_{III}...X
H ₂ O ₂	-42.7	-3.8	-6.0	-7.4	-9.2
H ₂ O	-53.8	-3.1	-4.8	-6.4	-8.6
O ₃	-17.8	-3.8	-6.4	-6.2	-8.5
N ₂	-11.4	-1.0	-2.6	-3.7	-4.9
Cl ₂	-3.6	-1.9	-5.1	-6.6	-7.3
Cl ⁻	-171.0	-14.5	-21.3	-26.9	-32.6
F ⁻	-240.3	-21.1	-33.7	-38.1	-50.8
BF ₄ ⁻	-145.4	-8.9	-18.6	-21.5	-24.9
NO ₃ ⁻	-167.4	-14.3	-20.8	-26.7	-31.2
SO ₄ ²⁻	-279.6	^a	-48.6	-62.6	-75.6
ClO ⁻	-205.9	-18.6	-27.0	-30.7	-36.2
ClO ₂ ⁻	-183.0	-13.8	-24.0	-30.0	-35.4
ClO ₃ ⁻	-161.3	-15.7	-17.5	-22.7	-27.9
ClO ₄ ⁻	-139.9	-13.9	-18.5	-22.1	-26.8

^aSO₄²⁻ forms an anionic σ -complex with HFB

The free energy change (ΔG) for the formation of the receptor-guest complexes are summarized in Table 4.2. The complexes of the receptors with neutral molecules associated with lower binding energies (except **R_{III}...Cl₂** and **R_{III}...O₃**) are characterized by positive ΔG values signifying endergonic reactions which cannot occur spontaneously. ΔG values for **R_{III}...Cl₂** and **R_{III}...O₃** are negative indicating the exergonic or spontaneous formation of host-guest complex in both cases. The complexes of **R_I**, **R_{II}** and **R_{III}** with all anionic guest molecules show large negative ΔG values. Binding energies of a representative set of complexes computed at IPCM solvation model ($E_{\text{int-IPCM}}$) are presented in Table 4.3. In comparison with the gas phase, the binding energy is reduced slightly in the solvent phase, but it is favorable, indicating that receptors based on the lone pair/anion- π interaction are competitive in solvents too.

Table 4.2 Free energy change (ΔG) of $\mathbf{R_I...X}$, $\mathbf{R_{II}...X}$ and $\mathbf{R_{III}...X}$ complexes in kcal/mol.

X	ΔG (kcal/mol)		
	$\mathbf{R_I...X}$	$\mathbf{R_{II}...X}$	$\mathbf{R_{III}...X}$
H ₂ O ₂	3.1	2.1	1.4
H ₂ O	1.3	2.9	1.3
O ₃	4.6	4.2	-0.3
N ₂	4.9	4.3	2.8
Cl ₂	2.3	0.7	-2.6
Cl ⁻	-15.9	-18.7	-25.9
F ⁻	-28.7	-29.6	-40.4
BF ₄ ⁻	-7.7	-9.1	-13.2
NO ₃ ⁻	-9.7	-10.0	-20.8
SO ₄ ²⁻	-40.4	-53.4	-67.6
ClO ⁻	-19.9	-21.6	-28.4
ClO ₂ ⁻	-15.7	-15.6	-28.9
ClO ₃ ⁻	-9.1	-8.9	-21.3
ClO ₄ ⁻	-9.6	-12.7	-18.7

Table 4.3 Binding energy values of receptor-guest complexes in aqueous phase using IPCM solvation model in kcal/mol.

System	$E_{\text{int-IPCM}}$	System	$E_{\text{int-IPCM}}$
$\mathbf{R_I...H_2O_2}$	-6.0	$\mathbf{R_I...ClO_2^-}$	-24.0
$\mathbf{R_I...H_2O}$	-4.6	$\mathbf{R_I...ClO_4^-}$	-18.4
$\mathbf{R_I...O_3}$	-6.4	$\mathbf{R_{II}...H_2O_2}$	-7.2
$\mathbf{R_I...N_2}$	-2.6	$\mathbf{R_{II}...O_3}$	-5.9
$\mathbf{R_I...Cl_2}$	-5.1	$\mathbf{R_{II}...N_2}$	-3.5
$\mathbf{R_I...Cl^-}$	-21.3	$\mathbf{R_{II}...Cl_2}$	-6.4
$\mathbf{R_I...F^-}$	-33.7	$\mathbf{R_{II}...Cl^-}$	-26.6
$\mathbf{R_I...BF_4^-}$	-18.6	$\mathbf{R_{II}...F^-}$	-37.9
$\mathbf{R_I...NO_3^-}$	-20.8	$\mathbf{R_{III}...N_2}$	-5.1
$\mathbf{R_I...ClO^-}$	-27.0	$\mathbf{R_{III}...BF_4^-}$	-27.5

The noncovalent anion- π /lone pair- π interaction in the receptor-guest complexes have been further explored using AIM analysis which reveals bcps and bond paths connecting the atoms of the guest molecules with the ring C atoms of the fluorinated arms of the receptors.

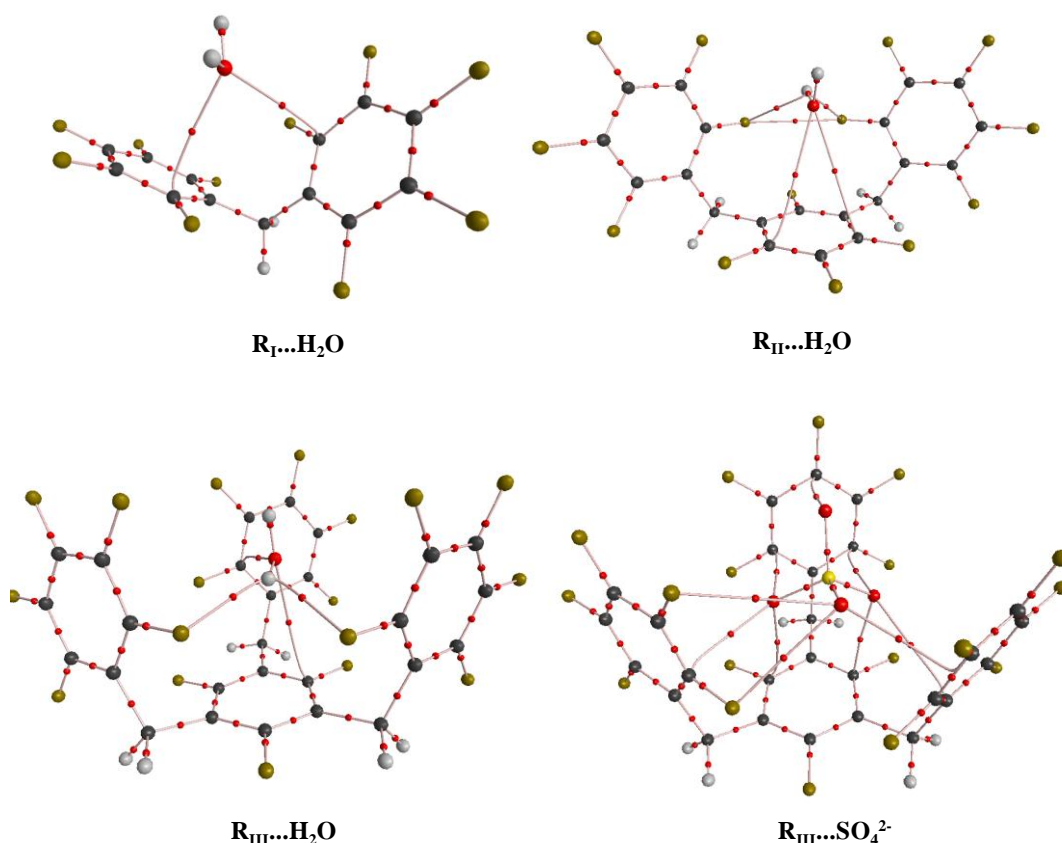


Figure 4.8 AIM Molecular graphs of $R_I \dots H_2O$, $R_{II} \dots H_2O$, $R_{III} \dots H_2O$ and $R_{III} \dots SO_4^{2-}$. Small red spheres and lines represent bond critical points (BCPs) and bond paths, respectively.

Bcps and bond paths can be considered as signatures of lone pair/anion- π interactions. In Figure 4.8, the AIM molecular graphs of $R_I \dots H_2O$, $R_{II} \dots H_2O$, $R_{III} \dots H_2O$ and $R_{III} \dots SO_4^{2-}$ are shown as representative cases. $R_I \dots H_2O$ exhibits two bcps, each one connecting the O and a ring carbon atom suggesting the presence of two lone pair- π interactions. $R_{II} \dots H_2O$ display two bcps linking the O atom with the ring C atoms of the

central HFB core. Additional stabilization by hydrogen bonding interaction of the H atoms of H₂O and F atoms of C₆F₅ rings of **R_{II}** are also revealed in the molecular graphs. **R_{III}...SO₄²⁻** complex displays multiple lone pair- π interactions and halogen bonds (between O and F atoms). The value of $\rho(\mathbf{r})$ at bcp varies between 0.002 to 0.028 au, while the corresponding $\nabla^2\rho(\mathbf{r})$ values are all positive in the range 0.011 to 0.091 au. Thus it is clear that lone pair- π /anion- π interactions coupled with hydrogen and halogen bonds bring about the efficient binding of the receptor molecules with neutral and anionic guest molecules.

Part B – Cage Receptors for Noble Gas Atoms and Molecular Hydrogen

4.5 Introduction

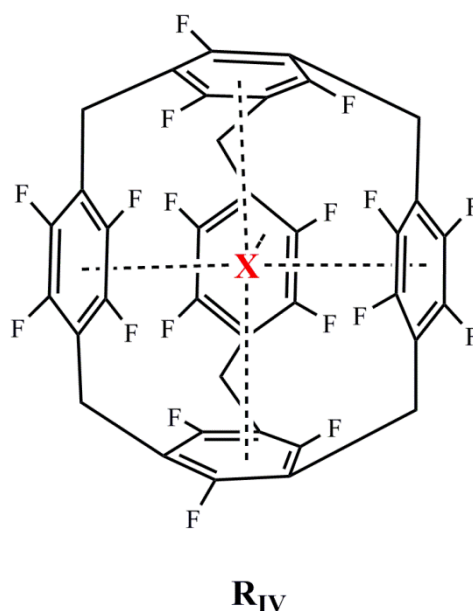
Non covalent complexes formed between rare gas atoms and aromatic molecules (RG- π) have been the subject of many theoretical and experimental investigations [Dessent and Müller-Dethlefs 2000; Felker *et al.* 1994; Hobza *et al.* 1994; Kim *et al.* 2000; Neusser and Krause 1994; van der Avoird *et al.* 1994]. The chemical inertness of noble gases was considered to be absolute for many years [Christe 2001] since their discovery until 1930 when Pauling [Pauling 1933] suggested that chemical bonding may be possible for heavier noble gas atoms like xenon where the outermost electronic shell is less stable. Later, Neil Bartlett [Bartlett 1962] demonstrated that the inertness of noble gases is not a basic tenet of chemistry by synthesizing the first noble gas compound, $\text{Xe}^+[\text{PtF}_5]^-$ which triggered the search for interactions between rare gases and other elements. Noble gas atoms, due to their spherical electron density distribution, do not possess any permanent electric multipole moment and hence the electrostatic component of the interaction energy is absent in the case of the complexes of rare gas atoms with aromatic molecules [Chalasinski and Szczesniak 1994; Hobza *et al.* 1994]. Being chemically inert, rare gas atoms interact by van der Waals forces, which at large distances are governed by attractive dispersion forces. The van der Waals complexes of argon with a number of prototype benzene-related systems including benzene, fluorinated benzenes, aniline, furan and oxazoles have been probed [Bohn *et al.* 1989; Brupbacher and Bauder 1990; Hobza *et al.* 1996; Hobza *et al.* 1992; Hobza *et al.* 1991; Hobza *et al.* 1993; Kraka *et al.* 1995; Kukolich 1983; Tarakeshwar *et al.* 2001]. These studies have shown that exchange repulsion forces preferentially dictate the equilibrium

geometry whereas, the dispersion forces determine the stability of RG- π complexes. Structure adapted perturbation theory (SAPT) studies by Kim et al. [Tarakeshwar *et al.* 2001] on the complexes of argon with benzene and fluoro-substituted benzenes *viz.* fluorobenzene and p-difluorobenzene showed that fluorine substitution does not affect the stability of the complexes strongly since it causes a reduction in both the stabilizing induction and dispersion forces as well as the destabilizing exchange-repulsion and exchange-induction forces.

Encapsulation of charged or neutral molecules in the inner cavities of organic host molecules is a fascinating area of research and various theoretical and experimental efforts exploring the viability of cage like molecules having endohedrally trapped noble gas atoms have been reported [Cerpa *et al.* 2009; Jiménez-Vázquez *et al.* 2001; Krapp and Frenking 2007; Pan *et al.* 2013; Saunders *et al.* 1993]. Clathrates and hydrates are the earlier noble gas compounds known where the noble gas atoms are caged in cavities in the crystal lattice of the host compound formed by a network of hydrogen bonds between covalently bound molecules. The superior Xe binding characteristics of cryptophane molecules through van der Waals forces has also been demonstrated [Bartik *et al.* 1998; Brotin and Dutasta 2009; Jacobson *et al.* 2011]. Noble gas atoms encapsulated in cage-molecules functionalized to target biological receptors are employed in magnetic resonance imaging techniques for various medical applications [Berthault *et al.* 2008; Spence *et al.* 2001]. In view of the importance of cage like molecules for the encapsulation of noble gas atoms, theoretical approaches are employed to design a substituted hexafluorobenzene based caged structure that can effectively bind noble gas atoms. The binding affinity of the cage receptor for molecular hydrogen is also probed due to the increasing interest of receptors in hydrogen storage. The theoretical predictions presented in this chapter would be of interest to synthetic chemists for the synthesizing highly efficient novel receptors for noble gas atoms.

4.6 Design Strategy and Computational Methods

The cage receptor is modelled in a stepwise manner by substituting the electron-deficient core of hexafluorobenzene at 1, 3, and 5 positions with pentafluorobenzyl ($C_6F_5CH_2-$) groups. The tripodal platform of **R_{III}** reported in Part A of this chapter is used for the construction of the cage receptor by moving it from an open to closed cavity *i.e.*, to a cage (**R_{IV}**). The receptor model, **R_{IV}** and its possible noncovalent interactions with any incoming guest molecule is presented in Scheme 4.2.



Scheme 4.2 The cage receptor model, **R_{IV}**. **X** = He, Ne, Ar, Kr and H₂. Dotted lines represent the possible interactions of the guest molecule with the electron-deficient rings of the receptor.

Geometry optimization of **R_{IV}** as well as the complexes of the **R_I**, **R_{II}**, **R_{III}** (reported in Part A of this chapter) and **R_{IV}** with noble gas atoms and H₂ are carried out at M06L/6-311++G(d,p) level [Zhao and Truhlar 2006] using Gaussian09 [Frisch *et al.* 2010] suite of programs. BSSE corrected interaction or stabilization energies (E_{int}) of the complexes are calculated using the supermolecule approach. The comparison of E_{int} values for the **R_{IV}...X** with E_{int} for **HFB...X**, **R_I...X**, **R_{II}...X** and **R_{III}...X** complexes

demonstrates the systematic improvement in the interaction energy on moving from HFB with single electron-deficient ring to the cage receptor with five electron-deficient rings. Topological properties of molecular electron density at the bond critical points (BCP) are obtained by AIM methodology [Bader 1985] as implemented in AIM2000 program [Biegler-König and Schönbohm 2002; Biegler-König *et al.* 2001]. Molecular electrostatic potential (MESP) topography of the receptor molecule is analyzed at the same level of theory.

To test the suitability of M06L/6-311++G(d,p) level for the binding energy calculations, the E_{int} of benzene-argon complex computed at M06L/6-311++G(d,p) level is compared with experimental binding energy value. E_{int} of benzene-argon complex is 0.962 kcal/mol which is indeed very close to the experimental binding energy obtained by Krause and Neusser [Krause and Neusser 1993] (0.972 kcal/mol) suggesting the adequacy of this level for the calculations.

4.7 Results and Discussion

Figure 4.9 presents the optimized geometry of \mathbf{R}_{IV} and the MESP textured on the 0.003 au electron density surface to demonstrate the most negative potential (blue) and most positive potential (red) regions of the receptor. All the five aromatic rings of \mathbf{R}_{IV} are electron-deficient and form noncovalent interactions with guest molecules in the internal cavity. The inner cavity of \mathbf{R}_{IV} is 6.38 Å in length and 5.47 Å in width. The interaction distances for the complexes of He, Ne, Ar, Kr and Xe with HFB are 3.06 Å, 3.24 Å, 3.60 Å, 3.55 Å and 3.81 Å respectively. This shows that the cavity of the \mathbf{R}_{IV} is large enough to encapsulate He, Ne, Ar and Kr whereas Xe is too large to be contained in the \mathbf{R}_{IV} cavity.

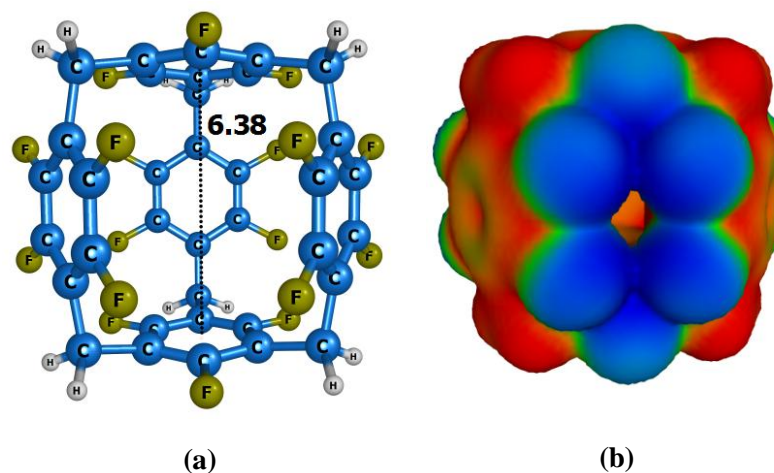


Figure 4.9 (a) Optimized geometry of the cage receptor and (b) MESP textured on the 0.003 au electron density surface.

Figure 4.10 presents the endohedral complexes of \mathbf{R}_{IV} with noble gas atoms He, Ne, Ar and Kr. It is clear that the noble gas atom is placed symmetrically relative to the center of the cage in all the endohedral complexes. The interaction energies of the noncovalent complexes of noble gas atoms (He, Ne, Ar and Kr) and H_2 with \mathbf{R}_I , \mathbf{R}_{II} , \mathbf{R}_{III} and \mathbf{R}_{IV} are presented in Table 4.4. The stabilization energy for the van der Waals complexes of He, Ne, Ar and Kr with the cage receptor is -4.07, -5.97, -6.00 and -6.11 kcal/mol, respectively. As the number of fluorinated aromatic units is increased from one to five, the binding energies of the noble gas complexes have increased steadily. Compared to HFB...He complex, magnitude of E_{int} is increased by 5.9-fold for \mathbf{R}_{IV} ...He complex. Similarly 6.4-fold, 7.9-fold and 6.1-fold increase in the magnitude of E_{int} is observed in the complexes of Ne, Ar and Kr with \mathbf{R}_{IV} in comparison with HFB. The DFT-SAPT interaction energies of endohedral complexes of the C_{60} fullerene with He, Ne, Ar and Kr atoms reported by Hesselmann and Korona [Hesselmann and Korona 2011] are -1.58, -2.86, -7.88 and -8.26 kcal/mol, respectively. Slanina *et al.* [Slanina *et al.* 2006] reported the stabilization energy of $\text{Ne}@C_{60}$ at MP2/6-311G(2d, 2p) and MPWB1K/6-311G(2d, 2p) as -5.39 and -7.20 kcal/mol, respectively. These results

indicate that compared to fullerene, the newly proposed cage receptor \mathbf{R}_{IV} binds more effectively with He and Ne while the interaction of the \mathbf{R}_{IV} is slightly as good or slightly weaker with Ar and Kr.

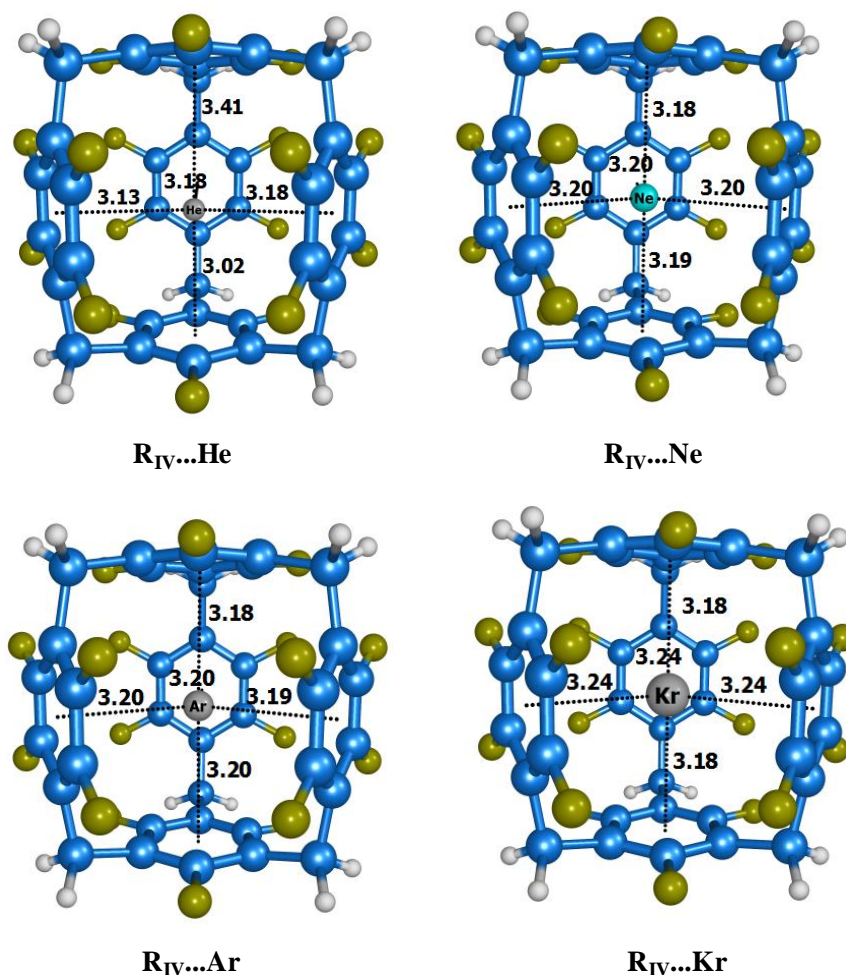


Figure 4.10 Optimized geometries of $\mathbf{R}_{IV}\dots\text{He}$, $\mathbf{R}_{IV}\dots\text{Ne}$, $\mathbf{R}_{IV}\dots\text{Ar}$ and $\mathbf{R}_{IV}\dots\text{Kr}$ complexes. Interaction distances in Å.

$\mathbf{R}_{IV}\dots\text{H}_2$ complex (Figure 4.11) is highly stable with an E_{int} value of -7.08 kcal/mol which is considerably higher than the reported values for $\text{H}_2@\text{C}_{60}$ and $\text{H}_2@\text{C}_{70}$. The stabilization energy of $\text{H}_2@\text{C}_{70}$ calculated from diffusion Monte Carlo (DMC) [Sebastianelli *et al.* 2010] calculations is -3.83 kcal/mol while the energy calculated from DFT-SAPT [Korona *et al.* 2009] is -3.46 kcal/mol, SCS-MP2 [Kruse and Grimme 2009] method is -6.50 kcal/mol and MPWBK [Murata *et al.* 2008] method is -

6.90 kcal/mol. The reported stabilization energies for $\text{H}_2@C_{60}$ from DMC [Sebastianelli *et al.* 2010] calculations is -4.29 kcal/mol, DFT-SAPT [Korona *et al.* 2009] is -4.63 kcal/mol and MP 2.5/CBS' (2,3) [Kruse and Grimme 2009] method is -7.30 kcal/mol. It is also evident that there almost 10-fold increase in E_{int} for $\mathbf{R}_{\text{IV}}\dots\text{H}_2$ complex compared to $\mathbf{HFB}\dots\text{H}_2$ complex. These results clearly show the efficiency of \mathbf{R}_{IV} to trap and store molecular hydrogen.

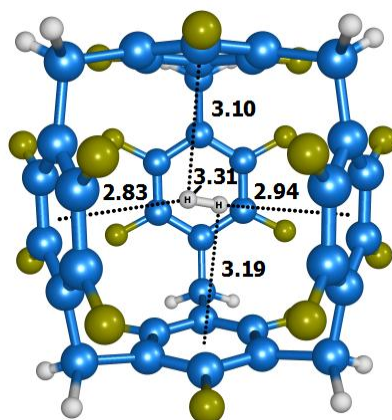


Figure 4.11 Optimized geometry of $\mathbf{R}_{\text{IV}}\dots\text{H}_2$ complex. Interaction distances in Å.

Table 4.4 Interaction energy values (E_{int}) of $\mathbf{HFB}\dots\text{X}$, $\mathbf{R}_{\text{I}}\dots\text{X}$, $\mathbf{R}_{\text{II}}\dots\text{X}$, $\mathbf{R}_{\text{III}}\dots\text{X}$ and $\mathbf{R}_{\text{IV}}\dots\text{X}$ in kcal/mol.

X	E_{int}				
	$\mathbf{HFB}\dots\text{X}$	$\mathbf{R}_{\text{I}}\dots\text{X}$	$\mathbf{R}_{\text{II}}\dots\text{X}$	$\mathbf{R}_{\text{III}}\dots\text{X}$	$\mathbf{R}_{\text{IV}}\dots\text{X}$
He	-0.69	-1.04	-1.53	-2.54	-4.07
Ne	-0.93	-1.40	-2.29	-3.23	-5.97
Ar	-0.76	-2.10	-2.95	-4.16	-6.00
Kr	-1.00	-2.54	-3.60	-4.33	-6.11
H_2	-0.72	-1.34	-2.52	-3.85	-7.08

The presence of nonbonding interactions between the noble gas atoms and H_2 with the cage receptor is confirmed by AIM topological features *viz.* the existence of bcps and bond paths linking the atoms of the guest molecule and one or more ring carbon atoms of \mathbf{R}_{IV} . Electron density, $\rho(\mathbf{r})$ and Laplacian of electron density, $\nabla^2 \rho(\mathbf{r})$ at bcps for $\mathbf{R}_{\text{IV}}\dots\mathbf{X}$ complexes are summarized in Table 4.5. The bond paths and bcps between the ring carbon atoms of \mathbf{R}_{IV} and the atoms of the guest species are depicted in the molecular graphs of the $\mathbf{R}_{\text{IV}}\dots\text{He}$, $\mathbf{R}_{\text{IV}}\dots\text{Ne}$, $\mathbf{R}_{\text{IV}}\dots\text{Ar}$ and $\mathbf{R}_{\text{IV}}\dots\text{Kr}$ shown in Figure 4.12 and molecular graph of $\mathbf{R}_{\text{IV}}\dots\text{H}_2$ shown in Figure 4.13.

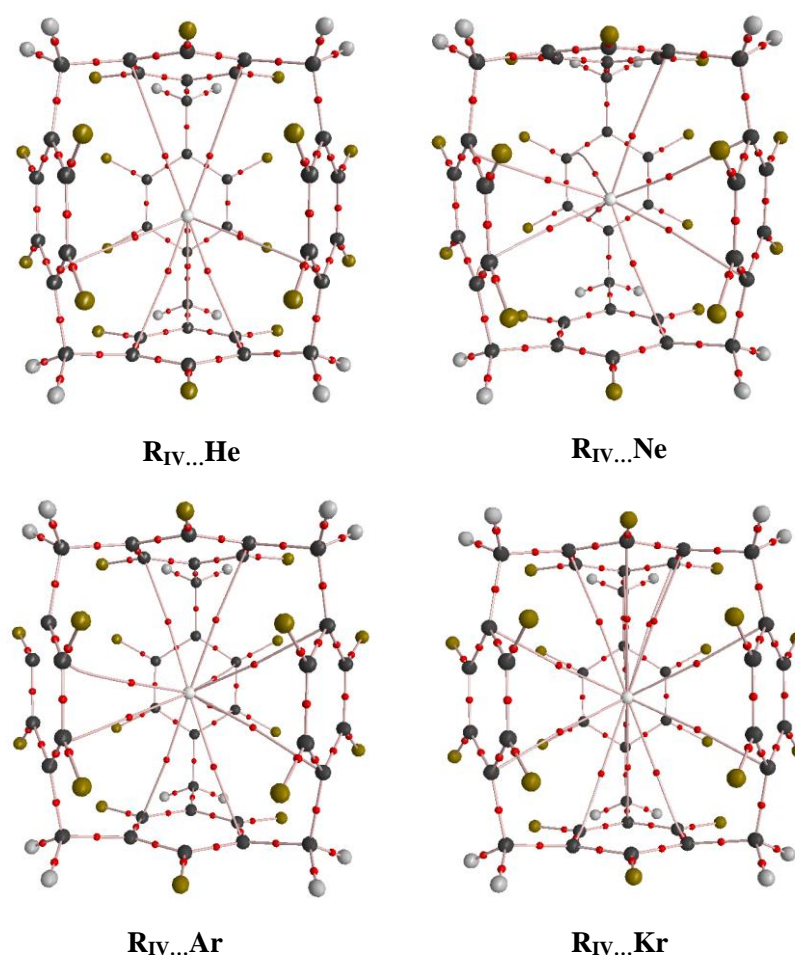


Figure 4.12 AIM molecular graph of the endohedral complexes of \mathbf{R}_{IV} with He, Ne, Ar and Kr. Small red spheres represent bond critical points (bcps) and red lines represent bond paths.

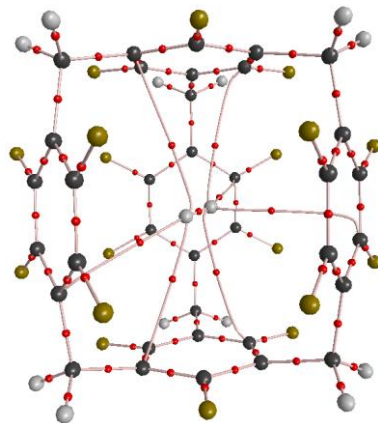


Figure 4.13 AIM molecular graph of the $\mathbf{R}_{IV}\dots\mathbf{H}_2$ complex. Small red spheres represent bond critical points (bcps) and red lines represent bond paths.

Table 4.5 Electron density ($\rho(\mathbf{r})$) and Laplacian of electron density ($\nabla^2\rho(\mathbf{r})$) at bcps for $\mathbf{R}_{IV}\dots\mathbf{X}$ complexes. I, II, III, IV and V represent the five aromatic rings in the cage receptor. Values in au.

X	I		II		III		IV		V	
	$\rho(\mathbf{r})$	$\nabla^2\rho(\mathbf{r})$	$\rho(\mathbf{r})$	$\nabla^2\rho(\mathbf{r})$	$\rho(\mathbf{r})$	$\nabla^2\rho(\mathbf{r})$	$\rho(\mathbf{r})$	$\nabla^2\rho(\mathbf{r})$	$\rho(\mathbf{r})$	$\nabla^2\rho(\mathbf{r})$
He	0.002	0.009	0.002	0.011	0.002	0.009	0.001	0.005	0.002	0.010
Ne	0.003	0.014	0.003	0.014	0.003	0.014	0.003	0.014	0.003	0.014
Ar	0.006	0.022	0.006	0.024	0.006	0.023	0.006	0.022	0.006	0.023
Kr	0.008	0.027	0.008	0.026	0.007	0.024	0.007	0.024	0.007	0.024
H ₂	0.003	0.010	0.004	0.012	0.003	0.010	0.004	0.011	0.003	0.009

It is found that the number of bcps and bond paths linking the noble gas atom with the ring carbon atoms of \mathbf{R}_{IV} increases with the strength of the interaction. For instance weaker complexes, $\mathbf{R}_{IV}\dots\mathbf{He}$ and $\mathbf{R}_{IV}\dots\mathbf{Ne}$ are characterized by 8 bcps and 8 bond paths whereas stronger $\mathbf{R}_{IV}\dots\mathbf{Ar}$ and $\mathbf{R}_{IV}\dots\mathbf{Kr}$ complexes exhibits 10 and 12 bcps respectively. The values of $\rho(\mathbf{r})$ and $\nabla^2\rho(\mathbf{r})$ also increase with the strength of the interaction.

4.8 Conclusions

In Part A of this chapter, neutral molecular receptors capable of binding lone pair bearing molecules including anions through multiple lone pair- π interactions have been proposed through density functional theory calculations. The bidentate (**R_I**), tridentate (**R_{II}**) and tetradentate (**R_{III}**) receptor models bind to electron-rich guest molecules (*viz.* N₂, O₃, H₂O, H₂O₂, F⁻, Cl⁻, BF₄⁻, NO₃⁻, ClO⁻, ClO₂⁻, ClO₃⁻, ClO₄⁻ and SO₄²⁻) through two, three and four or more lone pair- π interactions. **R_{III}**, due to its flexible tripodal structure and the most electron-deficient character of the aromatic rings provide the maximum number of interaction sites and hence complexes more effectively to the electron-rich guest molecules. The favorable interactions between the receptor models and guest molecules in both gas phase and solution phase suggest that these molecules which exploit lone pair- π /anion- π interactions can indeed serve as excellent lead molecules towards the synthesis of neutral receptors for small molecules and anions with potential applications in chemistry and biology. The present study also underlines our previous observation that V_{\min} is a good descriptor to measure the strength of the interaction between the lone pair bearing molecule and an electron-deficient π -system since the E_{int} data of the host-guest complexes follow more or less the same trend as the lone pair strength of the molecules revealed from their V_{\min} values. By systematically increasing the number of electron-deficient aromatic rings, substantial increase in anion- π interaction can be achieved, and this strategy is useful for developing molecular motifs for the recognition of weakly binding organic anions and neutral molecules with lone pairs.

Part B reports fluorinated cage receptor (**R_{IV}**) molecule for the encapsulation of noble gas atoms and molecular hydrogen using density functional theory calculations. The cages are constructed by pentafluorobenzyl (C₆F₅CH₂-) substitution of HFB core to

form a cage cavity. Stable van der Waals complexes of \mathbf{R}_{IV} with noble gas atoms and H_2 predicted from DFT calculations suggest that this molecule could find potential applications as molecular receptors for rare gases and for hydrogen storage.

List of publications

A) Articles in Journals

1. Comparison of Aromatic NH... π , OH... π and CH... π Interactions of Alanine Using MP2, CCSD, and DFT Methods. **Mohan, N.**; Vijayalakshmi, K. P.; Koga, N.; Suresh, C. H. *J. Comp. Chem.* **2010**, 31, 2874.
2. Mechanism of Epoxide Hydrolysis in Microsolvated Nucleotide Bases Adenine, Guanine and Cytosine: A DFT Study. Vijayalakshmi, K. P.; **Mohan, N.**; Ajitha, M. J.; Suresh, C. H. *Org. Biomol. Chem.* **2011**, 9, 5115.
3. Molecular Electrostatics for Probing Lone Pair- π Interactions. **Mohan, N.**; Suresh, C. H.; Kumar, A.; Gadre, S. R. *Phys. Chem. Chem. Phys.*, **2013**, 15, 18401.
4. Lone Pairs: An Electrostatic Viewpoint. Kumar, A.; Gadre, S. R.; **Mohan, N.**; Suresh, C. H. *J. Phys. Chem. A*, **2014**, 118, 526.
5. A Molecular Electrostatic Potential Analysis of Hydrogen, Halogen, and Dihydrogen Bonds. **Mohan, N.**; Suresh, C. H. *J. Phys. Chem. A*, **2014**, DOI: 10.1021/jp4115699.
6. Energies of Hydrogen Bonds, Halogen Bonds and Dihydrogen Bonds: A Comparison of MP2, MP4, M06L and W1BD methods. **Mohan, N.**; Suresh, C. H. (*submitted*).
7. Anion Receptors Based on Highly Fluorinated Aromatic Scaffolds. **Mohan, N.**; Suresh, C. H. (*submitted*).

B) Published contributions to academic conferences

1. Presented a poster entitled "Quantifying Lone Pair Strength and Lone Pair- π Interactions Using Molecular Electrostatic Potential" in the 3rd Indo-German Conference on "Modeling Chemical and Biological (Re)Activity (MCBR 2013)" held at NIIPER and IISER, Mohali, during 26th February to 1st March 2013.
2. Presented a poster entitled "Design of novel receptors for lone pairs and anions based on lone pair- π interactions" in the "Symposium on Theoretical and Computational Chemistry-Frontiers and Challenges" held at Bharathidasan University, Tiruchirappalli, during June 14-15, 2013.

References

- Ahuja, R.; Samuelson, A. G. "Non-Bonding Interactions of Anions with Nitrogen Heterocycles and Phenyl Rings: A Critical Cambridge Structural Database Analysis" *CrystEngComm* 5, **2003**, 395.
- Alabugin, I. V.; Manoharan, M.; Peabody, S.; Weinhold, F. "Electronic Basis of Improper Hydrogen Bonding: A Subtle Balance of Hyperconjugation and Rehybridization" *J. Am. Chem. Soc.* 125, **2003**, 5973.
- Alkorta, I.; Blanco, F.; Deyá, P. M.; Elguero, J.; Estarellas, C.; Frontera, A.; Quiñonero, D. "Cooperativity in Multiple Unusual Weak Bonds" *Theor. Chem. Acc.* 126, **2010**, 1.
- Alkorta, I.; Rozas, I.; Elguero, J. "An Attractive Interaction Between the π -cloud of C₆F₆ and Electron-Donor Atoms" *J. Org. Chem.* 62, **1997**, 4687.
- Alkorta, I.; Rozas, I.; Elguero, J. "Radicals as Hydrogen Bond Acceptors" *Ber. Bunsenges. Phys. Chem.* 102, **1998**, 429.
- Alkorta, I.; Rozas, I.; Elguero, J. "Interaction of Anions with Perfluoro Aromatic Compounds" *J. Am. Chem. Soc.* 124, **2002**, 8593.
- Allen, L. C.; Karo, A. M. "Basis Functions for Ab Initio Calculations" *Rev. Modern Phys.* 32, **1960**, 275.
- Allerhand, A.; Schleyer, P. v. R. "A Survey of C-H Groups as Proton Donors in Hydrogen Bonding" *J. Am. Chem. Soc.* 85, **1963**, 1715.
- Amendola, V.; Fabbrizzi, L.; Mosca, L. "Anion Recognition by Hydrogen Bonding: Urea-Based Receptors" *Chem. Soc. Rev.* 39, **2010**, 3889.
- Amicangelo, J. C.; Irwin, D. G.; Lee, C. J.; Romano, N. C.; Saxton, N. L. "Experimental and Theoretical Characterization of a Lone Pair- π Complex: Water-Hexafluorobenzene" *J. Phys. Chem. A* 14, **2012**, 1014.

- Arunan, E.; Desiraju, G. R.; Klein, R. A.; Sadlej, J.; Scheiner, S.; Alkorta, I.; Clary, D. C.; Crabtree, R. H.; Dannenberg, J. J.; Hobza, P.; Kjaergaard, H. G.; Legon, A. C.; Mennucci, B.; Nesbitt, D. J. "Defining the Hydrogen Bond: An Account (IUPAC Technical Report)" *Pure Appl. Chem.* 83, **2011**, 1619.
- Auffinger, P.; Hays, F. A.; Westhof, E.; Shing, H. P. "Halogen Bonds in Biological Molecules" *Proc. Nat. Acad. Sci.* 101, **2004**, 16789.
- Bader, R. F. W. "Atoms in Molecules" *Acc. Chem. Res.* 18, **1985**, 9.
- Bader, R. F. W. *Atoms in Molecules: A Quantum Theory*. Clarendon Press: Oxford, **1990**.
- Bader, R. F. W. "A Quantum Theory of Molecular Structure and its Applications" *Chem. Rev.* 91, **1991**, 893.
- Bader, R. F. W.; Essén, H. "The Characterization of Atomic Interactions" *J. Chem. Phys.* 80, **1984**, 1943.
- Balanarayan, P.; Kavathekar, R.; Gadre, S. R. "Electrostatic Potential Topography for Exploring Electronic Reorganizations in 1,3 Dipolar Cycloadditions" *J. Phys. Chem. A* 111, **2007**, 2733.
- Barnes, E. C.; Petersson, G. A.; Montgomery Jr, J. A.; Frisch, M. J.; Martin, J. M. L. "Unrestricted Coupled Cluster and Brueckner Doubles Variations of W1 Theory" *J. Chem. Theory Comput.* 5, **2009**, 2687.
- Bartik, K.; Luhmer, M.; Dutasta, J.-P.; Collet, A.; Reisse, J. "¹²⁹Xe and ¹H NMR Study of the Reversible Trapping of Xenon by Cryptophane-A in Organic Solution" *J. Am. Chem. Soc.* 120, **1998**, 784.
- Bartlett, N. "Xenon Hexafluoroplatinate(V) Xe⁺[PtF₆]⁻" *Proc. Chem. Soc.* 218, **1962**.

- Bartlett, R. J.; Silver, D. M. "Many-Body Perturbation Theory Applied to Electron Pair Correlation Energies. I. Closed-Shell First-Row Diatomic Hydrides" *J. Chem. Phys.* 62, **1975**, 3258.
- Bauzá, A.; Mooibroek, T. J.; Frontera, A. "Tetrel-Bonding Interaction: Rediscovered Supramolecular Force?" *Angew. Chem. Int. Ed.* 52, **2013**, 12317.
- Bauzá, A.; Quiñonero, D.; Deyà, P. M.; Frontera, A. "Theoretical Ab Initio Study of Anion- π Interactions in Inorganic Rings" *Chem. Phys. Lett.* 530, **2012**, 145.
- Becke, A. D. "Density-Functional Exchange-Energy Approximation with Correct Asymptotic Behavior" *Phys. Rev. A* 38, **1988**, 3098.
- Becke, A. D.; Edgecombe, K. E. "A Simple Measure of Electron Localization in Atomic and Molecular Systems" *J. Chem. Phys.* 92, **1990**, 5397.
- Beer, P. D.; Gale, P. A. "Anion Recognition and Sensing: The State of the Art and Future Perspectives" *Angew. Chem. Int. Ed.* 40, **2001**, 486.
- Begum, R.; Kang, S. O.; Bowman-James, K. "Amide-Based Ligands for Anion Coordination" *Angew. Chem. Int. Ed.* 45, **2006**, 7882.
- Benabicha, F.; Pichon-Pesme, V.; Jelsch, C.; Lecomte, C.; Khmou, A. "Experimental Charge Density and Electrostatic Potential of Glycyl-L-Threonine Dihydrate" *Acta Cryst. B* 56, **2000**, 155.
- Benesi, H. A.; Hildebrand, J. H. "A Spectrophotometric Investigation of the Interaction of Iodine with Aromatic Hydrocarbons" *J. Am. Chem. Soc.* 71, **1949**, 2703.
- Bent, H. A. "Structural Chemistry of Donor-Acceptor Interactions" *Chem. Rev.* 68, **1968**, 587.
- Berger, I.; Egli, M. "The Role of Backbone Oxygen Atoms in the Organization of Nucleic Acid Tertiary Structure: Zippers, Networks, Clamps, and C-H...O Hydrogen Bonds" *Chem. Eur. J.* 3, **1997**, 1400.

- Berger, I.; Egli, M.; Rich, A. "Inter-Strand C-H...O Hydrogen Bonds Stabilizing Four-Stranded Intercalated Molecules: Stereoelectronic Effects of O4' in Cytosine-Rich DNA" *Proc. Natl. Acad. Sci. U.S.A.* 93, **1996**, 12116.
- Berryman, O. B.; Bryantsev, V. S.; Stay, D. P.; Johnson, D. W.; Hay, B. P. "Structural Criteria for the Design of Anion Receptors: The Interaction of Halides with Electron-Deficient Arenes" *J. Am. Chem. Soc.* 129, **2007**, 48.
- Berthault, P.; Bogaert-Buchmann, A.; Desvaux, H.; Huber, G.; Boulard, Y. "Sensitivity and Multiplexing Capabilities of MRI Based on Polarized ^{129}Xe Biosensors" *J. Am. Chem. Soc.* 130, **2008**, 16456.
- Bianchi, A.; Bowman-James, K.; García-España, E. *Supramolecular Chemistry of Anions*. Wiley-VCH: New York, **1997**.
- Biegler-König, F.; Schönbohm, J. "An Update to the AIM2000 - Program for Atoms in Molecules" *J. Comp. Chem.* 23, **2002**, 1489.
- Biegler-König, F.; Schönbohm, J.; Bayles, D. "AIM2000 - A Program to Analyze and Visualize Atoms in Molecules" *J. Comp. Chem.* 22, **2001**, 545.
- Binkley, J. S.; Pople, J.; Hehre, W. J. "Self-Consistent Molecular Orbital Methods. 21. Small Split-Valence Basis Sets for First-Row Elements" *J. Am. Chem. Soc.* 102, **1980**, 939.
- Blake, G. A.; Laughlin, K. B.; Cohen, R. C.; Busarow, K. L.; Gwo, D.-H.; Schmuttenmaer, C. A.; Steyert, D. W.; Saykally, R. J. "The Berkeley Tunable Far Infrared Laser Spectrometers" *Rev. Sci. Instrum.* 62, **1991**, 1701.
- Bobadova-Parvanova, P.; Galabov, B. "Ab Initio Molecular-Orbital Study of Hydrogen-Bonded Complexes of Carbonyl Aliphatic Compounds and Hydrogen Fluoride" *J. Phys. Chem. A* 102, **1998**, 1815.

- Boese, A. D.; Martin, J. M. L.; Klopper, W. "Basis Set Limit Coupled Cluster Study of H-Bonded Systems and Assessment of More Approximate Methods" *J. Phys. Chem. A* 111, **2007**, 11122.
- Boese, R.; Kirchner, M. T.; Billups, W. E.; Norman, L. R. "Cocrystallization with Acetylene: Molecular Complexes with Acetone and Dimethyl Sulfoxide" *Angew. Chem. Int. Ed.* 42, **2003**, 1961.
- Bohn, R. K.; Hillig, K. W., II; Kuczkowski, R. L. "Pyrrole-Argon: Microwave Spectrum, Structure, Dipole Moment, and Nitrogen-14 Quadrupole Coupling Constants" *J. Phys. Chem.* 93, **1989**, 3456.
- Bondy, C. R.; Loeb, S. J. "Amide Based Receptors for Anions" *Coord. Chem. Rev.* 240, **2003**, 77.
- Born, M.; Oppenheimer, J. R. "Zur Quantentheorie der Molekeln" *Ann. Phys.* 84, **1927**, 457.
- Botschwina, P.; Oswald, R. "The Totally Symmetric Vibrations of NH₃...HF and NH₃...HCN: A CCSD(T) Study Including Anharmonicity Effects" *Z.Phys.Chem.* 219, **2005**, 399.
- Bouhmaida, N.; Germani, N.-E.; Lecomte, C.; Thalal, A. "Modelling Electrostatic Potential from Experimentally Determined Charge Densities. II. Total Potential" *Acta Cryst. A*53, **1997**, 556.
- Bouhmaida, N.; Ghermani, N.-E.; Lecomte, C.; Thalal, A. "Molecular Fragment Electric Moments Derived From the Fit of The Experimental Electrostatic Potential. Application to the Water Molecule" *Acta Cryst. A*55, **1999**, 729.
- Bowen, J. P.; Allinger, N. L. "Molecular Mechanics: The Art and Science of Parameterization" *Rev. Comp. Chem.* 2, **1991**, 81.

- Boyd, D. B.; Lipkowitz, K. B. "Molecular Mechanics: The Method and its Underlying Philosophy" *J. Chem. Educ.* 59, **1982**, 269.
- Boyd, R. J.; Choi, S. C. "A Bond-Length-Bond-Order Relationship for Intermolecular Interactions Based on the Topological Properties of Molecular Charge Distributions" *Chem. Phys. Lett.* 120, **1985**, 80.
- Boyd, R. J.; Choi, S. C. "Hydrogen Bonding Between Nitriles and Hydrogen Halides and the Topological Properties of Molecular Charge Distributions" *Chem. Phys. Lett.* 129, **1986**, 62.
- Boys, S. F. "Electronic Wave Functions. I. A General Method of Calculation for the Stationary States of Any Molecular System" *Proc. Roy. Soc.* 200, **1950**, 542.
- Boys, S. F.; Bernardi, F. "The Calculation of Small Molecular Interactions by the Differences of Separate Total Energies. Some Procedures with Reduced Errors" *Mol. Phys.* 19, **1970**, 553.
- Bretschneider, A.; Andrada, D. M.; Dechert, S.; Meyer, S.; Mata, R. A.; Meyer, F. "Preorganized Anion Traps for Exploiting Anion- π Interactions: An Experimental and Computational Study" *Chem. Eur. J.* 19, **2013**, 16988.
- Brillouin, L. "Les Champs Self-Consistents de Hartree et de Fock" *Actualities Sci. Ind.* 159, **1934**, 37.
- Brinck, T.; Murray, J. S.; Politzer, P. "Surface Electrostatic Potentials of Halogenated Methanes as Indicators of Directional Intermolecular Interactions" *Int. J. Quantum. Chem.* 44, **1992**, 57.
- Brinck, T.; Murray, J. S.; Politzer, P. "Molecular Surface Electrostatic Potentials and Local ionization Energies of Group V-VII Hydrides and Their Anions: Relationships for Aqueous and Gas-Phase Acidities" *Int. J. Quantum. Chem.* 48, **1993**, 73.

- Brotin, T.; Dutasta, J.-P. "Cryptophanes and Their Complexes-Present and Future" *Chem. Rev.* 109, **2009**, 88.
- Brupbacher, T.; Bauder, A. "Rotational Spectrum and Dipole Moment of the Benzene-Argon van der Waals Complex" *Chem. Phys. Lett.* 173, **1990**, 435.
- Buckingham, A. D.; Fowler, P. W.; Hutson, J. M. "Theoretical Studies of van der Waals Molecules and Intermolecular Forces" *Chem. Rev.* 88, **1988**, 963.
- Canagaratna, M.; Phillips, J. A.; Ott, M. E.; Leopold, K. R. J. "The Nitric Acid-Water Complex: Microwave Spectrum, Structure, and Tunneling" *J. Phys. Chem. A* 102, **1998**, 1489.
- Carroll, W. R.; Pellechia, P.; Shimizu, K. D. "A Rigid Molecular Balance for Measuring Face-To-Face Arene-Arene Interactions" *Org. Lett.* 10, **2008**, 3547.
- Carter, M.; Voth, A. R.; Scholfield, M. R.; Rummel, B.; Sowers, L. C.; Ho, P. S. "Enthalpy-Entropy Compensation in Biomolecular Halogen Bonds Measured in DNA Junctions" *Biochemistry* 29, **2013**, 4891.
- Casellas, H.; Massera, C.; Buda, F.; Gamez, P.; Reedijk, J. "Crystallographic Evidence of Theoretically Novel Anion- π Interactions" *New J. Chem.* 30, **2006**, 1561.
- Cerpa, E.; Krapp, A.; Flores-Moreno, R.; Donald, K. J.; Merino, G. "Influence of Endohedral Confinement on the Electronic Interaction Between He atoms: A He₂@C₂₀H₂₀ Case Study" *Chem. Eur. J.* 15, **2009**, 1985.
- Chalasinski, G.; Szczesniak, M. M. "Origins of Structure and Energetics of van der Waals Clusters from Ab Initio Calculations" *Chem. Rev.* 94, **1994**, 1723.
- Chambers, R. D.; Todd, M. "A New Approach to Di(Perfluoroaryl)Methanes Utilising Sulphone-Stabilised Carbanions" *J. Fluorine Chem.* 27, **1985**, 237.
- Chen, Y.; Wang, D.-X.; Huang, Z.-T.; Wang, M.-X. "Ion Pair Receptors Based on Anion- π Interaction" *Chem. Commun.* 47, **2011**, 8112.

- Chesnut, D. B. "The Contribution to Bonding by Lone Pairs" *Chem. Phys.* 291, **2003**, 141.
- Chiavarino, B.; Crestoni, M. E.; Fornarini, S.; Lanucara, F.; Lemaire, J.; Maître, P.; Scuderi, D. "Molecular Complexes of Simple Anions with Electron-Deficient Arenes: Spectroscopic Evidence for Two Types of Structural Motifs for Anion-Arene Interactions" *Chem. Eur. J.* 15, **2009**, 8185.
- Chifotides, H. T.; Dunbar, K. R. "Anion- π Interactions in Supramolecular Architectures" *Acc. Chem. Res.* 46, **2013**, 894.
- Choi, K.; Hamilton, A. D. "Macrocyclic Anion Receptors Based on Directed Hydrogen Bonding Interactions" *Coord. Chem. Rev.* 240, **2003**, 101.
- Christe, K. O. "A Renaissance in Noble Gas Chemistry" *Angew. Chem. Int. Ed.* 4, **2001**, 1419.
- Čížek, J. "On the Correlation Problem in Atomic and Molecular Systems. Calculation of Wavefunction Components in Ursell-Type Expansion Using Quantum-Field Theoretical Methods" *J. Chem. Phys.* 45, **1966**, 4256.
- Clark, T.; Hennemann, M.; Murray, J. S.; Politzer, P. "Halogen Bonding: The σ -Hole" *J. Mol. Model.* 13, **2007**, 291.
- Cockroft, S. L.; Hunter, C. A. "Chemical Double-Mutant Cycles: Dissecting Non-Covalent Interactions" *Chem. Soc. Rev.* 36, **2007**, 172.
- Corradi, E.; Meille, S. V.; Messina, M. T.; Metrangolo, P.; Resnati, G. "Halogen Bonding Versus Hydrogen Bonding in Driving Self-Assembly Processes" *Angew. Chem. Int. Ed.* 39, **2000**, 1782.
- Cossi, M.; Barone, V.; Cammi, R.; Tomasi, J. "Ab Initio Study of Solvated Molecules: A New Implementation of the Polarizable Continuum Model" *Chem. Phys. Lett.* 255, **1996**, 327.

- Crabtree, R. H.; Siegbahn, P. E. M.; Eisenstein, O.; Rheingold, A. L.; Koetzle, T. F. "A New Intermolecular Interaction: Unconventional Hydrogen Bonds with Element-Hydride Bonds as Proton Acceptor" *Acc. Chem. Res.* 29, **1996**, 348.
- Cramer, C. J. *Essentials of Computational Chemistry*. John Wiley & Sons: Chichester, **2004**.
- Cramer, C. J.; Truhlar, D. G. "Implicit Solvation Models: Equilibria, Structure, Spectra, and Dynamics" *Chem. Rev.* 99, **1999**, 2161.
- Cybulski, H.; Pecul, M.; Sadleja, J. "Characterization of Dihydrogen-Bonded D-H...H-A Complexes on the Basis of Infrared and Magnetic Resonance Spectroscopic Parameters" *J. Chem. Phys.* 119, **2003**, 5094.
- Danten, Y. "On the Nature of the Water-Hexafluorobenzene Interaction" *J. Phys. Chem. A* 103, **1999**, 3530.
- Davidson, E. R.; Feller, D. "Basis Set Selection for Molecular Calculations" *Chem. Rev.* 86, **1986**, 681.
- Dawson, R. E.; Hennig, A.; Weimann, D. P.; Emery, D.; Ravikumar, V.; Montenegro, J.; Takeuchi, T.; Gabutti, S.; Mayor, M.; Mareda, J.; Schalley, C. A.; Matile, S. "Experimental Evidence for the Functional Relevance of Anion- π Interactions" *Nat. Chem.* 2, **2010**, 533.
- De Hoog, P.; Gamez, P.; Mutikainen, I.; Turpeinen, U.; Reedijk, J. "An Aromatic Anion Receptor: Anion- π Interactions Do Exist" *Angew. Chem. Int. Ed.* 43, **2004**, 5815.
- Debye, P. *Polar Molecules*. Chemical Catalog Company: New York, **1929**.
- Demeshko, S.; Dechert, S.; Meyer, F. "Anion- π Interactions in a Carousel Copper(II)-Triazine Complex" *J. Am. Chem. Soc.* 126, **2004**, 4508.

- Deshmukh, M. M.; Gadre, S. R.; Tonner, R.; Frenking, G. "Molecular Electrostatic Potentials of Divalent Carbon(0) Compounds" *Phys. Chem. Chem. Phys.* 10, **2008**, 2298.
- Desiraju, G. R. "Hydrogen Bridges in Crystal Engineering: Interactions Without Borders" *Acc. Chem. Res.* 35, **2002**, 565.
- Desiraju, G. R. "A Bond by Any Other Name" *Angew. Chem. Int. Ed.* 50, **2011**, 52.
- Desiraju, G. R.; Ho, P. S.; Kloo, L.; Legon, A. C.; Marquardt, R.; Metrangola, P.; Politzer, P. A.; Resnati, G.; Rissanen, K. "Definition of the Halogen Bond" *Pure Appl. Chem.* 85, **2013**, 1711.
- Desiraju, G. R.; Parthasarathy, R. "The Nature of Halogen...Halogen Interactions: Are Short Halogen Contacts Due to Specific Attractive Forces or Due to Close Packing of Nonspherical Atoms?" *J. Am. Chem. Soc.* 111, **1989**, 8725.
- Desiraju, G. R.; Steiner, T. *The Weak Hydrogen Bond: In Structural Chemistry and Biology*. Oxford University Press: New York, **2001**.
- Dessent, C. E. H.; Müller-Dethlefs, K. "Hydrogen-Bonding and van der Waals Complexes Studied by ZEKE and REMPI Spectroscopy" *Chem. Rev.* 100, **2000**, 3999.
- Di Paolo, T.; Sandorfy, C. "On the Biological Importance of the Hydrogen Bond Breaking Potency of Fluorocarbons" *Chem. Phys. Lett.* 26, **1974a**, 466.
- Di Paolo, T.; Sandorfy, C. "On the Hydrogen Bond Breaking Ability of Fluorocarbons Containing Higher Halogens" *Can. J. Chem.* 52, **1974b**, 3612.
- Dian, B. C.; Longarte, A.; Mercier, S.; Evans, D. A.; Wales, D. J.; Zwier, T. S. "The Infrared and Ultraviolet Spectra of Single Conformations of Methyl-Capped Dipeptides: N-Acetyl Tryptophan Amide and N-Acetyl Tryptophan Methyl Amide" *J. Chem. Phys.* 117, **2002a**, 10688.

- Dian, B. C.; Longarte, A.; Zwier, T. S. "Conformational Dynamics in a Dipeptide After Single-Mode Vibrational Excitation" *Science* 296, **2002b**, 2369.
- Dietrich, B. "Design of Anion Receptors: Applications" *Pure Appl. Chem.* 65, **1993**, 1457.
- Dietrich, B.; Fyles, T. M.; Lehn, J. M.; Pease, L. G.; Fyles, D. L. "Anion Receptor Molecules. Synthesis and Some Anion Binding Properties of Macrocyclic Guanidinium Salts" *J. Chem. Soc., Chem. Commun.* **1978**, 934.
- Dietrich, B.; Hosseini, M. W.; Lehn, J. M.; Sessions, R. B. "Anion Receptor Molecules. Synthesis and Anion-Binding Properties of Polyammonium Macrocycles" *J. Am. Chem. Soc.* 103, **1981**, 1282.
- Dimitrova, V.; Ilieva, S.; Galabov, B. "Electrostatic Potential at Atomic Sites as a Reactivity Descriptor for Hydrogen Bonding. Complexes of Monosubstituted Acetylenes and Ammonia" *J. Phys. Chem. A* 106, **2002**, 11801.
- Dimitrova, V.; Ilieva, S.; Galabov, B. "Electrostatic Potential at Nuclei as a Reactivity Index in Hydrogen Bond Formation. Complexes of Ammonia with C-H, N-H and O-H Proton Donor Molecules" *J. Mol. Struct. THEOCHEM* 637, **2003**, 73.
- Dinur, U.; Hagler, A. T. "New Approaches to Empirical Force Fields" *Rev. Comp. Chem.* 2, **1991**, 99.
- Dirac, P. A. M. "Note on Exchange Phenomena in the Thomas-Fermi Atom" *Proc. Cambridge Phil. Roy. Soc.* 26, **1930**, 376.
- Ditchfield, R.; Hehre, W. J.; Pople, J. A. "Self-Consistent Molecular-Orbital Methods. IX. An Extended Gaussian-Type Basis for Molecular-Orbital Studies of Organic Molecules" *J. Chem. Phys.* 54, **1971**, 724.
- Doll, J.; Freeman, D. L. "Monte Carlo Methods in Chemistry" *IEEE Comput. Sci. Eng.* 1, **1994**, 22.

- Dumas, J.-M.; Peurichard, H.; Gomel, M. J. "Some Observations of Halogenated Solvent" *J. Chem. Res. Synop.* **1978**, 54.
- Dumas, J. M.; Geron, C.; Peurichard, H.; Gomel, M. J. "MX₄-Organic Bases Interactions (M= C, SI-X= Cl, Br)-Study of Influence of Central Element and Halogen" *Bull. Soc. Chim. Fr.* **1976**, 720.
- Dunning, T. H. J. "Gaussian Basis Sets for Use in Correlated Molecular Calculations. I. The Atoms Boron Through Neon and Hydrogen" *J. Chem. Phys.* 90, **1989**, 1007.
- Egli, M.; Gessner, R. V. "Stereoelectronic Effects of Deoxyribose O4' on DNA Conformation" *Proc. Natl. Acad. Sci. U.S.A.* 92, **1995**, 180.
- Eisenschitz, R.; London, F. "Über das Verhältnis der van der Waalsschen Kräfte zu den homöopolaren Bindungskräften" *Z. Phys.* 60, **1930**, 491.
- Estarellas, C.; Frontera, A.; Quiñonero, D.; Deyà, P. M. "Anion- π Interactions in Flavoproteins" *Chem. Eur. J.* 6, **2011a**, 2316.
- Estarellas, C.; Frontera, A.; Quiñonero, D.; Deyà, P. M. "Relevant Anion- π Interactions in Biological Systems: The Case of Urate Oxidase" *Angew. Chem. Int. Ed.* 50, **2011b**, 415.
- Estarellas, C.; Rotger, M. C.; Capó, M.; Quiñonero, D.; Frontera, A.; Costa, A.; Deyà, P. M. "Anion- π interactions in Four-Membered Rings" *Org. Lett.* 11, **2009**, 1987.
- Felker, P. M.; Maxton, P. M.; Schaeffer, M. W. "Nonlinear Raman Studies of Weakly Bound Complexes and Clusters in Molecular Beams" *Chem. Rev.* 94, **1994**, 1787.
- Feller, D.; Davidson, E. R. Basis Sets for Ab Initio Molecular Orbital Calculations and Intermolecular Interactions. In *Reviews in Computational Chemistry*, K. B. Lipkowitz, D. B. Boyd, Eds. VCH: New York, **1990**; Vol. 1.
- Fermi, E. "Un Metodo Statistiche per la Determinazione di Alcune Oroprieta Dell'atomo" *Rend. Accad. Nazl. Lincei* 6, **1927**, 602.

- Fermi, E. "Eine statistische Methode zur Bestimmung einiger Eigenschaften des Atomes und ihre Anwendung auf die Theorie des periodischen Systems der Elemente" *Z. Phys.* 48, **1928**, 73.
- Fersht, A. R. "The Hydrogen Bond in Molecular Recognition" *Trends Biochem. Sci.* 12, **1987**, 301.
- Flurry, R. L. J. "Molecular Orbital Theory of Electron Donor-Acceptor Complexes. I. A Simple Semiempirical Treatment" *J. Phys. Chem.* 69, **1965**, 1927.
- Flurry, R. L. J. "Molecular Orbital Theory of Electron Donor-Acceptor Complexes. II. Charged Donors and Acceptors" *J. Phys. Chem.* 73, **1969**, 2111.
- Fock, V. "Näherungsmethode zur Lösung des Quantenmechanischen Mehrkörper Problems" *Z. Phys.* 61, **1930**, 126.
- Foresman, J. B.; Head-Gordon, M.; Pople, J. A.; Frisch, M. J. "Toward a Systematic Molecular Orbital Theory for Excited States" *J. Phys. Chem.* 96, **1992**, 135.
- Foresman, J. B.; Keith, T. A.; Wiberg, K. B.; Snoonian, J.; Frisch, M. J. "Solvent Effects 5. The Influence of Cavity Shape, Truncation of Electrostatics, and Electron Correlation on Ab Initio Reaction Field Calculations" *J. Phys. Chem.* 100, **1996**, 16098.
- Frisch, M. J.; Trucks, G. W.; Schlegel, H. B.; Scuseria, G. E.; Robb, M. A.; Cheeseman, J. R.; Scalmani, G.; Barone, V.; Mennucci, B.; Petersson, G. A.; Nakatsuji, H.; Caricato, M.; Li, X.; Hratchian, H. P.; Izmaylov, A. F.; Bloino, J.; Zheng, G.; Sonnenberg, J. L.; Hada, M.; Ehara, M.; Toyota, K.; Fukuda, R.; Hasegawa, J.; Ishida, M.; Nakajima, T.; Honda, Y.; Kitao, O.; Nakai, H.; Vreven, T.; Montgomery, Jr., J. A.; Peralta, J. E.; Ogliaro, F.; Bearpark, M.; Heyd, J. J.; Brothers, E.; Kudin, K. N.; Staroverov, V. N.; Keith, T.; Kobayashi, R.; Normand, J.; Raghavachari, K.; Rendell, A.; Burant, J. C.; Iyengar, S. S.; Tomasi,

- J.; Cossi, M.; Rega, N.; Millam, J. M.; Klene, M.; Knox, J. E.; Cross, J. B.; Bakken, V.; Adamo, C.; Jaramillo, J.; Gomperts, R.; Stratmann, R. E.; Yazyev, O.; Austin, A. J.; Cammi, R.; Pomelli, C.; Ochterski, J. W.; Martin, R. L.; Morokuma, K.; Zakrzewski, V. G.; Voth, G. A.; Salvador, P.; Dannenberg, J. J.; Dapprich, S.; Daniels, A. D.; Farkas, O.; Foresman, J. B.; Ortiz, J. V.; Cioslowski, J.; Fox, D. J. *Gaussian 09, Revision C.01*, Gaussian, Inc.: Wallingford CT, 2010.
- Frontera, A.; Quiñonero, D.; Costa, A.; Ballester, P.; Deyà, P. M. "MP2 Study of Cooperative Effects Between Cation- π , Anion- π and π - π Interactions" *New J. Chem.* 31, **2007**, 556.
- Frontera, A.; Quiñonero, D.; Deyà, P. M. "Cation- π and Anion- π Interactions" *WIREs Comput. Mol. Sci.* 1, **2011**, 440.
- Frontera, A.; Quiñonero, D.; Garau, C.; Costa, A.; Ballester, P.; Deyà, P. M. "MP2 Study of Cation-(π)_n- π Interactions (n = 1-4)" *J. Phys. Chem. A* 110, **2006**, 9307.
- Frontera, A.; Saczewski, F.; Gdaniec, M.; Dziemidowicz-Borys, E.; Kurland, A.; Deyà, P. M.; Quiñonero, D.; Garau, C. "Anion- π Interactions in Cyanuric Acids: A Combined Crystallographic and Computational Study" *Chem. Eur. J.* 11, **2005**, 6560.
- Gadre, S. R.; Bhadane, P. K. "Patterns in Hydrogen Bonding via Electrostatic Potential Topography" *J. Chem. Phys.* 107, **1997**, 5625.
- Gadre, S. R.; Bhadane, P. K.; Pundlik, S. S.; Pingale, S. S. Molecular Recognition via Electrostatic Potential Topography. In *Molecular Electrostatic Potentials: Concepts and Applications*, J. S. Murray, K. Sen, Eds. Elsevier: Amsterdam, **1996**; Vol. 3.

- Gadre, S. R.; Kölmel, C.; Shrivastava, I. H. "Deriving Chemical Parameters From Electrostatic Potential Maps of Molecular Anions" *Inorg. Chem.* 31, **1992a**, 2279.
- Gadre, S. R.; Kulkarni, S. A.; Shrivastava, I. H. "Molecular Electrostatic Potentials: A Topographical Study" *J. Chem. Phys.* 96, **1992b**, 5253.
- Gadre, S. R.; Pathak, R. K. "Maximal and Minimal Characteristics of Molecular Electrostatic Potentials" *J. Chem. Phys.* 93, **1990a**, 1770.
- Gadre, S. R.; Pathak, R. K. "Nonexistence of Local Maxima in Molecular Electrostatic Potential Maps" *Proc. Ind. Acad. Sci. (Chem. Sci.)* 102, **1990b**, 189.
- Gadre, S. R.; Pundlik, S. S. "Complementary Electrostatics for the Study of DNA Base-Pair Interactions" *J. Phys. Chem. B* 101, **1997**, 3298.
- Gadre, S. R.; Shirsat, R. N. *Electrostatics of Atoms and Molecules*. Universities Press: Hyderabad, India, **2000**.
- Gadre, S. R.; Shrivastava, I. H. "Topography Driven Electrostatic Charge Models for Molecules" *Chem. Phys. Lett.* 205, **1993**, 350.
- Galabov, B.; Bobadova-Parvanova, P. "Molecular Electrostatic Potential as Reactivity Index in Hydrogen Bonding: Ab Initio Molecular Orbital Study of Complexes of Nitrile and Carbonyl Compounds with Hydrogen Fluoride" *J. Phys. Chem. A* 103, **1999**, 6793.
- Galabov, B.; Bobadova-Parvanova, P.; Ilieva, S.; Dimitrova, V. "The Electrostatic Potential at Atomic Sites as a Reactivity Index in the Hydrogen Bond Formation" *J. Mol. Struct. THEOCHEM* 630, **2003**, 101.
- Gallivan, J. P.; Dougherty, D. A. "Can Lone Pairs Bind to a π System? The Water...Hexafluorobenzene Interaction" *Org. Lett.* 1, **1999**, 103.

- Garau, C.; Frontera, A.; Quiñonero, D.; Ballester, P.; Costa, A.; Deyá, P. M. “A Topological Analysis of the Electron Density in Anion- π Interactions” *ChemPhysChem* 4, **2003a**, 1344.
- Garau, C.; Frontera, A.; Quiñonero, D.; Ballester, P.; Costa, A.; Deyá, P. M. “Cation- π Versus Anion- π Interactions: A Comparative Ab Initio Study Based on Energetic, Electron Charge Density and Aromatic Features” *Chem. Phys. Lett.* 392, **2004a**, 85.
- Garau, C.; Frontera, A.; Quiñonero, D.; Ballester, P.; Costa, A.; Deyá, P. M. “Cation- π versus Anion- π Interactions: Energetic, Charge Transfer, and Aromatic Aspects” *J. Phys. Chem. A* 108, **2004b**, 9423.
- Garau, C.; Quiñonero, D.; Frontera, A.; Ballester, P.; Costa, A.; Deyá, P. M. “Approximate Additivity of Anion- π Interactions: An Ab Initio Study on Anion- π , Anion- π_2 and Anion- π_3 Complexes” *J. Phys. Chem. A* 109, **2005**, 9341.
- Garau, C.; Quiñonero, D.; Frontera, A.; Ballester, P.; Costa, A.; Deyá, P. M. “Anion- π Interactions: Must the Aromatic Ring be Electron Deficient?” *New J. Chem.* 27, **2003b**, 211.
- Garau, C.; Quiñonero, D.; Frontera, A.; Ballester, P.; Costa, A.; Deyá, P. M. “Interplay Between Cation- π , Anion- π and π - π Interactions” *ChemPhysChem* 7, **2006**, 2487.
- Garcia-Raso, A.; Albertí, F. M.; Fiol, J. J.; Tasada, A.; Barceló-Oliver, M.; Molins, E.; Escudero, D.; Frontera, A.; Quiñonero, D.; Deyá, P. M. “Anion- π Interactions in Bisadenine Derivatives: A Combined Crystallographic and Theoretical Study” *Inorg. Chem.* 46, **2007**, 10724.
- Garrett, R. H.; Grisham, C. M. *Biochemistry*. Harcourt Brace College: Orlando, **1995**.

- Gillespie, R. J. "The Valence-Shell Electron-Pair Repulsion (VSEPR) Theory of Directed Valency" *J. Chem. Educ.* 40, **1963**, 295.
- Gillespie, R. J.; Nyholm, R. S. "Inorganic Stereochemistry" *Q. Rev. Chem. Soc.* 11, **1957**, 339.
- Gilli, G.; Gilli, P. "Towards an Unified Hydrogen-Bond Theory" *J. Mol. Struct.* 552, **2000**, 1.
- Gilli, G.; Gilli, P. *The Nature of the Hydrogen Bond: Outline of a Comprehensive Hydrogen Bond Theory*. Oxford University Press: Oxford, **2009a**.
- Gilli, P.; Bertolasi, V.; Ferretti, V.; Gilli, G. "Covalent Nature of the Strong Homonuclear Hydrogen Bond. Study of the O-H-O System by Crystal Structure Correlation Methods" *J. Am. Chem. Soc.* 116, **1994**, 909.
- Gilli, P.; Pretto, L.; Bertolasi, V.; Gilli, G. "Predicting Hydrogen-Bond Strengths from Acid-Base Molecular Properties. The pK_a Slide Rule: Toward the Solution of a Long-Lasting Problem" *Acc. Chem. Res.* 42, **2009b**, 33.
- Glendening, E. D.; Landis, C. R.; Weinhold, F. "Natural Bond Orbital Methods" *WIREs Comput. Mol. Sci.* 2, **2002**, 1.
- Godbout, N.; Salahub, D. R.; Andzelm, J.; Wimmer, E. "Optimization of Gaussian-Type Basis Sets for Local Spin Density Functional Calculations. Part I. Boron Through Neon, Optimization Technique and Validation" *Can. J. Chem.* 70, **1992**, 560.
- Gorteau, V.; Bollot, G.; Mareda, J.; Perez-Velasco, A.; Matile, S. "Rigid Oligonaphthalenediimide Rods as Transmembrane Anion- π Slides" *J. Am. Chem. Soc.* 128, **2006**, 14788.
- Gotch, A. J.; Zwier, T. S. "The Spectroscopy and Dynamics of π Hydrogen-Bonded Complexes: Benzene-HCl/DCl and Toluene-HCl/DCl" *J. Chem. Phys.* 93, **1990**, 6977.

- Grabowski, S. J. "Ab Initio Calculations on Conventional and Unconventional Hydrogen Bonds-Study of the Hydrogen Bond Strength" *J. Phys. Chem. A* 105, **2001a**, 10739.
- Grabowski, S. J. "A New Measure of Hydrogen Bonding Strength – Ab Initio and Atoms in Molecules Studies" *Chem. Phys. Lett.* 338, **2001b**, 361.
- Grabowski, S. J. "Hydrogen Bonding Strength - Measures Based on Geometric and Topological Parameters" *J. Phys. Org. Chem.* 17, **2004**, 18.
- Grabowski, S. J. "What is the Covalency of Hydrogen Bonding?" *Chem. Rev.* 111, **2011**, 2597.
- Grabowski, S. J. "Hydrogen and Halogen Bonds are Ruled by the Same Mechanisms" *Phys. Chem. Chem. Phys.* 15, **2013**, 7249.
- Grabowski, S. J.; Sokalski, W. A. "Different Types of Hydrogen Bonds: Correlation Analysis of Interaction Energy Components" *J. Phys. Org. Chem.* 18, **2005**, 779.
- Grabowski, S. J.; Sokalski, W. A.; Dyguda, E.; Leszczyński, J. "Quantitative Classification of Covalent and Noncovalent H-bonds" *J. Phys. Chem. B* 110, **2006**, 6444.
- Graf, E.; Lehn, J. M. "Anion Cryptates: Highly Stable and Selective Macrotricyclic Anion Inclusion Complexes" *J. Am. Chem. Soc.* 98, **1976**, 6403.
- Guthrie, F. "On the Iodide of Iodammonium" *J. Chem. Soc.* 16, **1863**, 239.
- Hall, G. G. "The Molecular Orbital Theory of Chemical Valency. VIII. A Method of Calculating Ionization Potentials" *Proc. Roy. Soc. (London) A* 205, **1951**, 541.
- Hantzsch, A. "Gelbe und rote Formen von Salzen und Hydraten der Oxyazokörper" *Ber. Dtsch. Chem. Ges.* 43, **1910**, 3049.
- Hartree, R. R. "The Wave Mechanics of an Atom with a Non-Coulomb Central Field. Part I. Theory and Methods" *Proc. Cambridge Phil. Soc.* 24, **1928**, 89.

- Hassel, O. "Structural Aspects of Interatomic Charge-Transfer Bonding" *Science* 170, **1970**, 497.
- Hassel, O.; Stromme, K. O. "Halogen-Molecule Bridges in Solid Addition Compounds" *Nature* 182, **1958a**, 1155.
- Hassel, O.; Stromme, K. O. "Structure of the Crystalline Compound Benzene-Bromine (1:1)" *Acta Chem. Scand.* 12, **1958b**, 1146.
- Hay, B. P.; Bryantsev, V. S. "Anion-Arene Adducts: C-H Hydrogen Bonding, Anion- π Interaction, and Carbon Bonding Motifs" *Chem. Commun.* 21, **2008**, 2417.
- Hay, B. P.; Custelcean, R. "Anion- π Interactions in Crystal Structures: Commonplace or Extraordinary?" *Cryst. Growth Des.* 9, **2009**, 2539.
- He, J. J.; Quioco, F. A. "Stabilization of Charges on Isolated Ionic Groups Sequestered in Proteins by Polarized Peptide Units" *Science* 251, **1991**, 1479.
- Hehre, W. J.; Ditchfield, R.; Pople, J. "Self-Consistent Molecular Orbital Methods. XII. Further Extensions of Gaussian-Type Basis Sets for Use in Molecular Orbital Studies of Organic Molecules" *J. Chem. Phys.* 56, **1972**, 2257.
- Hehre, W. J.; Random, L.; Schleyer, P. v. R.; Pople, J. A. *Ab Initio Molecular Orbital Theory*. Wiley: New York, **1986**.
- Hehre, W. J.; Stewart, R. F.; Pople, J. A. "Self-Consistent Molecular-Orbital Methods. I. Use of Gaussian Expansions of Slater-Type Atomic Orbitals" *J. Chem. Phys.* 51, **1969**, 2657.
- Hernández-Trujillo, J.; Vela, A. "Molecular Quadrupole Moments for the Series of Fluoro- and Chlorobenzenes" *J. Phys. Chem.* 100, **1996**, 6524.
- Hesselmann, A.; Korona, T. "On the Accuracy of DFT-SAPT, MP2, SCS-MP2, MP2C, and DFT+Disp Methods for the Interaction Energies of Endohedral Complexes of

- the C₆₀ Fullerene with a Rare Gas Atom” *Phys. Chem. Chem. Phys.* 13, **2011**, 732.
- Hill, J. G.; Hu, X. “Theoretical Insights into the Nature of Halogen Bonding in Prereactive Complexes” *Chem. Eur. J.* 19, **2013**, 3620.
- Hirschfelder, J. O.; Curtiss, C. F.; Bird, R. B. *Molecular Theory of Gases and Liquids*. Wiley: New York, **1964**.
- Hobza, P. “Theoretical Studies of Hydrogen Bonding” *Annu. Rep. Prog. Chem., Sect. C* 100, **2004**, 3.
- Hobza, P.; Bludský, O.; Selzle, H. L.; Schlag, E. W. “Ab Initio Second and Fourth Order Møller–Plesset Study on Structure, Stabilization Energy, and Stretching Vibration of Benzene-X (X=He, Ne, Ar, Kr, Xe) van der Waals Molecules” *J. Chem. Phys.* 97, **1992**, 335.
- Hobza, P.; Bludský, O.; Selzle, H. L.; Schlag, E. W. “Ab Initio Calculations on the Structure, Vibrational Frequencies, and Valence Excitation Energies of the Benzene...Ar and Benzene...Ar₂ Cluster” *Chem. Phys. Lett.* 250, **1996**, 402.
- Hobza, P.; Havlas, Z. “Blue-Shifting Hydrogen Bonds” *Chem. Rev.* 100, **2000**, 4253.
- Hobza, P.; Müller-Dethlefs, K. *Non-Covalent Interactions: Theory and Experiment*. Royal Society of Chemistry: Cambridge, **2010**.
- Hobza, P.; Selzle, H. L.; Schlag, E. W. “Ab Initio Calculations on the Structure, Stabilization, and Dipole Moment of Benzene...Ar Complex” *J. Chem. Phys.* 95, **1991**, 391.
- Hobza, P.; Selzle, H. L.; Schlag, E. W. “Properties of Fluorobenzene-Ar and p-Difluorobenzene-Ar Complexes: Ab Initio Study” *J. Chem. Phys.* 99, **1993**, 2809.

- Hobza, P.; Selzle, H. L.; Schlag, E. W. "Structure and Properties of Benzene-Containing Molecular Clusters: Nonempirical Ab Initio Calculations and Experiments" *Chem. Rev.* 94, **1994**, 1767.
- Hobza, P.; Špirko, V.; Selzle, H. L.; Schlag, E. W. "Anti-Hydrogen Bond in the Benzene Dimer and Other Carbon Proton Donor Complexes" *J. Phys. Chem. A* 102, **1998**, 2501.
- Hohenberg, P.; Kohn, W. "Inhomogeneous Electron Gas" *Phys. Rev. B* 136, **1964**, 864.
- Huggins, M. L. "Hydrogen Bridges in Organic Compounds" *J. Org. Chem.* 1, **1936**, 407.
- Humphreys, C. J. "Electrons Seen in Orbit" *Nature* 401, **1999**, 21.
- Jacobson, D. R.; Khan, N. S.; Collé, R.; Fitzgerald, R.; Laureano-Pérez, L.; Bai, Y.; Dmochowski, I. J. "Measurement of Radon And Xenon Binding to a Cryptophane Molecular Host" *Proc. Natl. Acad. Sci. USA* 108, **2011**, 10969.
- Jain, A.; Purohit, C. S.; Verma, S.; Sankararamakrishnan, R. "Close Contacts between Carbonyl Oxygen Atoms and Aromatic Centers in Protein Structures: $\pi\cdots\pi$ or Lone-Pair $\cdots\pi$ Interactions?" *J. Phys. Chem. B* 111, **2007**, 8680.
- Jain, A.; Ramanathan, V.; Sankararamakrishnan, R. "Lone Pair $\cdots\pi$ Interactions Between Water Oxygens and Aromatic Residues: Quantum Chemical Studies Based on High-Resolution Protein Structures and Model Compounds" *Protein Sci.* 18, **2009**, 595.
- Janesko, B. G. "Rung 3.5 Density Functionals" *J. Chem Phys.* 133, **2010**, 104103.
- Janesko, B. G. "Rung 3.5 Density Functionals: Another Step on Jacob's Ladder" *Int. J. Quantum Chem.* 113, **2013**, 83.
- Janowski, T.; Pulay, P. "High Accuracy Benchmark Calculations on the Benzene Dimer Potential Energy Surface" *Chem. Phys. Lett.* 447, **2007**, 27.

- Jeffrey, G. A. *An Introduction to Hydrogen Bonding*. Oxford University Press: Oxford, **1997**.
- Jeffrey, G. A.; Saenger, W. *Hydrogen Bonding in Biological Structures*. Springer-Verlag: California, **1994**.
- Jensen, F. *Introduction to Computational Chemistry*. John Wiley and Sons: New York, **1999**.
- Jiménez-Vázquez, H. A.; Tamariz, J.; Cross, R. J. "Binding Energy in and Equilibrium Constant of Formation for the Dodecahedrane Compounds He@C₂₀H₂₀ and Ne@C₂₀H₂₀" *J. Phys. Chem. A* 105, **2001**, 1315.
- Jonas, V.; Frenking, G.; Reetz, M. T. "Comparative Theoretical Study of Lewis Acid-Base Complexes of BH₃, BF₃, BCl₃, AlCl₃, and SO₂" *J. Am. Chem. Soc.* 116, **1994**, 8141.
- Joseph, J.; Jemmis, E. D. "Red-, Blue-, or No-Shift in Hydrogen Bonds: A Unified Explanation" *J. Am. Chem. Soc.* 129, **2007**, 4620.
- Joyce, L. A.; Shabbir, S. H.; Anslyn, E. V. "The Uses of Supramolecular Chemistry in Synthetic Methodology Development: Examples of Anion and Neutral Molecular Recognition" *Chem. Soc. Rev.* 39, **2010**, 3621.
- Kelly, H. P. *Advances in Chemical Physics*. John Wiley & Sons: New York, **1969**.
- Kim, D.; Tarakeshwar, P.; Kim, K. S. "Theoretical Investigations of Anion- π Interactions: The Role of Anions and the Nature of π Systems" *J. Phys. Chem. A* 108, **2004**, 1250.
- Kim, K. S.; Tarakeshwar, P.; Lee, J. Y. "Molecular Clusters of π -Systems: Theoretical Studies of Structures, Spectra, and Origin of Interaction Energies" *Chem. Rev.* 100, **2000**, 4145.

- Kitaura, K.; Morokuma, K. "A New Energy Decomposition Scheme for Molecular Interactions Within the Hartree-Fock Approximation" *Int. J. Quantum Chem.* 10, **1976**, 325.
- Knop, O.; Rankin, K. N.; Boyd, R. J. "Coming to Grips with N-H...N bonds. 2. Homocorrelations Between Parameters Deriving from the Electron Density at the Bond Critical Point" *J. Phys. Chem. A* 107, **2003**, 272.
- Koch, U.; Popelier, P. L. A. "Characterization of C-H-O Hydrogen Bonds on the Basis of the Charge Density" *J. Phys. Chem.* 99, **1995**, 9747.
- Kohn, W.; Sham, L. J. "Self-Consistent Equations Including Exchange and Correlation Effects" *Phys. Rev. A* 140, **1965**, 1133.
- Kollman, P.; McKelvey, J.; Johansson, A.; Rothenberg, S. "Theoretical Studies of Hydrogen-Bonded Dimers. Complexes Involving HF, H₂O, NH₃, HCl, H₂S, PH₃, HCN, HNC, HCP, CH₂NH, H₂CS, H₂CO, CH₄, CF₃H, C₂H₂, C₂H₄, C₆H₆, F, and H₃O⁺" *J. Am. Chem. Soc.* 97, **1975**, 955.
- Kollman, P. A.; Allen, L. C. "An SCF Partitioning Scheme for the Hydrogen Bond" *Theor. Chim. Acta* 18, **1970**, 399.
- Kollman, P. A.; Allen, L. C. "Theory of the Hydrogen Bond" *Chem. Rev.* 72, **1972**, 283.
- Korona, T.; Hesselmann, A.; Dodziuk, H. "Symmetry-Adapted Perturbation Theory Applied to Endohedral Fullerene Complexes: A Stability Study of H₂@C₆₀ and 2H₂@C₆₀" *J. Chem. Theory Comput.* 5, **2009**, 1585.
- Kovács, A.; Varga, Z. "Halogen Acceptors in Hydrogen Bonding" *Coord. Chem. Rev.* 250, **2006**, 710.
- Kraka, E.; Cremer, D.; Spoerel, U.; Merke, I.; Stahi, W.; Dreizler, H. "Intermolecular Forces in Argon van der Waals Complexes. Rotational Spectrum and Ab Initio Investigation of Ar-Oxazole" *J. Phys. Chem.* 99, **1995**, 12466.

- Krapp, A.; Frenking, G. "Is This a Chemical Bond? A Theoretical Study of Ng₂@C₆₀ (Ng=He, Ne, Ar, Kr, Xe)" *Chem. Eur. J.* 13, **2007**, 8256.
- Krause, H.; Neusser, H. J. "Dissociation Energy of Neutral and Ionic Benzene-Noble Gas Dimers by Pulsed Field Threshold Ionization Spectroscopy" *J. Chem. Phys.* 99, **1993**, 6278.
- Krishnan, R.; Pople, J. A. "Approximate Fourth-Order Perturbation Theory of the Electron Correlation Energy" *Int. J. Quantum Chem.* 14, **1978**, 91.
- Kristyán, S.; Pulay, P. "Can (Semi)Local Density Functional Theory Account for the London Dispersion Forces?" *Chem. Phys. Lett.* 229, **1994**, 175.
- Kruse, H.; Grimme, S. "Accurate Quantum Chemical Description of Non-Covalent Interactions in Hydrogen Filled Endohedral Fullerene Complexes" *J. Phys. Chem. C* 113, **2009**, 17006.
- Kukolich, S. G. "Microwave Structure Measurements on the Furan-Argon Complex" *J. Am. Chem. Soc.* 105, **1983**, 2207.
- Kumar, A.; Gadre, S. R.; Mohan, N.; Suresh, C. H. "Lone Pairs: An Electrostatic Viewpoint" *J. Phys. Chem. A* 118, **2014**, 526.
- Kümmel, H. G. A Biography of the Coupled Cluster Method. In *Recent Progress in Many-Body Theories Proceedings of the 11th International Conference*, R. F. Bishop, T. Brandes, K. A. Gernoth, N. R. Walet, Y. Xian, Eds. World Scientific Publishing: Singapore, **2002**.
- Kuswandi, B.; Nuriman; Verboom, W.; Reinhoudt, D. N. "Tripodal Receptors for Cation and Anion Sensors" *Sensors* 6, **2006**, 978.
- Laidig, K. E. "The Atomic Basis of the Molecular Quadrupole Moments of Benzene and Hexafluorobenzene" *Chem. Phys. Lett.* 185, **1991**, 483.

- Lane, J. R.; Kjaergaard, H. G. "Explicitly Correlated Intermolecular Distances and Interaction Energies of Hydrogen Bonded Complexes" *J. Chem. Phys.* 131, **2009**, 034307.
- Langmuir, I. "Isomorphism, Isosterism and Covalence" *J. Am. Chem. Soc.* 41, **1919a**, 1543.
- Langmuir, I. "The Structure of Atoms and the Octet Theory of Valence" *Proc. Natl. Acad. Sci. USA* 5, **1919b**, 252.
- Latimer, W. M.; Rodebush, W. H. "Polarity and Ionization from the Standpoint of the Lewis Theory of Valence" *J. Am. Chem. Soc.* 42, **1920**, 1419.
- Legon, A. C. " π -electron 'Donor-Acceptor' Complexes B...ClF and the Existence of the 'Chlorine Bond'" *Chem. Eur. J.* 4, **1998**, 1890.
- Legon, A. C. "Prereactive Complexes of Dihalogens XY with Lewis Bases B in the Gas Phase: A Systematic Case for the Halogen Analogue B...XY of the Hydrogen Bond B...HX" *Angew. Chem. Int. Ed.* 38, **1999**, 2686.
- Legon, A. C. The Interaction of Dihalogens and Hydrogen Halides with Lewis Bases in the Gas Phase: An Experimental Comparison of the Halogen Bond and the Hydrogen Bond. In *Halogen Bonding: Fundamentals and Applications*, P. Metrangolo, G. Resnati, Eds. Springer: Berlin, **2008**.
- Legon, A. C. "The Halogen Bond: An Interim Perspective" *Phys. Chem. Chem. Phys.* 12, **2010**, 7736.
- Lehn, J.-M. *Supramolecular Chemistry: Concepts and Perspectives*. VCH: New York, **1995**.
- Lehn, J. M.; Sonveaux, E.; Willard, A. K. "Molecular Recognition. Anion Cryptates of a Macrobicyclic Receptor Molecule for Linear Triatomic Species" *J. Am. Chem. Soc.* 100, **1978**, 4914.

- Leopold, K. R.; Canagaratna, M.; Phillips, J. A. "Partially Bonded Molecules from the Solid State to the Stratosphere" *Acc. Chem. Res.* 30, **1997**, 57.
- Leroy, G.; Louterman-Leloup, G.; Ruelle, P. "Contribution to the Theoretical Study of the Hydrogen Bond-I" *Bull. Soc. Chim. Belg.* 85, **1976**, 205.
- Lewis, G. N. "The Atom and the Molecule" *J. Am. Chem. Soc.* 38, **1916**, 762.
- Lewis, G. N. *Valence and structure of Atoms and Molecules*. The Chemical Catalog Co., Inc.: New York, **1923**.
- Lhoták, P. "Anion Receptors Based on Calixarenes" *Top. Curr. Chem.* 255, **2005**, 65.
- Li, A.-F.; Wang, J.-H.; Wang, F.; Jiang, Y.-B. "Anion Complexation and Sensing Using Modified Urea and Thiourea-Based Receptors" *Chem. Soc. Rev.* 39, **2010a**, 3729.
- Li, Q.; Jing, B.; Liu, Z.; Li, W.; Cheng, J.; Gong, B.; Sun, J. "Surprising Enhancing Effect of Methyl Group on the Strength of OX...F and S...XF (X = Cl and Br) Halogen Bonds" *J. Chem. Phys.* 133, **2010b**, 114303.
- Li, Q.; Li, R.; Liu, Z.; Li, W.; Cheng, J. "Interplay Between Halogen Bond and Lithium Bond in MCN-LiCN-XCCH (M = H, Li, and Na; X = Cl, Br, and I) Complex: The Enhancement of Halogen Bond by a Lithium Bond" *J. Comp. Chem.* 32, **2011**, 3296.
- Limtrakul, J. P.; Hannongbua, S. V.; Kokpol, S. U.; Rode, B. M. "Cation Binding Effect on Hydrogen Bonded Dimer of Imidazole and Water" *Inorg. Chim. Acta.* 138, **1987**, 131.
- Liu, X.; Xu, Y. "Infrared and Microwave Spectra of the Acetylene–Ammonia and Carbonyl Sulfide–Ammonia Complexes: A Comparative Study of a Weak C–H...N Hydrogen Bond and an S...N Bond" *Phys. Chem. Chem. Phys.* 13, **2011**, 14235.

- Llinares, J. M.; Powell, D.; Bowman-James, K. "Ammonium Based Anion Receptors" *Coord. Chem. Rev.* 240, **2003**, 57.
- Lommerse, J. P. M.; Stone, A. J.; Taylor, R.; Allen, F. H. "The Nature and Geometry of Intermolecular Interactions between Halogens and Oxygen or Nitrogen" *J. Am. Chem. Soc.* 118, **1996**, 3108.
- London, F. "Über einige Eigenschaften und Anwendungen der Molekularkräfte" *Z. Phys. Chem.* B11, **1930a**, 222.
- London, F. "Zur Theorie und Systematik der Molekularkräfte" *Z. Phys.* 63, **1930b**, 245.
- López, R.; Rico, J. F.; Ramírez, G.; Ema, I.; Zorrilla, D. "DAMQT: A Package for the Analysis of Electron Density in Molecules" *Comput. Phys. Commun.* 180, **2009**, 1654.
- Luecke, H.; Quiocho, F. A. "High Specificity of a Phosphate Transport Protein Determined by Hydrogen Bonds" *Nature* 347, **1990**, 402.
- Luque, F. J.; Orozco, M.; Bhadane, P. K.; Gadre, S. R. "Effect of Solvation on the Shapes, Sizes and Anisotropies of Polyatomic Anions via Molecular Electrostatic Potential Topology: An Ab Initio Self Consistent Reaction Field Approach" *J. Chem. Phys.* 100, **1994**, 6718.
- Ma, J. C.; Dougherty, D. A. "The Cation- π Interaction" *Chem. Rev.* 97, **1997**, 1303.
- MacKie, I. D.; DiLabio, G. A. "Approximations to Complete Basis Set-extrapolated, Highly Correlated Non-covalent Interaction Energies" *J. Chem. Phys.* 135, **2011**, 134318.
- Madsen, G. K. H.; Iversen, B. B.; Larsen, F. K.; Kapon, M.; Reisner, G. M.; Herbstein, F. H. "Topological Analysis of the Charge Density in Short Intramolecular O-H...O Hydrogen Bonds. Very Low Temperature X-Ray and Neutron Diffraction Study of Benzoylacetone" *J. Am. Chem. Soc.* 120, **1998**, 10040.

- Mahadevi, A. S.; Sastry, G. N. "Modulation of Hydrogen Bonding upon Ion Binding: Insights into Cooperativity" *Int. J. Quantum Chem.* 114, **2014**, 145.
- Martin, J. M. L.; De Oliveira, G. "Towards Standard Methods for Benchmark Quality Ab Initio Thermochemistry - W1 and W2 Theory" *J. Chem. Phys.* 111, **1999**, 1843.
- Mascal, M. "Precedent and Theory Unite in the Hypothesis of a Highly Selective Fluoride Receptor" *Angew. Chem. Int. Ed.* 45, **2006**, 2890.
- Mascal, M.; Armstrong, A.; Bartberger, M. D. "Anion-Aromatic Bonding: A Case for Anion Recognition by π -Acidic Rings" *J. Am. Chem. Soc.* 124, **2002**, 6274.
- Mathew, J.; Suresh, C. H. "Use of Molecular Electrostatic Potential at the Carbene Carbon as A Simple and Efficient Electronic Parameter of N-Heterocyclic Carbenes" *Inorg. Chem.* 49, **2010**, 4665.
- Mathew, J.; Thomas, T.; Suresh, C. H. "Quantitative Assessment of the Stereoelectronic Profile of Phosphine Ligands" *Inorg. Chem.* 46, **2007**, 10800.
- Matile, S.; Mareda, J. "Anion- π Slides for Transmembrane Transport" *Chem. Eur. J.* 15, **2009**, 28.
- McKee, V.; Nelson, J.; Town, R. M. "Caged Oxoanions" *Chem. Soc. Rev.* 32, **2003**, 309.
- Mecozzi, S.; West Jr., A. P.; Dougherty, D. A. "Cation- π Interactions in Aromatics of Biological and Medicinal Interest: Electrostatic Potential Surfaces as a Useful Qualitative Guide" *Proc. Natl. Acad. Sci. USA* 93, **1996a**, 10566.
- Mecozzi, S.; West Jr, A. P.; Dougherty, D. A. "Cation- π Interactions in Simple Aromatics: Electrostatics Provide a Predictive Tool" *J. Am. Chem. Soc.* 118, **1996b**, 2307.
- Merritt, J. M.; Rudić, S.; Miller, R. E. "Infrared Laser Spectroscopy of CH₃...HF in Helium Nanodroplets: The Exit-Channel Complex of the F + CH₄ Reaction" *J. Chem. Phys.* 124, **2006**, 084301.

- Metrangolo, P.; Neukirch, H.; Pilati, T.; Resnati, G. "Halogen Bonding Based Recognition Processes: A World Parallel to Hydrogen Bonding" *Acc. Chem. Res.* **38**, **2005**, 386.
- Mingos, D. M. P. *Supramolecular Assembly via Hydrogen Bonds*. Springer: New York, **2004**.
- Mintz, B. J.; Parks, J. M. "Benchmark Interaction Energies for Biologically Relevant Noncovalent Complexes Containing Divalent Sulfur" *J. Phys. Chem. A* **116**, **2012**, 1086.
- Mohan, N.; Suresh, C. H.; Kumar, A.; Gadre, S. R. "Molecular Electrostatics for Probing Lone Pair- π Interactions" *Phys. Chem. Chem. Phys.* **15**, **2013**, 18401.
- Møller, C.; Plesset, M. S. "Note on an Approximation Treatment for Many-Electron Systems" *Phys. Rev.* **46**, **1934**, 618.
- Mooibroek, T. J.; Black, C. A.; Gamez, P.; Reedijk, J. "What's New in the Realm of Anion- π Binding Interactions? Putting the Anion- π Interaction in Perspective" *Cryst. Growth Des.* **8**, **2008**, 1082.
- Moore, T. S.; Winmill, T. F. "The State of Amines in Aqueous Solution" *J. Chem. Soc., Trans.* **101**, **1912**, 1635.
- Morales, J. L.; Nocedal, J. "Remark on Algorithm 778: L-BFGS-B: Fortran Subroutines for Large-Scale Bound Constrained Optimization" *ACM Trans. Math. Softw.* **38**, **2011**, 7.
- Morokuma, K. "Why Do Molecules Interact? The Origin of Electron Donor-Acceptor Complexes, Hydrogen Bonding, and Proton Affinity" *Acc. Chem. Res.* **10**, **1977**, 294.
- Müller-Dethlefs, K.; Hobza, P. "Noncovalent Interactions: A Challenge for Experiment and Theory" *Chem. Rev.* **100**, **2000**, 143.

- Müller-Dethlefs, K.; Sander, M.; Schlag, E. W. "A Novel Method Capable of Resolving Rotational Ionic States by the Detection of Threshold Photoelectrons with a Resolution of 1.2 cm^{-1} " *Z. Naturf. A* 39, **1984a**, 1089.
- Müller-Dethlefs, K.; Sander, M.; Schlag, E. W. "Two-Colour Photoionization Resonance Spectroscopy of NO: Complete Separation of Rotational Levels of NO^+ at the Ionization Threshold" *Chem. Phys. Lett.* 112, **1984b**, 291.
- Mulliken, R. S. "Molecular Compounds and Their Spectra. II" *J. Am. Chem. Soc.* 74, **1952**, 811.
- Mulliken, R. S.; Person, W. B. *Molecular Complexes: A Lecture and Reprint Volume*. Wiley-Interscience: New York, **1969**.
- Murata, M.; Maeda, S.; Morinaka, Y.; Murata, Y.; Komatsu, K. "Synthesis and Reaction of Fullerene C_{70} Encapsulating Two Molecules of H_2 " *J. Am. Chem. Soc.* 130, **2008**, 15800.
- Murray-Rust, P.; Motherwell, W. D. S. "Computer Retrieval and Analysis of Molecular Geometry. 4. Intermolecular Interactions" *J. Am. Chem. Soc.* 101, **1979**, 4374.
- Murray-Rust, P.; Stallings, W. C.; Monti, C. T.; Preston, R. K.; Glusker, J. P. "Intermolecular Interactions of the Carbon-Fluorine Bond: The Crystallographic Environment of Fluorinated Carboxylic Acids and Related Structures" *J. Am. Chem. Soc.* 105, **1983**, 3206.
- Murray, J. S.; Concha, M. C.; Lane, P.; Hobza, P.; Politzer, P. "Blue Shifts vs Red Shifts in σ -Hole Bonding" *J. Mol. Model.* 14, **2008**, 699.
- Murray, J. S.; Paulsen, K.; Politzer, P. "Molecular Surface Electrostatic Potentials in the Analysis of Non-Hydrogen-Bonding Noncovalent Interactions" *Proc. Ind. Acad. Sci. (Chem. Sci.)* 106, **1994**, 267.

- Murray, J. S.; Sen, K. *Molecular Electrostatic Potentials: Concepts and Applications*. Elsevier: Amsterdam, **1996**; Vol. 3.
- Nernst, W. "Über die Löslichkeit von Mischkrystallen" *Z. Phys. Chem.* **8**, **1892**, 110.
- Neusser, H. J.; Krause, K. "Binding Energy and Structure of van der Waals Complexes of Benzene" *Chem. Rev.* **94**, **1994**, 1829.
- Nir, E.; Janzen, C.; Imhof, P.; Kleinermanns, K.; de Vries, M. S. "Guanine Tautomerism Revealed by UV–UV and IR–UV Hole Burning Spectroscopy" *J. Chem. Phys.* **115**, **2001**, 4604.
- Nir, E.; Janzen, C.; Imhof, P.; Kleinermanns, K.; de Vries, M. S. "Pairing of the Nucleobases Guanine and Cytosine in the Gas Phase Studied by IR–UV Double-Resonance Spectroscopy and Ab Initio Calculations" *Phys. Chem. Chem. Phys.* **4**, **2002**, 732.
- Oddo, G.; Puxeddu, E. "Sui 5-Azoeugenoli e La Costituzione Dei Cosidetti *o*-Ossiazocomposti" *Gazz. Chim. It.* **36**, **1906**, 1.
- Onnes, H. K. The Liquefaction of Helium. In *KNAW, Proceedings*, Proc. R. Netherlands Acad. Arts Sci. (KNAW): Amsterdam, **1909**; Vol. 11, p 168.
- Paldus, J.; Čížek, J.; Shavitt, I. "Correlation Problems in Atomic and Molecular Systems. IV. Extended Coupled-Pair Many-Electron Theory and its Application to the BH₃ Molecule" *Phys. Rev. A* **5**, **1972**, 50.
- Palusiak, M. "On the Nature of Halogen Bond – The Kohn–Sham Molecular Orbital Approach" *J. Mol. Struct. THEOCHEM* **945**, **2010**, 89.
- Pan, S.; Contreras, M.; Romero, J.; Reyes, A.; Chattaraj, P. K.; Merino, G. "C₅Li₇⁺ and O₂Li₅⁺ as Noble-Gas-Trapping Agents" *Chem. Eur. J.* **19**, **2013**, 2322.

- Park, C. H.; Simmons, H. E. "Macrobicyclic Amines. II. Out-out In-in Prototropy in 1, (k + 2)-Diazabicyclo [k.l.m] Alkaneammonium Ions" *J. Am. Chem. Soc.* 90, **1968a**, 2429.
- Park, C. H.; Simmons, H. E. "Macrobicyclic Amines. III. Encapsulation of Halide Ions by in,in-1,(k + 2)-Diazabicyclo[k.l.m.]Alkane Ammonium Ions" *J. Am. Chem. Soc.* 90, **1968b**, 2431.
- Parr, R. G.; Yang, W. *Density-Functional Theory of Atoms and Molecules*. Oxford University Press: Oxford, **1989**.
- Parthasarathi, R.; Subramanian, V.; Sathyamurthy, N. "Hydrogen Bonding Without Borders: An Atoms-In-Molecules Perspective" *J. Phys. Chem. A* 110, **2006**, 3349.
- Parthiban, S.; Martin, J. M. L. "Assessment of W1 and W2 Theories for the Computation of Electron Affinities, Ionization Potentials, Heats of Formation, and Proton Affinities" *J. Chem. Phys.* 114, **2001**, 6014.
- Pathak, R. K.; Gadre, S. R. "Nonexistence of Local Maxima in Molecular Electrostatic Potential Maps" *Proc. Ind. Acad. Sci. (Chem. Sci.)* 102, **1990**, 189.
- Patkowski, K. "Basis Set Converged Weak Interaction Energies from Conventional and Explicitly Correlated Coupled-Cluster Approach" *J. Chem. Phys.* 138, **2013**, 154101.
- Patwari, G. N.; Ebata, T.; Mikami, N. "Gas Phase Dihydrogen Bonded Phenol–Borane–Trimethylamine Complex" *J. Chem. Phys.* 114, **2001**, 8877.
- Patwari, G. N.; Ebata, T.; Mikami, N. "Gas phase Dihydrogen Bonding: Clusters of Borane-Amines with Phenol and Aniline" *Chem. Phys.* 283, **2002**, 193.

- Pauling, L. "The Nature of the Chemical Bond. Application of Results Obtained from the Quantum Mechanics and from a Theory of Paramagnetic Susceptibility to the Structure of Molecules" *J. Am. Chem. Soc.* 53, **1931a**, 1367.
- Pauling, L. "The Formulas of Antimonic Acid and the Antimonates" *J. Am. Chem. Soc.* 55, **1933**, 1895.
- Pauling, L. "The Structure and Entropy of Ice and of Other Crystals with Some Randomness of Atomic Arrangement" *J. Am. Chem. Soc.* 57, **1935**, 2680.
- Pauling, L. *The Nature of the Chemical Bond*. Cornell University Press: Ithaca, **1939**.
- Pauling, L.; Corey, R. B. "Two Hydrogen-Bonded Spiral Configurations of the Polypeptide Chain" *J. Am. Chem. Soc.* 72, **1950**, 5349.
- Pauling, L.; Corey, R. B.; Branson, H. R. "The Structure of Proteins: Two Hydrogen-Bonded Helical Configurations of the Polypeptide Chain" *Proc. Natl. Acad. Sci. USA* 37, **1951**, 205.
- Pauling, L. T. "The Nature of the Chemical Bond. Application of Results Obtained from the Quantum Mechanics and from a Theory of Paramagnetic Susceptibility to the Structure of Molecules" *J. Am. Chem. Soc.* 53, **1931b**, 1367.
- Perdew, J. P. "Density-Functional Approximation for the Correlation Energy of the Inhomogeneous Electron Gas" *Phys. Rev. B* 33, **1986**, 8822.
- Perdew, J. P.; Chevary, J. A.; Vosko, S. H.; Jackson, K. A.; Pederson, M. R.; Singh, D. J.; Fiolhais, J. C. "Atoms, Molecules, Solids, and Surfaces: Applications of the Generalized Gradient Approximation for Exchange and Correlation" *Phys. Rev. B* 46, **1992**, 6671.
- Perdew, J. P.; Schmidt, K. Jacob's Ladder of Density Functional Approximations for the Exchange-Correlation Energy. In *Density Functional Theory and its Applications*

- to Materials*, V. E. Van Doren, K. Van Alseoy, P. Geerlings, Eds. AIP Press: New York, **2001**.
- Perez-Jorda, J. M.; Becke, A. D. "A Density-functional Study of van der Waals Forces: Rare Gas Diatomics" *Chem. Phys. Lett.* 233, **1995**, 134.
- Pernal, K.; Podeszwa, R.; Patkowski, K.; Szalewicz, K. "Dispersionless Density Functional Theory" *Phys. Rev. Lett.* 103, **2009**, 263201.
- Peverati, R.; Truhlar, D. G. "Improving the Accuracy of Hybrid Meta-GGA Density Functionals by Range Separation" *J. Phys. Chem. Lett.* 2, **2011**, 2810.
- Peverati, R.; Truhlar, D. G. "An Improved and Broadly Accurate Local Approximation to the Exchange-Correlation Density Functional: The MN12-L Functional for Electronic Structure Calculations in Chemistry and Physics" *Phys. Chem. Chem. Phys.* 14, **2012**, 13171.
- Pfeiffer, P.; Fischer, P.; Kuntner, J.; Monti, P.; Pros, Z. "Zur Theorie der Farblacke, II" *Justus Liebigs Ann. Chem.* 398, **1913**, 137.
- Pflugrath, J. W.; Quioco, F. A. "Sulphate Sequestered in the Sulphate-Binding Protein of Salmonella Typhimurium is Bound Solely by Hydrogen Bonds" *Nature* 314, **1985**, 257.
- Pflugrath, J. W.; Quioco, F. A. "The 2 Å Resolution Structure of the Sulfate-Binding Protein Involved in Active Transport in Salmonella Typhimurium" *J. Mol. Biol.* 200, **1988**, 163.
- Pichon-Pesme, V.; Lecomte, C. "Experimental Charge Density and Electrostatic Potential of Triglycine" *Acta Cryst.* B54, **1998**, 485.
- Pimentel, G. C.; McClellan, A. L. *The Hydrogen Bond*. W. H. Freeman: San Francisco, **1960**.

- Politzer, P.; Laurence, P. R.; Jayasuriya, K. "Molecular Electrostatic Potentials: An Effective Tool for the Elucidation of Biochemical Phenomena" *Environ. Health Perspect.* 61, **1985**, 191.
- Politzer, P.; Murray, J. S. Molecular Electrostatic Potentials and Chemical Reactivity. In *Reviews in Computational Chemistry*, K. B. Lipkowitz, D. B. Boyd, Eds. John Wiley & Sons, Inc.: Hoboken, NJ, USA, **1991**; Vol. 2.
- Politzer, P.; Murray, J. S. "The Fundamental Nature and Role of the Electrostatic Potential in Atoms and Molecules" *Theor. Chem. Acc.* 108, **2002**, 134.
- Politzer, P.; Murray, J. S.; Clark, T. "Halogen bonding: An Electrostatically-Driven Highly Directional Noncovalent Interaction" *Phys. Chem. Chem. Phys.* 12, **2010**, 7748.
- Politzer, P.; Murray, J. S.; Clark, T. "Halogen Bonding and Other σ -Hole Interactions: A Perspective" *Phys. Chem. Chem. Phys.* 15, **2013**, 11178.
- Politzer, P.; Murray, J. S.; Peralta-Inga, Z. "Molecular Surface Electrostatic Potentials in Relation to Noncovalent Interactions in Biological Systems" *Int. J. Quantum Chem.* 85, **2001**, 676.
- Politzer, P.; Truhlar, D. G. *Chemical Applications of Atomic and Molecular Electrostatic Potentials*. Plenum Press: New York, **1981**.
- Popelier, P. L. A. "Characterization of a Dihydrogen Bond on the Basis of the Electron Density" *J. Phys. Chem. A* 102, **1998**, 1873.
- Popelier, P. L. A.; Logothetis, G. "Characterization of an Agostic Bond on the Basis of the Electron Density" *J. Organomet. Chem.* 555, **1998**, 101.
- Pople, J. A.; Beveridge, D. L. *Approximate Molecular Orbital Theory*. McGraw-Hill: New York, **1970**.

- Pople, J. A.; Binkley, J. S.; Seeger, R. "Theoretical Models Incorporating Electron Correlation" *Int. J. Quantum Chem. Symp.* 10, **1976**, 1.
- Pople, J. A.; Head-Gordon, M.; Raghavachari, K. "Quadratic Configuration Interaction - A General Technique for Determining Electron Correlation Energies" *J. Chem. Phys.* 87, **1987**, 5968.
- Prescott, A. B. "Notes on a Few Pyridine Alkyl Iodides" *J. Am. Chem. Soc.* 18, **1896**, 91.
- Pugliano, N.; Saykally, R. J. "Measurement of Quantum Tunneling Between Chiral Isomers of the Cyclic Water Trimer" *Science* 257, **1992**, 1937.
- Pullman, B. "A Lucid Introduction to Biological Applications of MESP" *Int. J. Quantum Chem. Quantum Biol. Symp.* 17, **1990**, 609.
- Pundlik, S. S.; Gadre, S. R. "Structure and Stability of DNA Base Trimers: An Electrostatic Approach" *J. Phys. Chem. B* 101, **1997**, 9657.
- Quiñonero, D.; Garau, C.; Frontera, A.; Ballester, P.; Costa, A.; Deyá, P. M. "Counterintuitive Interaction of Anions with Benzene Derivatives" *Chem. Phys. Lett.* 359, **2002a**, 486.
- Quiñonero, D.; Garau, C.; Rotger, C.; Frontera, A.; Ballester, P.; Costa, A.; Deyá, P. M. "Anion- π Interactions: Do They Exist?" *Angew. Chem. Int. Ed.* 41, **2002b**, 3539.
- Raghavachari, K.; Anderson, J. B. "Electron Correlation Effects in Molecules" *J. Phys. Chem.* 100, **1996**, 12960.
- Raghavachari, K.; Pople, J. A. "Approximate 4th-Order Perturbation-Theory of Electron Correlation Energy" *Int. J. Quantum Chem.* 14, **1978**, 91.
- Rapaport, D. C. *The Art of Molecular Dynamics Simulation*. Cambridge University Press: Cambridge, **2004**.
- Ratajczak, H.; Orville-Thomas, W. J. *Molecular Interactions*. John Wiley & Sons: Chichester, **1980**; Vol. 1.

- Rebek, J. J.; Askew, B.; Ballester, P.; Buhr, C.; Jones, S.; Nemeth, D.; Williams, K. "Molecular Recognition: Hydrogen Bonding and Stacking Interactions Stabilize a Model for Nucleic Acid Structure" *J. Am. Chem. Soc.* 109, **1987**, 5033.
- Reed, A. E.; Curtiss, L. A.; Weinhold, F. "Intermolecular Interactions from a Natural Bond Orbital, Donor-Acceptor Viewpoint" *Chem. Rev.* 88, **1988**, 899.
- Remsen, I.; Norris, J. F. "The Action of Halogens on the Methylamines" *Am. Chem. J.* 18, **1896**, 90.
- Remya, K.; Suresh, C. H. "Which Density Functional is Close to CCSD Accuracy to Describe Geometry and Interaction Energy of Small Non-Covalent Dimers? A Benchmark Study Using Gaussian09" *J. Comput. Chem.* 34, **2013**, 1341.
- Řezáč, J.; Hobza, P. "Describing Noncovalent Interactions Beyond the Common Approximations: How Accurate is the "Gold Standard," CCSD(T) at the Complete Basis Set Limit?" *J. Chem. Theory Comput.* 9, **2013**, 2151.
- Řezáč, J.; Riley, K. E.; Hobza, P. "S66: A Well-balanced Database of Benchmark Interaction Energies Relevant to Biomolecular Structures" *J. Chem. Theory Comput.* 7, **2011**, 2427.
- Rico, J. F.; Lòpez, R.; Ema, I.; Ramírez, G. "Deformed Atoms in Molecules: Analytical Representation of Atomic Densities for Gaussian Type Orbitals" *J. Mol. Struct-THEOCHEM* 727, **2005**, 115.
- Rico, J. F.; Lòpez, R.; Ema, I.; Ramírez, G.; Ludeña, E. V. "Electrostatic Potentials and Fields from Density Expansions of Deformed Atoms in Molecules" *J. Comput. Chem.* 25, **2004**, 1347.
- Riley, K. E.; Hobza, P. "Investigations into the Nature of Halogen Bonding Including Symmetry Adapted Perturbation Theory Analyses" *J. Chem. Theory Comput.* 4, **2008**, 232.

- Riley, K. E.; Murray, J. S.; Fanfrlík, J.; Řezáč, J.; Solá, R. J.; Concha, M. C.; Ramos, F. M.; Politzer, P. "Halogen Bond Tunability II: The Varying Roles of Electrostatic and Dispersion Contributions to Attraction in Halogen Bonds" *J. Mol. Model.* 19, **2013**, 4651.
- Riley, K. E.; Murray, J. S.; Politzer, P.; Concha, M. C.; Hobza, P. "Br...O Complexes as Probes of Factors Affecting Halogen Bonding: Interactions of Bromobenzenes and Bromopyrimidines with Acetone" *J. Chem. Theory Comput.* 5, **2009**, 155.
- Rode, B. M. "The Influence of Metal Ions on Neighbouring Hydrogen Bonds" *Theoret. Chim. Acta* 56, **1980**, 245.
- Rode, B. M.; Sagarik, K. P. "The Influence of Small Monovalent Cations on Neighbouring N...H...O Hydrogen Bonds" *Chem. Phys. Lett.* 88, **1982**, 337.
- Roothaan, C. C. J. "New Developments in Molecular Orbital Theory" *Rev. Mod. Phys.* 23, **1951**, 69.
- Sagarik, K. P.; Rode, B. M. "The Influence of Small Monovalent Cations on Neighbouring Hydrogen Bonds of Aquo-Protein Complexes" *Z. Naturforsch. A* 36, **1981**, 1357.
- Sagarik, K. P.; Rode, B. M. "The Influence of Magnesium(II) on the Hydrogen Bonds of the Adenine-Thymine Base Pair" *Inorg. Chim. Acta* 78, **1983a**, 177.
- Sagarik, K. P.; Rode, B. M. "The Influence of Small Monovalent Cations on the Hydrogen Bonds of Base Pairs of DNA" *Inorg. Chim. Acta* 78, **1983b**, 81.
- Sakai, N.; Mareda, J.; Vauthey, E.; Matile, S. "Core-substituted Naphthalenediimides" *Chem. Commun.* 46, **2010**, 4225.
- Salonen, L. M.; Ellermann, M.; Diederich, F. "Aromatic Rings in Chemical and Biological Recognition: Energetics and Structures" *Angew. Chem. Int. Ed.* 50, **2011**, 4808.

- Sarkhel, S.; Rich, A.; Egli, M. "Water-Nucleobase "Stacking": H- π and Lone Pair- π Interactions in the Atomic Resolution Crystal Structure of an RNA Pseudoknot" *J. Am. Chem. Soc.* 125, **2003**, 8998.
- Saunders, M.; Jiménez-Vázquez, H. A.; Cross, R. J.; Poreda, R. J. "Stable Compounds of Helium and Neon: He@C₆₀ and Ne@C₆₀" *Science* 259, **1993**, 1428.
- Sayyed, F. B.; Suresh, C. H. "Quantitative Assessment of Substituent Effects on Cation- π Interactions Using Molecular Electrostatic Potential Topography" *J. Phys. Chem. A* 115, **2011**, 9300.
- Scerri, E. R. "Have Orbitals Really Been Observed?" *J. Chem. Educ.* 77, **2000**, 1492.
- Schiøtt, B.; Iversen, B. B.; Madsen, G. K. H.; Bruice, T. C. "Characterization of the Short Strong Hydrogen Bond in Benzoylacetone by Ab Initio Calculations and Accurate Diffraction Experiments. Implications for the Electronic Nature of Low-Barrier Hydrogen Bonds in Enzymatic Reactions" *J. Am. Chem. Soc.* 120, **1998**, 12117.
- Schlick, T. *Molecular Modeling and Simulation*. Springer-Verlag: New York, **2002**.
- Schmidtchen, F. P. "Inclusion of Anions in Macrotricyclic Quaternary Ammonium Salts" *Angew. Chem. Int. Ed.* 16, **1977**, 720.
- Schmidtchen, F. P.; Berger, M. "Artificial Organic Host Molecules for Anions" *Chem. Rev.* 97, **1997**, 1609.
- Schmidtchen, F. P.; Müller, G. "Anion Inclusion Without Auxiliary Hydrogen Bonds: X-Ray Structure of the Iodide Cryptate of a Macrotricyclic Tetra-quaternary Ammonium Receptor" *J. Chem. Soc., Chem. Commun.* **1984**, 1115.
- Schneider, H.; Vogelhuber, K. M.; Schinle, F.; Weber, J. M. "Aromatic Molecules in Anion Recognition: Electrostatics Versus H-Bonding" *J. Am. Chem. Soc.* 129, **2007**, 13022.

- Schnieder, H.-J.; Werner, F.; Blatter, T. "Attractive Interactions Between Negative Charges and Polarizable Aryl Parts of Host–Guest Systems" *J. Phys. Org. Chem.* **6**, **1993**, 590.
- Schottel, B. L.; Chifotides, H. T.; Dunbar, K. R. "Anion- π Interactions" *Chem. Soc. Rev.* **37**, **2008**, 68.
- Schrödinger, E. "Quantisierung als Eigenwertproblem" *Ann. Phys.* **79**, **1926**, 361.
- Schuster, P.; Zundel, G.; Sandorfy, C. *The Hydrogen Bond: Recent Developments in Theory and Experiments*. North-Holland Pub. Co.: Amsterdam, **1976**.
- Scrocco, E.; Tomasi, J. "Electronic Molecular Structure, Reactivity and Intermolecular Forces: An Euristic Interpretation by Means of Electrostatic Molecular Potentials" *Adv. Quantum Chem.* **11**, **1978**, 116.
- Sebastianelli, F.; Xu, M.; Bačić, Z.; Lawler, R.; Turro, N. J. "Hydrogen Molecules inside Fullerene C₇₀: Quantum Dynamics, Energetics, Maximum Occupancy, And Comparison with C₆₀" *J. Am. Chem. Soc.* **132**, **2010**, 9826.
- Sen, K. D.; Politzer, P. "Characteristic Features of the Electrostatic Potentials of Singly Negative Monoatomic Ions" *J. Chem. Phys.* **90**, **1989**, 4370.
- Senn, H. M.; Thiel, W. "QM/MM Methods for Biomolecular Systems" *Angew. Chem. Int. Ed.* **48**, **2009**, 1198.
- Shavitt, I. *Methods in Computational Physics*. Academic Press: New York, **1963**.
- Shirsat, R. N.; Bapat, S. V.; Gadre, S. R. "Molecular Electrostatics: A Comprehensive Topographical Approach" *Chem. Phys. Lett.* **200**, **1992**, 373.
- Sidgwick, N. V.; Powell, H. E. "Bakerian Lecture. Stereochemical Types and Valency Groups" *Proc. R. Soc. A* **176**, **1940**, 153.
- Simmons, H. E.; Park, C. H. "Macrobicyclic Amines. I. Out-in Isomerism of 1,(k+2)-Diazabicyclo[k.l.m] Alkanes" *J. Am. Chem. Soc.* **90**, **1968**, 2428.

- Sjoberg, P.; Politzer, P. "Use of the Electrostatic Potential at the Molecular Surface to Interpret and Predict Nucleophilic Processes" *J. Phys. Chem.* 94, **1990**, 3959.
- Slanina, Z.; Pulay, P.; Nagase, S. "H₂, Ne, and N₂ Energies of Encapsulation into C₆₀ Evaluated with the MPWB1K Functional" *J. Chem. Theory Comput.* 2, **2006**, 782.
- Slater, J. C. "Note on Hartree's Method" *Phys. Rev.* 35, **1930**, 210.
- Slater, J. C. "A Simplification of the Hartree-Fock Method" *Phys. Rev.* 81, **1951**, 385.
- Slater, J. C. "Atomic Radii in Crystals" *J. Chem. Phys.* 41, **1964**, 3199.
- Spence, M. M.; Rubin, S. M.; Dimitrov, I. E.; Ruiz, E. J.; Wemmer, D. E.; Pines, A.; Yao, S. Q.; Tian, F.; Schultz, P. G. "Functionalized Xenon as a Biosensor" *Proc. Natl. Acad. Sci. USA* 98, **2001**, 10654.
- Steiner, T. "The Hydrogen Bond in the Solid State" *Angew. Chem. Int. Ed.* 41, **2002**, 48.
- Stewart, J. J. P. "Semiempirical Molecular Orbital Methods" *Rev. Comp. Chem.* 1, **1990**, 45.
- Stewart, R. F. "Small Gaussian Expansions of Slater-Type Orbitals" *J. Chem. Phys.* 52, **1970**, 431.
- Sundararajan, K.; Sankaran, K.; Viswanathan, K. S.; Kulkarni, A. D.; Gadre, S. R. "H- π complexes of Acetylene-Ethylene: A Matrix Isolation and Computational Study" *J. Phys. Chem. A* 106, **2002**, 1504.
- Suresh, C. H. "Molecular Electrostatic Potential Approach to Determining the Steric Effect of Phosphine Ligands in Organometallic Chemistry" *Inorg. Chem.* 45, **2006**, 4982.
- Suresh, C. H.; Alexander, P.; Vijayalakshmi, K. P.; Sajith, P. K.; Gadre, S. R. "Use of Molecular Electrostatic Potential for Quantitative Assessment of Inductive Effect" *Phys. Chem. Chem. Phys.* 10, **2008**, 6492.

- Suresh, C. H.; Gadre, S. R. "Electrostatic Potential Minimum of the Aromatic Ring as a Measure of Substituent Constant" *J. Phys. Chem. A* 111, **2007**, 710.
- Suresh, C. H.; Mohan, N.; Vijayalakshmi, K. P.; George, R.; Mathew, J. M. "Typical Aromatic Noncovalent Interactions in Proteins: A Theoretical Study Using Phenylalanine" *J. Comput. Chem.* 30, **2009**, 1392.
- Szabo, A.; Ostlund, N. S. *Modern Quantum Chemistry Introduction to Advanced Electronic Structure Theory*. Dover: New York, **1996**.
- Szczesniak, M. M.; Scheiner, S. "Effects of External Ions on The Dynamics of Proton Transfer Across a Hydrogen Bond" *J. Phys. Chem.* 89, **1985**, 1835.
- Tarakeshwar, P.; Kim, K. S.; Kraka, E.; Cremer, D. "Structure and Stability of Fluorine-Substituted Benzene-Argon Complexes: The Decisive Role of Exchange-Repulsion and Dispersion Interactions" *J. Chem. Phys.* 115, **2001**, 6018.
- Taylor, P. G.; Bassindale, A. R.; El Aziz, Y.; Pourny, M.; Stevenson, R.; Hursthouse, M. B.; Coles, S. J. "Further Studies of Fluoride Ion Entrapment in Octasilsesquioxane Cages; X-ray Crystal Structure Studies and Factors that Affect their Formation" *Dalton Trans.* 41, **2012**, 2048.
- Thanthiriwatte, K. S.; Hohenstein, E. G.; Burns, L. A.; Sherrill, C. D. "Assessment of the Performance of DFT and DFT-D Methods for Describing Distance Dependence of Hydrogen-bonded Interactions" *J. Chem. Theory Comput.* 7, **2010**, 88.
- Thomas, L. H. "The Calculation of Atomic Fields" *Proc. Cambridge Phil. Soc.* 23, **1927**, 542.
- Tomasi, J.; Alagona, G.; Bonaccorsi, R.; Ghio, C.; Cammi, R. Semiclassical Interpretation of Intramolecular Interactions. In *Theoretical Models of Chemical Bonding*, Z.B. Maksic, Ed. Springer: Berlin, **1991**; Vol. 3.

- Tomasi, J.; Mennucci, B.; Cammi, R. MEP: A Tool for Interpretation and Prediction. From Molecular Structure to Solvation Effects. In *Molecular Electrostatic Potentials Concepts and Applications*, J. S. Murray, K. Sen, Eds. Elsevier: Amsterdam, **1996**; Vol. 3.
- Tomasi, J.; Persico, M. "Molecular Interactions in Solution: An Overview of Methods Based on Continuous Distributions of the Solvent" *Chem. Rev.* 94, **1994**, 2027.
- Townes, C. H.; Schawlow, A. L. *Microwave Spectroscopy*. Dover: New York, **1975**.
- Tsuzuki, S.; Honda, K.; Uchimaru, T.; Mikami, M.; Tanabe, K. "The Magnitude of the CH/ π Interaction between Benzene and Some Model Hydrocarbons" *J. Am. Chem. Soc.* 122, **2000**, 3746.
- Tuma, C.; Boese, A. D.; Handy, N. C. "Predicting the Binding Energies of H-Bonded Complexes : A Comparative DFT Study" *Phys. Chem. Chem. Phys.* 1, **1999**, 3939.
- Umeyama, H.; Morokuma, K. "The Origin of Hydrogen Bonding. An Energy Decomposition Study" *J. Am. Chem. Soc.* 99, **1977**, 1316.
- van der Avoird, A.; Wormer, P. E. S.; Moszynski, R. "From Intermolecular Potentials to the Spectra of van der Waals Molecules, and Vice Versa" *Chem. Rev.* 94, **1994**, 1931.
- Vijay, D.; Zipse, H.; Sastry, G. N. "On the Cooperativity of Cation- π and Hydrogen Bonding Interactions" *J. Phys. Chem. B* 112, **2008**, 8863.
- Vosko, S. H.; Wilk, L.; Nusair, M. "Accurate Spin-Dependent Electron Liquid Correlation Energies for Local Spin Density Calculations: A Critical Analysis" *Can. J. Phys.* 58, **1980**, 1200.
- Voth, A. R.; Hays, F. A.; Ho, P. S. "Directing Macromolecular Conformation Through Halogen Bonds" *Proc. Nat. Acad. Sci.* 104, **2007**, 6188.

- Voth, A. R.; Ho, P. S. "The Role of Halogen Bonding in Inhibitor Recognition and Binding by Protein Kinases" *Curr. Top. Med. Chem.* 7, **2007**, 1336.
- Wang, F.-F.; Hou, J.-H.; Li, Z.-R.; Wu, D.; Li, Y.; Lu, Z.-Y.; Cao, W.-L. "Unusual Halogen-Bonded Complex FBr...BrF and Hydrogen-Bonded Complex FBr...HF Formed by Interactions Between Two Positively Charged Atoms of Different Polar Molecules" *J. Chem. Phys.* 126, **2007**, 144301.
- Wang, W.; Wong, N.-B.; Zheng, W.; Tian, A. "Theoretical Study on the Blueshifting Halogen Bond" *J. Phys. Chem. A* 108, **2004**, 1799.
- Watson, J. D.; Crick, F. H. C. "Molecular Structure of Nucleic Acids" *Nature* 171, **1953**, 737.
- Weiner, P. K.; Kollman, P. A. "AMBER: Assisted Model Building with Energy Refinement. A General Program for Modeling Molecules and Their Interactions" *J. Comput. Chem.* 2, **1981**, 287.
- Weinhold, F. Natural Bond Orbital Methods. In *Encyclopedia of Computational Chemistry*, P. v. R. Schleyer, N. L. Allinger, T. Clark, J. Gasteiger, P. A. Kollman, H. F. Schaefer, III, P. R. Schreiner, Eds. Wiley: Chichester, UK, **1998**; Vol. 3, p 1792.
- Werner, A. "Ueber Haupt- und Nebenvalenzen und die Constitution der Ammoniumverbindungen" *Justus Liebigs Ann. Chem.* 322, **1902**, 261.
- Wiberg, K. B. "Basis Set Effects on Calculated Geometries: 6-311++G** vs. aug-ac-pvdz" *J. Comput. Chem.* 25, **2004**, 1342.
- Wolters, L. P.; Bickelhaupt, F. M. "Halogen Bonding Versus Hydrogen Bonding: A Molecular Orbital Perspective" *ChemistryOpen* 1, **2012**, 96.
- Xu, X.; Goddard, W. A. "Assessment of Handy-Cohen Optimized Exchange Density Functional (OPTX)" *J. Phys. Chem. A* 108, **2004**, 8495.

- Yap, G. P. A.; Rheingold, A. L.; Das, P.; Crabtree, R. H. "A Three-Center Hydrogen Bond in 2,6-Diphenylpyridinium Tetrachloroaurate" *Inorg. Chem.* 34, **1995**, 3474.
- Yeole, S. D.; Gadre, S. R. "Topography of Scalar Fields: Molecular Clusters and π -Conjugated Systems" *J. Phys. Chem. A* 115, **2011**, 12769.
- Yeole, S. D.; Lòpez, R.; Gadre, S. R. "Rapid Topography Mapping of Scalar Fields: Large Molecular Clusters" *J. Chem. Phys.* 137, **2012**, 074116.
- Yoon, J.; Kim, S. K.; Singh, N. J.; Kim, K. S. "Imidazolium Receptors for the Recognition of Anions" *Chem. Soc. Rev.* 35, **2006**, 355.
- Zhang, J.; Chen, P.; Yuan, B.; Ji, W.; Cheng, Z.; Qiu, X. "Real-Space Identification of Intermolecular Bonding with Atomic Force Microscopy" *Science* 342, **2013**, 611.
- Zhao, Y.; Beuchat, C.; Domoto, Y.; Gajewy, J.; Wilson, A.; Mareda, J.; Sakai, N.; Matile, S. "Anion- π Catalysis" *J. Am. Chem. Soc.* 136, **2014**, 2101.
- Zhao, Y.; Schultz, N. E.; Truhlar, D. G. "Design of Density Functionals by Combining the Method of Constraint Satisfaction with Parametrization for Thermochemistry, Thermochemical Kinetics, and Noncovalent Interactions" *J. Chem. Theory Comput.* 2, **2005a**, 364.
- Zhao, Y.; Schultz, N. E.; Truhlar, D. G. "Exchange-Correlation Functional with Broad Accuracy for Metallic and Nonmetallic Compounds, Kinetics, and Noncovalent Interactions" *J. Chem. Phys.* 123, **2005b**, 161103.
- Zhao, Y.; Tishchenko, O.; Truhlar, D. G. "How Well Can Density Functional Methods Describe Hydrogen Bonds to π Acceptors?" *J. Phys. Chem. B* 109, **2005c**, 19046.
- Zhao, Y.; Truhlar, D. G. "Hybrid Meta Density Functional Theory Methods for Thermochemistry, Thermochemical Kinetics, and Noncovalent Interactions: The

- MPW1B95 And MPWB1K Models and Comparative Assessments for Hydrogen Bonding and van der Waals Interactions” *J. Phys. Chem. A* 108, **2004**, 6908.
- Zhao, Y.; Truhlar, D. G. “Benchmark Databases for Nonbonded Interactions and Their Use to Test Density Functional Theory” *J. Chem. Theory Comput.* 1, **2005a**, 415.
- Zhao, Y.; Truhlar, D. G. “Design of Density Functionals That are Broadly Accurate for Thermochemistry, Thermochemical Kinetics, and Nonbonded Interactions” *J. Phys. Chem. A* 109, **2005**, 5656.
- Zhao, Y.; Truhlar, D. G. “Density Functional for Spectroscopy: No Long-Range Self-Interaction Error, Good Performance for Rydberg and Charge-Transfer States, and Better Performance on Average than B3LYP for Ground States” *J. Phys. Chem. A* 110, **2006a**, 13126.
- Zhao, Y.; Truhlar, D. G. “A New Local Density Functional for Main-Group Thermochemistry, Transition Metal Bonding, Thermochemical Kinetics, and Noncovalent Interactions” *J. Chem. Phys.* 125, **2006b**, 194101.
- Zhao, Y.; Truhlar, D. G. “Exploring the Limit of Accuracy of the Global Hybrid Meta Density Functional for Main-Group Thermochemistry, Kinetics, and Noncovalent Interactions” *J. Chem. Theory Comput.* 4, **2008a**, 1849.
- Zhao, Y.; Truhlar, D. G. “The M06 Suite of Density Functionals for Main Group Thermochemistry, Thermochemical Kinetics, Noncovalent Interactions, Excited States, and Transition Elements: Two New Functionals and Systematic Testing of Four M06-Class Functionals and 12 Other Functionals” *Theor. Chem. Acc.* 120, **2008b**, 215.
- Zhu, W. L.; Tan, X. J.; Puah, C. M.; Gu, J. D.; Jiang, H. L.; Chen, K. X.; Felder, C. E.; Silman, I.; Sussman, J. L. “How Does Ammonium Interact with Aromatic

- Groups? A Density Functional Theory (DFT/B3LYP) Investigation” *J. Phys. Chem. A* 104, **2000**, 9573.
- Zuo, J. M.; Kim, M.; O’Keeffe, M.; Spence, J. C. H. “Direct Observation of d-Orbital Holes and Cu–Cu Bonding in Cu₂O” *Nature* 401, **1999**, 49.